

University of Warwick institutional repository: <http://go.warwick.ac.uk/wrap>

**A Thesis Submitted for the Degree of PhD at the University of Warwick**

<http://go.warwick.ac.uk/wrap/55294>

This thesis is made available online and is protected by original copyright.

Please scroll down to view the document itself.

Please refer to the repository record for this item for information to help you to cite it. Our policy information is available from the repository home page.

## Library Declaration and Deposit Agreement

### 1. STUDENT DETAILS

Please complete the following:

Full name: JONATHAN ROSS SNELLING

University ID number: 0859742

### 2. THESIS DEPOSIT

2.1 I understand that under my registration at the University, I am required to deposit my thesis with the University in BOTH hard copy and in digital format. The digital version should normally be saved as a single pdf file.

2.2 The hard copy will be housed in the University Library. The digital version will be deposited in the University's Institutional Repository (WRAP). Unless otherwise indicated (see 2.3 below) this will be made openly accessible on the Internet and will be supplied to the British Library to be made available online via its Electronic Theses Online Service (EThOS) service.

[At present, theses submitted for a Master's degree by Research (MA, MSc, LL.M, MS or MMedSci) are not being deposited in WRAP and not being made available via EThOS. This may change in future.]

2.3 In exceptional circumstances, the Chair of the Board of Graduate Studies may grant permission for an embargo to be placed on public access to the hard copy thesis for a limited period. It is also possible to apply separately for an embargo on the digital version. (Further information is available in the *Guide to Examinations for Higher Degrees by Research*.)

2.4 If you are depositing a thesis for a Master's degree by Research, please complete section (a) below. For all other research degrees, please complete both sections (a) and (b) below:

#### (a) Hard Copy

I hereby deposit a hard copy of my thesis in the University Library to be made publicly available to readers (please delete as appropriate) EITHER immediately OR after an embargo period of ..... months/years as agreed by the Chair of the Board of Graduate Studies.

I agree that my thesis may be photocopied.

☒ YES ☐ NO (Please delete as appropriate)

#### (b) Digital Copy

I hereby deposit a digital copy of my thesis to be held in WRAP and made available via EThOS.

Please choose one of the following options:

EITHER My thesis can be made publicly available online. ☒ YES ☐ NO (Please delete as appropriate)

OR My thesis can be made publicly available only after .....[date] (Please give date)  
YES / NO (Please delete as appropriate)

OR My full thesis cannot be made publicly available online but I am submitting a separately identified additional, abridged version that can be made available online.  
YES / NO (Please delete as appropriate)

OR My thesis cannot be made publicly available online. YES / NO (Please delete as appropriate)

### 3. GRANTING OF NON-EXCLUSIVE RIGHTS

Whether I deposit my Work personally or through an assistant or other agent, I agree to the following:

Rights granted to the University of Warwick and the British Library and the user of the thesis through this agreement are non-exclusive. I retain all rights in the thesis in its present version or future versions. I agree that the institutional repository administrators and the British Library or their agents may, without changing content, digitise and migrate the thesis to any medium or format for the purpose of future preservation and accessibility.

### 4. DECLARATIONS

(a) I DECLARE THAT:

- I am the author and owner of the copyright in the thesis and/or I have the authority of the authors and owners of the copyright in the thesis to make this agreement. Reproduction of any part of this thesis for teaching or in academic or other forms of publication is subject to the normal limitations on the use of copyrighted materials and to the proper and full acknowledgement of its source.
- The digital version of the thesis I am supplying is the same version as the final, hard-bound copy submitted in completion of my degree, once any minor corrections have been completed.
- I have exercised reasonable care to ensure that the thesis is original, and does not to the best of my knowledge break any UK law or other Intellectual Property Right, or contain any confidential material.
- I understand that, through the medium of the Internet, files will be available to automated agents, and may be searched and copied by, for example, text mining and plagiarism detection software.

(b) IF I HAVE AGREED (in Section 2 above) TO MAKE MY THESIS PUBLICLY AVAILABLE DIGITALLY, I ALSO DECLARE THAT:

- I grant the University of Warwick and the British Library a licence to make available on the Internet the thesis in digitised format through the Institutional Repository and through the British Library via the EThOS service.
- If my thesis does include any substantial subsidiary material owned by third-party copyright holders, I have sought and obtained permission to include it in any version of my thesis available in digital format and that this permission encompasses the rights that I have granted to the University of Warwick and to the British Library.

### 5. LEGAL INFRINGEMENTS

I understand that neither the University of Warwick nor the British Library have any obligation to take legal action on behalf of myself, or other rights holders, in the event of infringement of intellectual property rights, breach of contract or of any other right, in the thesis.

---

*Please sign this agreement and return it to the Graduate School Office when you submit your thesis.*

Student's signature: \_\_\_\_\_

Date: \_\_\_\_\_

*Monell* 14th February 2014

Characterisation of pharmaceutical and polymer  
formulations by novel mass spectrometry  
approaches

Jonathon R. Snelling B.Sc. (Hons)

A thesis submitted for the degree of Doctor of Philosophy

University of Warwick  
School of Life Sciences

August 2012

谨以此论文献给我的爱妻君宜  
十分感谢你对我始终如一的包容与无微不至的照顾

# Table of Contents

List of Figures .....	iv
List of Tables.....	x
Acknowledgements .....	xi
Declaration .....	xii
Summary .....	xiii
Abbreviations .....	xiv
<b>Chapter 1 - Mass Spectrometry Introduction.....</b>	<b>1</b>
1.1 Birth of Mass Spectrometry .....	2
1.2 Basics of Mass Spectrometry .....	3
1.3 Established Ionisation techniques.....	3
1.3.1 Matrix Assisted Laser Desorption Ionisation (MALDI) .....	5
1.3.2 Electrospray Ionisation (ESI).....	7
1.4 Established Mass Analysers.....	10
1.4.1 Quadrupole Mass Filter .....	10
1.4.2 Time of Flight Mass Analyser .....	11
1.5 Tandem Mass Spectrometry .....	14
1.6 Ion Detection .....	16
1.7 Evaluating capabilities of novel mass spectrometry techniques.....	17
1.8 Ambient Ionisation Techniques.....	19
1.8.1 ESI based Ambient Ionisation Techniques .....	22
1.8.1.1 Desorption Electrospray Ionisation (DESI) .....	22
1.8.1.2 Extractive Electrospray Ionisation (EESI).....	25
1.8.2 APCI based Ambient Ionisation techniques .....	29
1.8.2.1 Atmospheric pressure solids analysis probe (ASAP) .....	29
1.9 Separation Science Coupled to Mass Spectrometry .....	32
1.9.1 Ion Mobility-Mass Spectrometry .....	32
1.9.1.1 Drift Cell Ion Mobility Spectrometry .....	33
1.9.1.2 Travelling Wave Ion Mobility-Mass Spectrometry (TWIMS) .....	36
1.10 Aims of project .....	42
1.10 Research Papers .....	45
1.11 Oral Presentations.....	45
1.12 Conference Papers (Peer Reviewed) .....	46
<b>Chapter 2 - Materials and Methods .....</b>	<b>65</b>
2.1 Materials.....	66
2.1.1 Reagents.....	66

2.1.2 Pharmaceutical samples.....	66
2.1.3 Polymer Samples.....	68
<b>2.2 Methods.....</b>	<b>69</b>
2.2.1 Ion mobility mass spectrometer instrument.....	69
2.2.2 Calibration of Synapt G2.....	70
2.2.2.1 Calibration of mass analyser.....	70
2.2.2.2 Calibration of ion mobility cell.....	70
2.2.3 Analysis of Pharmaceutical Samples.....	72
2.2.3.1 ASAP analysis of pharmaceutical formulations.....	72
2.2.3.2 DESI analysis of pharmaceutical formulations.....	73
2.2.3.3 ESI analysis of pharmaceutical formulations.....	74
2.2.3.4 TA-EESI analysis of pharmaceutical formulations.....	75
2.2.4 Analysis of Tween and tyloxapol formulations.....	76
2.2.4.1 ASAP analysis of Tween and tyloxapol formulations.....	76
2.2.4.2 ESI analysis of Tween and tyloxapol formulations.....	77
2.2.4.3 MALDI analysis of Tween and tyloxapol formulations.....	77
2.2.4.4 TA-EESI analysis of Tween and tyloxapol formulations.....	78
2.2.5 Analysis of Polyrotaxane formulation.....	79
2.2.5.1 Analysis of polyrotaxane formulations by ESI.....	79
2.2.5.2 Analysis of polyrotaxane formulations by MALDI.....	79
<b>2.4 Benzocaine purity assay by gas chromatography – MS (GC-MS).....</b>	<b>80</b>
<b>2.5 Modelling.....</b>	<b>80</b>
<b>2.6 References.....</b>	<b>82</b>
<b>Chapter 3 - Pharmaceutical Formulations.....</b>	<b>83</b>
<b>3.1 Pharmaceutical formulations.....</b>	<b>84</b>
<b>3.2 Characterisation of Pharmaceutical formulations.....</b>	<b>84</b>
<b>3.3 Characterisation by Mass Spectrometry.....</b>	<b>85</b>
<b>3.4 Characterisation of pharmaceuticals by ambient ionisation.....</b>	<b>85</b>
<b>3.5 Ion mobility mass spectrometry (IM-MS) in pharmaceutical analysis.....</b>	<b>86</b>
<b>3.6 Aims.....</b>	<b>87</b>
<b>3.7 Development of thermally assisted – extractive electrospray ionisation (TA-EESI).....</b>	<b>88</b>
3.7.1 TA-EESI of Salbutamol.....	89
3.7.2 TA-EESI analysis of decongestant sprays.....	92
3.7.3 Benzocaine.....	98
<b>3.8 Evaluation of ASAP technique.....</b>	<b>111</b>
<b>3.8.1 ASAP analysis of benzocaine.....</b>	<b>111</b>
3.8.2 ASAP analysis of decongestant sprays.....	114
3.8.3 ASAP analysis of Anadin extra.....	116
3.8.4 Deep heat spray case study.....	118

<b>3.9 Conclusions.....</b>	<b>123</b>
<b>3.10 References.....</b>	<b>124</b>
<b>Chapter 4 - Polymer Characterisation.....</b>	<b>129</b>
<b>4.1 Introduction to synthetic polymers.....</b>	<b>130</b>
<b>4.2 Existing characterisation techniques for polymer formulations .....</b>	<b>133</b>
4.2.1 Characterisation of polymers by established mass spectrometry techniques .....	136
4.2.2 Use of Direct Analysis techniques for polymer analysis.....	138
4.2.3 Use of ion mobility-mass spectrometry for polymer analysis .....	138
<b>4.3 Aims of work reported in chapter .....</b>	<b>139</b>
<b>4.4 Results – Ambient ionisation for tyloxapol analysis .....</b>	<b>140</b>
4.4.1 Comparison of ionisation techniques for a Tyloxapol formulation .....	140
4.4.2 Metal Ion adduct formation in ambient ionisation techniques.....	149
4.4.3 Analysis of Tyloxapol by ambient ionisation conclusions .....	151
<b>4.5 Polysorbate formulations .....</b>	<b>152</b>
4.5.1 ASAP analysis of Tween formulations for ester determination .....	156
4.5.2 ESI-IMMS analysis of Tween formulations .....	160
4.5.3 MALDI-IMMS analysis of Tween formulations .....	162
4.5.4 Polysorbate case study conclusions.....	173
<b>4.6 Polyrotaxane characterisation .....</b>	<b>175</b>
4.6.1 Rotaxanes.....	175
4.6.2 Polyrotaxanes .....	175
4.6.3 Characterisation Methods .....	176
4.6.4 Results .....	178
4.6.5 Polyrotaxane case study conclusions .....	189
<b>4.7 References.....</b>	<b>190</b>
<b>Chapter 5 - Conclusions and Future Perspectives.....</b>	<b>199</b>
<b>5.1 Conclusions and Future Perspectives .....</b>	<b>200</b>
<b>5.2 References.....</b>	<b>205</b>



# List of Figures

<b>Figure 1.1</b> - Schematic of a mass spectrometer. ....	3
<b>Figure 1.2</b> - Common ion formation reaction during methane CI. ....	4
<b>Figure 1.3</b> - Schematic of MALDI ionisation process. ....	6
<b>Figure 1.4</b> - Schematic showing two proposed ESI mechanisms – Adapted from Kerbale (2000). ....	9
<b>Figure 1.5</b> - Schematic of a quadrupole mass filter. An ion with a stable trajectory (green) will reach the detector, while the ion with an unstable trajectory (blue) will not. ....	11
<b>Figure 1.6</b> - Schematic of Reflectron-ToF instrument. Both ions are the same $m/z$ but have different initial kinetic energies. ....	13
<b>Figure 1.7</b> - A schematic representation of the droplet pickup mechanism of ion formation in DESI, adapted from (Cooks 2006). 1+2 represent film formation and extraction of solid phase analytes into film. 3 represents secondary ions formed from secondary droplets. ....	23
<b>Figure 1.8</b> - Schematic Diagram of the EESI setup, (adapted from (Law, Wang et al. 2010)). ....	25
<b>Figure 1.9</b> - (A) Schematic of ND-EESI, (B) Schematic of EESI (TA-EESI is similar but with a hot plate placed below the bottle). ....	28
<b>Figure 1.10</b> - Schematic of ASAP, with legend. ....	29
<b>Figure 1.11</b> - Main mechanisms for formation of radical cation, and protonated ion (adapted from (Horning, Carroll et al. 1974)). ....	30
<b>Figure 1.12</b> - Schematic of DCIMS experiment, with typical ATD readout. Adapted from (Eiceman and Stone 2004). ....	35
<b>Figure 1.13</b> - Schematic representation of a SRIG. Adapted from (Giles 2004) ....	36
<b>Figure 1.14</b> - Schematic showing the progression of the travelling wave voltage pulse along the TWIG (Adapted from Giles 2004) ....	37
<b>Figure 1.15</b> - Schematic diagram of Synapt G2. The ionisation region shown is a z-spray ESI source and is one of many that can be interfaced to the instrument. .	39
<b>Figure 2.1</b> - Structures, formulae and exact mass for active ingredients studied ....	67
<b>Figure 2.2</b> - Photograph of EESI setup. ....	75

<b>Figure 3.1</b> - Mass spectra of the salbutamol spray obtained by TA-EESI-MS analysis at three different temperatures, (A) ambient temperature, (B) $200 \pm 10$ °C and (C) $340 \pm 10$ °C. Spectra are displayed with intensity axes linked.....	89
<b>Figure 3.2</b> - Precursor-selected MS/MS spectrum of $m/z$ 577.3 ion. This is characterised as protonated salbutamol sulphate, a dimer of salbutamol in coordination with a sulphate group. This ion was observed when the TA-EESI temperature was increased to ( $\sim 340^{\circ}\text{C} \pm 10^{\circ}\text{C}$ ). .....	90
<b>Figure 3.3</b> - Product ion spectra of salbutamol obtained by means of (A) mobility-separated CID/MS and (B) precursor-selected ESI-MS/MS.....	91
<b>Figure 3.4</b> - The proposed fragmentation pathway for the singly-protonated ion of salbutamol. ....	91
<b>Figure 3.5</b> - Structures, formulae and exact mass data for Oxymetazoline and Xylometazoline.....	92
<b>Figure 3.6</b> - Mass spectra of Vicks Sinex Decongestant obtained by TA-EESI-MS analysis at three different temperatures.(A) ambient temperature, (B) $240 \pm 10^{\circ}\text{C}$ and (C) $340 \pm 10^{\circ}\text{C}$ . .....	93
<b>Figure 3.7</b> - Mass spectra of Sudafed obtained by TA-EESI-MS analysis at three different temperatures, (A) ambient temperature, (B) $240 \pm 10$ °C and (C) $370 \pm 10$ °C. Spectra are displayed with intensity axes linked. ....	94
<b>Figure 3.8</b> - Arrival time distributions for the singly-protonated ions of (A) xylometazoline and (B) oxymetazoline, with their corresponding mobility-separated product ion spectra inset. Experiment performed with TA temperature of $240 \pm 10$ °C. ....	95
<b>Figure 3.9</b> - (A) TA-EESI-Mobility-separated product ion spectrum for Sudafed (same spectrum as in Figure 3.8A) and (B) ESI-precursor-selected MS/MS product ion spectrum for $m/z$ 245.2. CID voltages were set at 30 V in both experiments. ....	96
<b>Figure 3.10</b> - Proposed structures of some fragments generated from xylometazoline. ....	97
<b>Figure 3.11</b> - Structure, formula and exact mass of benzocaine.....	98
<b>Figure 3.12</b> - Mass spectra of AAA Sore Throat Spray obtained by TA-EESI-MS analysis at (A) ambient temperature and (B) $110 \pm 10$ °C.....	98

<b>Figure 3.13</b> - Precursor selected MS/MS of the $m/z$ 155.1 ion observed within the formulation (A), MS/MS of menthone standard (B), and MS/MS of eucalyptol standard (C). CID voltage set at 20V.....	99
<b>Figure 3.14</b> - The extracted arrival time distribution for the singly-protonated ion of benzocaine ( $m/z$ 166.1), which shows two distinct peaks with arrival times of 4.29 ms and 5.33 ms respectively. Their corresponding mobility-separated product ion spectra are shown inset. Product ion spectra generated in same sub second experiment with energy in transfer cell set at 30 volts.....	100
<b>Figure 3.15</b> - Comparison of (A) combined mobility separated MS/MS spectra with (B) MS/MS spectrum generated by ESI-MS/MS with no mobility separation (conventional mass spectrometry example). ....	101
<b>Figure 3.16</b> - The extracted arrival time distribution for the singly-protonated ion of a benzocaine ( $m/z$ 166.1) standard. The two extracted mobility resolved product ion spectra are shown either side of their respective peaks .....	102
<b>Figure 3.17</b> - ATDs for ortho isomer (A) and meta isomer (B) of Benzocaine. ....	103
<b>Figure 3.18</b> - Precursor-selected TWIM-MS/MS spectra for the singly-protonated ions of (A) benzocaine (compact conformation), (B) benzocaine (extended conformation), (C) ethyl 2-aminobenzoate (ortho isomer) and (D) ethyl 3-aminobenzoate (meta isomer). ....	104
<b>Figure 3.19</b> - GC-MS chromatograms of benzocaine (para) and ethyl-3-aminobenzoate (meta). One peak is observed within each chromatogram and benzocaine is shown to have a longer elution time than ethyl-3-aminobenzoate .The difference in elution time, is not due to differences in boiling point, but likely polarity. A non-polar column was used, and the observation would suggest that benzocaine (the para isomer) is less polar than the meta isomer. ....	105
<b>Figure 3.20</b> - ATDs and estimated cross sections experimentally derived by the group of Mike Bowers. ....	106
<b>Figure 3.21</b> - The extracted arrival time distributions for the $m/z$ 138 fragment ion of (A) benzocaine and (B) ethyl 3-aminobenzoate (meta isomer).....	107
<b>Figure 3.22</b> - Proposed differences in protonation site, with larger CCS a result of rearrangement.....	110
<b>Figure 3.23</b> - Relative intensities of radical cation and protonated ion of benzocaine with different source conditions. ....	111

<b>Figure 3.24</b> - Mobility extracted ATDs for radical cations of benzocaine (A) and protonated molecular ion of benzocaine (B). Ions were generated by the ASAP technique .....	112
<b>Figure 3.27</b> - ATDs of radical cation and protonated ion of oxymetazoline.....	115
<b>Figure 3.28</b> - Comparison of the MS/MS spectra for protonated and radical cation of oxymetazoline.....	115
<b>Figure 3.29</b> - Spectra obtained during ASAP analysis of an Anadin Extra tablet at (A) 600 °C (no solvent infusing), (B) 600 °C (solvent infusing), (C) negative polarity with solvent infused, and (D) 300 °C (solvent infusing). ....	116
<b>Figure 3.30</b> - Structure, formula and exact mass of methyl nicotinate. ....	118
<b>Figure 3.31</b> - ATDs for the charged radical and protonated molecule ion of methyl nicotinate produced by ASAP ionisation. ....	118
<b>Figure 3.32</b> - (A) Mobility separation spectrum of protonated methyl nicotinate, (B) corresponding radical cation product ion spectrum (C) NIST spectrum generated by EI.....	119
<b>Figure 3.33</b> - MS/MS of para (A) and ortho (B) isomers of methyl nicotinate.....	120
<b>Figure 3.34</b> - Structure, formula and exact mass of nicotinic acid.....	121
<b>Figure 3.35</b> - Pseudo MS <sup>3</sup> of <i>m/z</i> 124 ion from methyl nicotinate (A) and MS/MS of nicotinic acid (B). ....	121
<b>Figure 3.36</b> - ATD of methyl nicotinate product ion with <i>m/z</i> 124 (A) compared with ATD of nicotinic acid (B) .....	122
<b>Figure 4.1</b> - Generation by step-wise polymerisation of PET.....	131
<b>Figure 4.2</b> - Chain growth of polystyrene via free radical polymerisation with benzoyl peroxide as initiator, and combination termination. ....	132
<b>Figure 4.3</b> - Chemical Structures of (A) Tyloxapol, and the structurally similar (B) p-tert octylphenol ethoxylate.....	140
<b>Figure 4.4</b> - Comparison of TA-EESI-MS/MS spectra when <i>m/z</i> 559.5 ion precursor selected.....	141
<b>Figure 4.5</b> - Proposed formation of product ion that has a neutral loss of 112 Daltons .....	142
<b>Figure 4.6</b> - Proposed structures for ions below <i>m/z</i> 300. This region is very similar for all the p-tert octyl phenol ethoxylate series observed from a Tyloxapol formulation. ....	142

<b>Figure 4.7</b> - Spectra obtained when a 99% pure tyloxapol standard analysed using four different ionisation techniques. ....	143
<b>Figure 4.8</b> - Estimated cross sections of 3 extracted ion series generated by means of ASAP. ....	145
<b>Figure 4.9</b> - Mobility-extracted ASAP MS spectra observed in a Tyloxapol formulation. ....	145
<b>Figure 4.10</b> - Comparison of MS/MS spectra for the radical cation (top) and the protonated molecule ion (bottom) of p-tertoctylphenol ethoxylate with 10 ethylene oxide repeat units. ....	146
<b>Figure 4.11</b> - Estimated Cross sections of 3 extracted ion series observed when TA-EESI used to generate ions. ....	147
<b>Figure 4.12</b> - Comparison of MS/MS spectra for $m/z$ 575 ion generated by TA-EESI (top) and ASAP analysis (bottom). ....	148
<b>Figure 4.13</b> - Spectra observed during investigation into lithiation by different ionisation techniques. ....	150
<b>Figure 4.14</b> - Schematic of Tween synthesis, inset shows the carboxylic acid. ....	153
<b>Figure 4.15</b> - Typical mass spectrum observed when Tween 20 formulation is analysed by ASAP (600C). ....	156
<b>Figure 4.16</b> - Characteristic dioxolanylium ions observed for (A) Tween 20, (B) Tween 40, (C) Tween 60, (D) Tween 80. ....	157
<b>Figure 4.17</b> - ESI-Mobility spectra of Tween 80 formulation (top), mobilogram of formulation (middle) with two trendlines A and B, and repsective extracted spectra (bottom). ....	161
<b>Figure 4.18</b> - Summed MALDI-TWIM-MS spectrum of Tween 20, with major chemical families highlighted. ....	164
<b>Figure 4.20</b> - (A) - Estimated cross-section versus $m/z$ for three isobaric isosorbide families (B) - ATD for nominal $m/z$ of 1165 and (C) - (I) Mobility separated product ion spectrum for isosorbide polyethoxylate 23-mer. (II) Isosorbide polyethoxylate oleate 17-mer and (III) isosorbide polyethoxylate dioleate 11-mer. ....	168
<b>Figure 4.21</b> - (A) - Estimated collision cross section versus $m/z$ for three isobaric sorbitan families. (B) - ATD signal for $m/z$ of 1227. (C) - Mobility separated product ion spectrum for (I) Sorbitan Polyethoxylate 24-mer (II) Sorbitan	

ethoxylate monooleate 18-mer (III) Sorbitan polyethoxylate dioleate 12-mer. .....	169
<b>Figure 4.22</b> - Schematic of a simple rotaxane molecule. ....	175
<b>Figure 4.23</b> - Structure of polyrotaxane system studied. ....	177
<b>Figure 4.24</b> - MALDI-MS spectrum of Grubbs polyrotaxane system. ....	178
<b>Figure 4.25</b> - MS/MS spectra of 1:1 species differing in carbon number. ....	179
<b>Figure 4.26</b> - MS/MS analysis of species with 1:1 (top), 2:2 (middle) and 3:3 (bottom).....	180
<b>Figure 4.27</b> - MS/MS spectra for $m/z$ 388, which has been mobility extracted from the TAP fragmentation of $m/z$ 990.....	181
<b>Figure 4.28</b> - ESI-MS spectrum of polyrotaxane system. ....	182
<b>Figure 4.29</b> - MALDI-MS/MS and ATD (top) and ESI-MS/MS and ATD (bottom) spectra of $m/z$ 990.6 ion. ....	183
<b>Figure 4.30</b> - Product ion spectrum for $m/z$ 2262.3 (top). The MS/MS spectrum for $m/z$ 2109.3 (bottom) was mobility extracted from a TAP fragmentation of the $m/z$ 2262.3 ion. ....	184
<b>Figure 4.31</b> - Proposed radical fragmentation .....	186
<b>Figure 4.32</b> - ATD for polyrotaxane species. ....	187
<b>Figure 4.33</b> - Estimated CCS for polyrotaxane species and their fragments. ....	188
<b>Figure 5.1</b> - Comparison showing differences (orange) and similarities (blue) between Tween 40 and Tween 80. ....	203

# List of Tables

<b>Table 1.1</b> - Summary of major ambient ionisation techniques .....	21
<b>Table 4.1</b> - Approximate ester content measured, by percentage, for each Tween formulation studied .....	159
<b>Table 4.2</b> - Commercial specification (Sigma Aldrich). Ticks indicate manufacturer includes these in the balance of the formulation, crosses indicate not listed by manufacturer as part of formulation .....	159
<b>Table 4.3</b> - Chemical families observed by MALDI-IMS-MS, categorised as major, minor and trace series. ....	162
<b>Table 4.4 A-D</b> - Polydispersity index (PDI), number average molecular weight (Mn) and weight average molecular weight (Mw) for selected species in (A)Tween 20, (B) Tween 40, (C) Tween 60 and (D) Tween 80. Data derived from three replicates carried out on different days SD < 0.2%.....	171

# Acknowledgements

Although I am the sole author of this thesis, I am by no means the sole contributor. Many people have supported me with their encouragement, and it is this support and belief which has enabled me to complete this research.

I should like to thank Professor Jim Scrivens for giving me the opportunity to undertake this PhD. Thank you to the Royal Society of Chemistry and the EPSRC who provided the financial support for this work.

I would like to thank members of the Scrivens lab past and present including Dr Gill Hilton who advised me in my first year of this PhD, and gave me encouragement and support, without which, the journey to this stage would have been more difficult. Thanks to Dr Charlotte Scarff with whom I collaborated with on a number of projects. Thanks to Dr Kostas Thalassinou for explaining to me the intricacies of ion mobility and for being a good mentor within the lab. Thank you also to Fran, Nisha, Elle, Sue, Krisztina and Matt.

I would also like to thank Professor Charles Wilkins for his wisdom, and for providing the polyrotaxane sample, and thanks to Dr Andrew Boyston for synthesising it. I would like to thank Dr Luca Salassa for theoretical calculations, and Dr Christian Bleiholder and Professor Mike Bowers of UCSB for further calculations and for running samples on their home-built drift cell mobility instrument.

Finally, I would like to thank my family for supporting me over the years, and to my wife Junyi, thank you for putting up with me and my PhD over the last four years.



# Declaration

I hereby declare that this thesis, submitted in partial fulfilment of the requirements for the degree of Doctor of Philosophy and entitled “Characterisation of pharmaceutical and polymer formulations by novel mass spectrometry approaches”, represents my own work and has not been previously submitted to this or any other institution for any degree, diploma or other qualification. Work undertaken by my collaborators is explicitly stated where appropriate.

Jonathon R. Snelling

August 2012

# Summary

Since its inception at the beginning of the twentieth century, the field of mass spectrometry has progressed from the realm of physics to an analytical tool that can be found in many fields of science. This is in large part due to continued development and innovation in instrument design.

This thesis explores two significant areas of development in mass spectrometry in the last ten years. The first is the development of ambient ionisation techniques. These techniques require little or no sample preparation, and as a result can provide a rapid means of direct analysis. The second development is the commercialisation of ion mobility – mass spectrometry (IM-MS). This technique enables information on the shape of the analyte of interest to be obtained in addition to its mass-to-charge ratio. The technique has the potential to simplify the spectra acquired from complex mixtures and to separate out isobaric species that cannot be resolved by mass spectrometry alone.

Both of these developments have been applied to two important areas of analytical science – the characterisation of pharmaceutical commercial products and synthetic polymer formulations.

A modification of the extractive electrospray ionisation (EESI) technique has been developed and has been termed thermally assisted – EESI (TA-EESI). TA-EESI and the atmospheric pressure solids analysis probe (ASAP) have been coupled with IM-MS.

IM-MS has been used as a rapid separation technique to resolve isomeric species within complex polysorbate formulations. Recently introduced novel polymer architectures synthesised by simple methods have been studied using IM-MS experiments.

# Abbreviations

## Two

2D Two Dimensional

## A

Å Angstrom  
ACN Acetonitrile  
AFM Atomic force microscopy  
AIBN Azobisisobutyronitrile  
APCI Atmospheric pressure chemical ionisation  
ASAP Atmospheric pressure solids analysis probe  
ATD Arrival time distribution

## C

CCS Collisional cross section  
CI Chemical ionisation  
CID Collisional induced dissociation  
CRM Charge residual model

## D

DAMS Direct analysis mass spectrometry  
DAPCI Desorption atmospheric pressure chemical ionisation  
DAPPI Desorption atmospheric pressure photo ionisation  
DART Direct analysis in real time  
DB24C8 Dibenzo 24 crown ether 8  
DBDI Dielectric barrier discharge ionisation  
DC Direct current  
DCIMS Drift cell ion mobility spectrometry  
DESI Desorption electrospray ionisation  
DHB 2,5-dihydroxybenzoic acid

DSC Differential scanning calorimetry

## **E**

EASI Easy ambient sonic spray ionisation  
ECD Electron capture dissociation  
EESI Extractive electrospray ionisation  
EI Electron impact  
ELDI Electrospray laser desorption ionisation  
ELSD Evaporative light scattering detection  
EM Electromagnetism  
ESI Electrospray ionisation  
ETD Electron transfer dissociation  
eV Electron volt

## **F**

F6P Hexafluorophosphate  
FAB Fast atom bombardment  
FAIMS Field asymmetric waveform ion mobility spectrometry  
FD-ESI Field desorption - electrospray ionisation  
FT-ICR Fourier transform - ion cyclotron resonance  
FTIR Fourier transform infrared spectroscopy

## **G**

GC Gas chromatography  
GC-MS Gas chromatography – mass spectrometry  
GPC Gel permeation chromatography

## **H**

HDMS High definition mass spectrometer  
HILIC Hydrophilic interaction chromatography  
HLB Hydrophilic - lipophilic balance

## I

IEM	Ion evaporation model
IM-MS	Ion mobility - mass spectrometry
IMS	Ion mobility spectrometry

## L

LAESI	Laser ablation electrospray ionisation
LC	Liquid chromatography
LC-MS	Liquid chromatography - mass spectrometry
LESA	Liquid extraction surface analysis
LiCl	Lithium chloride
LM	Light microscopy
LMJ-SSP/ESI	Liquid micro-junction surface sampling probe/electrospray ionisation

## M

$m/z$	Mass to charge ratio
$M^+$	Molecular ion
MALDI	Matrix assisted laser desorption ionisation
MCP	Multichannel plate
MeOH	Methanol
$M_n$	Number average molecular weight
MS	Mass spectrometry
MS/MS	Tandem mass spectrometry
$M_w$	Weight average molecular weight

## N

ND-EESI	Neutral desorption - extractive electrospray ionisation
NIST	National Institute for Science and Technology
NMR	Nuclear magnetic resonance

## O

O/W	Oil in water
oa-ToF	orthogonal acceleration - Time of flight

## P

PADI	Plasma assisted desorption ionisation
PCA	Principal components analysis
PDE-5	Phosphodiesterase type-5
PDI	Polydispersity index
PDPA	Phase doppler particle analysis
PE	Polyethylene
PEG	Polyethylene glycol
PET	Polyethylene terephthalate
pH	Potential hydrogen
PhD	Doctor of Philosophy
PP	Polypropylene
PSI	Paper spray ionisation

## Q

QQQ	Triple quadrupole mass spectrometer
Q-ToF	Quadrupole - Time of flight

## R

RF	Radiofrequency
----	----------------

## S

S/N	Signal to noise ratio
SEM	Scanning electron microscope
SESI	Secondary electrospray ionisation
SIMS	Secondary ion mass spectrometry

SOA	Secondary organic aerosol
SRIG	Stack ring ion guide
SRM	Selected reaction monitoring

## **T**

TA-EESI	Thermally assisted - extractive electrospray ionisation
TAP	Time aligned parallel fragmentation
TEM	Transmission electron microscope
TLC	Thin layer chromatography
ToF	Time of flight
T-WAVE	Travelling wave
TWIG	Travelling wave ion guide
TWIM-MS	Travelling wave ion mobility - mass spectrometry
TWIMS	Travelling wave ion mobility spectrometry

## **U**

UCSB	University of California, Santa Barbara
UV	Ultraviolet

## **W**

W/O	Water in Oil
-----	--------------

## **X**

XPS	X-ray photoelectron spectroscopy
-----	----------------------------------

## **Z**

ZEKE-PFI	Zero electron kinetic energy – pulsed field ionisation spectroscopy
----------	---

# **Chapter 1 – Mass Spectrometry Introduction**



## 1.1 Birth of Mass Spectrometry

The development of mass spectrometry begins in the 19<sup>th</sup> century, with experiments on electrical discharges in gases within a vacuum (Svec 1985). In 1869, Hittorf discovered cathode rays, which are beams emitted from a cathode within a vacuum tube (Hittorf 1869). Further research by Goldstein on these beams led to the discovery of canal/anode rays (Goldstein 1876). J. J. Thomson was fundamental in the thorough understanding of the nature of these beams. Building upon the research of Perrin, who demonstrated that cathode rays consisted of negatively charged carriers and could be deflected by a magnetic field (Perrin 1895), Thomson determined the mass-to-charge ratios ( $m/z$ ) of these carriers at 1/1800 the mass relative to hydrogen (Thomson 1897). This was performed by sending parallel streams of beams through magnetic and electric fields.

While Thomson was discovering the electron, Wien showed that canal rays deflected in an opposite direction from cathode rays when a magnetic field was applied, and established these carried a positive charge (Wien 1898). After winning the Nobel Prize for the discovery of the electron, Thomson shifted his attention to canal rays, or positive rays of electricity as he termed them. He discovered they were composed of ions of different masses. When a photographic plate was placed in front of the beam, it recorded parabolic streaks characteristic of ions of a specific ( $m/z$ ) (Thomson 1911). Thomson's parabolic spectrograph enabled the discovery of isotopes of Neon-20 and Neon-22, each with a characteristic parabolic trajectory. This crude instrument can be considered the first mass spectrometer.

Francis Aston, a student of Thomson, developed an instrument with velocity focusing, improving mass accuracy and resolving power, allowing him to discover over 200 naturally occurring isotopes (Aston 1920).

Over the last 100 years, mass spectrometry has evolved from a tool for physicists into one of the most powerful techniques for chemical identification and characterisation. Scientific fields as diverse as geochronology to proteomics all benefit from its unrivalled sensitivity, selectivity, dynamic range and speed.

## 1.2 Basics of Mass Spectrometry

Mass spectrometry is based upon the motion of a gas phase ion in an electrical and/or magnetic field. The motion is dependent on the mass-to-charge ratio of the ion. If the number of charges on the ion is known, then the mass of the ion and a subsequent identification may be made. Figure 1.1 shows the essential components in a modern mass spectrometer. The first stage introduces the sample to the mass spectrometer, resulting in the generation of gas phase ions of analytes found within the sample. Ions formed then pass into a mass analyser, where these are resolved according to their  $m/z$ . An ion detector measures and amplifies the ion current of mass-resolved ions and a computer system records the resulting data, presenting it in a user-friendly format. Variations in each of the components of the instrument give rise to a wide variety of mass spectrometer, suitable for different applications.

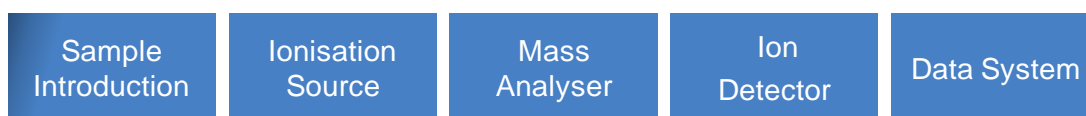


Figure 1.1 - Schematic of a mass spectrometer.

## 1.3 Established Ionisation techniques

For many samples, transferring an analyte into the gas phase in the form of an ion presents the biggest challenge, rather than the analysis itself. Developments in ionisation have expanded the application range of mass spectrometry, to most areas of science. The first major development in ionisation was the introduction of electron ionisation (EI) by Dempster in 1918, a method still used today (Dempster 1918).

In EI a beam of electrons is emitted from a heated filament and accelerated toward an anode. These electrons bombard the gas phase sample introduced into the source, resulting in the formation of a molecular ion ( $M^+$ ). The kinetic energy imparted to an electron, and the chemistry of the analyte can determine the ionisation efficiency. A broad maximum ionisation efficiency is achieved with an electric potential of 70 electron volts (eV). Approximately 2 eV is transferred to the molecular ion resulting

in high internal energy, and thus extensive fragmentation. This fragmentation is reproducible, and structurally diagnostic, properties that make it useful to generate libraries of spectra. Sample identification can then be made by comparing the spectrum generated from an unknown with a spectral database.

Extensive fragmentation is not always desirable, however, as little or no molecular ion may remain. Chemical ionisation (CI), which was introduced by Munson and Field in the mid 1960s (Munson and Field 1966), improves upon EI, in that the beam of electrons interacts with a reagent gas such as methane. A neutral analyte then collides with reagent gas ions previously formed. Proton transfer is the predominant ionisation mechanism. Figure 1.2 shows one simple path of proton transfer, with methane as the reagent. Proton transfer is a lower energy process compared to the hard ionisation mechanism found in EI, and so the analyte ion possesses less residual energy, and fragmentation is reduced, resulting in a higher amount of intact molecular ion. CI still requires samples to be thermally stable, as vapourisation into the gas phase is by heating, and thus is limited to relatively small non-polar molecules. EI and CI give complementary information, and a number of sources have been developed that allow the user to perform both.

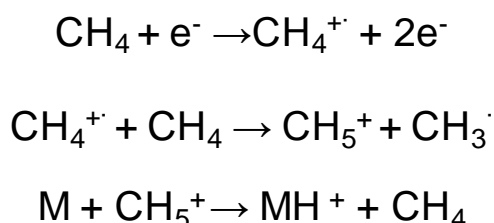


**Figure 1.2** - Common ion formation reaction during methane CI.

Introduced in 1974, atmospheric pressure CI (APCI) was one of the first techniques where ion formation takes place outside of a vacuum (Horning, Carroll et al. 1974). This method enables ionisation of volatile and semi-volatile compounds from solution, although is limited up to 1,500 Daltons (Da). In APCI, the sample solution is nebulised in a capillary, desolvated, before interacting with a corona discharge. The discharge ionises a reagent gas (often nitrogen), which then collide with

vapourised solvent molecules to form secondary reactant ions such as hydronium ( $\text{H}_3\text{O}^+$ ). These then ionise the neutral analyte, predominately by proton transfer mechanisms.

By the 1980s EI was the main method of ionisation, although numerous others including those not described were used. However, most were only sufficient to analyse small organic molecules that vapourised well. Major difficulties were encountered with getting large molecules into the gas phase as ions, and even when they did, would fragment and decompose extensively. Non volatile small molecules were also difficult to analyse. The introduction of fast atom bombardment (FAB), enabled for the first time non-derivitised polar molecules up to 5000 Da to be analysed. During FAB analysis, the sample is dissolved into a non-volatile liquid matrix such as glycerol and then bombarded by inert high energy atoms such as argon or xenon. This technique was beset by problems such as matrix associated chemical noise masking the signal of sample ions and the fact that relatively high concentration samples were needed. This technique did however start a renewed interest in ionisation techniques, culminating with the introduction of two revolutionary methods, matrix assisted laser desorption ionisation (MALDI) and electrospray ionisation (ESI).

### **1.3.1 Matrix Assisted Laser Desorption Ionisation (MALDI)**

MALDI, which is a pulsed rather than a continuous ionisation technique, allows for the production of intact gas-phase ions of large, non-volatile and thermally labile compounds. Developed in the 1980's by Karas and Hillenkamp (Karas and Hillenkamp 1988), there are similarities with another laser desorption method no longer routinely used, developed by Tanaka (Tanaka, Waki et al. 1988) who controversially won the Nobel Prize in 2002.

In the MALDI, method the sample is dissolved in a solution that is saturated with an organic matrix. The sample/matrix solution is then co-crystallised on a specially designed MALDI sample plate. Subsequent to this, within a vacuum, a short pulsed laser beam is fired at the sample-matrix crystal. Upon absorption of the laser energy, the crystalline structure of the matrix breaks down, to generate into a super-

compressed gas composed of ionised and neutral molecules. Although the mechanism of ionisation is not fully understood, the most accepted theory involves charge transfer reactions from matrix to analyte within this plume, including proton transfer, with the majority of ions formed singly charged. When synthetic polymers are analysed, transition and alkali metal salts may be included in the matrix solution, to promote cationisation by metal ion transfer. The proposed mechanism is shown in Figure 1.3.

The choice of matrix for MALDI analysis is critical, and can be dependent on the properties of the sample being analysed. While co-crystallised the matrix must isolate analyte molecules from one another to prevent sample cluster formation. The matrix employed must have a high molar absorptivity at the wavelength emitted by the laser used. The matrix absorbs the majority of the energy from the laser, thus minimising fragmentation of the analyte, but at the same time increases the efficiency of energy transfer from the laser to the analyte, thus maximising sensitivity. Due to the low cost, nitrogen lasers with wavelength of 337 nm are commonly used.

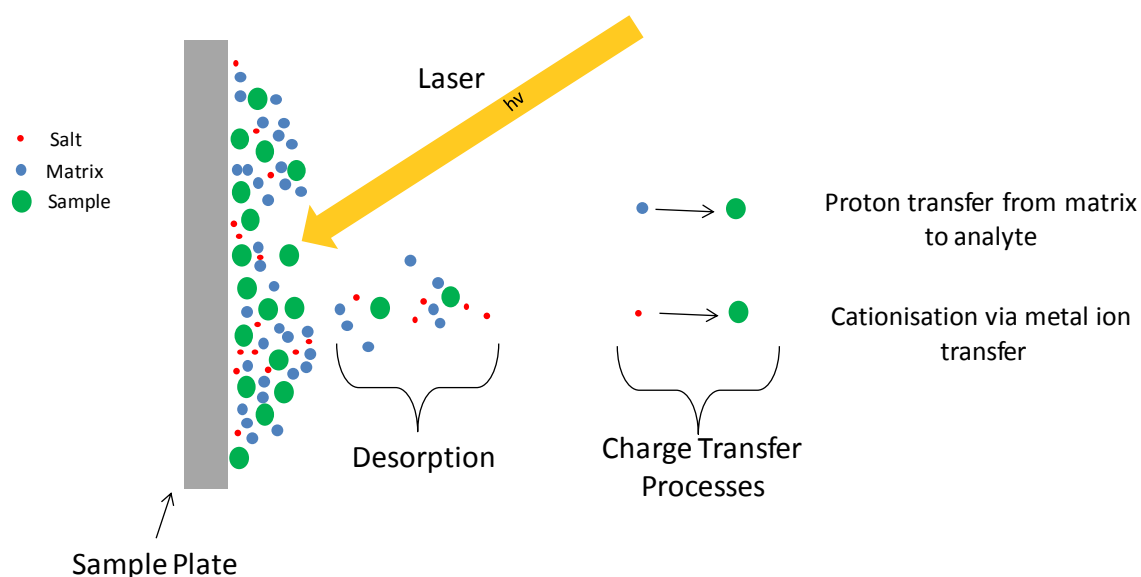


**Figure 1.3** - Schematic of MALDI ionisation process.

### 1.3.2 Electrospray Ionisation (ESI)

Concurrent with the introduction of MALDI, was the development of electrospray ionisation (ESI), which in contrast to the pulsed nature of MALDI is a continuous ionisation process. ESI is based on droplet production in the presence of a strong electric field.

Studies of electrospray had been commenced in the mid 18<sup>th</sup> century, when scientists such as Nollet observed the physical properties of liquids in glass capillaries to which an electrical potential had been applied (Nollet 1749). The use of electrospray for the application of paint to various surfaces caught the attention of Malcolm Dole in the 1960's. Dole and his co-workers were interested in determining the molecular mass of synthetic polymers, and thus required an ionisation technique that would enable the transfer of non volatile polymers into the gas-phase, with no degradation. Some limited success was observed by electrospraying benzene-acetone solutions of high-molecular weight polystyrene (Dole, Mack et al. 1968). Further studies were not vigorously pursued until the 1980's when the group of John Fenn demonstrated that ESI-MS could be used for the analysis of high molecular weight biomolecules (Yamashita and Fenn 1984).

In the ESI technique, the sample is dissolved into an aqueous solution containing suitable concentrations of volatile organic solvents such as methanol (MeOH) or acetonitrile (MeCN). When the instrument is operated in positive mode, an acid such as formic or acetic acid is also included to aid in the protonation of the analyte. The solvent composition is dependent on the properties of the sample. The sample solution is then sprayed through a capillary held at a high electrical potential in comparison to the counter-electrode at the entrance of the mass spectrometer. This electric field leads to the separation of positive and negative ions at the meniscus, formed at the tip of the capillary. In positive mode, positive ions accumulate at the surface of the meniscus forming a Taylor cone (Taylor 1964). The Taylor cone reduces the charge-to-surface ratio of the meniscus. A fine jet is created from the cone, when the repulsive force between the positive charges overcomes surface tension. A nebulising gas such as nitrogen, aids in the generation of a plume of highly charged droplets from the jet. There are two proposed mechanisms for the

generation of gas-phase ions from the highly charged droplets, the charge residue model (CRM) and the ion evaporation model (IEM).

With the CRM mechanism as proposed by Dole (Dole, Mack et al. 1968), the droplet size decreases due to solvent evaporation, and this results in an increase of the charge density at the surface of the droplet. A coulombic explosion occurs at the Rayleigh Limit, a critical point at which the cohesive forces of surface tension is less than the electrostatic repulsive forces of the ions present in the droplet. The coulombic explosion results in progeny droplets of smaller diameter. This cyclic process of solvent evaporation and fission by coulombic explosion continues until a single protonated analyte ion, free of solvent (and thus in the gas-phase) is produced. The ion produced may singly or multiply charged.

IEM as proposed by Iribarne and Thomson (Iribarne and Thomson 1976), is as the CRM mechanism in the initial stages, with solvent evaporation followed by coulombic explosion and progeny droplet formation. The cycle continues until droplets of a certain size are produced. At this point, direct ion emission from the droplets into the gas-phase will occur. Both proposed mechanisms are shown in Figure 1.4. It is believed that ions with a smaller  $m/z$  ratio will preferentially form via the IEM method, while for ions of a higher  $m/z$  ratio CRM is the dominant mechanism (Kearle 2000).

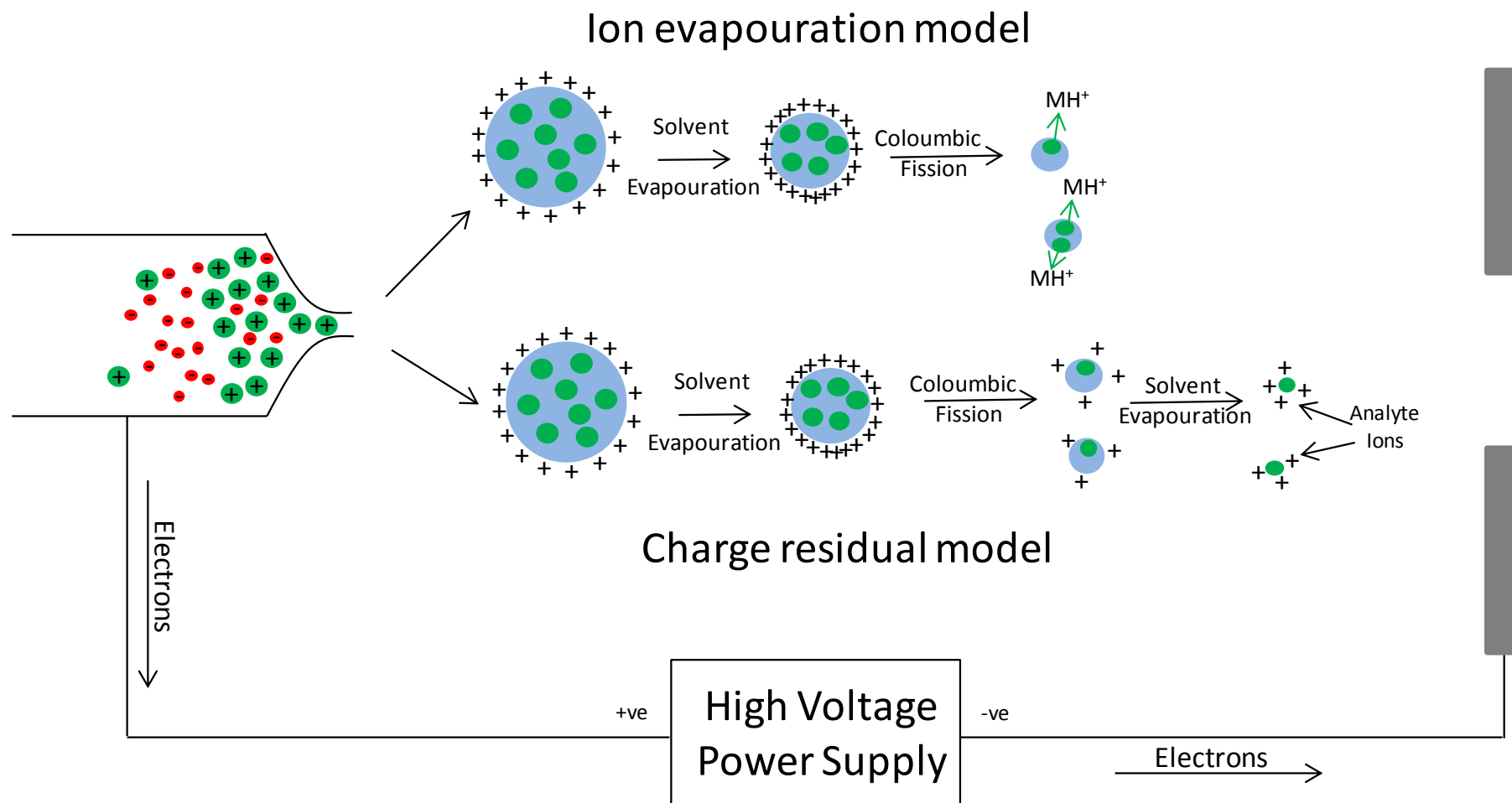


**Figure 1.4** - Schematic showing two proposed ESI mechanisms – Adapted from Kerbale (2000).



## 1.4 Established Mass Analysers

The mass analyser is the region of the mass spectrometer where gas phase ions produced in the ion source are separated according to their mass-to-charge ratio ( $m/z$ ). Common mass analysers used include scanning mass analysers such as quadrupole mass filters and magnetic sectors, which transmit ions of different  $m/z$  incrementally over a period of time. Mass analysers including time-of-flight (ToF), Fourier transform ion cyclotron resonance (FT-ICR), orbitrap and ion traps can almost simultaneously transmit all ions generated from a sample. Important characteristics of a mass analyser include accuracy, resolving power,  $m/z$  range, dynamic range, scan speed, transmission efficiency, operating pressure and cost.

Research presented in this thesis was performed utilising hybrid instruments that included a quadrupole mass filter and a ToF mass analyser, and these are discussed in detail here.

### 1.4.1 Quadrupole Mass Filter

The principle of the quadrupole mass filter was first described in 1953 (Paul 1953), and is based on the stability of an ions trajectory in an oscillating electric field. A quadrupole consists of four metal hyperbolic or circular rods that must be parallel (Figure 1.5). Opposite pairs of rods are connected electrically, and a direct current (DC) and alternating radio frequency (RF) voltages are applied. The amplitude of the voltage is the same for both pairs of rods, but differs in polarity (i.e. one set negative, the other positive). Gas-phase ions produced in the ion source travel through the centre of the quadrupole. Only ions with a specific  $m/z$  (and thus resonant frequency), will have a stable oscillating trajectory for a given ratio of voltages, and will then reach the detector. All other ions will have unstable trajectories, and will collide with the rods or wall of the analyser. A mass spectrum is obtained by varying the applied voltages, to allow other ions to have stable trajectories. If the rods have a suitable RF voltage applied and no direct current applied, then all ions above a certain  $m/z$  will have stable trajectories. This is often the case in hybrid quadrupole-time of flight (Q-ToF) instruments, where the quadrupole is often used for ion beam focussing, and can improve transmission efficiency.

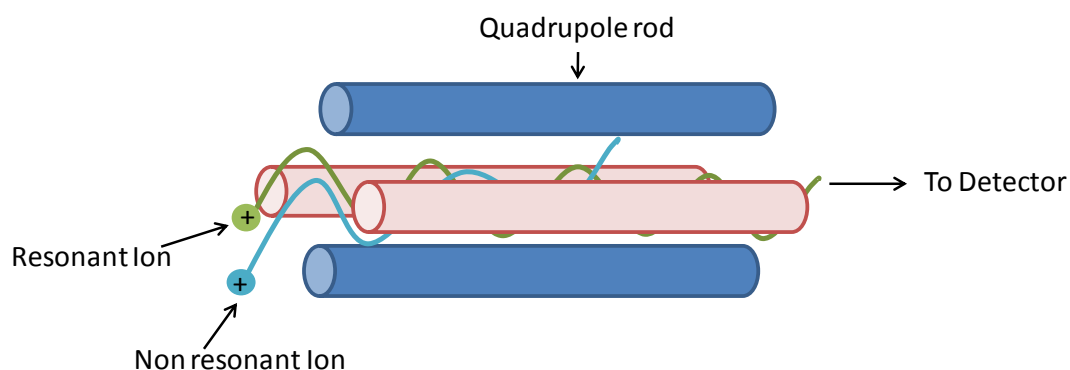


**Figure 1.5** - Schematic of a quadrupole mass filter. An ion with a stable trajectory (green) will reach the detector, while the ion with an unstable trajectory (blue) will not.

### 1.4.2 Time of Flight Mass Analyser

The concept of the time of flight (ToF) mass analyser was first discussed in 1946 at the American Physical Society in Cambridge (Stephens 1946). The first commercial linear ToF instrument was based on work published in 1955 (Wiley 1955). The ToF mass analyser allows almost simultaneous transmission of all ions generated from a sample. Measurement of the  $m/z$  of an ion is based on the time it takes to traverse a field free flight tube under vacuum conditions. ToF is a pulsed technique, requiring ions to be produced in packets, and so is well matched with MALDI. When ions are formed, they are accelerated into the ToF analyser by a potential ( $V$ ) applied between an electrode and extraction grid, which gives all ions the same amount of kinetic energy ( $E_k$ ). Ions possessing the same  $E_k$  but different mass ( $m$ ) will have different velocities ( $v$ ). Overall, the time taken for an ion to traverse the field free flight tube is inversely proportional to the square root of its mass.

The velocity ( $v$ ) of an ion with a mass ( $m$ ) and total charge ( $ze$ ) can be determined using Equation 1.1, where  $E_k$  is kinetic energy, and  $V$  the accelerating potential.

$$v = \frac{\sqrt{2E_k}}{m} = \frac{\sqrt{2zeV}}{m}$$

Equation 1.1

The time ( $t$ ) taken for an ion to fly through the flight tube of a fixed length ( $d$ ) is inversely proportional to  $v$ .

$$t = \frac{d}{v}$$

Equation 1.2

Given that  $v$  is constant and  $V$  and  $d$  are known:

$$t = \sqrt{\frac{m}{z}} \times \text{constant}$$

Equation 1.3

Smaller ions will have faster velocities than those ions with a larger  $m/z$ . The ToF analyser potentially has no upper limit in  $m/z$  range, and compared with a quadrupole has higher transmission efficiency and thus is more sensitive. A problem with the linear ToF is resolution. When ions of the same  $m/z$  are created, the initial spatial distribution means that those ions closest to the extraction grid will leave first but with slower velocities, while ions furthest from the extraction grid, leaving later will have higher velocities, and at the primary focal point will overtake the slower ions. This variation in ion velocity is termed the kinetic energy distribution, resulting in ions of the same  $m/z$  reaching the detector at slightly different times resulting in broad ion peaks, and so poor resolution.

Resolution can be improved by delayed pulsed extraction and by use of a reflectron, which is found in most modern instruments. In delayed pulsed extraction, those ions of the same  $m/z$  but with more energy will be closer to the detector than those with less energy after the primary focal point. An extraction pulse is applied after a time delay, and transmits more energy to those lower energy ions, which minimises the energy differences between ions of the same  $m/z$ , reducing peak width.

The reflectron is an electrostatic lens positioned at the end of the flight tube, and decreases the time difference at which ions of the same  $m/z$ , but differing kinetic energies reach the detector (Karataev 1972). Ions with higher kinetic energies and thus faster velocities penetrate the reflectron more deeply than those with lower

kinetic energy. The higher velocity ions will spend more time in the reflectron, and so will reach the detector at the same time as ions of the same  $m/z$  but lower initial kinetic energy. The reflectron effectively doubles the flight tube (Figure 1.6), and in theory, the longer the flight tube the better the resolution. As such the reflectron also enables improved separation of ions of different  $m/z$ .

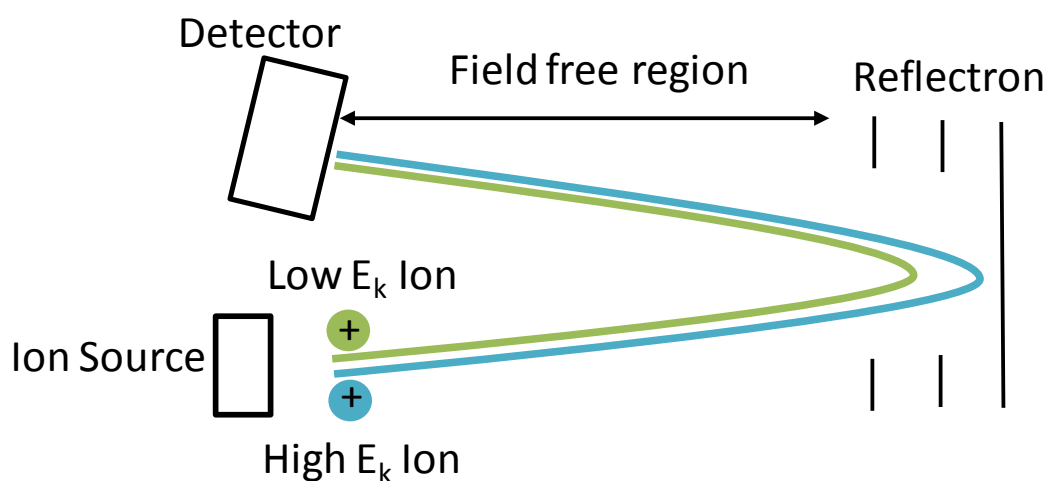


**Figure 1.6** - Schematic of Reflectron-ToF instrument. Both ions are the same  $m/z$  but have different initial kinetic energies.

Due to the pulsed nature of the ToF mass analyser, if a continuous ionisation source such as ESI is to be employed without compromising resolution then orthogonal acceleration ToF (oa-ToF) is required (Guilhas 2000). In an oa-ToF, a continuous (or pulsed) parallel ion beam of low kinetic energy enters an orthogonal accelerator. Here, a package of ions is pushed orthogonally from the original direction of the beam by a voltage pulse into the ToF analyser.

## 1.5 Tandem Mass Spectrometry

The development of softer ionisation techniques allowed for the analysis of analytes of increasing mass and/or involatility. Compared with EI, which generates fragment ion peaks, the softer ionisation techniques generate predominately quasi-molecular ions or adduct ions, which are useful for determining the molecular weight, but structurally informative fragments are required in mass spectrometry for determination of molecular structure. Tandem mass spectrometry (MS/MS) addresses this disadvantage of soft ionisation techniques.

MS/MS requires at least two steps of  $m/z$  analysis, and there are two basic instrumental concepts 1) tandem-in-space and 2) tandem-in-time. Tandem-in-space refers to those instruments with spatially separated mass analysers, with common examples including quadrupole-time of flight (Q-ToF) instruments, and triple quadrupole (QQQ) instruments. The first mass analyser is used to select an ion of a specific  $m/z$ , which passes into an intermediate region for dissociation into structurally useful fragments. The second mass analyser passes fragments generated to the detector to record a mass spectrum. Tandem-in-time refers to those instruments with a single mass analyser that is capable of trapping ions, fragmenting them, and subsequently characterising them, examples include FTICR and ion trap instruments. Tandem-in-time experiments can have an indeterminate number of stages ( $MS^n$ ), where fragments generated, can be selected for further fragmentation for additional structural information.

MS/MS experiments performed during the course of this research was by means of collision-induced dissociation (CID), which was introduced by Jennings in the late 1960s (Jennings 1968). In CID, an ion is passed through a collision cell containing inert gas molecules at a pressure higher than that of the surrounding vacuum. Translational energy from interactions between collision gas molecules and ions is converted into internal energy within the precursor ion. Further collisions increase the internal energy, eventually resulting in fragmentation, and generation of product ions. Other methods of ion fragmentation include among others, electron capture dissociation (ECD) (Zubarev, Kelleher et al. 1998), which is limited to FT-ICR instruments and electron transfer dissociation (ETD) (Syka, Coon et al. 2004).

There are four major types of MS/MS analysis that can be performed with CID: -

1. Product ion scan – A precursor ion of a specific  $m/z$  is selected in the first mass analysis step, and is fragmented in the collision cell. The second mass analyser scans for all product ions formed. This is the only type of scan available with a Q-ToF
2. Precursor ion scan – The first mass analyser scans for all precursor ions that fragment to give a specific product ion, which has been selected in the second mass analyser.
3. Neutral Loss Scan – This screens for ions that undergo a common loss. Both mass analysers scan, with the second analyser offset to a neutral loss that is expected.
4. Selected reaction monitoring (SRM) – Both the first and second mass analyser are set to a specific  $m/z$ , so that a specific precursor ion has to fragment to a specific product ion to be detected. This is a common experiment on QQQs, and is useful for quantitation.

## 1.6 Ion Detection

Ions separated by mass analysis are recorded by means of an ion detector. Since the initial photographic plate, more sophisticated ways of detection have developed, and can be divided into two categories: -

1. Direct measurement of charge detectors
2. Multiplier detectors

While direct measurement detectors such as the Faraday cup are well matched for quantitative analysis of isotope intensity, they suffer from poor sensitivity. The electron multiplier (EM) is widely employed as a detector, and is simple to understand. A gas-phase ion of positive or negative charge collides with a conversion dynode resulting in emission of secondary electrons. These secondary electrons are accelerated toward the next dynode where each electron generates more secondary electrons, and this cycle continues until the final electrode is reached. An electric current is generated, and passed through to a resistor to generate a voltage that is amplified and transferred to a detection system. Amplification of up to  $10^8$  of the original signal is possible.

An array detector, such as the micro channel plate (MCP), consists of a large number of mini electron multiplier channels assembled on a flat plate. These can detect and amplify several different ions simultaneously, and are thus more sensitive. If samples are too concentrated, then saturation of the MCP may occur. When saturation occurs, the MCP will not be able to detect smaller signals that occur immediately after a large signal. Ionisation methods that generate hundreds or thousands of ions simultaneously benefit from array detectors.

## 1.7 Evaluating capabilities of novel mass spectrometry techniques

Historically, the application range of mass spectrometry has been extended due to developments in instrument design. For instance before the development of ionisation techniques such as ESI or MALDI, the analysis of samples of a biological nature was challenging, if at all possible. Developments in mass analyser have enabled higher resolution spectra to be obtained, allowing the base line separation of ions of different  $m/z$  ratios. This is very important as there can be thousands of different species within a specific  $m/z$  range. Developments in mass analyser have also led to improvements in a number of other areas of analytical importance, including accuracy, sensitivity, dynamic range and  $m/z$  range. These developments have resulted in mass spectrometry becoming an ubiquitous analytical tool in laboratories with different application requirements both in academia and in industry.

Potential and existing applications of mass spectrometry may benefit from further developments in instrument design. Within the last ten years, there have been three major instrumentation developments in the field of mass spectrometry. This includes the introduction of a field of mass spectrometry termed ambient ionisation (Cooks 2006), the commercialisation of ion mobility-mass spectrometry (IM-MS) (Pringle 2007) and the commercialisation of a novel type of mass analyser, known as the Orbitrap (Makarov, Denisov et al. 2006). The analytical capabilities of these new areas of mass spectrometry have not been fully explored. The research presented in this thesis explores some of the capabilities of IM-MS and ambient ionisation.

Often in industry, such as in the pharmaceutical sector, high throughput and automated analyses are desired, but this can be challenging if substantial sample preparation is required. Ionisation techniques that do not require any sample preparation have the potential to speed up the analysis time, potentially permitting rapid high throughput analyses. These ambient ionisation techniques may also be able to produce gas-phase ions of samples where the use of established ionisation techniques is not feasible. Analytical techniques are often required to produce crucial information outside of the laboratory, such as in airports where rapid techniques that would allow for the direct analysis of passengers clothing, luggage or skin, without



the need for sample preparation. Section 1.8 provides a more detailed explanation of the field of ambient ionisation and those techniques that were used during the course of the research presented within this thesis.

Ion mobility spectrometry (IMS) is a gas-phase electrophoresis technique, which when combined with MS has the potential to form a powerful analytical technique. Ion mobility can allow for shape selective experiments to be performed, which can result in the separation of species with identical  $m/z$  ratios but different conformations. This separation is not achievable with high resolution mass spectrometry, and may not be achieved by conventional chromatographic techniques. IM-MS has the potential to impact a wide range of applications ranging from the life sciences to the chemical industry. The shape of biological molecules is closely related to the biological processes that they are involved in, and IM-MS can provide data comparable to more established methods such as X-Ray crystallography (Scarff 2008). The characterisation of complex formulations which may be composed of isomeric species is a requirement of the polymer industry. Established separation techniques such as liquid chromatography (LC) or gel permeation chromatography (GPC) may not fully resolve species present, and may benefit from the inclusion of mobility separation. A number of polymer species ionise favourably with MALDI, but online coupling of conventional separation techniques to MALDI is not possible, adding to the timescale and complexity of the analysis. Mobility separation is a post ionisation event and is suited to MALDI ionisation. IM-MS also has potential to provide more information on the ionisation mechanism, and to provide an additional method for determining site of ionisation on a molecule. Section 1.9 explains IM-MS in more detail.

## 1.8 Ambient Ionisation Techniques

The successful ionisation of a sample molecule into the gaseous phase is one of the major limitations of MS. The development of the ESI and MALDI ionisation techniques partially solved this problem, especially for large biomolecules and smaller molecules with polar properties. These techniques often require extensive sample preparation step, before the sample can be dissolved in an appropriate solvent (ESI) or mixed with a suitable matrix (MALDI). This sample preparation can be time-consuming, and can impede those applications that require high-throughput analyses. Sample preparation may introduce chemical interference that can affect the accuracy of the MS analysis.

Ambient ionisation or direct analysis mass spectrometry (DAMS) refers to those ionisation techniques that require little or no sample preparation, such as preconcentration, extraction, derivitisation, dissolution or chromatographic separation. These techniques allow for direct analysis of untreated samples, often in the open environment, allowing for unimpeded access to samples of any size or shape (Harris, Galhena et al. 2011; Huang, Cheng et al. 2011). This can afford a reduction in the time required the analysis.

The field of ambient ionisation has expanded to over 30 techniques since 2004, when the pioneering ambient ionisation techniques, desorption electrospray ionisation (DESI) (Takats, Wiseman et al. 2004) and direct analysis in real time (DART) (Cody 2005) were introduced to the MS community. Table 1.1 shows a list of prominent ambient ionisation approaches that have been developed since 2004. In this thesis, the techniques are classed according to the method of ionisation. The majority of the techniques are based on ESI or APCI. The analyte will be ionised via one of two ways:-

1. The analyte molecules will be formed and brought to the source for ionisation.
2. Charged species generated by an ionisation source are brought to the sample surface for desorption and subsequent ionisation.

<b>Ionisation Method</b>	<b>Acronym</b>	<b>Underlying Mechanism</b>	<b>Pioneering Reference</b>
<b>Atmospheric pressure solids analysis probe</b>	ASAP	Corona discharge based APCI	(McEwen 2005)
<b>Desorption atmospheric pressure chemical ionisation</b>	DAPCI	Corona discharge based APCI	(Takats, Cotte-Rodriguez et al. 2005)
<b>Desorption atmospheric pressure photoionisation</b>	DAPPI	Atmospheric pressure photoionisation (APPI)	(Haapala, Pól et al. 2007)
<b>Direct analysis in real time</b>	DART	Plasma based APCI	(Cody 2005)
<b>Dielectric barrier discharge ionisation</b>	DBDI	Plasma based APCI	(Na, Zhao et al. 2007)
<b>Desorption electrospray ionisation</b>	DESI	ESI	(Takats, Wiseman et al. 2004)
<b>Easy ambient sonic spray ionisation</b>	EASI	Sonic Spray Ionisation	(Haddad 2006)
<b>Extractive electrospray ionisation</b>	EESI	ESI	(Chen 2006)
<b>Electrospray laser desorption ionisation</b>	ELDI	Laser desorption (LD) + ESI	(Shiea 2005)

<b>Laser ablation electrospray ionisation</b>	LAESI	LD + ESI	(Nemes 2007)
<b>Liquid micro-junction surface sampling probe/electrospray ionisation</b>	LMJ-SSP/ESI	ESI	(Van Berkel and Kertesz 2009)
<b>Low temperature plasma</b>	LTP	Plasma based APCI	(Harper, Charipar et al. 2008)
<b>Neutral Desorption-extractive electrospray ionisation</b>	ND-EESI	ESI	(Chen 2007)
<b>Plasma-assisted desorption ionisation</b>	PADI	Plasma based APCI	(Ratcliffe, Rutten et al. 2007)
<b>Paper spray ionisation</b>	PSI	ESI	(Wang, Liu et al. 2010)

**Table 1.1** - Summary of major ambient ionisation techniques

### **1.8.1 ESI based Ambient Ionisation Techniques**

Ambient ionisation methods that are related to ESI such as DESI (Takats, Wiseman et al. 2004) and extractive electrospray ionisation (EESI) (Chen 2006) produce mass spectra that are similar to those obtained when ESI is utilised. The sample analysed can be a gas, vapour, liquid or solid. The ESI based ambient ionisation methods described here can all be performed on conventional mass spectrometers with little modification, assuming that an ESI source is present. Here DESI and EESI are discussed.

#### **1.8.1.1 Desorption Electrospray Ionisation (DESI)**

DESI, the pioneering ambient ionisation technique, first described by the group of Graham Cooks in 2004 (Takats, Wiseman et al. 2004), is still one of the more popular ambient ionisation techniques. DESI makes use of a pneumatically assisted electrospray, which is directed onto a sample surface in ambient conditions. The spray desorbs a minute part of the sample, which is carried away by secondary droplets that are scattered off the surface. A number of suggestions for the ion formation mechanism have been made, including chemical sputtering, droplet pickup and shockwave models (Takáts 2005). Measurements of droplet size and velocity by phase doppler particle analysis (PDPA) indicated that chemical sputtering was impossible, while the shockwave model was unlikely. A major mechanism proposed was the droplet pickup mechanism (Venter, Sojka et al. 2006). Further research using PDPA and computational fluid dynamic simulations support droplet pickup otherwise known as the multi-stage momentum transfer method (Costa and Cooks 2007; Costa 2008).

The droplet pickup mechanism as shown in Figure 1.7, can be simplified as a three step process (Costa and Cooks 2007; Harris, Nyadong et al. 2008) :-

1. *Formation of thin liquid on sample surface by impacting droplets.*
2. *Extraction of solid phase analytes into the thin film.*
3. *Collisions of primary droplets with film – secondary droplets are produced taking up part of the analyte containing film.*

It is assumed that secondary droplets formed will then produce gas phase ions, through either the IEM or CRM mechanism. This is supported by the experimental measurement of the internal energy distributions of ions formed by DESI, which are found to have similar shapes and mean values to those ions that produced by ESI (Nefliu, Smith et al. 2008).

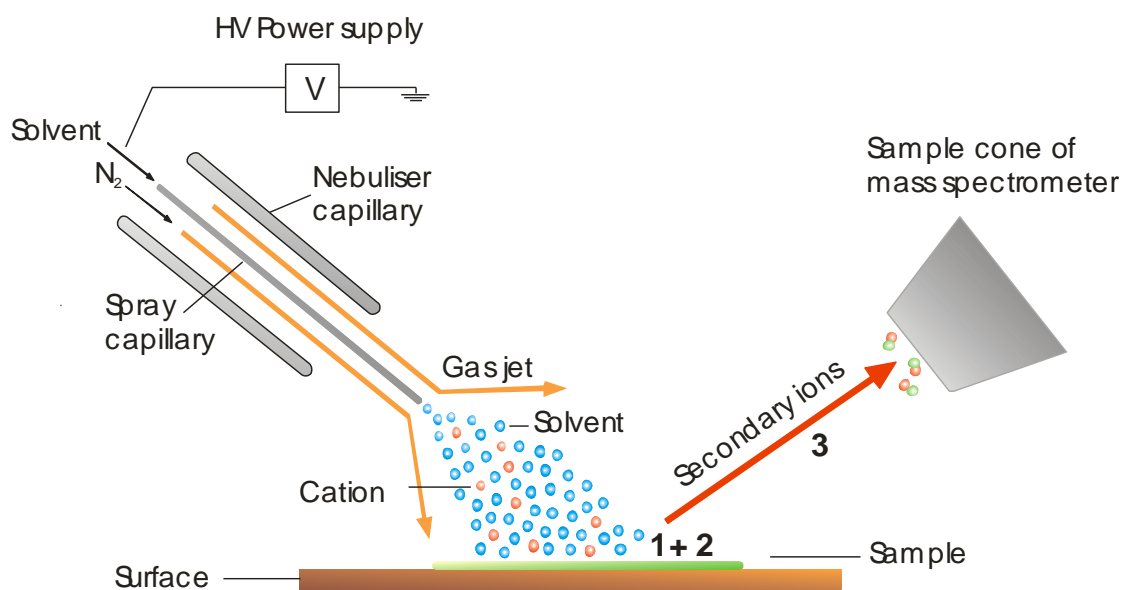


**Figure 1.7** - A schematic representation of the droplet pickup mechanism of ion formation in DESI, adapted from (Cooks 2006). 1+2 represent film formation and extraction of solid phase analytes into film. 3 represents secondary ions formed from secondary droplets.

A number of conditions affect the desorption/ionisation efficiency of DESI, including geometric conditions, such as the angle and distance of the spray relative to the sample surface, and the angle and distance between sample surface and sample cone of mass spectrometer, which can affect sensitivity. Spray conditions such as solvent and nebulising gas flow rates can determine the size and impact force of droplets onto the surface (Takáts 2005). High gas flow rates reduces the size of the droplets, improving desolvation, however once the size of the droplet becomes too small, premature evaporation may occur, decreasing ionisation efficiency (Volny, Venter et al. 2008). As with ESI, the solvent composition has to be optimised for the analyte being studied. A variant of DESI termed reactive DESI (Chen, Cotte-Rodriguez et al. 2006), dopes the DESI spray with selective chemical reagents, which increase the specificity of ionisation of particular analytes. An example of reactive DESI is for the analysis of a tissue section for cholesterol. No signal was observed with a methanol/water spray, but when betaine aldehyde was included as a reagent in the spray sample, a signal with high intensity was observed for the cholesterol derivative (Wu, Ifa et al. 2009).

The approximate number of research articles on DESI and the lower flow rate nanoDESI to March 2012 was 270 (Scifinder), and thus DESI is by far the most reported ambient ionisation technique within the literature. DESI has been successfully implements in areas such as: pharmaceutical analysis (Chen 2005; Weston, Bateman et al. 2005; Williams 2005; Williams 2006; Williams, Lock et al. 2006; Williams, Nibbering et al. 2006; Thunig, Flø et al. 2012), explosives detection (Cotte-Rodriguez, Chen et al. 2006; Sanders, Kothari et al. 2010), metabolomics (Kauppila, Talaty et al. 2007; Jackson 2008), MS imaging (Ifa 2007; Laskin, Heath et al. 2011), illicit and counterfeit drug detection (Fernández 2006; Leuthold 2006), thin layer chromatography analysis (Harry, Reynolds et al. 2009), chemical warfare agents (Paul and Claude 2010) polymers (JackSon 2006; Williams 2007) and in vivo testing (Wiseman 2005; Williams 2006; Katona, Denes et al. 2011).

### 1.8.1.2 Extractive Electrospray Ionisation (EESI)

Extractive electrospray ionisation (EESI) was initially developed for the rapid, in situ continuous, direct analysis of liquid samples. Samples are nebulised and directed into the plume of charged micro-droplets that had been produced by electrospraying an appropriate solvent (Chen 2006). It has since been extended to allow for the analysis of samples in various physical states such as vapour, aerosol, gas and solid samples. An example of the basic source setup found in the initial paper can be seen in Figure 1.8.

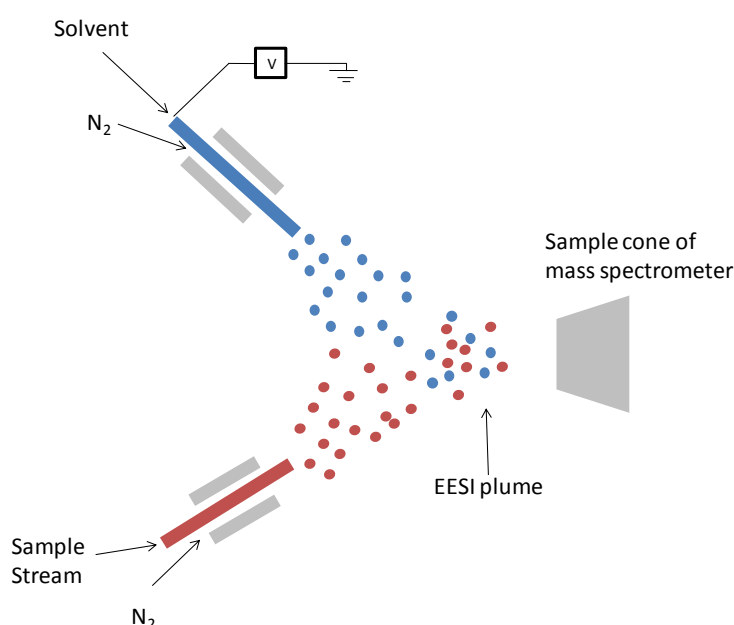


**Figure 1.8** - Schematic Diagram of the EESI setup, (adapted from (Law, Wang et al. 2010)).

There has been confusion and controversy within the literature on the similarities and differences of EESI when compared with secondary ESI (SESI) and fused droplet ESI (FD-ESI). This confusion over the similarities of techniques with different names and thus acronyms is a confusion that has been encountered with other ambient ionisation techniques. All three techniques involve a neutral sample being introduced into a charged solvent plume. SESI was introduced by the group of Hill (Wu, Siems et al. 1999) and introduces a vapour into an electrospray plume. A proponent of the SESI terminology recommends that when analytes ionised are



gases, then the technique should be termed SESI. When condensed phase samples are ionised then it is recommended the technique be referred to as EESI (Martínez-Lozano and de la Mora 2007; Martínez-Lozano, Rus et al. 2009). FD-ESI was introduced to characterise large analytes in a two-step ESI process, and is remarkably similar to the initial EESI experiment (Chang, Lee et al. 2002). For this thesis, those techniques that introduce a nebulised liquid, vapour, gas or aerosol into an electrospray plume are referred to as EESI.

There are believed to be a number of ionisation mechanisms within EESI.

- Liquid phase interaction between neutral droplet (formed from nebulised liquid or aerosol) and electrospray droplet. It is assumed that subsequent ESI like processes result in gas phase analyte ions.
- Gas phase ion-molecule reaction between neutral analyte molecule and ions generated from electrosprayed solvent droplets
- Samples that are introduced as gas phase molecules, bombard and dissolve into charged ESI droplet, and generation of gas phase ions via the IEM or CRM mechanism is believed to then occur.

Investigations into the ionisation mechanism for samples introduced in the liquid phase have included laser induced fluorescence and phase doppler anometry. These reveal that the predominant process involves liquid-liquid interactions (Law, Wang et al. 2010; Wang, Gröhn et al. 2012). This supports an earlier study that observed differences in spectra obtained when the polarity of the primary ESI spray was altered. The authors proposed that the difference in polarity of the ESI spray resulted in the extraction of different compounds of varying polarity via liquid phase interactions (Law, Chen et al. 2010).

Compared with ESI, EESI does not require sample pre-treatment and can allow for the direct analysis of samples, and thus is a much more rapid technique, allowing for higher throughput analyses.

The number of reports in the literature on EESI is noticeably smaller than that of DESI, but the application range is still quite varied. It has been observed that EESI is more tolerant of complex matrices (including salts) than ESI, the reasoning being that the neutral sample is dispersed in a relatively large space between the sample spray, electrospray and sample cone of the mass spectrometer. This, in addition to the rapid nature of EESI has been exploited for the rapid analysis of raw urine (Zhou, Jin et al. 2007).

The ability to analyse raw samples without sample pre-treatment is also suitable for other biological materials including proteins, which are often found in salty matrices, which can interfere with the performance of a mass spectrometer. EESI is very soft even when compared with ESI, as samples are isolated in time and in space from high voltages, resulting in minimal conformational changes enabling characterisation at the molecular level close to native conditions (Chen, Yang et al. 2010; Hu, Yang et al. 2011).

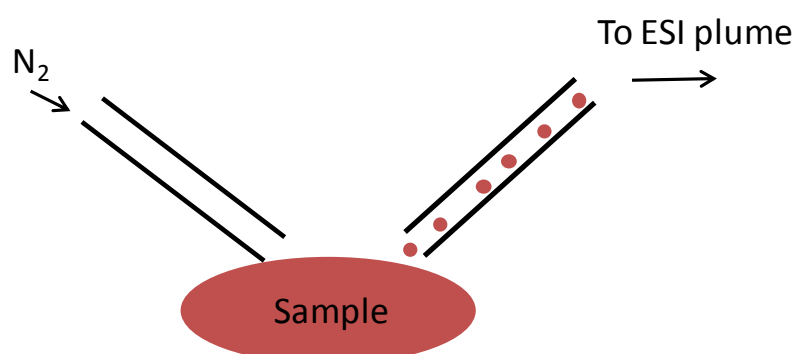
Metabolic changes within the body have been followed by in vivo profiling of the metabolites in breath by EESI sampling (Chen 2007; Ding, Yang et al. 2009; Berchtold, Meier et al. 2011). Ion molecule reactions have been observed for non-polar species in reactive EESI experiments, an example being silver adduct formation for sulphur containing compounds in breath (Chen 2007).

The in vivo analysis of sample surfaces by EESI has been facilitated by directing a neutral gas (such as nitrogen) at the surface. This results in desorption of molecules which are subsequently directed into an ESI plume. The technique is termed neutral desorption EESI (ND-EESI) (Chen 2007) and is shown in Figure 1.9A. Compared with DESI, ND-EESI is a more gentle method and does not bring charged particles to the sample, which is especially important when in vivo analysis of biological samples is required. ND-EESI has been coupled with principal components analysis (PCA) for rapid metabolomic analysis of biological surfaces including fresh and frozen meats, fish, and vegetables (Chen 2007; Chen and Zenobi 2008). Different types of cheese have also been differentiated by ND-EESI coupled to PCA (Wu, Chingin et al. 2010). ND-EESI has also been applied to the detection of explosives on skin, in a method that could be used for rapid screening at airports, and other high

risk public areas (Chen, Hu et al. 2009). A recent paper explores the analysis of secondary organic aerosols (SOA) in air (Doezema, Longin et al. 2012).

EESI and PCA have been used to differentiate the quality and maturity of different types of fruits. Fruit was placed into an airtight glass bottle, nitrogen then flowed into the bottle, and carried compounds released from the fruits upon leaving the bottle via the desolvation gas line of a conventional ESI source (Chen 2007). During the course of this PhD, all EESI experiments were performed by using a bottle in which the sample was placed. Figure 9B shows a simplified schematic. In Chapter 3 the development and evaluation of a modification of this experiment termed thermally assisted-EESI (TA-EESI) is discussed.

A



B

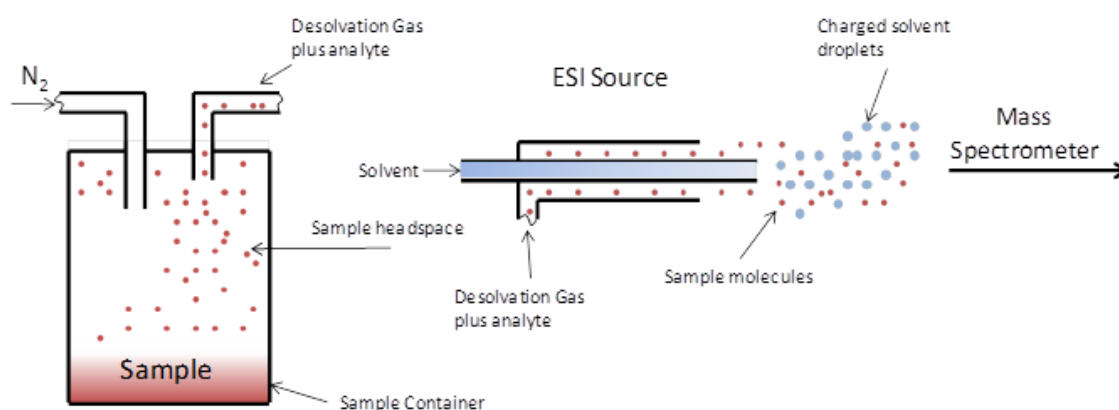


**Figure 1.9 - (A) Schematic of ND-EESI, (B) Schematic of EESI (TA-EESI is similar but with a hot plate placed below the bottle).**

## 1.8.2 APCI based Ambient Ionisation techniques

APCI based methods such as DART (Cody 2005), DAPCI (Takats, Cotte-Rodriguez et al. 2005) and ASAP (McEwen 2005), are among those ambient ionisation techniques that produce mass spectra similar to those spectra that are obtained when APCI is utilised. Here the atmospheric pressure solids analysis probe (ASAP) is discussed in detail.

### 1.8.2.1 Atmospheric pressure solids analysis probe (ASAP)

Atmospheric pressure solids analysis probe (ASAP) developed in 2005 by McEwen and co-workers (McEwen 2005) is a simple modification of an APCI source and allows for the analysis of volatile and semi-volatile analytes. The technique shares similarities with vacuum solids analysis probes, with the exception that ionisation is at atmospheric pressure. In this technique, a sample is deposited on a glass capillary probe. Sampling of solid samples simply requires the probe to wipe across a certain area. Liquid analytes can be sampled by dipping the glass probe into the containing bottle. Figure 1.10 shows a schematic of the ASAP experiment. A gas such as nitrogen whose temperature can be varied is directed at the sample holding capillary tube resulting in thermal evaporation of analyte molecules. The molecules are directed by the gas stream to an APCI needle tip, where they are ionised by a corona discharge.

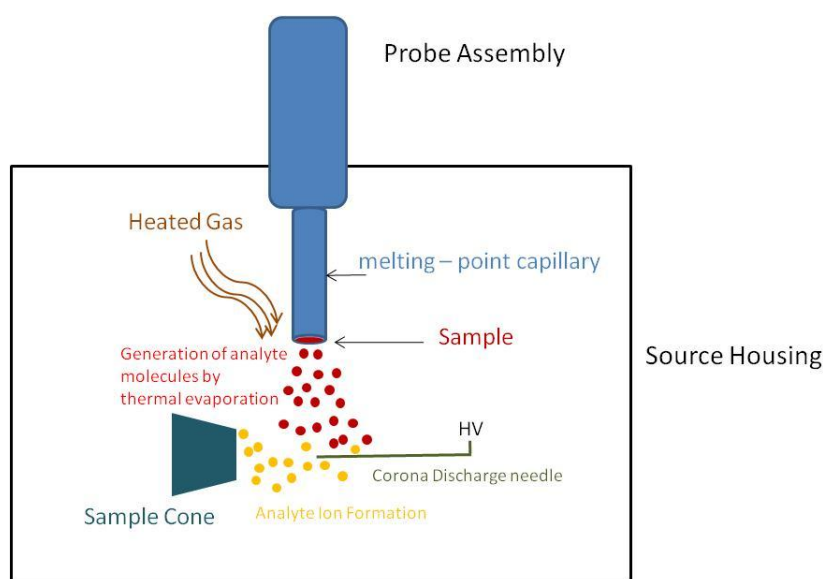
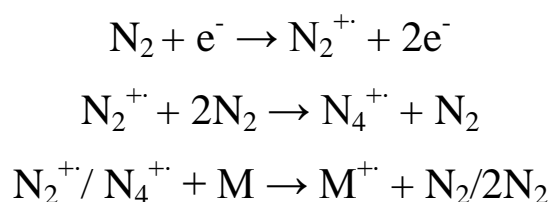


**Figure 1.10** - Schematic of ASAP, with legend.

There are two major ionisation mechanisms in ASAP. These are based on the mechanisms proposed by Horning for APCI (Horning, Carroll et al. 1974). Radical cation formation is the major ionisation mechanism when the ASAP source has been heated, and there is little water vapour present. This results in a dry atmosphere, and as such charge transfer between a nitrogen radical cation and the analyte molecule is predominant. The ASAP source commercially available from Waters, allows the user to infuse a lockspray, and can be modified to introduce water vapour into the source. In wet conditions, proton transfer from hydronium ions or water clusters resulting in protonated quasi-molecular ions is the major mechanism (as is normally seen in APCI coupled with liquid chromatography). Figure 1.11 shows the main mechanisms involved for generation of gas-phase radical cations and protonated ions.

### Formation of Radical Cation



### Formation of Protonated Ion

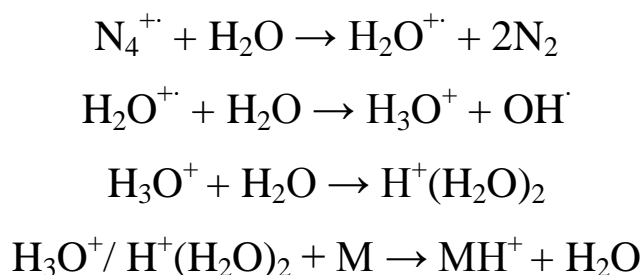


**Figure 1.11** - Main mechanisms for formation of radical cation, and protonated ion (adapted from (Horning, Carroll et al. 1974)).

The application range of ASAP is small, and in terms of reproducibility is limited to molecular weights of up to 1500 Da. Experiments utilising ASAP and other ambient ionisation techniques has enabled the identification of isobaric species based on ion fragments without prior separation (Barry and Wolff 2012). When coupled with ion mobility mass spectrometry (IM-MS), ASAP has been used to characterise structurally related compounds in crude oil. In that paper, ASAP was used to fractionate compounds according to their boiling point, and it was discovered that the addition or removal of hydrogen atoms from homologous series resulted in a discontinuous increase in collisional cross section (CCS), with increase in mass. This was attributed to addition or subtraction of a benzene ring (Ahmed, Cho et al. 2010). Steroids and the inhibition of the ergosterol pathway in fungi for production of sterol alcohols have both been investigated using ASAP-MS (McEwen and Gutteridge 2007; Ray 2010). The detection of pesticides in cereal, illegal food dyes and other contaminants by ASAP-MS was shown to have the potential to meet European union (EU) requirements for the identification of chemical contaminants in foods, but an improvement in the quantification aspects of the technique would be needed (Fussell, Chan et al. 2010). Another food application involves utilising ASAP-MS to try and understand the relationship between the flavour and compounds present in vanilla flavoured food products (Lee 2011).

ASAP has also been used to investigate counterfeit phosphodiesterase type-5 (PDE-5) inhibitors. PDE-5 inhibitors are successfully used to treat erectile dysfunction, and as such there is a large counterfeit market. In the same paper, herbal dietary supplements marketed as a natural alternative to the legitimate PDE-5 inhibitor tablets were found to contain them (Twohig, Skilton et al. 2010). Additional applications include polymer additive characterisation (Trimpin, Wijerathne et al. 2009), characterisation of SOAs (Bruns, Perraud et al. 2010) and high throughput screening of urine and bile (Twohig, Shockcor et al. 2010).

ASAP has been combined with DESI within a single ion source, that is easy to convert between, enabling rapid ionisation of polar non-volatile analytes to non-polar volatiles (Lloyd, Harron et al. 2009). The ASAP probe has also been used to introduce samples into a laserspray ionisation source (Zydel, Trimpin et al. 2010).

## **1.9 Separation Science Coupled to Mass Spectrometry**

Often, samples presented to the mass spectrometer are complex mixtures, or may include isomeric species that may not be resolved by MS on its own. Separation techniques such as gas chromatography (GC), liquid chromatography (LC) and ion mobility spectrometry (IMS) can be coupled to a mass spectrometer. Chromatography techniques separate components in mixtures as a function of their chemical and/or physical properties, with some components being retained on a column longer than others. The commercialisation of ion mobility – mass spectrometry (IM-MS) could have the potential to increase relevant data that can be extracted from a sample

### **1.9.1 Ion Mobility-Mass Spectrometry**

IMS is a gas phase electrophoretic technique that enables the separation of ions on the millisecond timescale, and is often the analytical technique of choice for the detection of explosives, drugs and chemical warfare agents (Hill, Siems et al. 1990; Creaser, Griffiths et al. 2004). A recent paper describes the use of IMS for occupational pharmaceutical exposure assessment (Armenta and Blanco 2012). The velocity at which an analyte ion migrates through a drift cell containing an inert buffer gas under the influence of an electrostatic field forms the basis of ion mobility. The velocity is based on the mobility of the ion, which is dependent on the reduced mass, charge and the collisional cross section (size and shape). Ions with different mobilities and thus velocities will reach the end of the flight tube at different time points. A thorough introductory review has been published (Kanu 2008).

### 1.9.1.1 Drift Cell Ion Mobility Spectrometry

Drift cell IMS (DCIMS) was introduced in 1970 as plasma chromatography (Cohen 1970). DCIMS is a post ionisation gas-phase separation technique that measures the time it takes an ion to migrate through a counter flowing neutral drift gas. In this instrument, ionisation by APCI mechanisms can be initiated by a  $^{63}\text{Ni}$  source which emits  $\beta$  particles. These particles ionise the drift gas, which in turn reacts with the trace amounts of water vapour present, resulting in formation of water clusters. Proton transfer from the water clusters to analyte molecules results in analyte ion formation. Common MS ionisation methods such as ESI (Wittmer, Chen et al. 1994) and MALDI (Gillig, Ruotolo et al. 2000) have also been interfaced to DCIMS instruments.

Electrodes in the drift cell provide a weak time-invariant electric field ( $E$ ,  $\text{V cm}^{-1}$ ), resulting in acceleration of ions present. Collisions with gas molecules decelerates the ions, resulting in a quasi-constant velocity ( $v_d$ ,  $\text{cm}^2 \text{s}^{-1}$ ) (Creaser, Griffiths et al. 2004).

The ion mobility ( $K$ ,  $\text{cm}^2 \text{s}^{-1} \text{V}^{-1}$ ) is the ratio of  $v_d$  to electric field strength  $E$ :

$$K = \frac{v_d}{E}$$

Equation 1.4

If the time taken to migrate through a drift cell of length  $d$  (cm) is  $t_d$  (s) then:

$$K = \frac{d}{t_d E}$$

Equation 1.5

The separation of two ions within a drift cell depends on the separation factor ( $\alpha$ ):

$$\alpha = \frac{K_1}{K_2}$$

Equation 1.6



Where  $K_1$  describes the higher mobility ion, and  $K_2$  the mobility of the slower moving ion.

To correct for standard temperature ( $T_0$  of 273.15 Kelvin) and pressure ( $P_0$  of 760 Torr), ion mobility is usually expressed as reduced mobility ( $K_0$ ):

$$K_0 = K \frac{PT_0}{TP_0} = K \frac{P \times 273}{T \times 760}$$

Equation 1.7

The reduced mobility  $K_0$  of an ion can be related to its collision cross-section by the Mason-Schamp equation (Revercomb and Mason 1975; Mason 1988):

$$K_0 = \frac{3ze}{16N_0} \times \frac{1}{\Omega} \sqrt{\left(\frac{2\pi}{\mu k_B T}\right)}$$

Equation 1.8

where  $z$  is the number of charges,  $e$  is the electronic charge  $N_0$  is the buffer gas number density at standard temperature and pressure,  $\mu$  is the reduced mass of the buffer gas and the ion,  $k_B$  is Boltzmann's constant,  $T$  is the temperature of the drift gas and  $\Omega$  the averaged collision cross section (CCS). The averaged CCS of an ion is calculated by averaging all possible collision geometries (Clemmer 1997). Currently DCIMS is the only form of IMS that allows CCS to be calculated directly from the ions drift time. Figure 1.12 shows a simplified schematic of the DCIMS experiment, and the arrival time distribution (ATD) data produced.

There are two major DCIMS modes of operation. Ambient pressure DCIMS experiments allow for the greatest separation resolution of any IMS technique, due to the increased number of ion/molecule interactions. This is the mode of operation in portable field monitoring IMS instruments. Reduced pressure DCIMS has a lower resolving power, but provides significant advantages when interfaced to mass spectrometry, including higher sensitivity. When IMS and MS are coupled the

technique is termed ion mobility-mass spectrometry (IM-MS). In the past decade, two alternative IMS methods have been introduced commercially, and incorporated into IM-MS instruments – travelling wave IMS (TWIMS) (Pringle 2007) and field asymmetric waveform IMS (FAIMS). In contrast to the pulsed nature of DCIMS and TWIMS, FAIMS can be operated with continuous introduction of ions, and is described in detail elsewhere (Guevremont 2004).

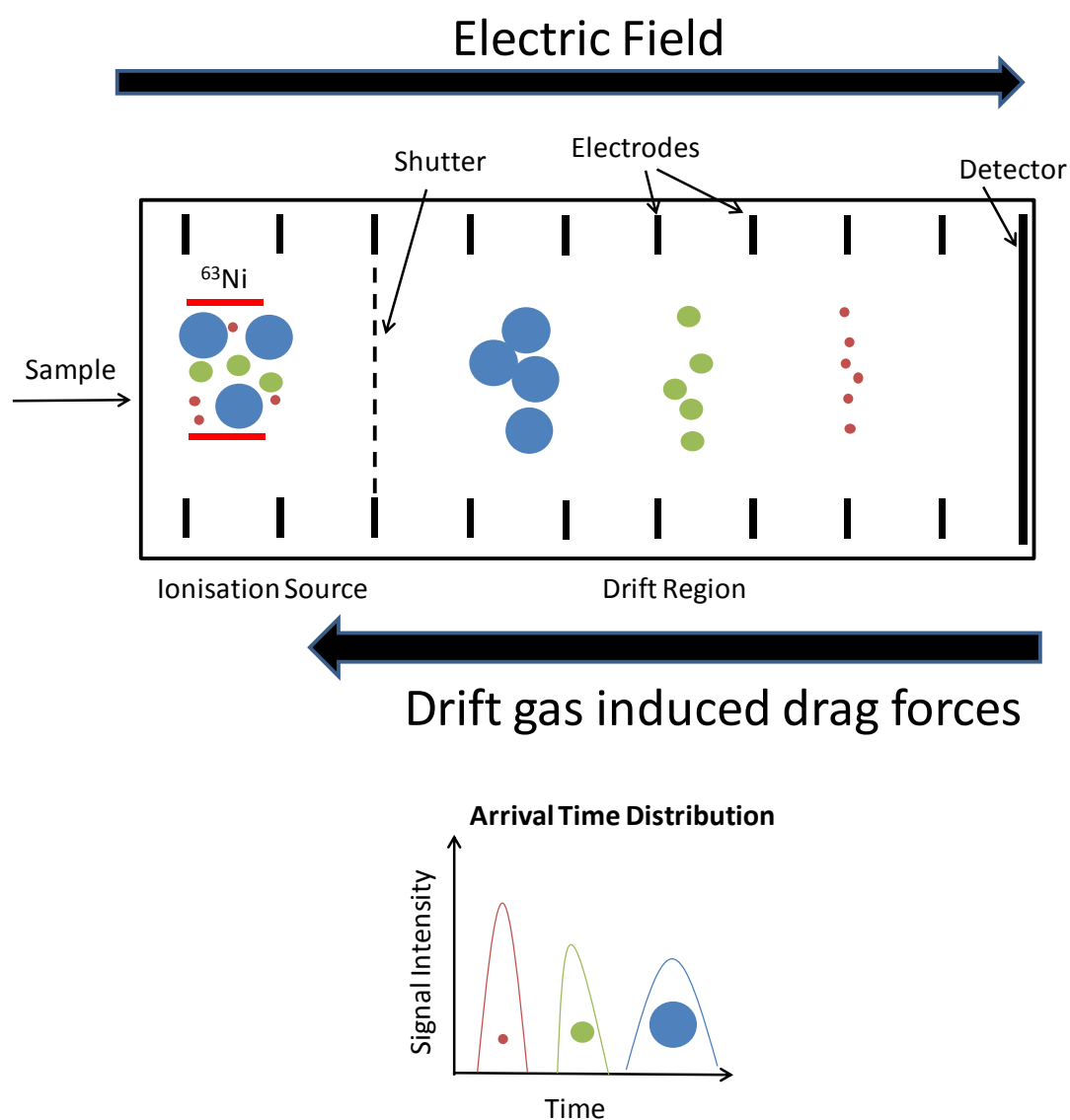


**Figure 1.12** - Schematic of DCIMS experiment, with typical ATD readout. Adapted from (Eiceman and Stone 2004).

### 1.9.1.2 Travelling Wave Ion Mobility-Mass Spectrometry (TWIMS)

In contrast to DCIMS experiments which use mobility cells that have a constant electric field applied, TWIMS uses a sequence of symmetric travelling waves that are continually propagated through a mobility cell. The travelling wave is produced by a series of transient direct current (DC) voltages that are superimposed onto a stack ring ion guide (SRIG), resulting in ion propulsion (Giles 2004). The SRIG consists of ring electrodes that are arranged orthogonally to the ion transmission axis. RF voltages are applied to consecutive electrodes. Opposite phases of RF voltages are applied to adjacent rings to radially confine and stabilise the trajectory of ions as they traverse through the SRIG, preventing ion loss via radial diffusion (Figure 1.13). The ring geometry creates axial traps that can slow or even stop ions in motion.

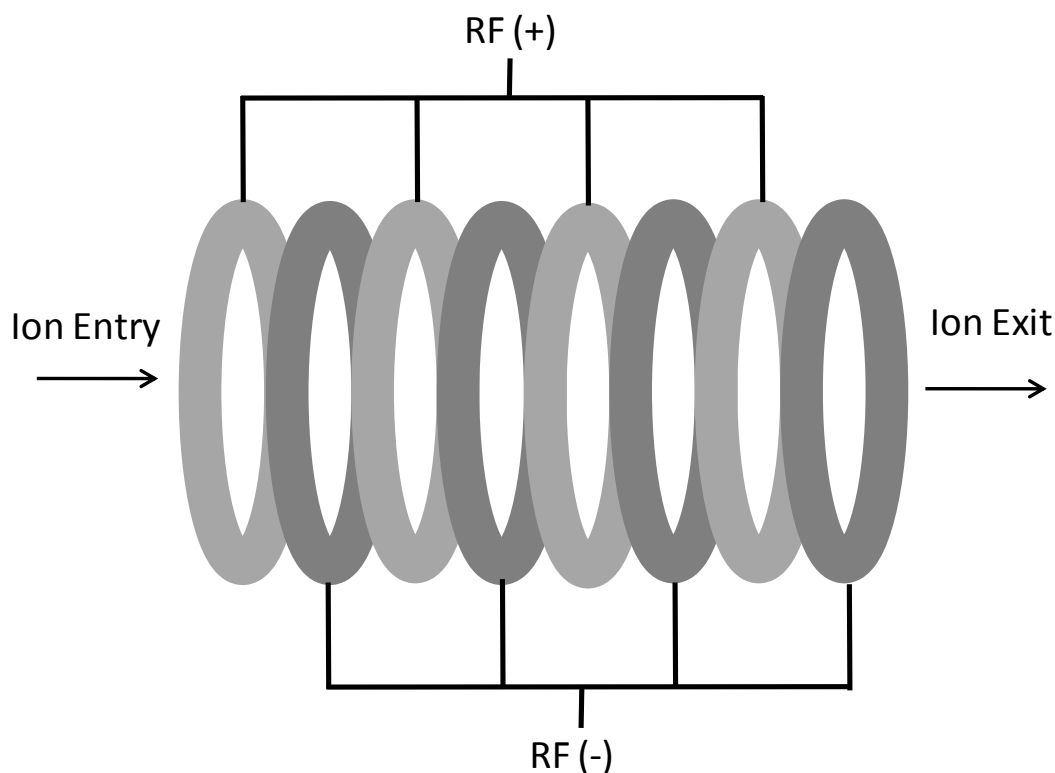


**Figure 1.13** - Schematic representation of a SRIG. Adapted from (Giles 2004)

A DC potential is applied to each pair of electrodes in succession, creating a moving potential along the ion guide that provides a travelling wave voltage on which ions

can surf. The SRIG in this context can be referred to as a travelling wave ion guide (TWIG). The TWIG can be used to separate ions based on their mobility because under a given gas pressure, travelling wave height and velocity conditions, ions with a high mobility can be carried with the wave, exiting the cell earlier, while ions of lower mobility roll over the wave top and require subsequent waves to propel them further, thus exit later (Figure 1.14).

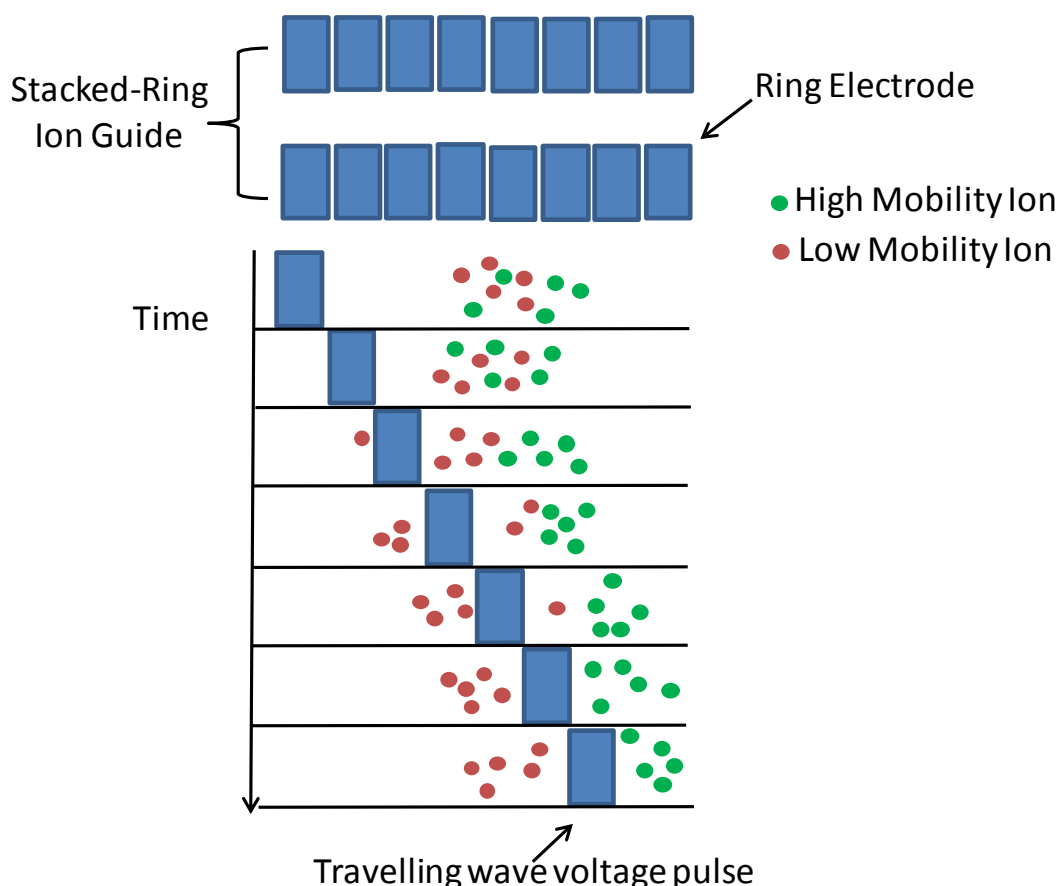


**Figure 1.14** - Schematic showing the progression of the travelling wave voltage pulse along the TWIG (Adapted from Giles 2004)

Three TWIGs forming a TriWave region were incorporated within a Q-ToF geometry to create the travelling wave ion mobility-mass spectrometry (TWIM-MS) Synapt G1 HDMS system (Waters, Manchester, UK) (Pringle 2007), and the recently introduced Synapt G2, which can perform higher resolution mobility separation (Giles 2011). Both instruments are hybrid quadrupole ion mobility oa-ToF mass spectrometers. With the Synapt G2 it is possible to rapidly change the

ionisation source which can include ESI, MALDI, APPI, APCI, ASAP, and all related ambient ionisation methods.

The first TWIG in the TriWave region is referred to as the trap cell, the second the mobility cell, and the third as the transfer cell. In both the Synapt G1 and G2 instruments the trap and transfer cells are both 100 mm long consisting of 64 electrodes.

A travelling wave is not applied to the trap, and the final electrode in the trap is DC-only, and the voltage is modulated so that periodically gates ion packets into mobility cell.

The mobility cell in the Synapt G1 is 185 mm, and consists of 122 electrodes grouped into 61 pairs, the G2 comprises a mobility cell that is longer at 254 mm consisting of 168 electrodes grouped into 84 pairs. This was implemented, as modelling by the manufacturer (Giles 2011) and theoretical studies on T-wave separation (Shvartsburg 2008) suggested that mobility resolution would increase as the square root of the length of the mobility cell increased. The maximum pressure of the buffer gas in the G2 is 2.5 mbar in contrast to 0.5 mbar in the G1, and is facilitated by the use of a helium entry cell consisting of four RF-only electrodes bounded by aperture plate, and with a length of 7 mm. In the G1 the travelling wave voltage is applied to the 1<sup>st</sup> and 7<sup>th</sup> pair of electrodes, then the 2<sup>nd</sup> and 8<sup>th</sup> pair of electrodes and so on. In the G2, the T-Wave pulse is applied to two pairs of electrodes, while progression along the cell is made in single electrode pair steps, with a repeat pattern of four electrode pairs, i.e. voltage applied to the 1<sup>st</sup>, 2<sup>nd</sup> and 5<sup>th</sup> and 6<sup>th</sup> pair of electrodes, and then to the 2<sup>nd</sup>, 3<sup>rd</sup>, 6<sup>th</sup> and 7<sup>th</sup> pair of electrodes.

The transfer cell is similar in both instruments, and has a travelling wave voltage pulse applied to it continually to maintain separation of ions from the mobility cell. This region transfers ions to the oa-ToF, which is synchronised with the gated release of ion packets from the trap cell. For each packet of ions released, there are 200 orthogonal pushes into the ToF analyser, thus for every cycle of mobility separation 200 mass spectra are recorded. Mobility cycles continue until a mass spectrum with desired signal to noise ratio (S/N) is acquired. A schematic of the

Synapt G2 on which the majority of results in this thesis were acquired is shown in Figure 1.15.

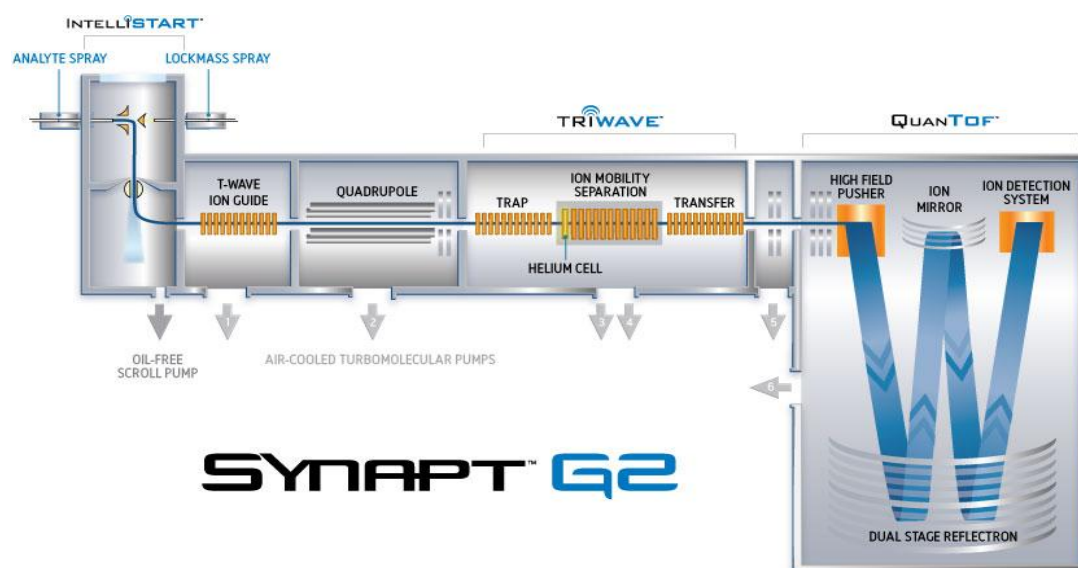


**Figure 1.15** - Schematic diagram of Synapt G2. The ionisation region shown is a z-spray ESI source and is one of many that can be interfaced to the instrument.

MS/MS can be performed by way of CID fragmentation in either, or both of the trap and transfer cells, enabling a number of experiments to take place, including:

- Mobility separation of ions in the mobility cell and subsequent fragmentation of these ions in the transfer cell – this is the method of choice for characterisation of complex mixtures, or for resolving isobaric species. This experiment does not always require quadrupole precursor selection.
- Fragmentation in the trap cell, and then mobility separation of product ions. A common use of this method is for mechanistic studies of precursor selected ions.
- Time-aligned parallel (TAP) fragmentation, where precursor selected ions are fragmented in the trap cell, produced ions are mobility separated and then

further fragmented in the trap cell. This provides a pseudo MS<sup>3</sup> mode of operation.

- Fragmentation without a travelling wave voltage applied to mobility cell can also take place in the trap or the transfer cell (Conventional CID).

Compared to many DCIM-MS instruments, TWIM-MS has a high sensitivity, and if instrument is properly optimised there should be no loss in sensitivity when switching between mobility and non mobility modes in the Synapt instruments. The mobility resolution in the G2 is around 45 ( $\Omega/\Delta\Omega$ ) and although an improvement on the G1, it is still significantly less than resolutions of achieved on high resolution atmospheric pressure DCIM-MS instruments, including 80 by the group of Hill (Wu, Siems et al. 1999) and up to 110 by the group of Bowers (Kemper, Dupuis et al. 2009).

While drift cells in DCIM-MS utilise uniform electric fields enabling direct calculations of cross sections of ions for structural information, the trajectory of an ion in a TWIMS device is complex because the electric field is non-uniform and not time dependent. While the fundamentals of ion motion in a TWIMS device have been investigated (Shvartsburg 2008) and initial attempts at direct measurement of cross sections reported (Giles 2010), accurate direct calculations are not yet possible. It is possible to obtain estimated cross-sections by acquiring data on calibration standards of established cross-sections and calibrating via reference.

The method of calibration used to determine cross sections within this body of work has been developed in-house by the Scrivens research group (Thalassinos, Grabenauer et al. 2008). This method requires the mobility measurements of standards with known absolute cross sections obtained by DCIM-MS, and should bracket the mobilities of the unknown samples. These calibrants are then analysed by TWIM-MS under the experimental conditions at which the analyte will be analysed, and is described below:

1. Measure the arrival time (scan number ( $n$ )) in which the calibrant ion arrives at the detector.
2. Convert  $n$  to time by multiplying by the oa-ToF pusher period ( $t_d = n \times \text{pusher period}$ ).
3. Correct for  $m/z$  dependent and  $m/z$  independent time of flight.  $m/z$  independent time is related to the velocity of the T-Wave, and is the time an ion spends in the mobility and transfer cells, and as name suggests the time taken is not dependent on  $m/z$ .  $m/z$  dependent time is the time taken from leaving the transfer cell to reaching the detector (in effect the time within the ToF analyser). The time is proportional to the square root of the  $m/z$  of the ion. An effective drift time is obtained ( $t(d)$ ).
4. Calibration coefficients from published cross section data are obtained. These are corrected for reduced mass and charge state to give a corrected coefficient ( $\Omega'$ ).
5. The corrected calibration coefficient is plotted against the effective drift time, and a curve is fitted to the data. For smaller calibrants and analytes a linear series is typically used, while a power series is applied for larger species.
6. Experimental T-Wave mobility measurements obtained for an analyte are converted into estimated cross-sections with the equation obtained from either the power fit or linear fit.

The mobility of an ion can be affected by the height of the T-Wave, its velocity and the pressure of the buffer gas, but these parameters will not affect calibration, provided that mobility measurements for the calibration standard are obtained under the same conditions as the analyte (Leary, Schenauer et al. 2009).



## **1.10 Aims of project**

The introduction of ambient ionisation techniques and the commercialisation of ion mobility mass spectrometry are arguably two of the biggest developments in mass spectrometry in the last ten years.

Ambient ionisation approaches are used to rapidly analyse complex matrices, from which complex ion populations are sampled and the spectra obtained may retain significant complexity. There has been little focus to date on the development of methods to address the spectral complexity found after ionisation. These experiments would benefit from chromatographic separation, but conventional chromatographic separation would require significant time and so reduce or eliminate an inherent benefit of ambient ionisation. The timescale of mobility separations is of the order of milliseconds, and therefore falls well within the timescale of an ambient ionisation experiment. Although the coupling of ambient ionisation techniques to IM-MS is clearly complementary, the field is in its infancy with few reports in the literature. These are based on coupling DESI with IM-MS to characterise either protein misfolding (Myung, Wiseman et al. 2006), tryptic peptides (Kaur-Atwal, Weston et al. 2007), pharmaceutical surfaces (Weston, Bateman et al. 2005; Williams and Scrivens 2008), pharmaceutical formulations on reverse-phase thin layer chromatography plates (Harry, Reynolds et al. 2009), or chemical warfare agents (D'Agostino and Chenier 2010).

Structural characterisation of complex polymer mixtures or polymers with novel architecture can be analytically challenging. IM-MS has the potential to simplify the spectra obtained. The level of structural detail provided by these IM-MS offers the potential to develop practical screening methods for complex formulations.

The aims of this work were to evaluate the capabilities of two ambient ionisation techniques and IM-MS for the characterisation of a selection of pharmaceutical and polymer formulations.

1. The rapid analysis of pharmaceutical formulations is a goal of the pharmaceutical industry, and would be more feasible if the sample preparation step was removed. A pharmaceutical formulation may be composed of both the active ingredient and a number of excipients that may act to deliver the active or to give a formulation a distinctive flavour or colour. An ambient ionisation source was developed and then evaluated for the rapid analysis of medicinal spray formulations containing components of differing volatilities. This technique would then be coupled to IM-MS to assess if additional information would be provided. This technique would also be evaluated for the analysis of polymer formulations
2. The ASAP technique is a novel method to generate ions. This was to be assessed for both polymer and pharmaceutical formulations. The technique can generate both protonated and radical cations. The fragmentation of radical cations is more reproducible compared with protonated ions, and identification methodologies utilising spectral libraries is a potential viability.
3. The use of IM-MS to analyse complex polysorbate formulations for individual component structural properties was to be assessed. Small differences in the formulations from batch to batch can potentially change the performance characteristics. Additional characterisation techniques are required by the polymer industry to fully characterise these formulations. IM-MS is one such technique that could improve the characterisation of these challenging formulations.
4. IM-MS was to be used to investigate the topology of a novel polymer architecture. These novel architectures are often analysed by ensemble analysis techniques such as NMR, which may not reveal the true complexity of these types of formulation. The conformation of these structures may have an effect on their properties.

The thesis has been split into five chapters:

1. Introduction – This chapter gives an overview of the established mass spectrometry techniques, and some of the advantages and challenges. Novel techniques are also introduced, and the aims of the PhD research are stated
2. Materials and methods – This chapter gives information on where to purchase materials, and how to perform the methods.
3. Characterisation of pharmaceutical formulations – The data generated by the analysis of a number of commercially available pharmaceutical formulations by established and novel techniques is presented in this chapter
4. Characterisation of polymer formulations – Data from the characterisation of the complex polymer formulations is presented here
5. Conclusions – This chapter gives an overview of what has been done during the research, but also indicates what still needs to be done.

### 1.10 Research Papers

The research involved in this project has resulted in two peer reviewed and published papers, with two others in preparation.

1. Scarff, C.A., **Snelling, J.R.**, Knust, M.M., Wilkins, C.L., Scrivens, J.H.,(2012) New structural insights into mechanically-interlocked polymers can be obtained by travelling wave ion mobility mass spectrometry *Journal of the American Chemical Society*, 2012, 134 (22), 9193-9198
2. **Snelling, J.R.**, Scarff, C.A., Scrivens J.H., (2012) The characterization of complex polysorbate formulations by means of shape-selective mass spectrometry *Analytical Chemistry*, **DOI:** 10.1021/ac300779p
3. **Snelling, J.R.**, Scarff, C.A., Scrivens J.H., (2012) Thermally-assisted extractive electrospray shape selective studies of medicinal spray formulations *Analytical Chemistry*, Submitted

### 1.11 Oral Presentations

**Snelling, J.R.**, Scarff, C.A., Scrivens J.H. Extractive electrospray ion mobility mass spectrometry characterisation of medicinal spray formulations, *BMSS 31<sup>st</sup> Annual Meeting, Cardiff* (2010)

### 1.12 Conference Papers (Peer Reviewed)

Scrivens, J.H., Scarff, C.A., Wilkins, C., **Snelling, J.R.**, The use of shape selective tandem mass spectrometry in the characterisation of complex formulations containing polymeric components, *60<sup>th</sup> ASMS Conference on Mass Spectrometry and Allied Topics* (2012)

Scrivens, J.H., Scarff, C.A., **Snelling, J.R.**, Knust, M., Wilkins, C.L., New structural insights into a novel geometry polymeric system by use of shape-selective MS studies. *BMSS 32<sup>nd</sup> Annual Meeting, Cardiff* (2011)

**Snelling, J.R.**, Scarff, C.A., Scrivens, J.H., Shape selective ambient ionisation mass spectrometry of pharmaceuticals and polymers, *BMSS 32<sup>nd</sup> Annual Meeting, Cardiff* (2011)

Scarff, C.A., **Snelling, J.R.**, Knust, M., Scrivens, J.H., Wilkins, C.L. New structural insights into a novel geometry polymeric system by use of shape-selective MS studies. *59<sup>th</sup> ASMS Conference on Mass Spectrometry and Allied Topics, Denver* (2011)

Scrivens, J.H., Scarff, C.A., Wilkins, C.L., **Snelling, J.R.** Applications of ASAP and EESI ionisation approaches coupled with travelling wave ion mobility mass spectrometry *59<sup>th</sup> ASMS Conference on Mass Spectrometry and Allied Topics, Denver* (2011)

Ray, A.D., Weston, D.J., Blatherwick, E.Q., **Snelling, J.R.**, Scrivens, J.H. Investigating Liquid Extraction Surface Analysis (LESA) for rapid analysis of pharmaceutical tablets. *BMSS 31<sup>st</sup> Annual Meeting, Cardiff* (2010)

Scrivens, J.H., Patel, N.A., Kondrat, F.D.L, **Snelling, J.R.**, Slade, S.E., Thalassinou, K., Scarff, C.A. Shape selective studies of complex systems utilizing travelling wave ion mobility mass spectrometry. *BMSS 31<sup>st</sup> Annual Meeting, Cardiff* (2010)

Scrivens, J.H., Scarff, C.A., **Snelling, J.R.** Thermally-assisted extractive electrospray ion mobility mass spectrometry characterisation of medicinal spray formulations. *58<sup>th</sup> ASMS Conference on Mass spectrometry and Allied Topics, Salt Lake City (2010)*

**Snelling, J.R.**, Hilton, G.R., Scrivens, J.H. Ambient ionisation combined with ion-mobility mass spectrometry and tandem mass spectrometry of pharmaceuticals and dietary supplements. *18<sup>th</sup> International Mass Spectrometry Conference, Bremen, Germany (2009)*

**Snelling, J.R.**, Hilton, G.R., Scrivens, J.H. A comparison of mass spectrometry ionisation techniques coupled to ion mobility mass spectrometry to differentiate between popular brands of pharmaceutical and dietary supplements. *Royal Society of Chemistry Analytical Research Forum, University of Kent (2009)*

### 1.13 References

**Ahmed, A., Cho, Y. J., No, M.-h., Koh, J., Tomczyk, N., Giles, K., Yoo, J. S. and Kim, S.** (2010). "Application of the Mason–Schamp Equation and Ion Mobility Mass Spectrometry To Identify Structurally Related Compounds in Crude Oil." *Analytical Chemistry* **83**(1): 77-83.

**Armenta, S. and Blanco, M.** (2012). "Ion Mobility Spectrometry: a comprehensive and versatile tool for occupational pharmaceutical exposure assessment." *Analytical Chemistry*.

**Aston, F. W.** (1920). "Isotopes and Atomic Weights." *Nature* **105**: 617-619.

**Barry, S. J. and Wolff, J.-C.** (2012). "Identification of isobaric amino-sulfonamides without prior separation." *Rapid Communications in Mass Spectrometry* **26**(4): 419-429.

**Berchtold, C., Meier, L. and Zenobi, R.** (2011). "Evaluation of extractive electrospray ionization and atmospheric pressure chemical ionization for the detection of narcotics in breath." *International Journal of Mass Spectrometry* **299**(2–3): 145-150.

**Bruns, E. A., Perraud, V., Greaves, J. and Finlayson-Pitts, B. J.** (2010). "Atmospheric Solids Analysis Probe Mass Spectrometry: A New Approach for Airborne Particle Analysis." *Analytical Chemistry* **82**(14): 5922-5927.

**Chang, D.-Y., Lee, C.-C. and Shiea, J.** (2002). "Detecting Large Biomolecules from High-Salt Solutions by Fused-Droplet Electrospray Ionization Mass Spectrometry." *Analytical Chemistry* **74**(11): 2465-2469.

**Chen, H., Cotte-Rodriguez, I. and Cooks, R. G.** (2006). "cis-Diol functional group recognition by reactive desorption electrospray ionization (DESI)." *Chemical Communications*(6): 597-599.

**Chen, H., Hu, B., Hu, Y., Huan, Y., Zhou, Z. and Qiao, X.** (2009). "Neutral Desorption Using a Sealed Enclosure to Sample Explosives on Human Skin for Rapid Detection by EESI-MS." *Journal of the American Society for Mass Spectrometry* **20**(4): 719-722.

**Chen, H., Talaty, N. N., Takats, Z., Cooks, R. G.** (2005). "Desorption Electrospray Ionization Mass Spectrometry for High-Throughput Analysis of Pharmaceutical Samples in the Ambient Environment." *Analytical Chemistry*. **77**(21): 6915-6927.

**Chen, H., Venter, Andre., Cooks, R. Graham.** (2006). "Extractive electrospray ionization for direct analysis of undiluted urine, milk and other complex mixtures without sample preparation." *Chemical Communications*(19): 2042-2044.

**Chen, H., Wortmann, A., Zenobi, A.,** (2007). "Neutral desorption sampling coupled to extractive electrospray ionization mass spectrometry for rapid differentiation of biosamples by metabolomic fingerprinting." *Journal of Mass Spectrometry* **42**(9): 1123-1135.

**Chen, H., Yang, S., Li, M., Hu, B., Li, J. and Wang, J.** (2010). "Sensitive Detection of Native Proteins Using Extractive Electrospray Ionization Mass Spectrometry." *Angewandte Chemie International Edition* **49**(17): 3053-3056.

**Chen, H., Yang, S., Wortmann, A., Zenobi, R.** (2007). "Neutral Desorption Sampling of Living Objects for Rapid Analysis by Extractive Electrospray Ionization Mass Spectrometry13." *Angewandte Chemie International Edition* **46**(40): 7591-7594.

**Chen, H. and Zenobi, R.** (2008). "Neutral desorption sampling of biological surfaces for rapid chemical characterization by extractive electrospray ionization mass spectrometry." *Nat. Protocols* **3**(9): 1467-1475.

**Clemmer, D. E., Jarrold, M.F.** (1997). "Ion mobility measurements and their applications to clusters and biomolecules." *Journal of Mass Spectrometry* **32**: 577-592.



**Cody, R. B., Laramée, J. A., Durst, H. D.** (2005). "Versatile New Ion Source for the Analysis of Materials in Open Air under Ambient Conditions." *Analytical Chemistry*. **77**(8): 2297-2302.

**Cohen, M. J., Karasek, F.W.** (1970). "Plasma Chromatography TM-New Dimension for Gas Chromatography and Mass Spectrometry." *J. Chromatogr Sci.* **8**: 330-337.

**Cooks, R. G., Ouyang, Z., Takats, Z., Wiseman, J. M.** (2006). "Ambient Mass Spectrometry." *Science* **311**(5767): 1566-1570.

**Costa, A. B. and Cooks, R. G.** (2007). "Simulation of atmospheric transport and droplet-thin film collisions in desorption electrospray ionization." *Chemical Communications*(38): 3915-3917.

**Costa, A. B., Cooks, R. G.** (2008). "Simulated splashes: Elucidating the mechanism of desorption electrospray ionization mass spectrometry." *Chemical Physics Letters* **464**(1-3): 1-8.

**Cotte-Rodriguez, I., Chen, H. and Cooks, R. G.** (2006). "Rapid trace detection of triacetone triperoxide (TATP) by complexation reactions during desorption electrospray ionization." *Chemical Communications*(9): 953-955.

**Creaser, C. S., Griffiths, J. R., Bramwell, C. J., Noreen, S., Hill, C. A. and Thomas, C. L. P.** (2004). "Ion mobility spectrometry: a review. Part 1. Structural analysis by mobility measurement." *The Analyst* **129**(11): 984-994.

**D'Agostino, P., A. and Chenier, C., L.** (2010). "Desorption electrospray ionization mass spectrometric analysis of organophosphorus chemical warfare agents using ion mobility and tandem mass spectrometry." *Rapid Communications in Mass Spectrometry* **24**(11): 1617-1624.

**Dempster, A. J.** (1918). "A new Method of Positive Ray Analysis." *Physical Review* **11**(4): 316-325.

**Ding, J., Yang, S., Liang, D., Chen, H., Wu, Z., Zhang, L. and Ren, Y.** (2009). "Development of extractive electrospray ionization ion trap mass spectrometry for in vivo breath analysis." *Analyst* **134**(10): 2040-2050.

**Doezema, L. A., Longin, T., Cody, W., Perraud, V., Dawson, M. L., Ezell, M. J., Greaves, J., Johnson, K. R. and Finlayson-Pitts, B. J.** (2012). "Analysis of secondary organic aerosols in air using extractive electrospray ionization mass spectrometry (EESI-MS)." *RSC Advances* **2**(7): 2930-2938.

**Dole, M., Mack, L. L., Hines, R. L., Mobley, R. C., Ferguson, L. D. and Alice, M. B.** (1968). "Molecular Beams of Macroions." *The Journal of Chemical Physics* **49**(5): 2240-2249.

**Eiceman, G. A. and Stone, J. A.** (2004). "Peer Reviewed: Ion Mobility Spectrometers in National Defense." *Analytical Chemistry* **76**(21): 390 A-397 A.

**Fernández, F. M., Cody, R.B., Green, M.D., Hampton,C.Y., McGready,R., Sengaloundeth,S., White,N.J., Newton,P.N.** (2006). "Characterization of Solid Counterfeit Drug Samples by Desorption Electrospray Ionization and Direct-analysis-in-real-time Coupled to Time-of-flight Mass Spectrometry." *ChemMedChem* **1**(7): 702-705.

**Fussell, R. J., Chan, D. and Sharman, M.** (2010). "An assessment of atmospheric-pressure solids-analysis probes for the detection of chemicals in food." *TrAC Trends in Analytical Chemistry* **29**(11): 1326-1335.

**Giles, K., Pringle, S. D., Worthington, K. R., Little, D., Wildgoose, J. L., Bateman, R.H.** (2004). "Applications of a travelling wave-based radio-frequency-only stacked ring ion guide." *Rapid Communications in Mass Spectrometry* **18**(20): 2401-2414.

**Giles, K., Wildgoose, J.L., Langridge, D.J., Campuzano, I.** (2010). "A method for direct measurement of ion mobilities using a travelling wave ion guide." *International Journal of Mass Spectrometry* **298**: 10-16.

**Giles, K., Williams, J.P., Campuzano, I.** (2011). "Enhancements in travelling wave ion mobility resolution." *Rapid Communications in Mass Spectrometry* **25**: 1559-1566.

**Gillig, K. J., Ruotolo, B., Stone, E. G., Russell, D. H., Fuhrer, K., Gonin, M. and Schultz, A. J.** (2000). "Coupling High-Pressure MALDI with Ion Mobility/Orthogonal Time-of-Flight Mass Spectrometry." *Analytical Chemistry* **72**(17): 3965-3971.

**Goldstein, E.** (1876). "Vorläufige Mittheilungen über electriche Entladungen Verdünnten Gasen." *Berlin Akd. Monatsber*: 279.

**Guevremont, R.** (2004). "High-field asymmetric waveform ion mobility spectrometry: A new tool for mass spectrometry." *Journal of Chromatography A* **1058**(1-2): 3-19.

**Guilhas, M., Selby, D., Mlynski, V.** (2000). "Orthogonal Acceleration Time-of-Flight Mass Spectrometry." *Mass Spectrometry Reviews* **19**: 65-107.

**Haapala, M., Pól, J., Saarela, V., Arvola, V., Kotiaho, T., Ketola, R. A., Franssila, S., Kauppila, T. J. and Kostianen, R.** (2007). "Desorption Atmospheric Pressure Photoionization." *Analytical Chemistry* **79**(20): 7867-7872.

**Haddad, R., Sparrapan, R., Eberlin, M. E.** (2006). "Desorption sonic spray ionization for (high) voltage-free ambient mass spectrometry." *Rapid Communications in Mass Spectrometry* **20**(19): 2901-2905.

**Harper, J. D., Charipar, N. A., Mulligan, C. C., Zhang, X., Cooks, R. G. and Ouyang, Z.** (2008). "Low-Temperature Plasma Probe for Ambient Desorption Ionization." *Analytical Chemistry* **80**(23): 9097-9104.

**Harris, G. A., Galhena, A. S. and Fernandez, F. M.** (2011). "Ambient Sampling/Ionization Mass Spectrometry: Applications and Current Trends." *Analytical Chemistry* **83**: 4508-4538.

**Harris, G. A., Nyadong, L. and Fernandez, F. M.** (2008). "Recent developments in ambient ionization techniques for analytical mass spectrometry." *The Analyst* **133**(10): 1297-1301.

**Harry, E., L., Reynolds, J., C., Bristow, A., W. T., Wilson, I., D. and Creaser, C., S.** (2009). "Direct analysis of pharmaceutical formulations from non-bonded reversed-phase thin-layer chromatography plates by desorption electrospray ionisation ion mobility mass spectrometry." *Rapid Communications in Mass Spectrometry* **23**(17): 2597-2604.

**Harry, E. L., Reynolds, J. C., Bristow, A. W. T., Wilson, I. D. and Creaser, C. S.** (2009). "Direct analysis of pharmaceutical formulations from non-bonded reversed-phase thin-layer chromatography plates by desorption electrospray ionisation ion mobility mass spectrometry." *Rapid Communications in Mass Spectrometry* **23**(17): 2597-2604.

**Hill, H. H., Siems, W. F. and St. Louis, R. H.** (1990). "Ion mobility spectrometry." *Analytical Chemistry*. **62**(23): 1201-1209.

**Hittorf, W.** (1869). "Ueber die Elektrizitätsleitung der Gase. Erste Mitteilung." *Ann Physik und Chemie* **136**(1).

**Horning, E. C., Carroll, D. I., Dzidic, I., Haegele, K. D., Horning, M. G. and Stillwell, R. N.** (1974). "Atmospheric Pressure Ionization (API) Mass Spectrometry. Solvent-Mediated Ionization of Samples Introduced in Solution and in a Liquid Chromatograph Effluent Stream." *Journal of Chromatographic Science* **12**(11): 725-729.

**Hu, B., Yang, S., Li, M., Gu, H. and Chen, H.** (2011). "Direct detection of native proteins in biological matrices using extractive electrospray ionization mass spectrometry." *Analyst* **136**(18): 3599-3601.

**Huang, M.-Z., Cheng, S.-C., Cho, Y.-T. and Shiea, J.** (2011). "Ambient ionization mass spectrometry: A tutorial." *Analytica Chimica Acta* **702**(1): 1-15.

**Ifa, D. R., Wiseman, J. M., Song, Q., Cooks, R. G.** (2007). "Development of capabilities for imaging mass spectrometry under ambient conditions with desorption electrospray ionization (DESI)." *International Journal of Mass Spectrometry* **259**(1-3): 8-15.

**Iribarne, J. V. and Thomson, B. A.** (1976). "On the evaporation of small ions from charged droplets." *The Journal of Chemical Physics* **64**(6): 2287-2294.

**Jackson, A. T., Williams, J.P., Scrivens, J.H.** (2006). "Desorption electrospray ionisation mass spectrometry and tandem mass spectrometry of low molecular weight synthetic polymers." *Rapid Communications in Mass Spectrometry* **20**(18): 2717-2727.

**Jackson, A. U., Werner, S. R., Talaty, N., Song, Y., Campbell, K., Cooks, R. G., Morgan, J. A.** (2008). "Targeted metabolomic analysis of Escherichia coli by desorption electrospray ionization and extractive electrospray ionization mass spectrometry." *Analytical Biochemistry* **375**(2): 272-281.

**Jennings, K. R.** (1968). "Collision-induced decompositions of aromatic molecular ions." *International Journal of Mass Spectrometry and Ion Physics* **1**(3): 227-235.

**Kanu, A. B., Dwivedi, P., Tam, M., Matz, L., Hill Jr., H.H.** (2008). "Ion mobility-mass spectrometry." *Journal of Mass Spectrometry*. **43**(1): 1-22.

**Karas, M. and Hillenkamp, F.** (1988). "Laser desorption ionization of proteins with molecular masses exceeding 10,000 daltons." *Analytical Chemistry* **60**(20): 2299-2301.

**Karataev, V. I., Mamyrin, B.A., Shmikk, D.V.** (1972). "New method for focusing ion bunches in time-of-flight mass spectrometers." *Sov. Phys.-Tech. Phys* **16**(7): 1177-1179.

**Katona, M., Denes, J., Skoumal, R., Toth, M. and Takats, Z.** (2011). "Intact skin analysis by desorption electrospray ionization mass spectrometry." *Analyst* **136**(4): 835-840.

**Kauppila, T. J., Talaty, N., Kuuranne, T., Kotiaho, T., Kostinen, R. and Cooks, R. G.** (2007). "Rapid analysis of metabolites and drugs of abuse from urine samples by desorption electrospray ionization-mass spectrometry." *The Analyst* **132**(9): 868-875.

**Kaur-Atwal, G., Weston, D., J., Green, P., S. , Crosland, S., Bonner, P., L. R. and Creaser, C., S.** (2007). "Analysis of tryptic peptides using desorption electrospray ionisation combined with ion mobility spectrometry/mass spectrometry." *Rapid Communications in Mass Spectrometry* **21**(7): 1131-1138.

**Kebarle, P.** (2000). "A brief overview of the present status of the mechanisms involved in electrospray mass spectrometry." *Journal of Mass Spectrometry* **35**(7): 804-817.

**Kemper, P. R., Dupuis, N. F. and Bowers, M. T.** (2009). "A new, higher resolution, ion mobility mass spectrometer." *International Journal of Mass Spectrometry* **287**(1-3): 46-57.

**Laskin, J., Heath, B. S., Roach, P. J., Cazares, L. and Semmes, O. J.** (2011). "Tissue Imaging Using Nanospray Desorption Electrospray Ionization Mass Spectrometry." *Analytical Chemistry* **84**(1): 141-148.

**Law, W. S., Chen, H. W., Balabin, R., Berchtold, C., Meier, L. and Zenobi, R.** (2010). "Rapid fingerprinting and classification of extra virgin olive oil by microjet

sampling and extractive electrospray ionization mass spectrometry." *Analyst* **135**(4): 773-778.

**Law, W. S., Wang, R., Hu, B., Berchtold, C., Meier, L., Chen, H. and Zenobi, R.** (2010). "On the Mechanism of Extractive Electrospray Ionization." *Analytical Chemistry* **82**(11): 4494-4500.

**Leary, J. A., Schenauer, M. R., Stefanescu, R., Andaya, A., Ruotolo, B. T., Robinson, C. V., Thalassinos, K., Scrivens, J. H., Sokabe, M. and Hershey, J. W. B.** (2009). "Methodology for Measuring Conformation of Solvent-Disrupted Protein Subunits using T-WAVE Ion Mobility MS: An Investigation into Eukaryotic Initiation Factors." *Journal of the American Society for Mass Spectrometry* **20**(9): 1699-1706.

**Lee, P. J., Ruel, A.M., Balogh, M.P., Young, P.B., Burgess, J.A.** (2011). "Analysis of vanilla flavoured food products using the atmospheric solids analysis probe." *Food Analysis* **21**(3).

**Leuthold, L. A., Mandscheff, J.F., Fathi, M., Giroud, C., Augsburger, M., Varesio, E., Hopfgartner, G.** (2006). "Desorption electrospray ionization mass spectrometry: direct toxicological screening and analysis of illicit Ecstasy tablets." *Rapid Communications in Mass Spectrometry* **20**(2): 103-110.

**Lloyd, J. A., Harron, A. F. and McEwen, C. N.** (2009). "Combination Atmospheric Pressure Solids Analysis Probe and Desorption Electrospray Ionization Mass Spectrometry Ion Source." *Analytical Chemistry* **81**(21): 9158-9162.

**Makarov, A., Denisov, E., Kholomeev, A., Balschun, W., Lange, O., Strupat, K. and Horning, S.** (2006). "Performance Evaluation of a Hybrid Linear Ion Trap/Orbitrap Mass Spectrometer." *Analytical Chemistry* **78**(7): 2113-2120.

**Martínez-Lozano, P. and de la Mora, J. F.** (2007). "Electrospray ionization of volatiles in breath." *International Journal of Mass Spectrometry* **265**(1): 68-72.

**Martínez-Lozano, P., Rus, J., Fernández de la Mora, G., Hernández, M. and Fernández de la Mora, J.** (2009). "Secondary Electrospray Ionization (SESI) of Ambient Vapors for Explosive Detection at Concentrations Below Parts Per Trillion." *Journal of the American Society for Mass Spectrometry* **20**(2): 287-294.

**Mason, E. A., McDaniel, E.W.** (1988). Transport Properties of Ions in Gases. *New York, Wiley*.

**McEwen, C. and Gutteridge, S.** (2007). "Analysis of the Inhibition of the Ergosterol Pathway in Fungi Using the Atmospheric Solids Analysis Probe (ASAP) Method." *Journal of the American Society for Mass Spectrometry* **18**(7): 1274-1278.

**McEwen, C. N., McKay, R. G., Larsen, B. S.** (2005). "Analysis of Solids, Liquids, and Biological Tissues Using Solids Probe Introduction at Atmospheric Pressure on Commercial LC/MS Instruments." *Analytical Chemistry*. **77**(23): 7826-7831.

**Munson, M. S. B. and Field, F. H.** (1966). "Chemical Ionization Mass Spectrometry. I. General Introduction." *Journal of the American Chemical Society* **88**(12): 2621-2630.

**Myung, S., Wiseman, J. M., Valentine, S. J., Takats, Z., Cooks, R. G. and Clemmer, D. E.** (2006). "Coupling Desorption Electrospray Ionization with Ion Mobility/Mass Spectrometry for Analysis of Protein Structure: Evidence for Desorption of Folded and Denatured States." *J. Phys. Chem. B* **110**(10): 5045-5051.

**Na, N., Zhao, M., Zhang, S., Yang, C. and Zhang, X.** (2007). "Development of a Dielectric Barrier Discharge Ion Source for Ambient Mass Spectrometry." *Journal of the American Society for Mass Spectrometry* **18**(10): 1859-1862.

**Nefliu, M., Smith, J. N., Venter, A. and Cooks, R. G.** (2008). "Internal Energy Distributions in Desorption Electrospray Ionization (DESI)." *Journal of the American Society for Mass Spectrometry* **19**(3): 420-427.



**Nemes, P., Vertes, A.** (2007). "Laser Ablation Electrospray Ionization for Atmospheric Pressure, in Vivo, and Imaging Mass Spectrometry." *Analytical Chemistry* **79**(21): 8098-8106.

**Nollet, J. A.** (1749). Recherches sur les causes particulieres des phenomenes eletriques. *Paris*.

**Paul, A. D. A. and Claude, L. C.** (2010). "Desorption electrospray ionization mass spectrometric analysis of organophosphorus chemical warfare agents using ion mobility and tandem mass spectrometry." *Rapid Communications in Mass Spectrometry* **24**(11): 1617-1624.

**Paul, W., Steinwedel, H.** (1953). "Ein neues Massenspektrometer ohne Magnetfeld (A new mass spectrometer without magnetic field)." *Zeitschrift fur Naturforschung*: 448-450.

**Perrin, J.** (1895). "Nouvelles proprietes des rayons cathodiques." *Comptes rendus de l'Académie des Sciences*, **121**: 1130-1135.

**Pringle, S. D., K. Giles et al.** (2007). "An investigation of the mobility separation of some peptide and protein ions using a new hybrid quadrupole/travelling wave IMS/oa-ToF instrument." *International Journal of Mass Spectrometry* **261**(1): 1-12.

**Ratcliffe, L. V., Rutten, F. J. M., Barrett, D. A., Whitmore, T., Seymour, D., Greenwood, C., Aranda-Gonzalvo, Y., Robinson, S. and McCoustra, M.** (2007). "Surface Analysis under Ambient Conditions Using Plasma-Assisted Desorption/Ionization Mass Spectrometry." *Analytical Chemistry* **79**(16): 6094-6101.

**Ray, A. D., Hammond, Janet., Major, Hilary.** (2010). "Molecular ions and protonated molecules observed in the atmospheric solids analysis probe analysis of steroids." *European Journal of Mass Spectrometry* **16**(2): 169-174.

**Revercomb, H. E. and Mason, E. A.** (1975). "Theory of plasma chromatography/gaseous electrophoresis. Review." *Analytical Chemistry* **47**(7): 970-983.

**Sanders, N. L., Kothari, S., Huang, G., Salazar, G. and Cooks, R. G.** (2010). "Detection of Explosives as Negative Ions Directly from Surfaces Using a Miniature Mass Spectrometer." *Analytical Chemistry* **82**(12): 5313-5316.

**Scarff, C. A., et al** (2008). "Travelling wave ion mobility mass spectrometry studies of protein structure: biological significance and comparison with X-ray crystallography and nuclear magnetic resonance spectroscopy measurements." *Rapid Communications in Mass Spectrometry* **22**(20): 3297-3304.

**Shiea, J., Huang, M-Z., HSu, H-J., Lee, C-Y., Yuan, C-H., Beech, I., Sunner, J** (2005). "Electrospray-assisted laser desorption/ionization mass spectrometry for direct ambient analysis of solids." *Rapid Communications in Mass Spectrometry* **19**(24): 3701-3704.

**Shvartsburg, A. A., Smith, R.D.** (2008). "Fundamentals of Travelling Wave Ion Mobility Spectrometry." *Analytical. Chemistry.* **80**: 9689-9699.

**Stephens, W.** (1946). "Pulsed Mass Spectrometer with Time Dispersion." *Bulletin of the American Physical Society* **21**(2): 22.

**Svec, H. J.** (1985). "Mass spectroscopy-ways and means. A historical prospectus." *International Journal of Mass Spectrometry and Ion Processes* **66**(1): 3-29.

**Syka, J. E. P., Coon, J. J., Schroeder, M. J., Shabanowitz, J. and Hunt, D. F.** (2004). "Peptide and protein sequence analysis by electron transfer dissociation mass spectrometry." *Proceedings of the National Academy of Sciences of the United States of America* **101**(26): 9528-9533.

**Takats, Z., Cotte-Rodriguez, I., Talaty, N., Chen, H. and Cooks, R. G.** (2005). "Direct, trace level detection of explosives on ambient surfaces by desorption

electrospray ionization mass spectrometry." *Chemical Communications*(15): 1950-1952.

**Takats, Z., Wiseman, J. M., Gologan, B. and Cooks, R. G.** (2004). "Mass spectrometry sampling under ambient conditions with desorption electrospray ionization." *Science* **306**(5695): 471-473.

**Takáts, Z., Wiseman, J.M., Cooks, R.G.** (2005). "Ambient mass spectrometry using desorption electrospray ionization (DESI): instrumentation, mechanisms and applications in forensics, chemistry, and biology." *Journal of Mass Spectrometry* **40**(10): 1261-1275.

**Tanaka, K., Waki, H., Ido, Y., Akita, S., Yoshida, Y., Yoshida, T. and Matsuo, T.** (1988). "Protein and polymer analyses up to  $m/z$  100 000 by laser ionization time-of-flight mass spectrometry." *Rapid Communications in Mass Spectrometry* **2**(8): 151-153.

**Taylor, G.** (1964). "Disintegration of Water Drops in an Electric Field." *Proceedings of the Royal Society of London. Series A. Mathematical and Physical Sciences* **280**(1382): 383-397.

**Thalassinos, K., Grabenauer, M., Slade, S. E., Hilton, G. R., Bowers, M. T. and Scrivens, J. H.** (2008). "Characterization of Phosphorylated Peptides Using Traveling Wave-Based and Drift Cell Ion Mobility Mass Spectrometry." *Analytical Chemistry* **81**(1): 248-254.

**Thomson, J. J.** (1897). "Cathode Rays." *Philosophical Magazine* **44**: 293.

**Thomson, J. J.** (1911). "Rays of positive electricity " *Philosophical Magazine* **6**: 752-767.

**Thunig, J., Flø, L., Pedersen-Bjergaard, S., Hansen, S. H. and Janfelt, C.** (2012). "Liquid-phase microextraction and desorption electrospray ionization mass

spectrometry for identification and quantification of basic drugs in human urine." *Rapid Communications in Mass Spectrometry* **26**(2): 133-140.

**Trimpin, S., Wijerathne, K. and McEwen, C. N.** (2009). "Rapid methods of polymer and polymer additives identification: Multi-sample solvent-free MALDI, pyrolysis at atmospheric pressure, and atmospheric solids analysis probe mass spectrometry." *Analytica Chimica Acta* **654**(1): 20-25.

**Twohig, M., Shockcor, J. P., Wilson, I. D., Nicholson, J. K. and Plumb, R. S.** (2010). "Use of an Atmospheric Solids Analysis Probe (ASAP) for High Throughput Screening of Biological Fluids: Preliminary Applications on Urine and Bile." *Journal of Proteome Research* **9**(7): 3590-3597.

**Twohig, M., Skilton, S. J., Fujimoto, G., Ellor, N. and Plumb, R. S.** (2010). "Rapid detection and identification of counterfeit of adulterated products of synthetic phosphodiesterase type-5 inhibitors with an atmospheric solids analysis probe." *Drug Testing and Analysis* **2**(2): 45-50.

**Van Berkel, G. J. and Kertesz, V.** (2009). "Application of a Liquid Extraction Based Sealing Surface Sampling Probe for Mass Spectrometric Analysis of Dried Blood Spots and Mouse Whole-Body Thin Tissue Sections." *Analytical Chemistry* **81**(21): 9146-9152.

**Venter, A., Sojka, P. E. and Cooks, R. G.** (2006). "Droplet Dynamics and Ionization Mechanisms in Desorption Electrospray Ionization Mass Spectrometry." *Analytical Chemistry* **78**(24): 8549-8555.

**Volny, M., Venter, A., Smith, S. A., Pazzi, M. and Cooks, R. G.** (2008). "Surface effects and electrochemical cell capacitance in desorption electrospray ionization." *Analyst* **133**(4): 525-531.

**Wang, H., Liu, J., Cooks, R. G. and Ouyang, Z.** (2010). "Paper Spray for Direct Analysis of Complex Mixtures Using Mass Spectrometry." *Angewandte Chemie International Edition* **49**(5): 877-880.

**Wang, R., Gröhn, A., Zhu, L., Dietiker, R., Wegner, K., Günther, D. and Zenobi, R.** (2012). "On the mechanism of extractive electrospray ionization (EESI) in the dual-spray configuration." *Analytical and Bioanalytical Chemistry* **402**(8): 2633-2643.

**Weston, D. J., Bateman, R., Wilson, I. D., Wood, T. R. and Creaser, C. S.** (2005). "Direct Analysis of Pharmaceutical Drug Formulations Using Ion Mobility Spectrometry/Quadrupole-Time-of-Flight Mass Spectrometry Combined with Desorption Electrospray Ionization." *Analytical Chemistry*. **77**(23): 7572-7580.

**Wien, W.** (1898). "Untersuchungen über die electrische Entladung in verdünnten Gasen." *Annalen der Physik* **301**(6): 440-452.

**Wiley, W. C., McLaren, I.H.,** (1955). "Time-of-Flight Mass Spectrometer with Improved resolution." *Review of Scientific Instruments* **26**: 1150-1157.

**Williams, J., P. and Scrivens, J., H** (2008). "Coupling desorption electrospray ionisation and neutral desorption/extractive electrospray ionisation with a travelling-wave based ion mobility mass spectrometer for the analysis of drugs." *Rapid Communications in Mass Spectrometry* **22**(2): 187-196.

**Williams, J. P., Hilton, G.R., Thalassinou, K., Jackson, A.T., Scrivens, J.H.** (2007). "The rapid characterisation of poly(ethylene glycol) oligomers using desorption electrospray ionisation tandem mass spectrometry combined with novel product ion peak assignment software." *Rapid Communications in Mass Spectrometry* **21**(11): 1693-1704.

**Williams, J. P., Lock, R., Patel, V. J. and Scrivens, J. H.** (2006). "Polarity switching accurate mass measurement of pharmaceutical samples using desorption electrospray ionization and a dual ion source interfaced to an orthogonal acceleration time-of-flight mass spectrometer." *Analytical Chemistry* **78**(21): 7440-7445.

**Williams, J. P., Nibbering, N. M. M., Green, B. N., Patel, V. J. and Scrivens, J. H.** (2006). "Collision-induced fragmentation pathways including odd-electron ion formation from desorption electrospray ionisation generated protonated and deprotonated drugs derived from tandem accurate mass spectrometry." *Journal of Mass Spectrometry* **41**(10): 1277-1286.

**Williams, J. P., Patel, V.J., Holland, R., Scrivens, J.H.** (2006). "The use of recently described ionisation techniques for the rapid analysis of some common drugs and samples of biological origin." *Rapid Communications in Mass Spectrometry* **20**(9): 1447-1456.

**Williams, J. P., Scrivens, J.H.** (2005). "Rapid accurate mass desorption electrospray ionisation tandem mass spectrometry of pharmaceutical samples." *Rapid Communications in Mass Spectrometry* **19**(24): 3643-3650.

**Wiseman, J. M., Satu M. Puolitaival Zoltán Takáts R. Graham Cooks Richard M. Caprioli** (2005). "Mass Spectrometric Profiling of Intact Biological Tissue by Using Desorption Electrospray Ionization13." *Angewandte Chemie International Edition* **44**(43): 7094-7097.

**Wittmer, D., Chen, Y. H., Luckenbill, B. K. and Hill, H. H.** (1994). "Electrospray Ionization Ion Mobility Spectrometry." *Analytical Chemistry* **66**(14): 2348-2355.

**Wu, C., Ifa, D. R., Manicke, N. E. and Cooks, R. G.** (2009). "Rapid, Direct Analysis of Cholesterol by Charge Labeling in Reactive Desorption Electrospray Ionization." *Analytical Chemistry* **81**(18): 7618-7624.

**Wu, C., Siems, W. F. and Hill, H. H.** (1999). "Secondary Electrospray Ionization Ion Mobility Spectrometry/Mass Spectrometry of Illicit Drugs." *Analytical Chemistry* **72**(2): 396-403.

**Wu, C., Siems, W. F., Klasmeier, J. and Hill, H. H.** (1999). "Separation of Isomeric Peptides Using Electrospray Ionization/High-Resolution Ion Mobility Spectrometry." *Analytical Chemistry* **72**(2): 391-395.

**Wu, Z., Chingin, K., Chen, H., Zhu, L., Jia, B. and Zenobi, R.** (2010). "Sampling analytes from cheese products for fast detection using neutral desorption extractive electrospray ionization mass spectrometry." *Analytical and Bioanalytical Chemistry* **397**(4): 1549-1556.

**Yamashita, M. and Fenn, J. B.** (1984). "Electrospray ion source. Another variation on the free-jet theme." *The Journal of Physical Chemistry* **88**(20): 4451-4459.

**Zhou, Z., Jin, M., Ding, J., Zhou, Y., Zheng, J. and Chen, H.** (2007). "Rapid detection of atrazine and its metabolite in raw urine by extractive electrospray ionization mass spectrometry." *Metabolomics* **3**(2): 101-104.

**Zubarev, R. A., Kelleher, N. L. and McLafferty, F. W.** (1998). "Electron Capture Dissociation of Multiply Charged Protein Cations. A Nonergodic Process." *Journal of the American Chemical Society* **120**(13): 3265-3266.

**Zydel, F., Trimpin, S. and McEwen, C.** (2010). "Laserspray ionization using an atmospheric solids analysis probe for sample introduction." *Journal of the American Society for Mass Spectrometry* **21**(11): 1889-1892.

## **Chapter 2**

### **Materials and Methods**



## **2.1 Materials**

### **2.1.1 Reagents**

High-grade chemical reagents including high purity water, formic acid, acetonitrile and methanol were obtained from J.T.Baker (Phillipsburg, NJ, USA). Tetrahydrofuran, polyalanine, alpha-cyano-4-hydroxycinnamic acid, 2,5-hydroxybenzoic acid, sodium iodide, caesium iodide, trifluoroacetic acid were purchased from Sigma-Aldrich (Gillingham, UK). Lithium chloride was acquired from ACROS Organics (Geel, Belgium).

### **2.1.2 Pharmaceutical samples**

Salbutamol sulphate was acquired with prescription, Deep Heat spray (The Mentholatum Co, Twyford, UK), AAA Sore Throat Spray (Manx Healthcare LTD, Warwick, UK), Vicks Sinex Decongestant (Proctor and Gamble, Weybridge, UK), Sudafed (McNeil products LTD, Maidenhead, UK) and Anadin Extra (Wyeth, UK) were all acquired commercially without prescription. Standards and isomers of methyl nicotinate and benzocaine were purchased from Sigma-Aldrich (Gillingham, UK) and Fluka (Gillingham, UK). Structures, formulae and exact mass information for the active pharmaceutical ingredients are shown in Figure 2.1.

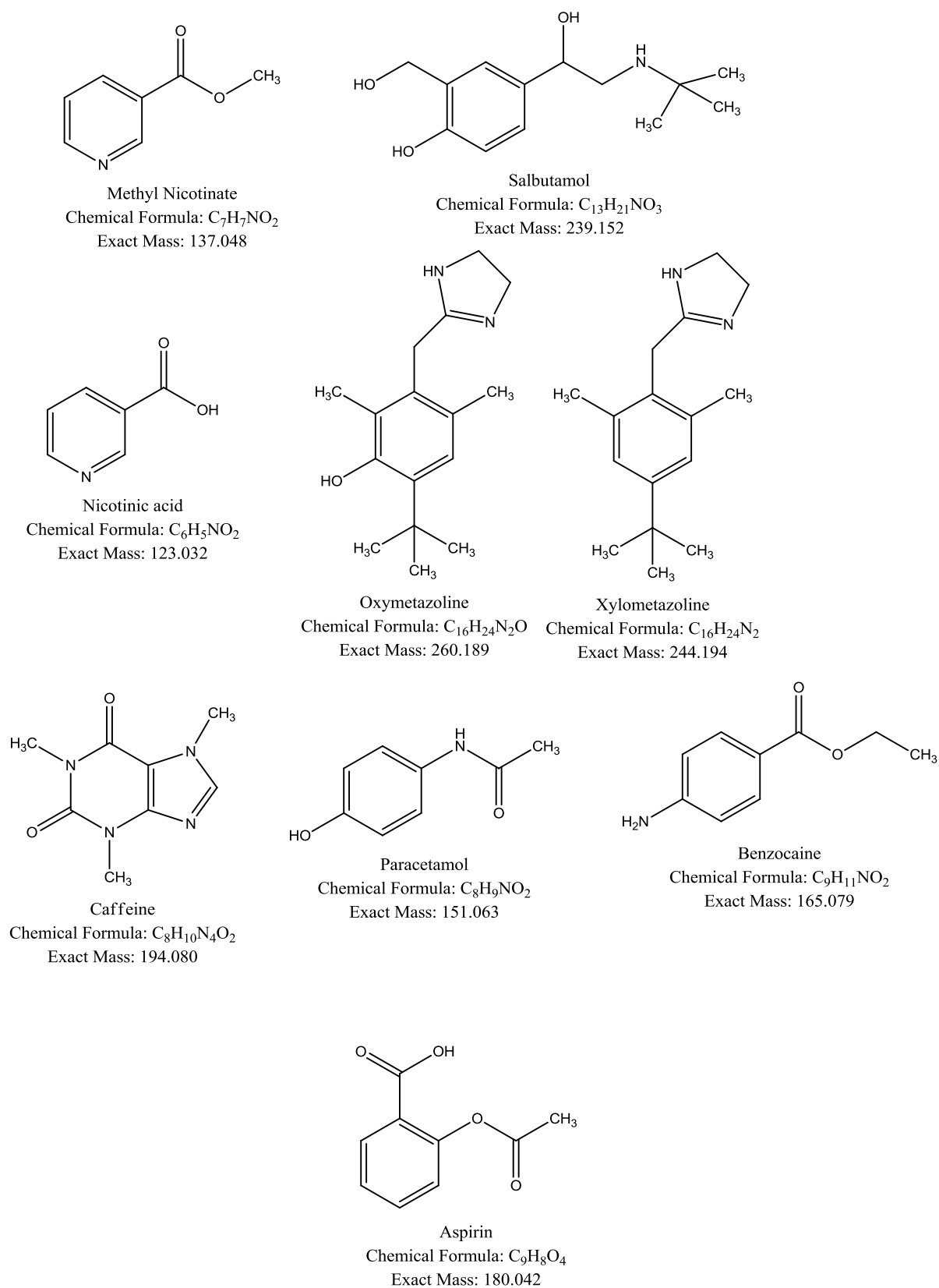


**Figure 2.1** - Structures, formulae and exact mass for active ingredients studied

### 2.1.3 Polymer Samples

Tyloxapol, PEG 1000 and complex polysorbate formulations (Tween 20, Tween 40, Tween 60, Tween 80) were purchased from Sigma-Aldrich (Gillingham, UK). The polyrotaxane sample was synthesized by acyclic diene metathesis polymerization as described by Momčilović *et al.* (Momčilović, Clark et al. 2011), and was generously donated by Dr Momčilović, Dr Paul Clark, Dr Andrew Boydston and Professor Robert Grubbs of the Californian Institute of Technology (Pasadena, USA). No single structure can accurately represent the complexity of these formulations.

## **2.2 Methods**

### **2.2.1 Ion mobility mass spectrometer instrument**

All samples investigated within this thesis were analysed by means of the Synapt G2 HDMS system (Waters, Manchester, UK). This instrument was used to perform mass spectrometry (MS), tandem MS (MS/MS) and travelling wave ion mobility (TWIM) experiments. The time of flight (ToF) analyser within the Synapt G2 instrument has three modes of operation. The ToF analyser has a resolution of around 10000 in sensitivity mode, 20000 in resolution mode and 40000 in high resolution mode. All experimental data within this thesis were acquired in resolution mode with a resolution of around 20000.

The Synapt G2 is equipped with a number of ionisation sources including electrospray ionisation (ESI), matrix assisted laser desorption ionisation (MALDI) and the atmospheric pressure solids analysis probe (ASAP). Those ambient ionisation techniques that are based on ESI or atmospheric pressure chemical ionisation (APCI) can be easily performed on the instrument. Information on how to prepare samples and the methodology for each ionisation technique is given in the relevant sections in this chapter.

## **2.2.2 Calibration of Synapt G2**

### **2.2.2.1 Calibration of mass analyser**

Mass calibration was performed by dissolving 1 mg of sodium iodide in 1 ml of 50% aqueous methanol/ 0.1% formic acid for ASAP, DESI, ESI and TA-EESI experiments. Sodiated PEG was used to mass calibrate MALDI experiments and was prepared in 3.6 mg/mL  $\alpha$ -cyano matrix in 50 % acetonitrile 49.95 % water 0.05 % trifluoroacetic acid.

### **2.2.2.2 Calibration of ion mobility cell**

As was mentioned in Chapter 1, the nature of travelling wave ion mobility spectrometry (TWIMS) means that absolute collision cross-sections of ions cannot be obtained directly from an ions drift time. This is in contrast to drift cell ion mobility spectrometry (DCIMS) where it is possible to directly measure an analytes collision cross section from its drift time. It has been shown that estimates of collision cross-sections can be made by calibrating the TWIMS instrument with calibrants of known cross-sections (Ruotolo, Benesch et al. 2008; Thalassinos, Grabenauer et al. 2009), assuming that the experimental conditions are identical to those conditions utilised when analysing samples. The Synapt G2 has three main parameters that can affect how long an ion spends within the mobility cell. These are the pressure of the counter flowing buffer gas within the cell, the height of the travelling wave, and the velocity of the travelling wave. The pressure of the counter flowing buffer gas was not changed in any experiment.

The calibration method used during this PhD research is an in-house procedure utilising polyalanine. Polyalanine is a polymeric species with known cross sections for its individual oligomers. Polyalanine is directly infused into the instrument by means of electrospray ionisation (ESI) for mobility experiments that utilised ESI, extractive-ESI (EESI) and ASAP ionisation methods for sample introduction, and introduced via MALDI for MALDI-mobility experiments.

1 milligram of polyalanine is dissolved in 1ml of solvent for an ESI calibration. The solvent utilised to dissolve polyalanine during the PhD research was 50% aqueous methanol/ 0.1% formic acid. 250  $\mu$ l of the solvent sample solution is then drawn by syringe, and injected into the ESI source with a flow rate of 5  $\mu$ l/min. The capillary voltage is set to 3.3 kV, the sample cone voltage to 40 volts, and the source temperature is set to 80 °C.

When a sample is to be ionised by MALDI, then the calibration should also be performed with MALDI as the ionisation technique. 20 milligrams of polyalanine is dissolved in 50% aqueous methanol/ 0.1% formic acid to form the analyte solution. The matrix solution is prepared by dissolving 6 mg of  $\alpha$ -cyano-4-hydroxycinnamic acid in 1 ml of a solution of acetonitrile/tetrahydrofuran (7:1, v/v). The sample solution is composed of a 1:1 ratio, v/v of the previously mentioned analyte and matrix solutions. 1  $\mu$ l of this sample solution is transferred onto each well of the MALDI sample holder. The plate is then presented to the MALDI source, and the laser set to just above threshold.

A series of oligomers is selected to span the experimental mobility space for each specific analyte. For instance, if the chemistry of an analyte suggests that the collision cross section of its gas phase ion would likely be around 150 Å<sup>2</sup>, then it would be appropriate to select oligomers of known cross section of between 100-200 Å<sup>2</sup>. A calibration curve of arrival time versus known cross section of a specific oligomer can be generated for the polyalanine series. Subsequent to this, estimates of cross sections of compounds with an unknown cross section can then be made. In the research presented in this thesis, a linear series was used to generate the calibration curve. It should be noted that more accurate estimations of collision cross section for large molecules, such as proteins would be made by fitting a power series to the data.

### **2.2.3 Analysis of Pharmaceutical Samples**

Pharmaceutical formulations were analysed by use of four different ionisation processes – (ASAP), (ESI), (MALDI) and thermally assisted – EESI (TA-EESI).

#### **2.2.3.1 ASAP analysis of pharmaceutical formulations**

An in depth explanation of ASAP is given in chapter 1, section 1.8.2.1. The ASAP probe that was used to analyse the pharmaceutical formulations has been modified to fit onto Waters instrumentation. The ASAP source is composed of three parts. The outer assembly is fixed to the source housing. The inner probe can be removed and reinserted for each experiment.

The method used to place analytes onto the glass capillary is dependent on the sample type. Solid pharmaceutical samples, such as tablets were broken in half, and then the glass capillary was swiped across the surface of the tablet. Medicinal sprays were sampled by initially spraying into a centrifuge tube. Subsequent to this, the glass capillary was then dipped into the centrifuge tube. Post sampling, the capillary was inserted in the inner probe tip.

The main ionisation parameters for an ASAP experiment are the corona discharge, the desolvation gas temperature, the desolvation gas temperature and the corona discharge current. The corona discharge current was set at 5 $\mu$ A for all positive and negative mode experiments. The desolvation gas temperature was ramped between 50-600°C and desolvation gas flow rate was ramped between 200-1200L/hr. Other ionisation settings that needed to be considered are the source block temperature and cone voltage. It was observed that a cone voltage set at 40 volts, resulted in the most efficient transfer of ions generated from pharmaceutical formulations. The source block temperature was ramped between 120-150°C. ASAP is a unique technique in that both protonated and radical cations can be produced, and this is a function of the water content present with the source atmosphere. In some cases, it was required to infuse solvent into the source atmosphere to promote protonation. This was achieved by infusing a solvent composed of 50% aqueous methanol 0.1% formic acid via the LockSpray line found on the source housing, at a flow rate of 5 $\mu$ L. The LockSpray

source is normally used to infuse a mass calibrant, to maintain calibration of the instrument during data acquisition.

During ASAP analysis of pharmaceutical formulations the mass range of the mass analyser was set between  $m/z$  50 -2000. For MS/MS experiments the collision energy in the transfer cell was set to between 20 to 30 volts for all active ingredients present within the formulation and between 10 to 45 volts for excipients. In experiments that utilised ion mobility, the separation was performed with a travelling – wave (T-Wave) height of 40 volts, and a T-Wave velocity of 1800 m/s. Data acquisition and processing were carried out using MassLynx (v4.1) software (Waters, Manchester, UK).

#### **2.2.3.2 DESI analysis of pharmaceutical formulations**

An in depth explanation of DESI is given in chapter 1, section 1.8.1.1. During the course of the PhD, DESI was only utilised for the analysis of medicinal spray formulations. These formulations were sprayed onto a 3 by 3 cm corrugated fibreboard and allowed to dry. This sample infused cardboard was then placed into the source region of an electrospray source at an angle of approximately 45 ° to the ESI spray and a distance of 5-10 mm from the sample cone. The solvent that was delivered via the ESI spray to the cardboard was composed of 50% aqueous methanol 0.1% formic acid. The ESI capillary had a voltage of 3.3 kilovolts. This resulted in the generation of secondary analyte ions which were directed into the sample cone of the mass spectrometer. The sample cone had a voltage of between 30 to 50 volts which was dependent on the sample type. Within the mass analyser, the range was set between  $m/z$  50-2000. MS/MS experiments were carried out when the transfer cell was set to 30 volts. No ion mobility experiments were performed with DESI as the ionisation source. Data acquisition and processing were carried out using MassLynx (v4.1) software (Waters, Manchester, UK).



### 2.2.3.3 ESI analysis of pharmaceutical formulations

An in depth explanation of ESI is given in chapter 1, section 1.3.2. ESI was performed on two types of pharmaceutical formulation - medicinal spray formulations and tablet formulations.

Medicinal spray formulations were prepared by initially spraying into a centrifuge tube. 10 µl of the formulation was then transferred into 990 µl of 50% aqueous methanol 0.1% formic acid. 1 µl of this solution was further diluted by transferring into 999 µl of 50% aqueous methanol 0.1% formic acid, to make a 1 in 100000 dilution. Tablets were crushed, and 1 mg of each tablet was dissolved in 1 ml of 50% aqueous methanol 0.1% formic acid.

Both types of samples were sprayed into the source at a flow rate of 5 µl/minute and a capillary voltage that was optimised between 3.3 to 3.5 kilovolts depending on sample. The sample cone was set to 40 volts in all instances.

During ESI analysis of pharmaceutical formulations the mass range of the mass analyser was set between  $m/z$  50 -2000. For MS/MS experiments the collision energy in the transfer cell was set to between 20 to 30 volts for all active ingredients present within the formulation and between 10 to 45 volts for excipients. In experiments that utilised ion mobility, the separation was performed with a travelling – wave (T-Wave) height of 40 volts, and a T-Wave velocity of 1800 m/s. Data acquisition and processing were carried out using MassLynx (v4.1) software (Waters, Manchester, UK).

#### 2.2.3.4 TA-EESI analysis of pharmaceutical formulations

An in depth explanation of EESI and TA-EESI are given in chapter 1, section 1.8.1.2. The TA-EESI experimental approach consisted of a sample bottle with a cap that could be removed easily. Inserted in this cap were two Teflon tubes, which allowed the desolvation gas for the ESI source to flow in and out. These were made air tight by a silicon based rubber. The EESI experiment was similar to the design utilised by Chen and Zenobi (Chen, Sun et al. 2007). Figure 2.2 shows a photograph of the basic construction. The TA-EESI approach places a heat block under the sample container

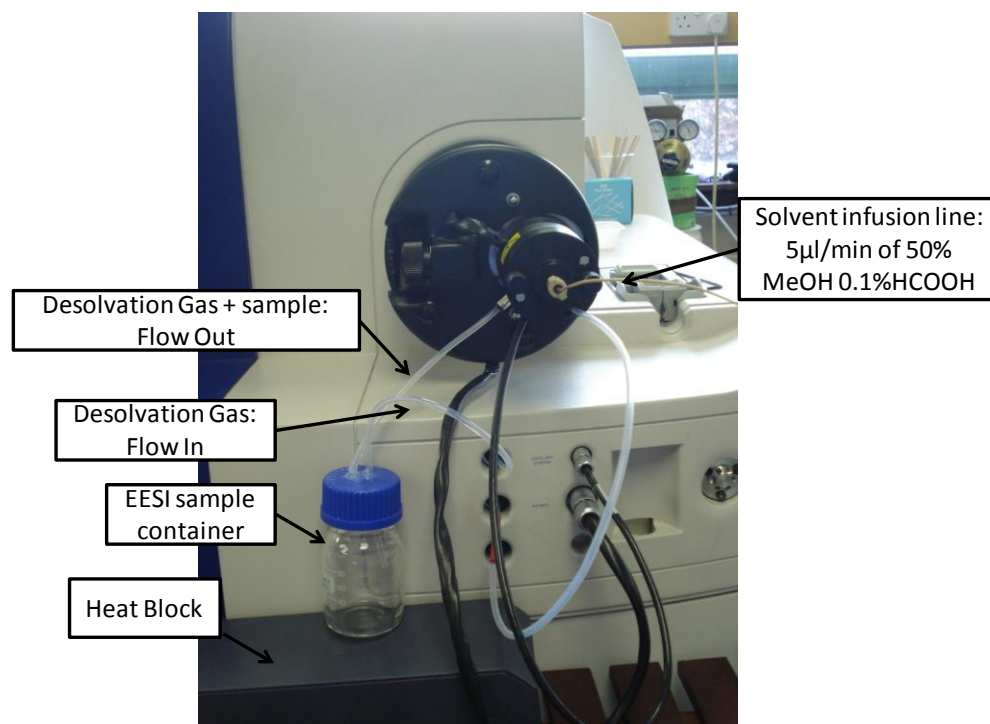


**Figure 2.2** - Photograph of EESI setup.

Only spray formulations were analysed using this approach. These were sampled simply by spraying one recommended dose into the sample container.

TA-EESI experiments were carried out by heating the sample bottle on a hotplate (FisherScientific, UK) between ambient temperature and 500°C in 50°C intervals. All samples were analysed by means of TA-EESI for approximately ten seconds at each temperature interval. The measured temperature, obtained from a thermocouple

inserted into the sample bottle, differed from the indicated hot plate temperature as a result of the cooling effect of the desolvation gas, with higher flow rates having larger cooling effects. The desolvation gas flow rate was set between 150 to 1000 L/hr. A thermocouple probe (HANNA instruments, Bedfordshire, UK) was used to determine the precise temperature used within each experiment. The cone voltage was set to 40 volts with a capillary voltage of 3.3 kilovolts. The ESI solvent was composed of 50% aqueous methanol 0.1% formic acid

During TA-EESI analysis of the medicinal spray formulations the mass range of the mass analyser was set between  $m/z$  50 -2000. For MS/MS experiments the collision energy in the transfer cell was set to between 20 to 30 volts for all active ingredients present within the formulation and between 10 to 45 volts for excipients. In experiments that utilised ion mobility, the separation was performed with a travelling – wave (T-Wave) height of 40 volts, and a T-Wave velocity of 1800 m/s. Data acquisition and processing were carried out using MassLynx (v4.1) software (Waters, Manchester, UK).

#### **2.2.4 Analysis of Tween and tyloxapol formulations**

The experimental conditions utilised for the analysis of Tween (a brand of polysorbate emulsifiers) and tyloxapol formulations were the same, and thus both have been grouped together. Four ionisation techniques were used for the analysis of these formulations – ASAP, ESI, MALDI and TA-EESI

##### **2.2.4.1 ASAP analysis of Tween and tyloxapol formulations**

Tween and tyloxapol formulations are both very viscous. These formulations were transferred onto the glass capillary by use of a spatula. The corona current was set at 5 $\mu$ A for the analysis of Tween and tyloxapol formulations (these formulations were only analysed in positive mode). Due to the non-volatile nature of the polymer species present within the Tween and tyloxapol formulations, the desolvation gas temperature was set at the maximum of 600°C and desolvation gas flow rate was ramped between 1000-1200L/hr. The source block temperature was set at 150°C and the cone voltage was set at 40 volts. This was achieved by infusing a solvent

composed of 50% aqueous methanol 0.1% formic acid via the LockSpray line found on the source housing, at a flow rate of 5 $\mu$ L. The mass analyser range was set between  $m/z$  50 – 2000. Separation in the ion mobility cell was carried out using a T-Wave height of 40 volts and a velocity of 600m/s in full scan mode. During MS/MS acquisition the T-Wave velocity was reduced to 400m/s, with all collision induced dissociation (CID) experiments taking place in the transfer cell, after precursor ion separation in the mobility cell. Data acquisition and processing were carried out using MassLynx (v4.1) software (Waters, Manchester, UK).

#### **2.2.4.2 ESI analysis of Tween and tyloxapol formulations**

Tween and tyloxapol samples were prepared by dissolving 1 mg in 1 ml in two different solvents. The first was 50% aqueous methanol 0.1% formic acid solvent, and the second with 50% aqueous methanol 0.5% lithium chloride. The samples had a capillary voltage optimised between 1.2 to 1.4 kilovolts with a sample cone voltage of 80 V when nanoflow ESI experiments were performed. Standard flow experiments had a capillary voltage of between 3.3 to 3.5 kilovolts and a sample cone voltage of 40V. A trap DC bias was changed from the default of 45 up to 60 volts during ESI analysis, to maintain sensitivity between mobility and non-mobility mode. Separation in the ion mobility cell was carried out using a T-Wave height of 40 volts and a velocity of 600m/s in full scan mode. During MS/MS acquisition the T-Wave velocity was reduced to 400m/s, with all collision induced dissociation (CID) experiments taking place in the transfer cell, after precursor ion separation in the mobility cell. Data acquisition and processing were carried out using MassLynx (v4.1) software (Waters, Manchester, UK).

#### **2.2.4.3 MALDI analysis of Tween and tyloxapol formulations**

Sample preparation for MALDI analysis of Tween and tyloxapol formulations was adapted and improved from a method developed by Ayorinde et al (Ayorinde, Gelain et al. 2000). The matrix solution employed was composed of 6 mg of alpha-cyano-4-hydroxycinnamic acid, which had been dissolved in 1 mL of acetonitrile/tetrahydrofuran (7:1, v/v). 20 mg of each Tween sample was dissolved in 1 mL of 50 % MeOH 40 % H<sub>2</sub>O 10% LiCl to prepare the analyte solution. The

sample solution was composed of a (1:1, v/v) of matrix and analyte solutions. 1 µl of the sample solution was then spotted onto the sample plate for MALDI ionisation. The energy of the MALDI laser was set at just above threshold. The Trap DC bias was set at 60 volts for the MALDI experiments. Separation in the ion mobility cell was carried out using a T-Wave height of 40 volts and a velocity of 600m/s in full scan mode. During MS/MS acquisition the T-Wave velocity was reduced to 400m/s, with all collision induced dissociation (CID) experiments taking place in the transfer cell, after precursor ion separation in the mobility cell. Data acquisition and processing were carried out using MassLynx (v4.1) software (Waters, Manchester, UK).

#### **2.2.4.4 TA-EESI analysis of Tween and tyloxapol formulations.**

A spatula transferred a small amount of the polymeric formulation into the sample containing bottle. The optimal temperature of for these formulations was when the heat pad was set at maximum (500 °C), and the flow rate of the gas was set at 1000 L/hr. The ESI solvent was composed of either 50% aqueous methanol 0.1% formic acid, or 50% methanol, 40% water and 10% lithium chloride. The cone voltage was set to 40 volts and the capillary voltage was set to 3.3 kilovolts. The mass analyser was set to detect ions with  $m/z$  between 50 – 2000. The collision energy in the transfer cell was set between 40 – 60 volts during MS/MS experiments. No ion mobility experiments were performed using TA-EESI for the analysis of Tween and tyloxapol formulations. Data acquisition and processing were carried out using MassLynx (v4.1) software (Waters, Manchester, UK).

### **2.2.5 Analysis of Polyrotaxane formulation**

The ionisation techniques utilised for the analysis of polyrotaxane formulations were ESI and MALDI

#### **2.2.5.1 Analysis of polyrotaxane formulations by ESI**

Optimisation for the sample preparation of the novel polyrotaxane system was carried out by collaborators at the University of Arkansas. It was determined that the best method for ESI analysis was to dissolve 0.5 mg in 1 ml of methanol. This was confirmed at Warwick by in – house preparation. Due to the small quantity of sample, nanoflow ESI was utilised. The sample cone was optimised to 80 volts, while the capillary voltage was optimised to 1.3 kilovolts.

CID-IMS-CID experiments, which utilise CID fragmentation in the trap and transfer cells, coupled with separation in the mobility cell, termed time-aligned-parallel (TAP) fragmentation experiments, were performed to provide additional characterization of components within the polyrotaxane system. The collision energy utilised in either the trap or transfer cell was ramped between 80 – 120 volts. Ion mobility experiments were conducted with a travelling-wave height of 40 volts and a travelling-wave velocity of 400 m/s. Data acquisition and processing were carried out using MassLynx (v4.1) software (Waters, Manchester, UK).

#### **2.2.5.2 Analysis of polyrotaxane formulations by MALDI**

Optimisation for the sample preparation of the novel polyrotaxane system was carried out by collaborators at the University of Arkansas. 1 mg of polyrotaxane sample was dissolved in 1 mL of 55 mg/mL 2,5-dihydroxybenzoic acid (DHB) in methanol and aliquoted onto a stainless steel MALDI target plate. The energy of the laser was set just above threshold.

CID-IMS-CID experiments, which utilise CID fragmentation in the trap and transfer cells, coupled with separation in the mobility cell, termed time-aligned-parallel (TAP) fragmentation experiments, were performed to provide additional

characterization of components within the polyrotaxane system. The collision energy utilised in either the trap or transfer cell was ramped between 80 – 120 volts. Ion mobility experiments were conducted with a travelling-wave height of 40 volts and a travelling-wave velocity of 400 m/s. Data acquisition and processing were carried out using MassLynx (v4.1) software (Waters, Manchester, UK).

## **2.4 Benzocaine purity assay by gas chromatography – MS (GC-MS)**

GC-MS analysis to assay purity of benzocaine was performed on a VG Trio-1 (VG/Micromass/Waters, Manchester, UK). The non polar column consisted of a phenyl arylene polymer (J & W Scientific, Folsom, USA). A temperature gradient was set up, and started at 50 °C increasing at a rate of 10 °C per minute up to 200 °C. The temperature remained at 200 °C for 5 minutes, and was subsequently decreased by 10 °C per minute down to 50 °C. The quadrupole on this machine as unit mass resolution, and the quadrupole mass analyzer scanned between 50 to 200 *m/z*. The electron energy was set to 70 eV. Data acquisition and processing were carried out using MassLynx (v4.1) software (Waters, Manchester, UK)

## **2.5 Modelling**

The collision cross-sections of benzocaine and its isomers were theoretically calculated by computational modelling and measured experimentally from ion mobility data. Computer modelling was carried out by collaborators at the University of California, Santa Barbara using Gaussian (Gaussian, Inc., Wallingford, CT, USA), which is a commercially available modelling software.

Briefly, geometry optimization calculations were performed on benzocaine and the meta and ortho isomers of benzocaine using the Gaussian 03 (G03) (Gaussian, Inc., Wallingford, CT, USA) program package employing the DFT method with the B3LYP and PBE1PBE functionals. The split-valence 6-311G\*\*++ basis set was applied with both functionals, while in the case of the B3LYP, the AUG-cc-p-VDZ was also used. Geometry optimizations were performed in the gas phase and the nature of all stationary points was confirmed by normal-mode analysis. These calculations were also performed on benzocaine molecules which had been

protonated on the nitrogen lone pair of electrons, the carbonyl oxygen and each of the carbon atoms in the aromatic ring. Rotationally-averaged collision cross-sections were calculated for the structures obtained by use of MOBCAL with the trajectory method employed.



## 2.6 References

**Ayorinde, F. O., Gelain, S. V., Johnson, J. H. and Wan, L. W. (2000).** "Analysis of some commercial polysorbate formulations using matrix-assisted laser desorption/ionization time-of-flight mass spectrometry." *Rapid Communications in Mass Spectrometry* 14(22): 2116-2124.

**Chen, H., Sun, Y., Wortmann, A., Gu, H. and Zenobi, R. (2007).** "Differentiation of Maturity and Quality of Fruit Using Noninvasive Extractive Electrospray Ionization Quadrupole Time-of-Flight Mass Spectrometry." *Analytical Chemistry* 79(4): 1447-1455.

**Momčilović, N., Clark, P. G., Boydston, A. J. and Grubbs, R. H. (2011).** "Facile synthesis of polyrotaxanes via acyclic diene metathesis polymerization of supramolecular monomers." *Journal of the American Chemical Society*: Submitted.

**Ruotolo, B. T., Benesch, J. L., Sandercock, A. M., Hyung, S. J. and Robinson, C. V. (2008).** "Ion mobility-mass spectrometry analysis of large protein complexes." *Nature Protocols* 3(7): 1139-1152.

**Thalassinos, K., Grabenauer, M., Slade, S. E., Hilton, G. R., Bowers, M. T. and Scrivens, J. H. (2009).** "Characterization of Phosphorylated Peptides Using Traveling Wave-Based and Drift Cell Ion Mobility Mass Spectrometry." *Analytical Chemistry* 81(1): 248-254.

## **Chapter 3**

# **Pharmaceutical Formulations**

### **3.1 Pharmaceutical formulations**

A pharmaceutical formulation consists of one or more active pharmaceutical ingredients and a number of excipient ingredients. These excipients may aid in drug delivery, or act as binders, disintegrants, diluents, glidants, emulsifying-solubilising agents, sweetening agents, coating agents or antimicrobial preservatives. Pharmaceutical formulations can be delivered by a number of mediums including, aerosols, tablets, capsules, creams and gels.

### **3.2 Characterisation of Pharmaceutical formulations**

The characterisation of pharmaceutical formulations should provide information on the identity, purity, quantity, content and stability of starting materials, excipients and active ingredients. Characterisation techniques are required for the drug discovery process through to development, and for quality control and counterfeit detection purposes.

Titrimetric methods are widely used for the analysis of pharmaceuticals mainly to determine the purity of a sample (Hansen, Pedersen-Bjergaard et al. 2011). Suppliers of raw starting materials often provide a specified purity that has been assayed titrimetrically. These methods are inexpensive to perform but are non-selective and require large amounts of sample.

UV and visible spectroscopy can be used to determine the quantity of active ingredients in formulations, reaction kinetics of drug degradation and for the determination of partition coefficients and solubilities of active ingredients. These techniques are easy to use and cost less than a number of techniques, but are limited to very simple formulations as excipients can interfere with the analysis due to the non-selective nature of such techniques (Görög, Rényi et al. 1989).

Nuclear magnetic resonance (NMR) spectroscopy is a powerful technique, and can be used to determine impurities and the exact structures of raw materials and finished products (Powers 2009). The technique suffers from significantly lower

sensitivity than other approaches and can sometimes have difficulty in identifying true components in complex mixtures.

### **3.3 Characterisation by Mass Spectrometry**

Mass spectrometry is a highly specific method for the determination and/or confirmation of the identity and structure of active ingredients and excipients (Klyuev 2002). When coupled to liquid chromatography (LC) or gas chromatography (GC), separation of components in a formulation can be achieved prior to  $m/z$  determination. This can provide an additional dimension of characterisation. MS is arguably the most widely used analytical chemistry technique in drug discovery and development. ESI-MS is often used for quality control purposes in therapeutic antibody and peptide manufacture (Janin-Bussat, Strub et al. 2010). The technique can be limited by higher costs. Significant data can be generated for complex samples by MS, but can often be limited by the extensive clean ups that may be required prior to analysis.

### **3.4 Characterisation of pharmaceuticals by ambient ionisation**

The development of a number of ambient ionisation techniques was facilitated by the analysis and characterisation of pharmaceutical formulations, and this presents the most widely studied application area of ambient ionisation techniques within the literature.

Desorption electrospray ionisation (DESI) has been used for the direct analysis of pharmaceutical formulations (Williams 2005; Jackson 2006; Williams, Lock et al. 2006; Williams, Nibbering et al. 2006; Williams and Scrivens 2008). A number of studies have evaluated the use of DESI to desorb active pharmaceutical ingredients that have been separated by thin layer chromatography (TLC) (Van Berkel and Kertesz 2006; Harry, Reynolds et al. 2009). DESI has also been used to identify pharmaceuticals and their metabolites in biological matrices including blood and urine (Kauppila, Wiseman et al. 2006; Huang, Chen et al. 2007; Kauppila, Talaty et al. 2007).

Extractive electrospray ionisation (EESI) has also been used to characterise pharmaceutical formulations (Williams and Scrivens 2008; Li, Hu et al. 2009; Gu, Hu et al. 2010; Meier, Berchtold et al. 2012; Meier, Berchtold et al. 2012). Online reaction monitoring for ethyl salicylate to salicylic acid by EESI has been demonstrated (McCullough, Bristow et al. 2011).

ASAP has been used to characterise medicinal steroids (Ray, Hammond et al. 2010) and to identify and differentiate between authentic and counterfeit phosphodiesterase inhibitors (Twohig, Skilton et al. 2010).

The interest in the direct analysis in real time (DART) technique in the pharmaceutical industry is demonstrated by a recent review on this specific technique and application area (Chernetsova and Morlock 2011). Specific examples of the DART technique for pharmaceutical analysis include its use in the routine and counterfeit identification of common prescribed antibiotics (Samms, Jiang et al. 2011), the quantification of a number of pharmaceuticals in plasma including anti-arrhythmics (Zhao, Lam et al. 2008), and for the detection of active pharmaceutical ingredients found in traditional Chinese medicines (Li, Wang et al. 2012). The plasma assisted desorption ionisation (PADI) technique has been compared to DESI for the surface analysis of pharmaceutical tablets (Ratcliffe, Rutten et al. 2007). Paper spray ionisation (PSI) has been evaluated for the quantification of pharmaceuticals in blood spots (Manicke, Abu-Rabie et al. 2011; Zhang, Xu et al. 2012).

### **3.5 Ion mobility mass spectrometry (IM-MS) in pharmaceutical analysis**

Ion mobility spectrometry (IMS) has been used as a standalone technique within the pharmaceutical industry mainly for verification of cleaning procedures for manufacturing equipment to prevent cross contamination with subsequent batches (O'Donnell, Sun et al. 2008). IMS has also been used to isolate pharmaceuticals from analogues, an example being the separation of a drug used in the treatment of Parkinson's disease from an isobaric molecule (Creaser, Griffiths et al. 2000).

IM-MS can bring an additional level of characterisation to pharmaceutical analysis, with selectivity increasing the confidence of identification of unknowns that may have been separated by ion mobility. MS analysis of pharmaceutical formulations can result in complex spectra, and often the pharmaceutical scientist may only be interested in the active pharmaceutical agent. IM-MS can simplify the spectra obtained. Both DESI (Weston, Bateman et al. 2005; Williams and Scrivens 2008; Harry, Reynolds et al. 2009) and ND-EESI (Williams and Scrivens 2008) techniques have been coupled with mobility separation for the characterisation of pharmaceutical formulations.

### **3.6 Aims**

Two ambient ionisation techniques were used to generate the data presented in this chapter. These techniques were also coupled with IM-MS to increase the level of information obtained. Specific aims of the research presented in this chapter were:

1. To develop and evaluate the capabilities of a modification of EESI. This modification will be utilised to analyse pharmaceutical formulations containing components of differing volatilities. There is a requirement within the pharmaceutical industry to be able to rapidly analyse formulations with components of differing volatility, but without resulting in sample carryover.
2. To couple the modified technique with IM-MS. This has the potential to both separate out species on the millisecond timescale, and to generate additional information, such as gas – phase conformation.
3. To evaluate the ASAP technique for pharmaceutical formulation analysis. The ASAP technique can enable both radical cation and protonated molecular ion formation simultaneously, rapidly and without sample preparation. There is the potential to compare ASAP generated spectra with EI library databases
4. To couple the ASAP technique with IM-MS to generate additional information, and to separate out ions on the millisecond timescale

### **3.7 Development of thermally assisted – extractive electrospray ionisation (TA-EESI)**

The predominant form of EESI within the literature is that which was first introduced by Huanwen Chen while at the Cooks lab (Chen 2006), whereby a nebulised spray is introduced into an ESI plume. Chen later moved to Zenobi's group, and introduced a variation of EESI whereby samples were placed into an airtight bottle and desolvation gas introduced, which upon leaving, can carry neutral sample gas and/or vapour which is then directed into the ESI plume (Chen, 2007). The sample must contain volatile components to fill the headspace. This EESI experiment is the easiest to use, and can be performed on almost any instrument that has an ESI source. The modification of the source is not time-consuming and can be carried out in a couple of minutes. The major disadvantage is that the sample must contain components volatile enough to fill the headspace.

A simple modification developed here termed thermally assisted EESI (TA-EESI) was evaluated. The sample container was heated by placing upon a hot plate. The temperature of the hotplate used in these experiments was limited up to 500 °C and could be increased in intervals of 50 °C. The temperature within the container differs from the temperature indicated on the hotplate due to the cooling effect of the desolvation gas. Higher flow rates have larger cooling effects. A thermocouple probe was used to determine a more accurate temperature for specific flow rates and hot plate settings.

### 3.7.1 TA-EESI of Salbutamol

Salbutamol sulphate is an active ingredient found in asthma inhalers and consists of two salbutamol molecules and a sulphate group. When salbutamol spray was analysed by means of extractive electrospray (EESI) at ambient temperature initially, only background ions were detected (Figure 3.1A). By use of TA-EESI-MS, the observation of salbutamol was made possible. A peak corresponding to the protonated monomer ion of salbutamol was observed in spectra obtained by TA-EESI-MS analysis at a measured temperature of approximately 200°C ( $\pm 10^\circ\text{C}$ ) (Figure 3.1B). When the temperature was increased ( $\sim 340^\circ\text{C} \pm 10^\circ\text{C}$ ), a peak at  $m/z$  577.3 was observed in the spectra obtained, along with the protonated monomer peak at  $m/z$  240.2 and heat induced fragments at  $m/z$  222.1 and 148.1 (Figure 3.1C). The spectrum in Figure 3.1C is similar to that obtained from an ESI spectrum of a standard (not shown).

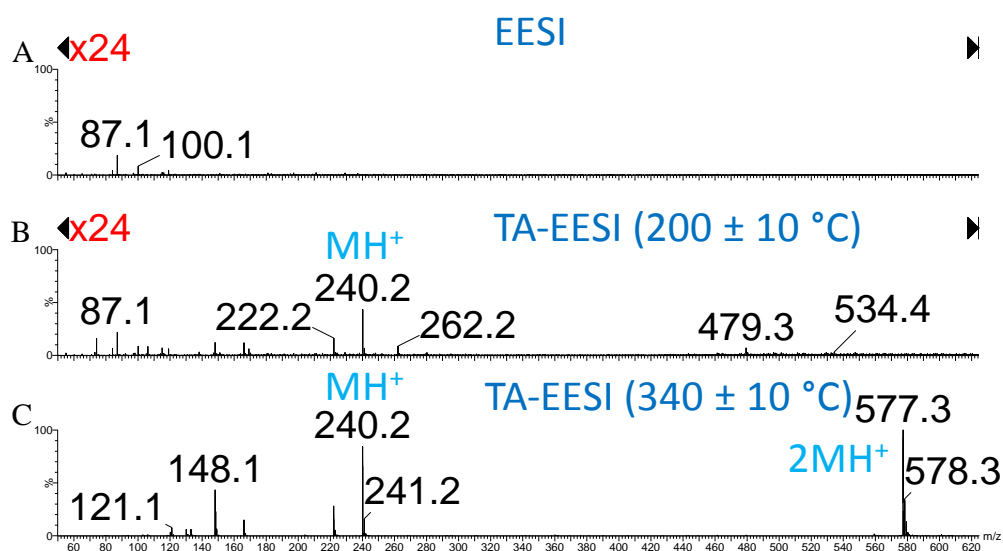


**Figure 3.1** - Mass spectra of the salbutamol spray obtained by TA-EESI-MS analysis at three different temperatures, (A) ambient temperature, (B)  $200 \pm 10^\circ\text{C}$  and (C)  $340 \pm 10^\circ\text{C}$ . Spectra are displayed with intensity axes linked.



The peak at  $m/z$  577.3 was characterised by TA-EESI-MS/MS as protonated salbutamol sulphate (Figure 3.2), and compares well with the spectrum obtained using ESI-MS/MS (not shown).

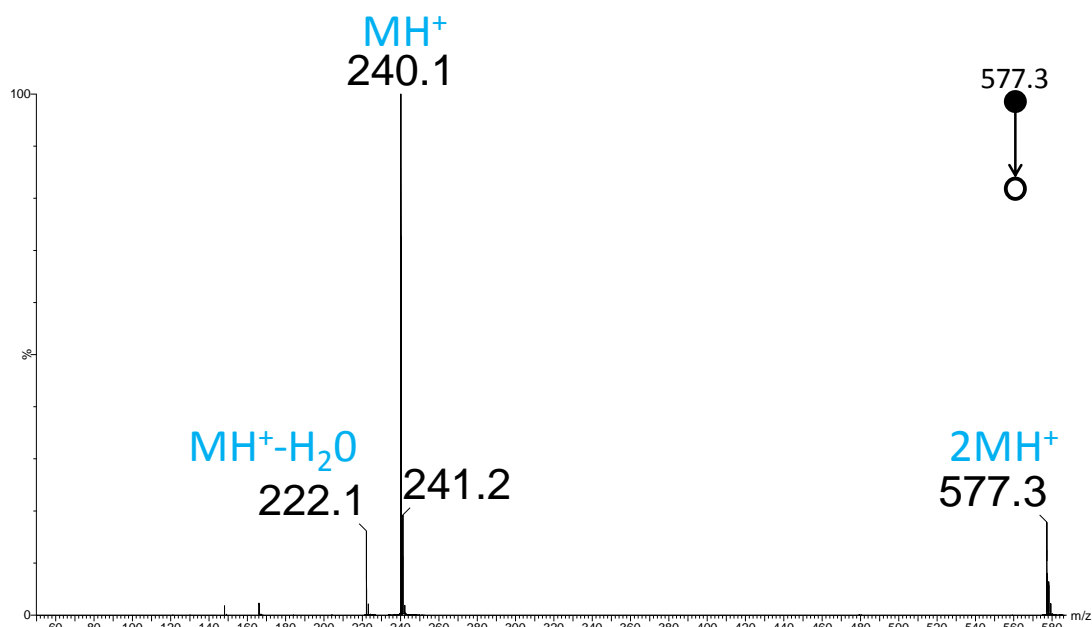


**Figure 3.2** - Precursor-selected MS/MS spectrum of  $m/z$  577.3 ion. This is characterised as protonated salbutamol sulphate, a dimer of salbutamol in coordination with a sulphate group. This ion was observed when the TA-EESI temperature was increased to ( $\sim 340^\circ\text{C} \pm 10^\circ\text{C}$ ).

Salbutamol is non-volatile molecule. The rapid analysis of this drug by an EESI based technique that does not require sample preparation and does not result in significant sample carryover can be demonstrated by TA-EESI.

The precursor-selected ESI-MS/MS spectrum of the protonated molecular ion of salbutamol and the mobility-separated TA-EESI-CID-MS spectrum are shown in Figure 3.3. Whilst the signal-to-noise ratio was better in the product ion spectrum obtained by precursor selection, the major fragment ions present within both spectra were similar and allowed for product characterisation. Major fragments ions were detected at  $m/z$  222, 166 and 148. A fragmentation pathway is proposed and presented in Figure 3.4.

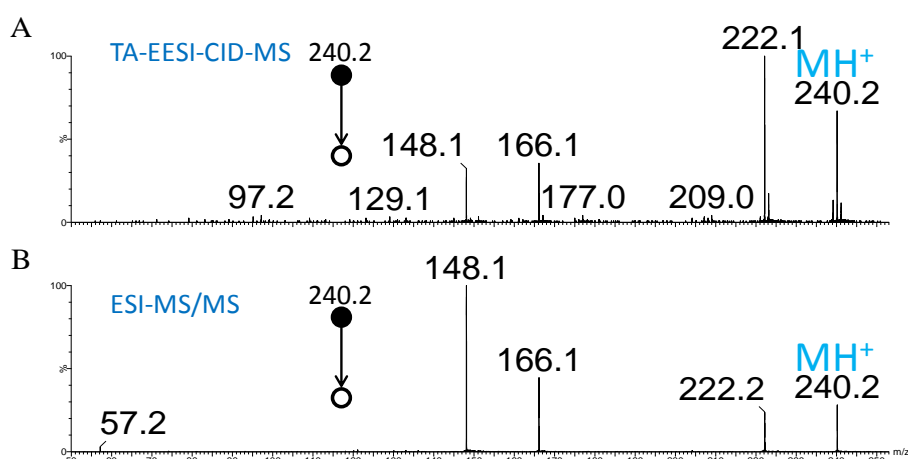


**Figure 3.3** - Product ion spectra of salbutamol obtained by means of (A) mobility-separated CID/MS and (B) precursor-selected ESI-MS/MS.

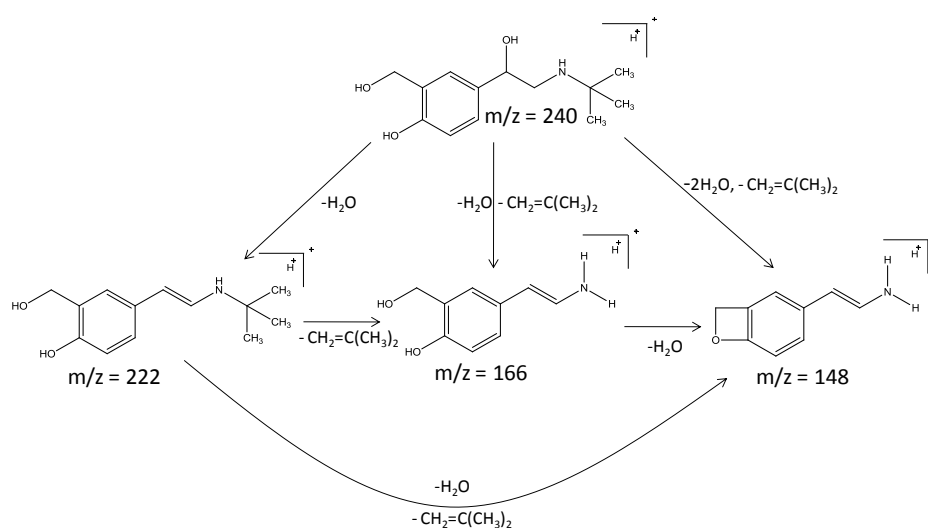


**Figure 3.4** - The proposed fragmentation pathway for the singly-protonated ion of salbutamol.

### 3.7.2 TA-EESI analysis of decongestant sprays

EESI-IM-MS analysis at ambient temperature of Vicks Sinex Decongestant and Sudafed did not result in the detection of the active pharmaceutical ingredient. The actives within these sprays (oxymetazoline and xylometazoline respectively) have relatively low volatilities, and thus were not present within the sample headspace at ambient temperatures. The structures, formulae and exact mass of both active pharmaceutical ingredients are presented in Figure 3.5.

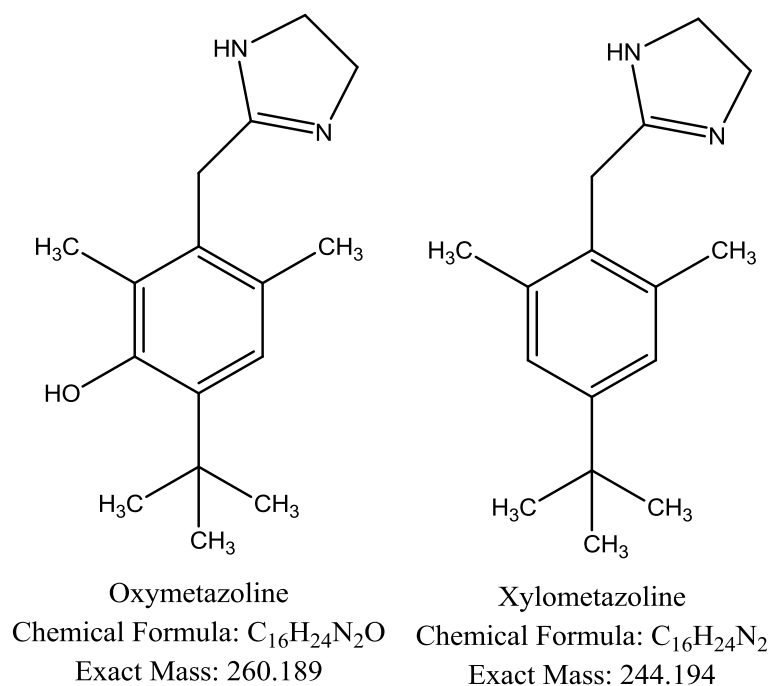


**Figure 3.5** - Structures, formulae and exact mass data for Oxymetazoline and Xylometazoline.

The ambient temperature spectrum of Vicks Sinex Decongestant, shown in Figure 3.6A, was dominated by a peak at  $m/z$  153.1. MS/MS analysis (data not shown) confirmed that this ion was camphor, a flavour excipient. The ion at  $m/z$  305.3 is the dimeric species. Other low intensity peaks observed in the spectrum corresponded to additional excipient ingredients.

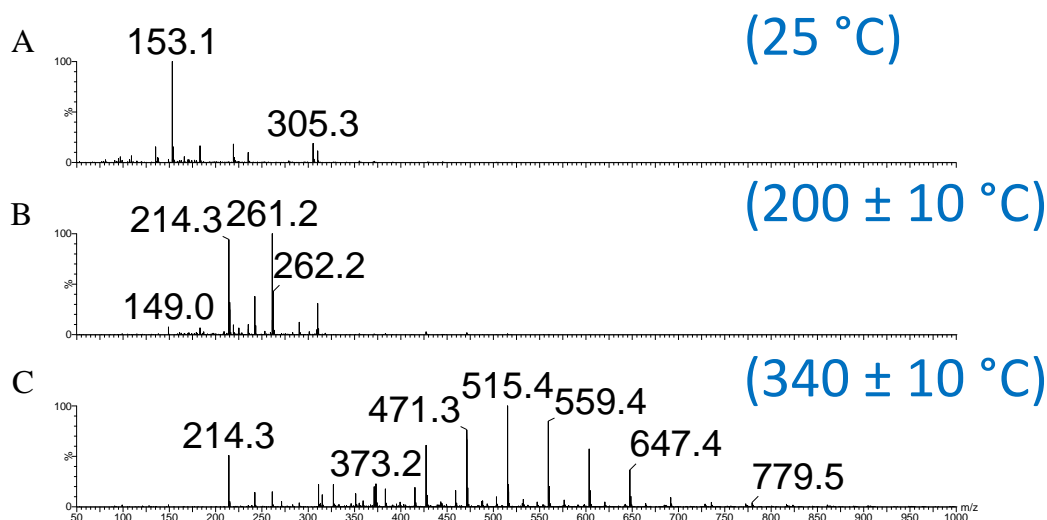


**Figure 3.6** - Mass spectra of Vicks Sinex Decongestant obtained by TA-EESI-MS analysis at three different temperatures. (A) ambient temperature, (B)  $240 \pm 10^\circ\text{C}$  and (C)  $340 \pm 10^\circ\text{C}$ .

The observation of the active ingredient, oxymetazoline, was facilitated by increasing the temperature of the sample container to  $\sim 240 \pm 10^\circ\text{C}$  (Figure 3.6B). At this temperature the base peak within the spectrum at  $m/z$  261 corresponded to the protonated molecular ion of oxymetazoline. When the temperature was increased to  $\sim 340^\circ\text{C} \pm 10^\circ\text{C}$ , a polymeric distribution was observed (Figure 3.6C). The active ingredient at  $m/z$  261 was still observed, but at a much lower relative intensity. The polymeric species was characterised as tyloxapol, an excipient present in the spray that acts as an expectorant and aids in liquefaction of the active. Results for the analysis of the tyloxapol component are presented with other polymer data in Chapter 4.

Figure 3.6 presents the first successful example of an ambient ionisation technique being applied to a formulation composed of active and excipient ingredients of differing volatilities, and does not result in significant sample carryover. This rapid analysis requires no sample preparation, and can be implemented by manufacturers on any mass spectrometer with an ESI source.

When the Sudafed formulation was analysed at ambient temperature, only low molecular weight excipients were detected in the spectra obtained, alongside background noise (Figure 3.7A). The protonated molecular ion of the active ingredient xylometazoline ( $m/z$  245) was observed in spectra when temperature was measured as  $\sim 240 \pm 10^\circ\text{C}$  (Figure 3.7B). On increasing the temperature, an ion corresponding to the xylometazoline dimer was observed ( $m/z$  489) (Figure 3.7C).

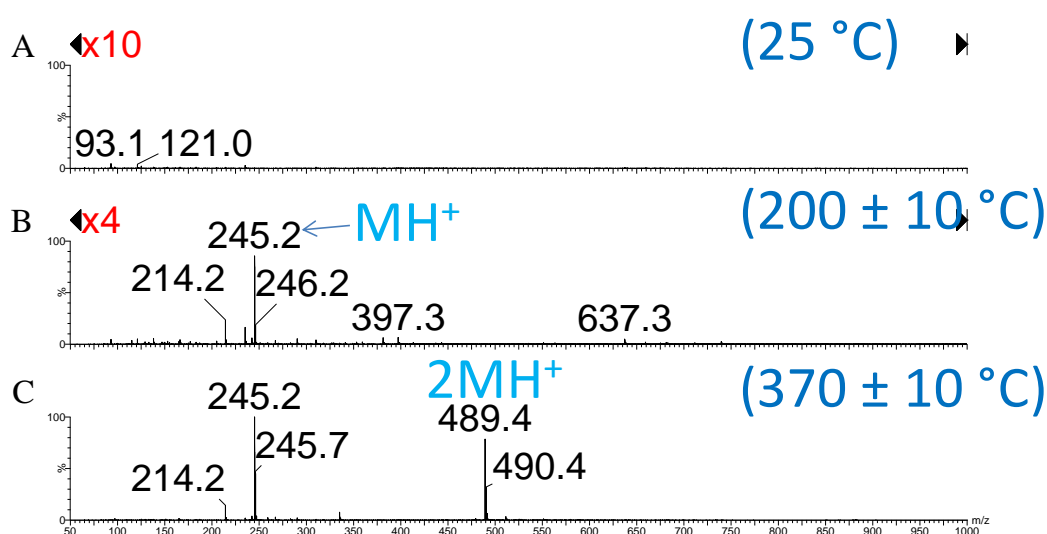


**Figure 3.7** - Mass spectra of Sudafed obtained by TA-EESI-MS analysis at three different temperatures, (A) ambient temperature, (B)  $240 \pm 10^\circ\text{C}$  and (C)  $370 \pm 10^\circ\text{C}$ . Spectra are displayed with intensity axes linked.

Xylometazoline has a similar structure to that of oxymetazoline (see Figure 3.5) differing only by a hydroxyl group that is attached to the aryl ring of oxymetazoline. When performing MS/MS analysis on a Q-ToF type instrument, it is conventional to set the quadrupoles to allow only the precursor ion of interest to pass into the collision cell. It is possible to obtain product ion spectra on the Synapt G2 instrument used here, by mobility separating precursor ions prior to fragmentation without precursor selection in the quadrupole. Both oxymetazoline and xylometazoline were analysed as components in a mixture of spray formulations by means of TA-EESI-TWIM-CID-MS. No precursor ions were selected and product ion spectra were

obtained from mobility separated peaks. The extracted ATDs for the protonated molecular ions of oxymetazoline and xylometazoline respectively are shown in Figure 3.8.

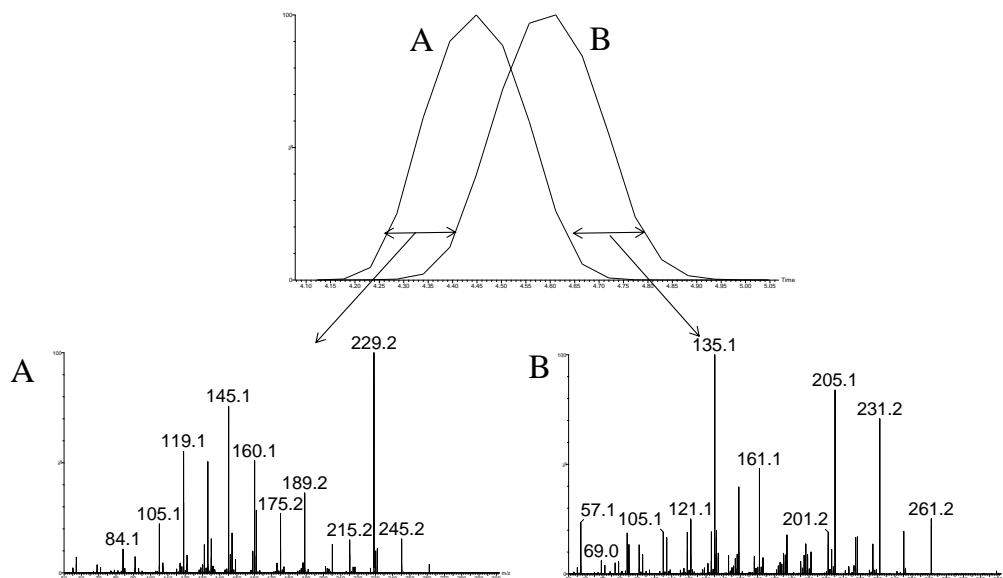


**Figure 3.8** - Arrival time distributions for the singly-protonated ions of (A) xylometazoline and (B) oxymetazoline, with their corresponding mobility-separated product ion spectrum inset. Experiment performed with TA temperature of  $240 \pm 10$  °C.

These ions, with very similar structures, were sufficiently separated by mobility to enable characterisation of each component from its corresponding mobility-separated product ion spectrum. Product ion spectra were extracted from regions on the ATDs that were not overlaid. Figure 3.9 compares the TA-EESI mobility separated product ion spectra with ESI precursor selected MS/MS spectra for xylometazoline.

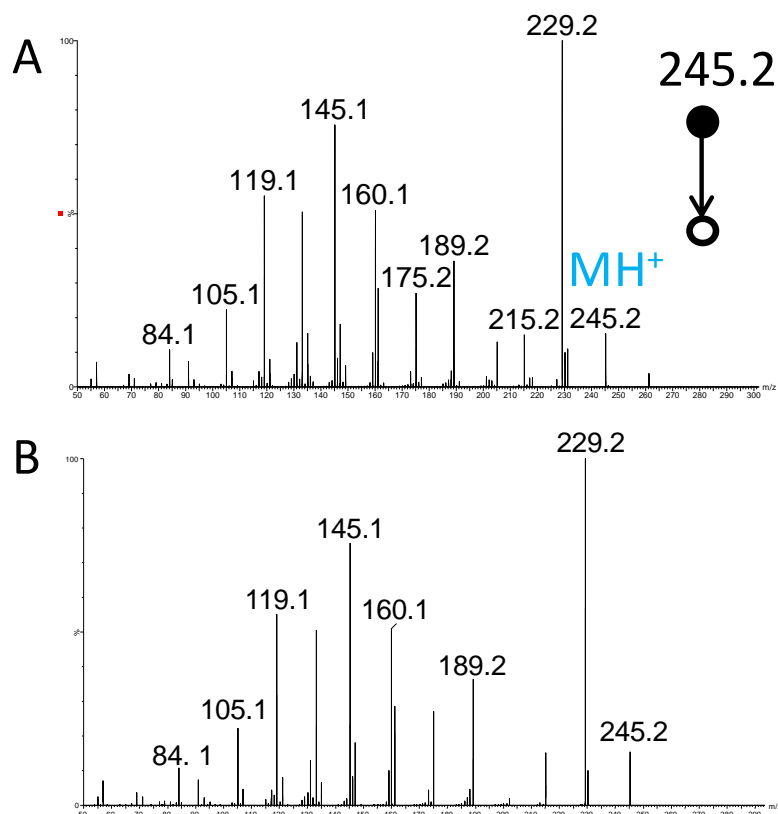


**Figure 3.9** - (A) TA-EESI-Mobility-separated product ion spectrum for Sudafed (same spectrum as in Figure 3.8A) and (B) ESI-precursor-selected MS/MS product ion spectrum for  $m/z$  245.2. CID voltages were set at 30 V in both experiments.

There are additional fragments present at minor levels (i.e.  $m/z$  205) in Figure 3.9A when compared with Figure 3.9B, however all major fragments observed were also generated from ESI precursor selected MS/MS of xylometazoline. The proposed structures of a number of these fragments are shown in Figure 3.10.

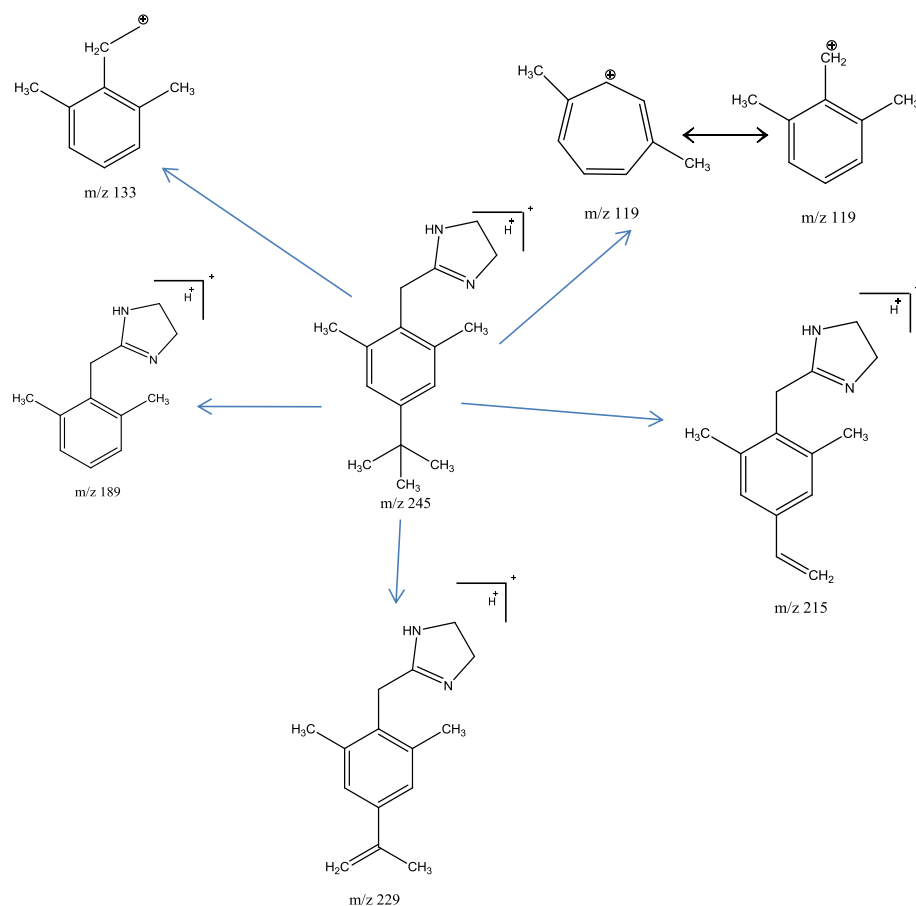


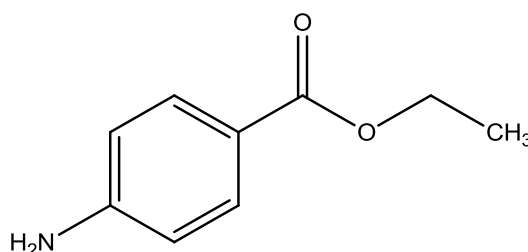
**Figure 3.10** - Proposed structures of some fragments generated from xylometazoline.

TA-EESI-TWIM-CID-MS provides a multidimensional, temperature resolved, ambient ionisation, shape selective, product ion spectral approach that can be performed in seconds with little or no sample preparation. The example presented above enabled the characterisation and differentiation of two structurally related decongestant active pharmaceutical ingredients without prior separation or precursor selection. If product ion spectra were required for components in more complex formulations, then precursor ion selection may be required. This is because as a formulation becomes more complicated, the probability that regions of an ATD of a specific component that does not overlay with the ATDs of other components decreases. If precursor selection is required the timescale of the experiment will naturally increase, although overall is less than the timescale required for ESI analysis coupled with separation science methods. Care needs to be taken to regulate the temperature applied, to avoid heat induced fragmentation.



### 3.7.3 Benzocaine

The active pharmaceutical ingredient in AAA sore throat spray is benzocaine (Figure 3.11). When this formulation was analysed by means of TA-EESI-MS at ambient temperature the spectra obtained showed a prominent ion at  $m/z$  155 (Figure 3.12A). The protonated molecular ion of benzocaine ( $m/z$  166) was observed in spectra obtained by TA-EESI-MS analysis at a measured temperature of approximately 110 °C (Figure 3.12B).



Benzocaine  
Chemical Formula: C<sub>9</sub>H<sub>11</sub>NO<sub>2</sub>  
Exact Mass: 165.079

**Figure 3.11** - Structure, formula and exact mass of benzocaine

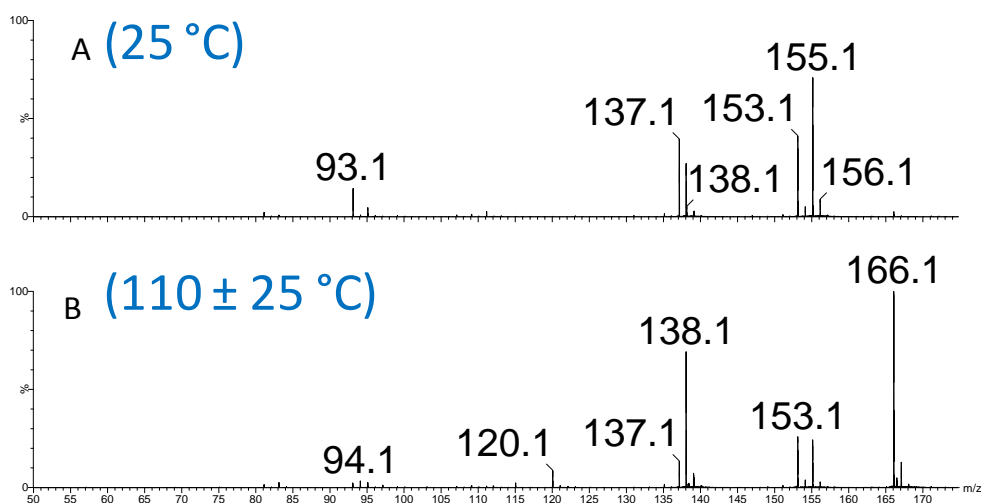


**Figure 3.12** - Mass spectra of AAA Sore Throat Spray obtained by TA-EESI-MS analysis at (A) ambient temperature and (B) 110 ± 10 °C.

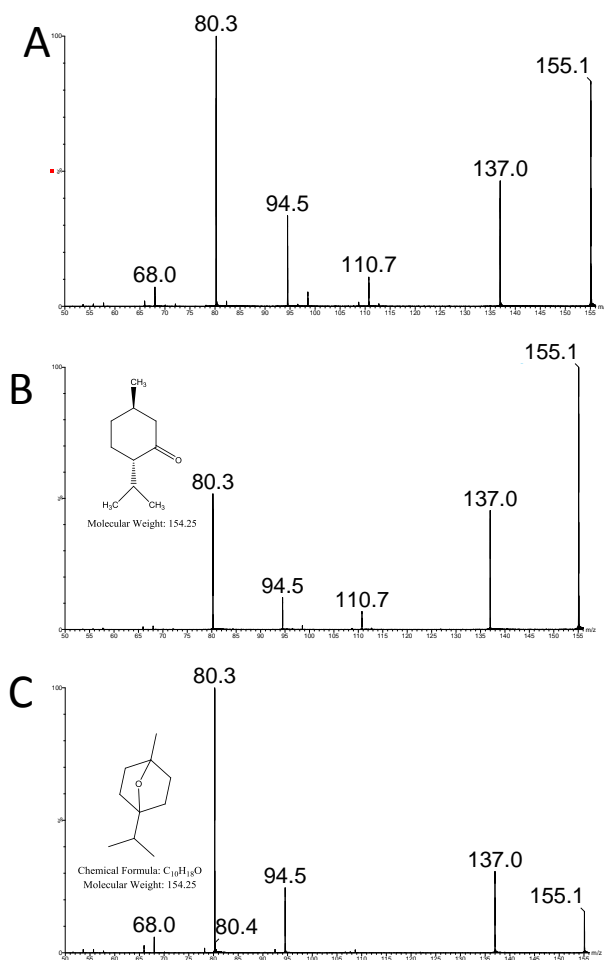


**Figure 3.13** - Precursor selected MS/MS of the  $m/z$  155.1 ion observed within the formulation (A), MS/MS of menthone standard (B), and MS/MS of eucalyptol standard (C). CID voltage set at 20V.

The spectrum shown in Figure 3.13A is that of the MS/MS spectrum for the  $m/z$  155.1 ion observed when the benzocaine formulation was analysed by TA-EESI at ambient temperature. The only excipient that was specified in the formulation that could result in an ion at  $m/z$  155.1 was peppermint oil. This excipient is composed of many volatile chemicals that give a pleasant aroma. Two isomeric species within peppermint oil that would produce an ion at  $m/z$  155.1 are eucalyptol and menthone. The MS/MS spectra of standards of menthone (Figure 3.13B) and eucalyptol (Figure C) are similar to the MS/MS spectrum of the formulation ion. Attempts at separating the standards by ion mobility were unsuccessful. The ATDs of the standards were

the same as for the formulation component (data not shown). No difference was observed for MS/MS or ATD results when experiments were performed using ESI.

Two well-resolved peaks were observed in the extracted ATD for the ion at  $m/z$  166, obtained from TA-EESI-TWIM-MS experiments (Figure 3.14). Subsequent MS/MS analysis resulted in the production of significantly different product ion spectra for the two mobility-separated precursors at  $m/z$  166 (Figure 3.14). This indicated that the peak observed at  $m/z$  166 was formed of a least two distinct ion species each with different mobilities. The overlaid combination of the two mobility separated MS/MS spectra is very similar to the MS/MS spectrum generated from a conventional (non-mobility) ESI-MS/MS experiment (Comparison shown in Figure 3.15). The two distinct ion species were estimated to have a difference in rotationally-averaged collision cross-section of 10-15 % ( $\sim 10 \text{ \AA}^2$ ). The species with an ATD of 4.29 ms was calculated to have an estimated collision cross section of  $77.1 \text{ \AA}^2$ , while the species with an ATD at 5.33 ms was calculated to have an estimated collision cross section of  $87.4 \text{ \AA}^2$ .

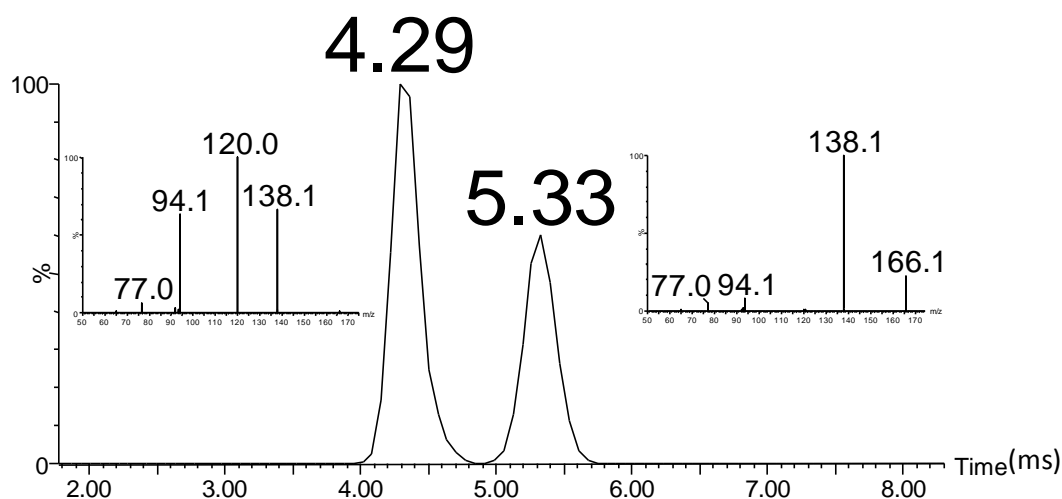


**Figure 3.14** - The extracted arrival time distribution for the singly-protonated ion of benzocaine ( $m/z$  166.1), which shows two distinct peaks with arrival times of 4.29 ms and 5.33 ms respectively. Their corresponding mobility-separated product ion spectra are shown inset. Product ion spectra generated in same sub second experiment with energy in transfer cell set at 30 volts.

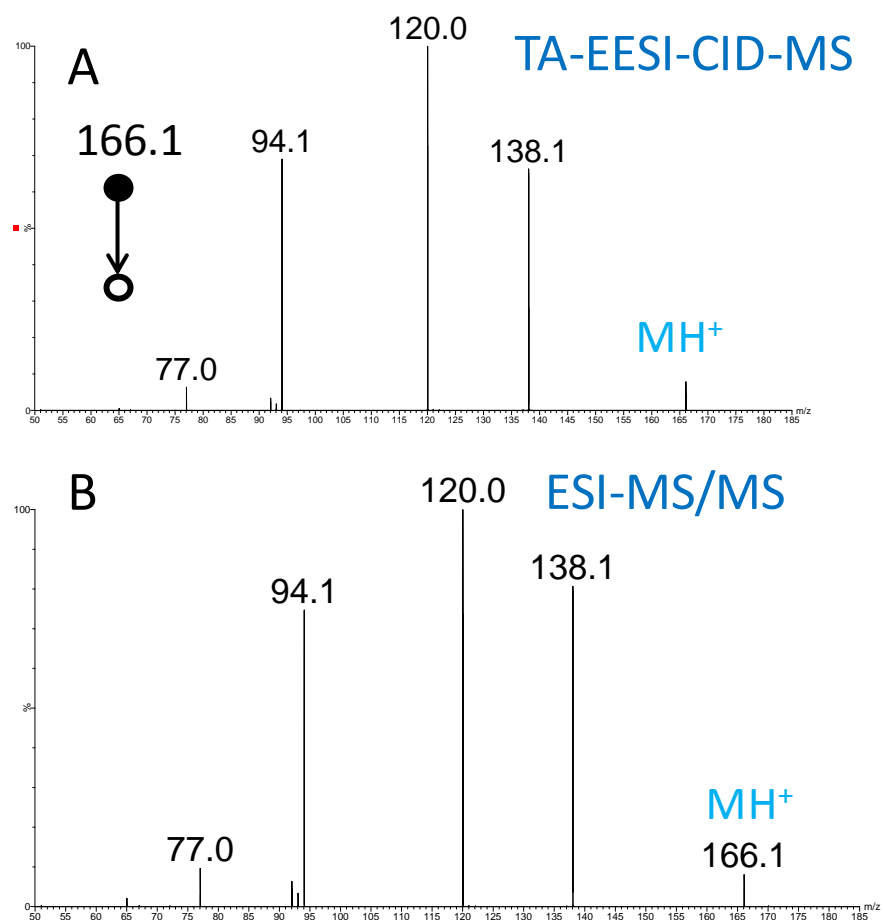


**Figure 3.15** - Comparison of (A) combined mobility separated MS/MS spectra with (B) MS/MS spectrum generated by ESI-MS/MS with no mobility separation (conventional mass spectrometry example).

The presence of two distinct ion species at  $m/z$  166 was unexpected and thus investigated further. It is important to note that both DESI and ESI analysis also produced the same ATD with two well defined and resolved peaks. It was initially thought that the observation of two species could be due to the presence of isobaric excipients, structural or geometric isomers of benzocaine or to the presence of benzocaine molecules with different sites of protonation. These species could, for example, relate to ortho and meta structural isomers, *trans* and *gauche* conformations or carbonyl- and amine-protonated ions.

The experimental results obtained from the spray formulation were compared with those acquired when two standards of benzocaine were analysed. The standards were obtained commercially from two different suppliers and both were indicated to have  $\geq 99$  % purity. The mobility spectra and fragmentation spectra obtained for the protonated molecular ion of benzocaine were very similar for the two standards and agreed with that obtained for the spray formulation. This indicated that the observance of two peaks in the extracted ATD for the ion at  $m/z$  166 in the spray formulation was not due to the presence of additional components, such as isobaric excipients (Figure 3.16).

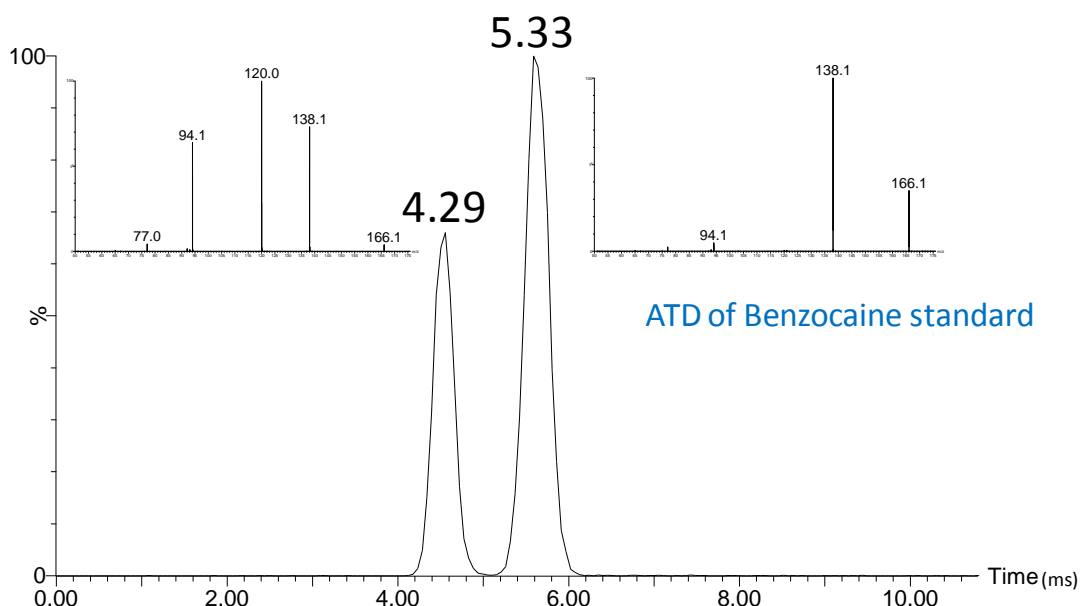


**Figure 3.16** - The extracted arrival time distribution for the singly-protonated ion of a benzocaine ( $m/z$  166.1) standard. The two extracted mobility resolved product ion spectra are shown either side of their respective peaks.

The spectra obtained following TA-EESI-TWIM-MS and MS/MS analysis of the ortho (99% pure) and meta (97% pure) isomers of benzocaine were compared with those obtained for benzocaine (the para isomer of the ethyl amino benzoates). The extracted ATDs for the ion at  $m/z$  166 representative of the meta and ortho isomers of benzocaine are shown in Figure 3.17. The corresponding product ion spectra are shown in Figure 3.18 for the four species (i.e. – both species of the para isomer, the meta isomer and the ortho isomer).

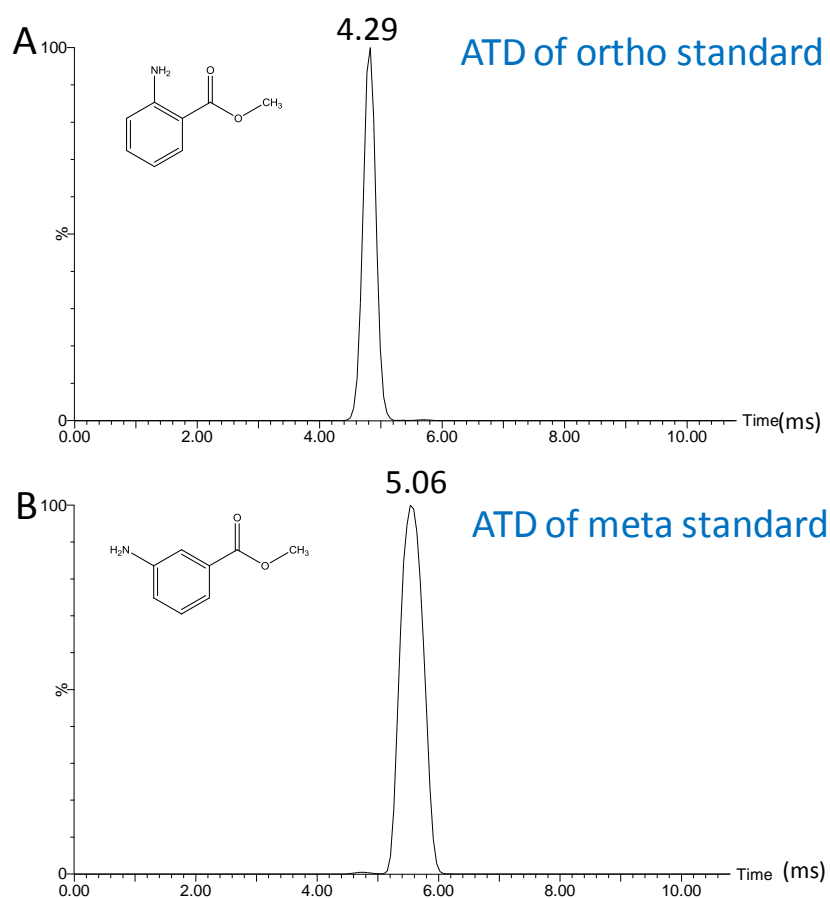


**Figure 3.17** - ATDs for ortho isomer (A) and meta isomer (B) of Benzocaine.

The ortho isomer has an ATD of 4.29 ms, and is calculated to have an estimated cross section of  $77.1 \text{ \AA}^2$  while the meta isomer has an ATD of 5.06 and is calculated to have an estimated cross section of  $86.1 \text{ \AA}^2$ .

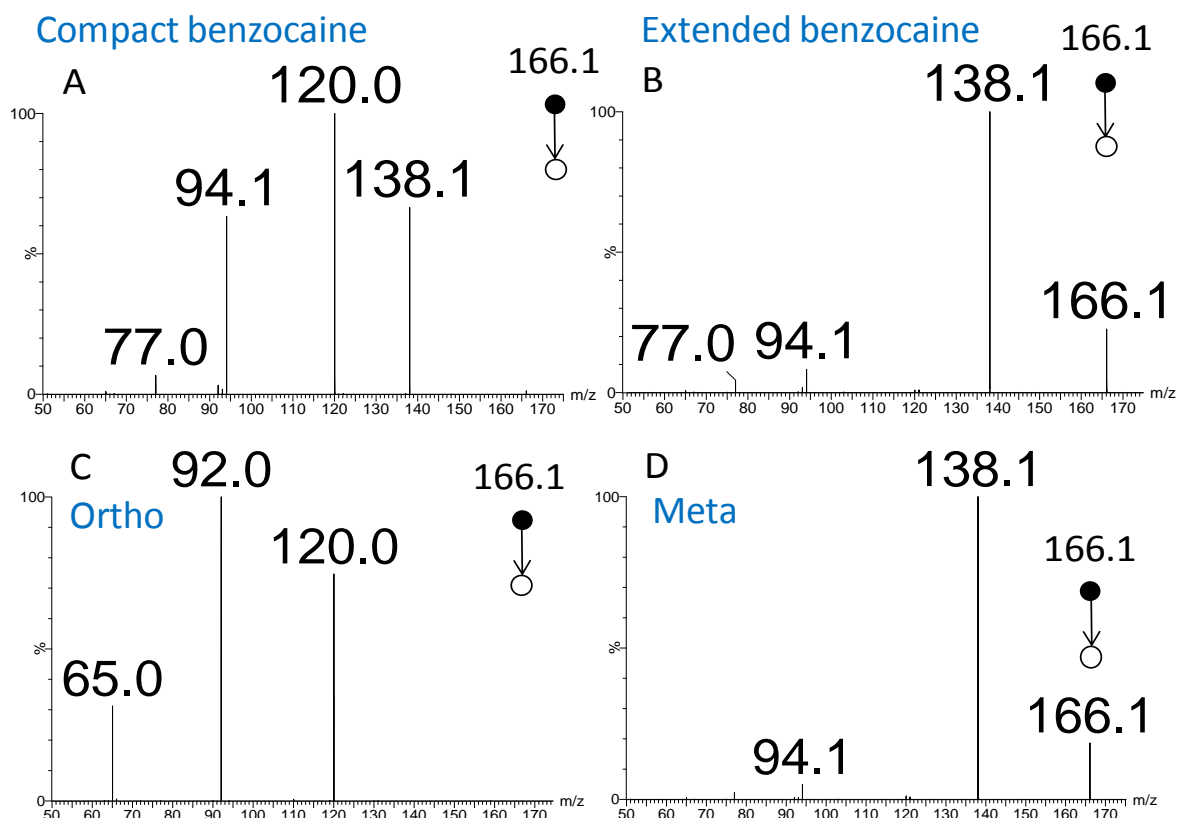


**Figure 3.18** - Precursor-selected TWIM-MS/MS spectra for the singly-protonated ions of (A) benzocaine (compact conformation), (B) benzocaine (extended conformation), (C) ethyl 2-aminobenzoate (ortho isomer) and (D) ethyl 3-aminobenzoate (meta isomer).

The ATDs and MS/MS spectra observed for the meta and ortho isomers indicated that neither were present within the AAA Sore Throat Spray or the benzocaine standard. The ortho isomer had a similar ATD to the species with a smaller cross section in the spray formulation but experimentally distinct MS/MS data. The ortho isomer did not fragment to give a product ion at  $m/z$  138 (Figure 3.18C compared with Figure 3.18A). TWIM-MS analysis of the protonated meta isomer did not correspond with that observed for either of the other isomers; a single peak was observed in the mobility trace. The benzocaine species with the longer drift time and the meta isomer provided similar product ion spectra (Figures 3.18B, D). Gas chromatography- MS (GC-MS) analysis of one of the benzocaine standards and the meta isomer standards showed one elution peak for each sample, separated by

approximately one minute (Figure 3.19). This provided supportive evidence that the peak with the longer drift time in the extracted ATD for benzocaine, in the spray and standards, was not due to the presence of meta isomer as a contaminant.

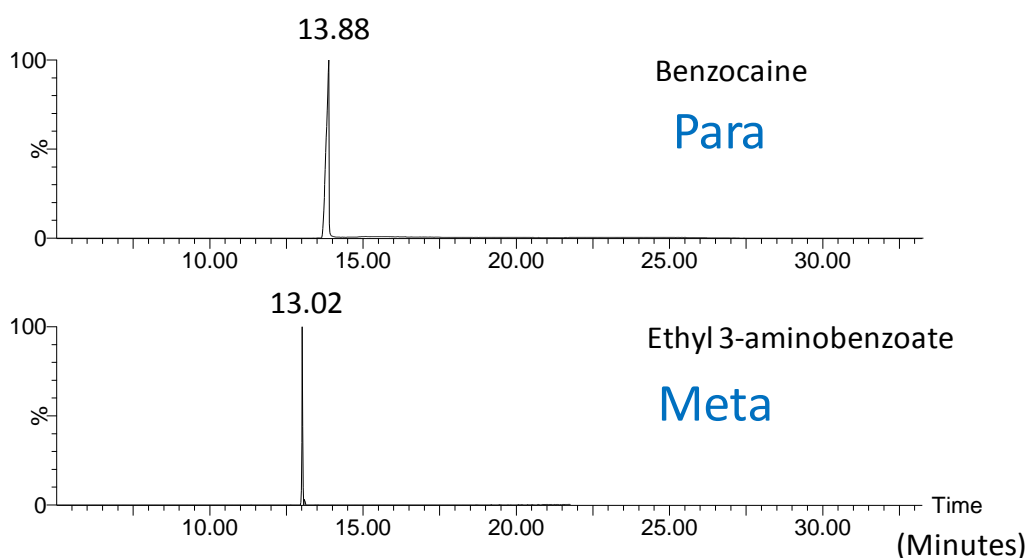


**Figure 3.19** - GC-MS chromatograms of benzocaine (para) and ethyl-3-aminobenzoate (meta). One peak is observed within each chromatogram and benzocaine is shown to have a longer elution time than ethyl-3-aminobenzoate. The difference in elution time, is not due to differences in boiling point, but likely polarity. A non-polar column was used, and the observation would suggest that benzocaine (the para isomer) is less polar than the meta isomer.



The drift gas used for mobility measurements in the Synapt G2 was nitrogen. Conventional ion mobility drift cells are often filled with helium. The group of Mike Bowers, based at the University of California, Santa Barbara (UCSB) agreed to collaborate in this work, and they ran three standards (ortho, para and meta isomers) using their home built stand alone drift cell based ion mobility spectrometer. Their results are presented in Figure 3.20. CCS can be determined directly from ATD using drift cell mobility instruments

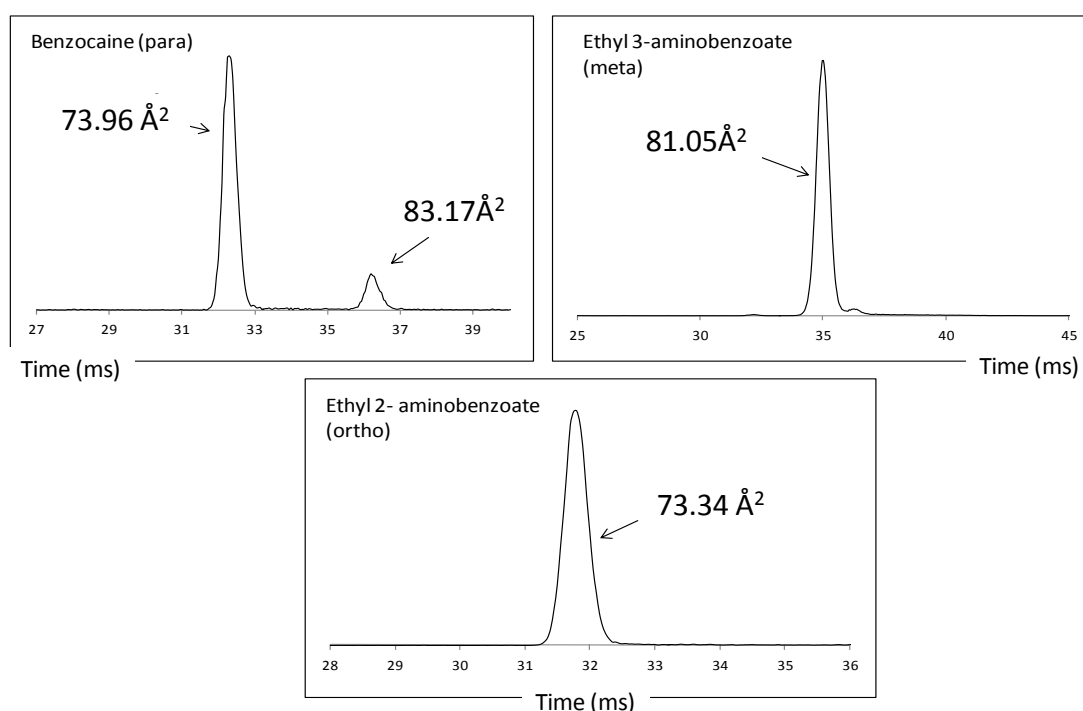


**Figure 3.20** - ATDs and estimated cross sections experimentally derived by the group of Mike Bowers.

Two peaks in the ATD of benzocaine were observed by the Bowers group, and although the estimated cross sections are smaller than the worked carried out on the Synapt G2, and the relative intensities vary, the difference in ATD between the two species is approximately the same (10-15%). The CCS of the ortho isomer (73.3 Å²) is less than an Angstrom different from that of the CCS for the benzocaine species with the faster mobility (73.9 Å²). The meta isomer has a CCS of 81.0 Å² which is

just over two Angstroms less than that of the larger benzocaine species. These results compare well with the results obtained on the Synapt G2

Aguado *et al.* (Aguado, Longarte et al. 2006) have previously used zero electron kinetic energy – pulsed field ionisation (ZEKE-PFI) spectroscopy, to study the number of conformations of benzocaine which can exist at room temperature. They discovered two interchangeable conformers, *trans* and *gauche*. It was therefore plausible that the two species observed related to *trans* and *gauche* conformers. Computational modelling of the two conformers indicated that they do not have significantly different rotationally-averaged collision cross-sections. Further MS analysis confirmed that the two species of benzocaine observed were not due to the presence of *trans* and *gauche* conformers. MS/MS analysis of the benzocaine molecular ion produced a fragment ion at  $m/z$  138, corresponding to the loss of an ethylene molecule. The ATD of that fragment ion (generated in the trap cell) showed two distinct peaks (Figure 3.21A). If the ions of *trans* and *gauche* conformers had different mobilities, then the fragment ion at  $m/z$  138 would have been found to have only one mobility, as the region that causes *trans/gauche* isomerism would have been lost. This was not the case. The ATD for the fragment ion at  $m/z$  138, from the meta isomer, showed only one ATD (Figure 3.21B).

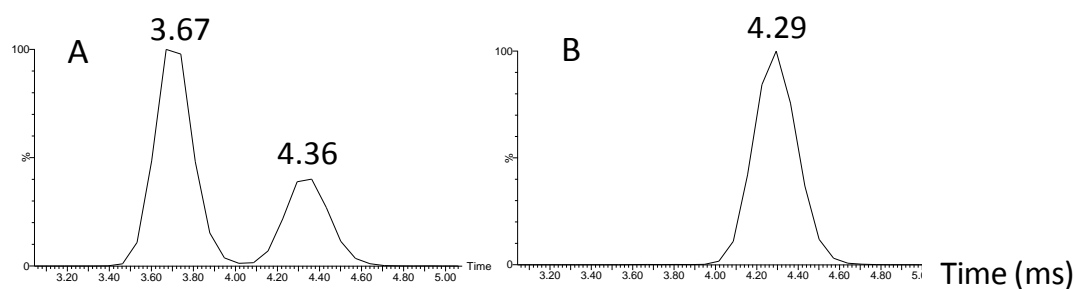


**Figure 3.21** - The extracted arrival time distributions for the  $m/z$  138 fragment ion of (A) benzocaine and (B) ethyl 3-aminobenzoate (meta isomer).

The peak in Figure 3.21A with an ATD of 3.67 ms is calculated to have an estimated cross section of  $71.3 \text{ \AA}^2$ , the peak with an ATD of 4.36 ms is calculated to have an

estimated cross section of  $79.3 \text{ \AA}^2$ . In Figure 3.21B the ATD is 4.29 ms for the  $m/z$  138 fragment ion, and is calculated to have an estimated cross section of  $77.1 \text{ \AA}^2$ .

In the late 1980's research by Karpas *et al.* (Karpas and Tironi 1991) investigated the mobility of anilines with differing ionisation protonation sites. They showed that ion interaction with neutral molecules in the gas phase can vary when the protonation site is different. This is likely due to the degree of charge delocalisation of the ion, itself dependent on site of protonation. The more an ion interacts with a molecule the lower its mobility and thus longer drift time in gas phase. Recent research by the group of Marcos Eberlin, utilised a Synapt G1 instrument to investigate if they could separate species termed protomers (Lalli, Iglesias et al. 2012).

Benzocaine has a number of potential protonation sites, including the nitrogen lone pair of electrons, the carbonyl oxygen and the aromatic ring. The two different species observed in the ATD for the benzocaine molecule ion could be related to ions with different protonation sites. Computer modelling carried out both at Warwick and at UCSB indicated that differences in protonation site should not result in experimentally significantly different cross sections.

A number of possible explanations for the observation of two peaks have been explored including:

- The possibility of impurities in the sample: – The observation of the two peaks was also seen for a pure standard (purity also established by in-house GC-MS experiments).
- The possibility that the sample contained additional isomeric components: – ATD, MS/MS and GC-MS experiments carried out on ortho and meta isomeric standards indicated that this was not the case.

- The additional peaks were due to artefacts caused by the mobility experiment: – Experimental results from a drift cell instrument carried out at UCSB also showed two peaks separated by similar mobility.
- The peaks were due to trans/gauche isomerisation: – Although superficially plausible this is impossible since two peaks were still observed in product ion mobility spectra even though the region that could give rise to this form of isomerisation had been lost.
- The peaks were due to differing protonation sites formed during the ionisation process forming differences in polarity of the molecules: – Theoretical calculations of protonated molecule ions with different protonation sites did not predict the experimentally observed difference in CCS.

The current hypothesis is that the observation of the two peaks is as an indirect result of differences in protonation site. Differences in protonation site potentially results in a rearrangement of the protonated molecule ion of the para isomer (benzocaine). This may also occur in the meta isomer as the measured CCS of the meta isomer was larger than that calculated by theory. The CCS of the meta isomer is similar to the larger CCS of the two benzocaine peaks. Figure 22 shows the potential rearrangement.

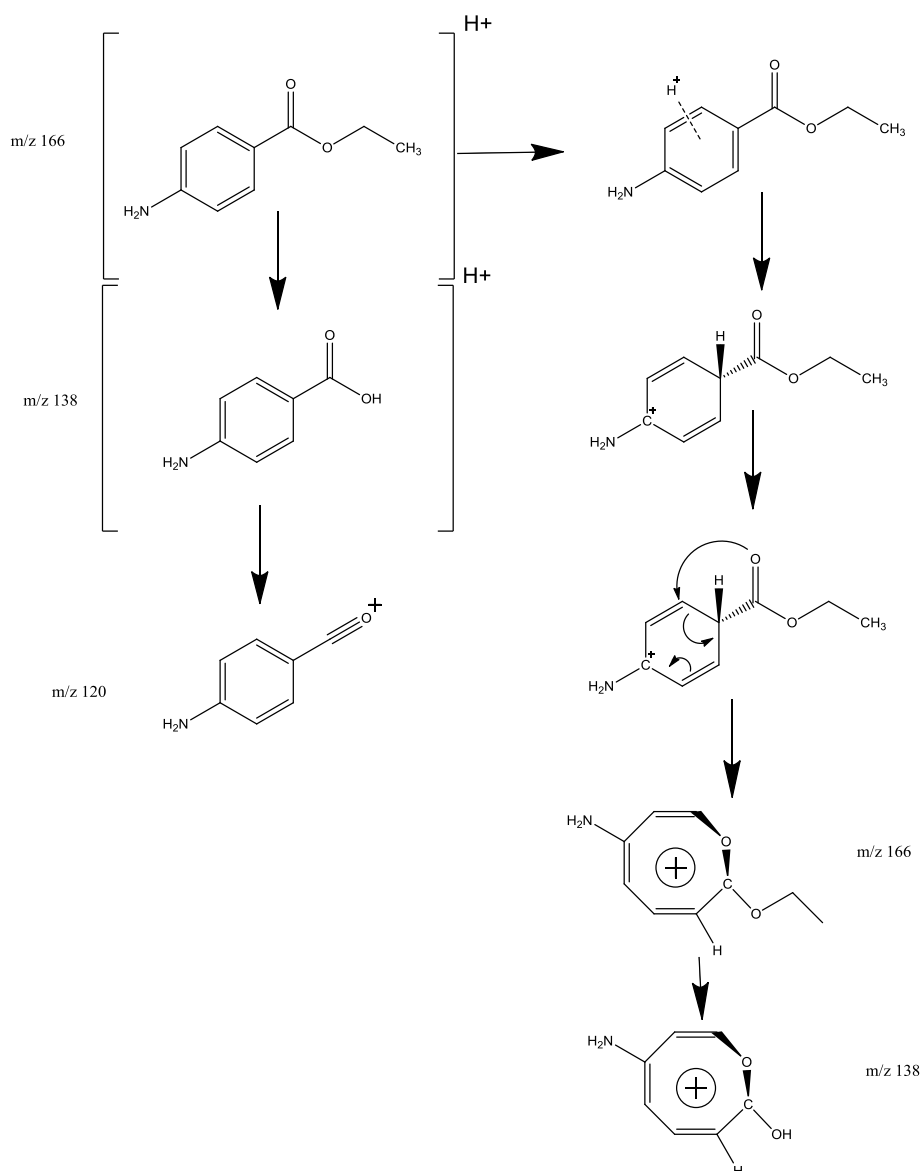


**Figure 3.22** - Proposed differences in protonation site, with larger CCS a result of rearrangement.

The separation of these two species would not have been possible with pre ionisation separation techniques such as liquid chromatography or gas chromatography, as the species are believed to be generated due to differences in ionisation site. Further theoretical and experimental work would need to be undertaken to fully understand the processes occurring that results in the observation of the two peaks. Further information about the mechanistic processes occurring in an ionisation technique may be revealed by utilising IM-MS, because this technique can separate and generate collision cross-section information of different protonated site species.

### 3.8 Evaluation of ASAP technique

The atmospheric pressure solids analysis probe (ASAP) approach has been utilised for the analysis of a number of pharmaceutical formulations. Methods can be found in Chapter 2.

#### 3.8.1 ASAP analysis of benzocaine

ASAP analysis can result in the generation of radical cations and/or protonated ions. The relative intensities of these ions will be dependent on the temperature of the probe, whether or not a solvent is infused into the source region( via the lockspray source), the volatility of the analyte of interest and if the analyte concerned can form a radical cation and/or protonated molecular ion. If no solvent is infused when the temperature of the probe is set to the maximum setting (600 °C) then the source region could be described as a dry environment. It is in these dry conditions that the greatest probability of radical cation generation occurs. Formation of protonated ions is still possible in such conditions, as water vapour in the source may still be present. If solvent is infused and the probe is set at the lowest temperature (i.e. – for those analytes that are volatile at ambient temperature), then the formation of a radical cation is less likely to occur. Figure 3.23 shows a comparison of the relative intensities of the radical cation ( $m/z$  165) and the protonated ion ( $m/z$  166) of benzocaine when the temperature of the probe was set at 600 °C.

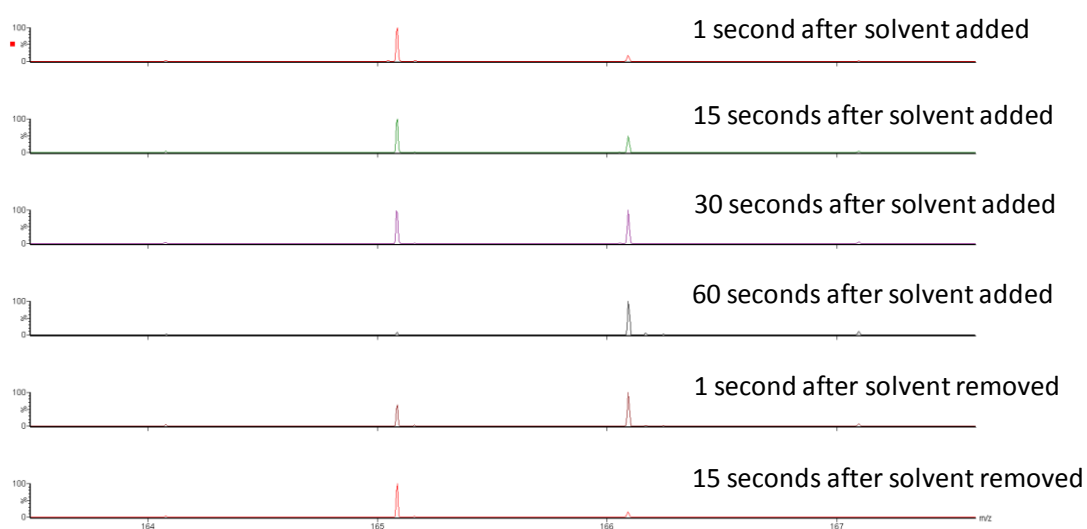


**Figure 3.23** - Relative intensities of radical cation and protonated ion of benzocaine with different source conditions.

Prior to infusion of solvent the majority of the benzocaine ions formed are radical cations. Once solvent is infused the relative intensity of the protonated ion increases until there are only trace levels of radical cation. Upon removal of solvent the relative intensity of the protonated ion decreases, while the relative intensity of the radical cation increases. If the temperature of the probe is set to a lower value (i.e. – 400 °C) then the proportion of protonated ion to radical cation can be higher, even if no solvent is infused. For benzocaine it was found that relatively equal amounts of radical cation, and the protonated ion could be observed when no solvent was infused and the temperature of the probe was set at 250 °C. Figure 3.24 shows the ATDs for the radical cation and protonated ion of benzocaine formed by the ASAP technique. The ATD of the radical cation consists of one peak at 4.5 ms, which was calculated to have an estimated cross section of 79.6 Å<sup>2</sup>. The ATD of the benzocaine molecule is composed of two peaks as previously shown by TA-EESI (CCS of 77.1 Å<sup>2</sup> and 87.4 Å<sup>2</sup>). The radical cation is thus shown to have a different cross section to either of the protonated species.

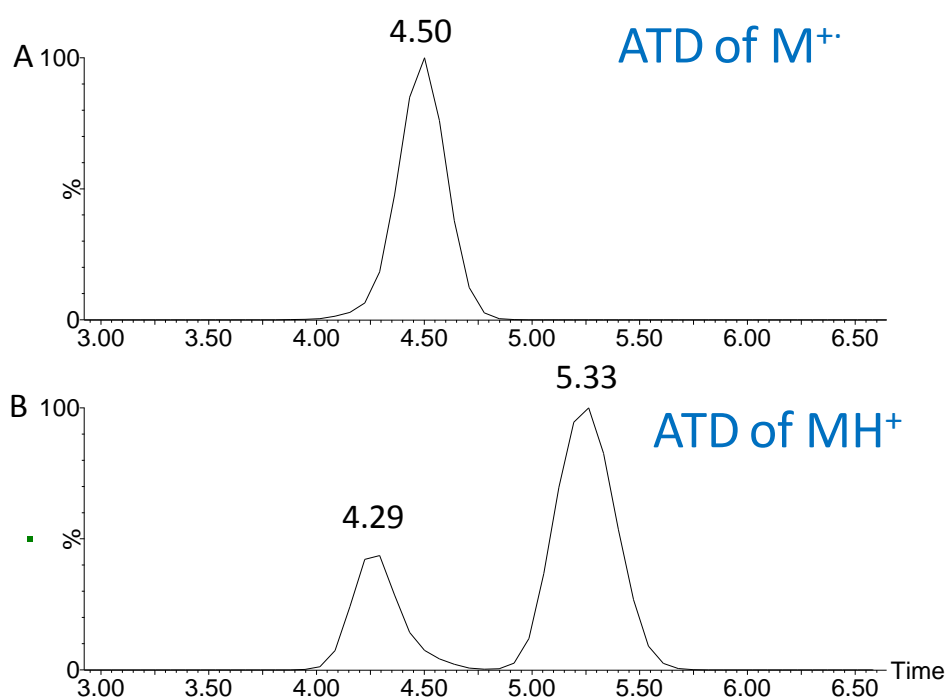


**Figure 3.24** - Mobility extracted ATDs for radical cations of benzocaine (A) and protonated molecular ion of benzocaine (B). Ions were generated by the ASAP technique

The MS/MS spectrum of the radical cation (Figure 3.25A) may be compared with the EI spectrum (Figure 3.25B)

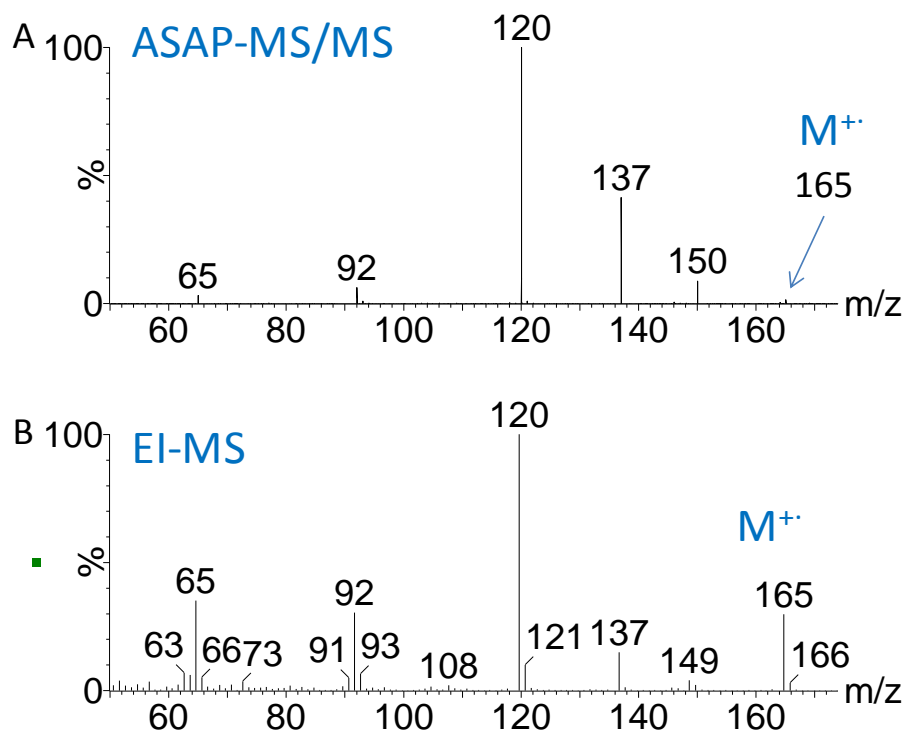


**Figure 3.25** - MS/MS spectrum of benzocaine radical cation generated by ASAP (A), compared with EI spectrum of Benzocaine (B).

The similarity between the MS/MS spectrum of the radical cation ion generated by ASAP and the spectrum generated by electron impact is significant. This may allow for the rapid generation of EI-like spectra without the need for sample pre-treatment, subsequently allowing for high throughput data generation.



### 3.8.2 ASAP analysis of decongestant sprays

Oxymetazoline and xylometazoline sprays were analysed using ASAP. The camphor excipient observed by TA-EESI analysis was not observed in ASAP analysis at any temperature, with or without solvent infusion. At higher temperatures the tyloxapol polymer distribution was observed (Chapter 4). Separation of xylometazoline and oxymetazoline protonated ions was possible. The ATDs are similar to those generated by TA-EESI and is shown in Figure 3.26A. Reproducible separation of their respective radical cations is also possible, although the degree of separation is not as great as that observed for the protonated molecules (Figure 3.26B).

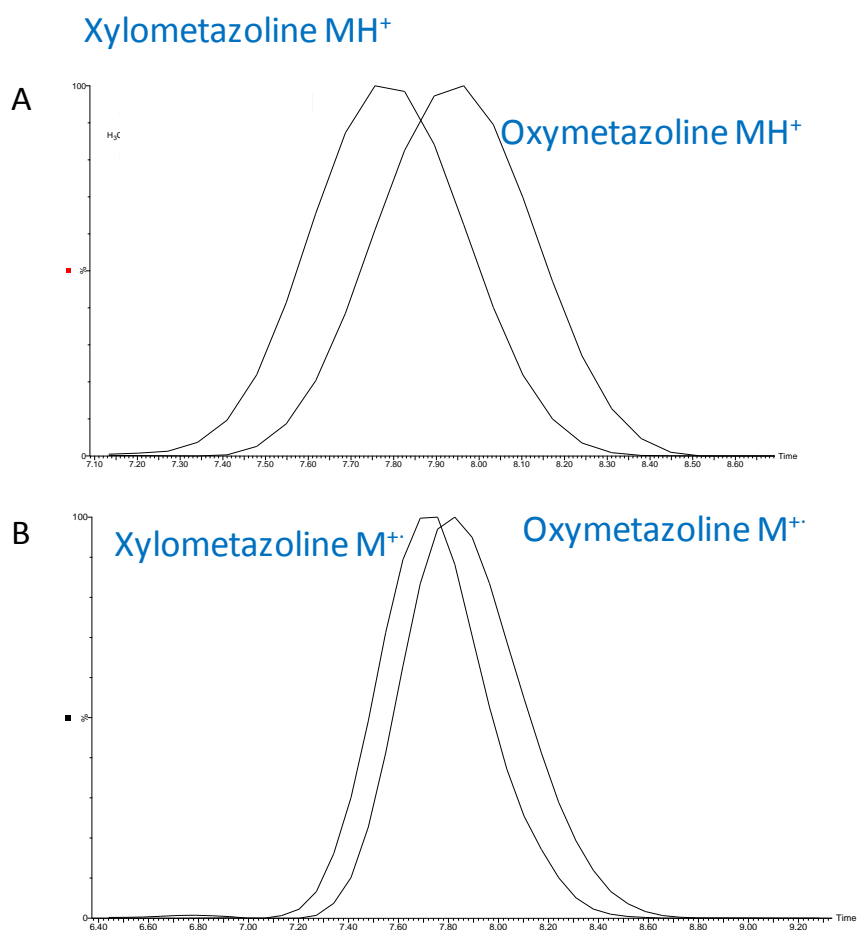


**Figure 3.26** - ATDs of the protonated ions of xylometazoline and oxymetazoline (A), and the radical cations of xylometazoline and oxymetazoline (B) generated by the ASAP method.

The separation of radical cation and protonated ion of oxymetazoline is small but reproducible (Figure 3.27). For a comparison to be made between the product ion spectra of the radical cation and protonated ion, precursor selected MS/MS experiments were performed (Figure 3.28).

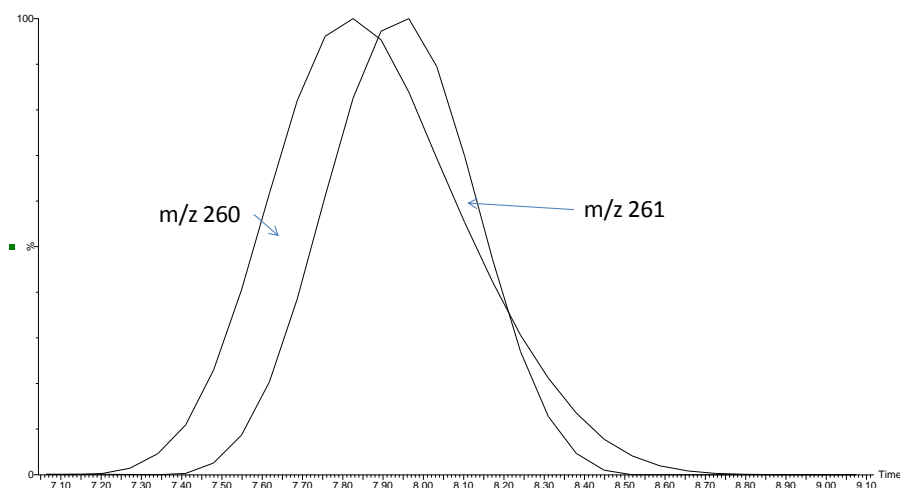


**Figure 3.27** - ATDs of radical cation and protonated ion of oxymetazoline.

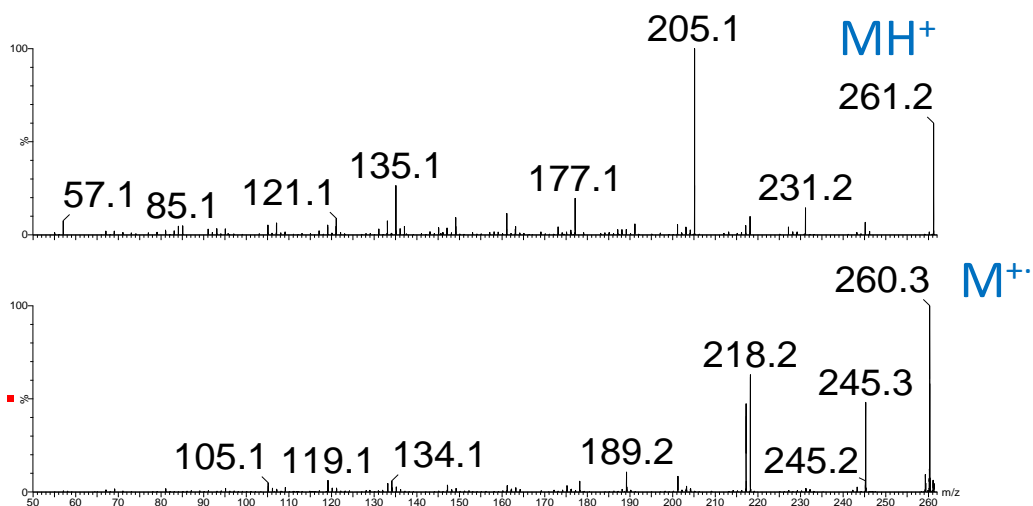


**Figure 3.28** - Comparison of the MS/MS spectra for protonated and radical cation of oxymetazoline.

### 3.8.3 ASAP analysis of Anadin extra

The work demonstrated here is the first research performed by the ASAP probe for a multi-active ingredient tablet. The analysis of pharmaceutical formulations containing more than one active ingredient has been demonstrated by other ionisation techniques in the past. One such example is that of Anadin Extra. This tablet contains paracetamol (mw 151), aspirin (mw 180) and caffeine (mw 194) as active pharmaceutical ingredients. The tablet was simply sampled by wiping the glass capillary against the surface of the tablet.

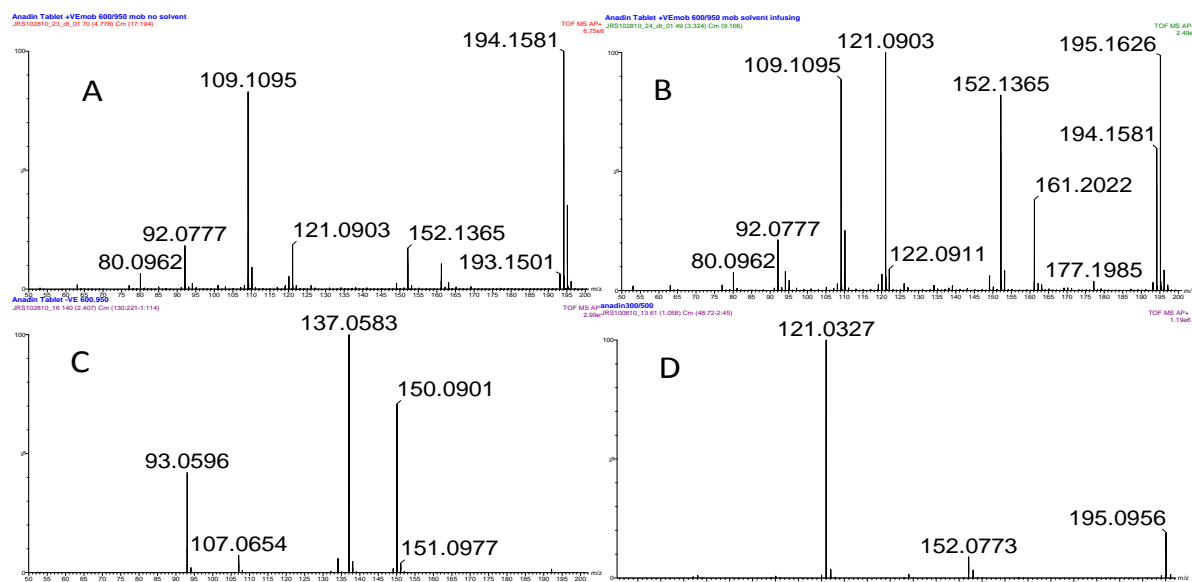


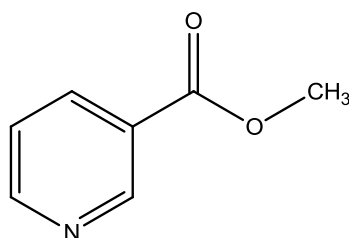
**Figure 3.29** - Spectra obtained during ASAP analysis of an Anadin Extra tablet at (A) 600 °C (no solvent infusing), (B) 600 °C (solvent infusing), (C) negative polarity with solvent infused, and (D) 300 °C (solvent infusing).

When the temperature is set to 600 °C and solvent is infused (Figure 3.29A), the predominant peak observed is the radical cation of caffeine ( $m/z$  194). Also present at a low intensity is the protonated molecule ion of paracetamol ( $m/z$  152). The fragment at  $m/z$  109 is a heat induced radical cation fragment formed from both caffeine and paracetamol. The peak at  $m/z$  121 is representative of a fragment of a protonated caffeine ion. When solvent is infused into the ASAP source region, the

amount of water vapour increases. Figure 3.29B shows the spectrum acquired when solvent was infused into the source and probe was set to 600 °C. The ion at  $m/z$  194 is still present, although the base peak is now the protonated caffeine ion ( $m/z$  195). The relative intensities of the ions at  $m/z$  152 and 121 have increased while the ion at  $m/z$  109 is similar. The corresponding fragment at  $m/z$  110 derived from protonated caffeine and paracetamol has increased in intensity. The negative ionisation mode ASAP spectrum for the Anadin Extra tablet is shown in Figure 3.29C. The aspirin active has not been observed in positive mode, and is more likely to produce deprotonated ions due to the presence of an acidic carboxylic group. Negative ionisation mode ASAP resulted in the observation of deprotonated paracetamol ( $m/z$  150) and fragments of aspirin at  $m/z$  137 and 93. No observation of deprotonated aspirin was observed (Figure 29C). DESI has been performed in negative mode previously and the deprotonated ion was observed (Williams, Lock et al. 2006). In positive mode when the temperature of the probe was decreased (300°C) and solvent infused, the spectrum shown in Figure 3.29D was observed. There are three main ions –  $m/z$  195,  $m/z$  152 and  $m/z$  121, which are representative of the protonated ion of caffeine, the protonated ion of paracetamol, and a fragment of caffeine respectively.

### 3.8.4 Deep heat spray case study

Deep heat spray is a commonly used spray formulation applied externally to provide comfort from muscular pain. The main active pharmaceutical ingredient in the formulation is methyl nicotinate (Figure 3.30).



Methyl Nicotinate  
Chemical Formula: C<sub>7</sub>H<sub>7</sub>NO<sub>2</sub>  
Exact Mass: 137.048

**Figure 3.30** - Structure, formula and exact mass of methyl nicotinate.

Methyl nicotinate is a volatile molecule, and desorbed from the ASAP glass capillary at ambient temperatures, resulting in a protonated peak. Increasing the temperature resulted in both a radical cation and the protonated molecule ion. The ATD of the protonated molecular ion and the ATD of the radical cation were significantly different (Figure 3.31).

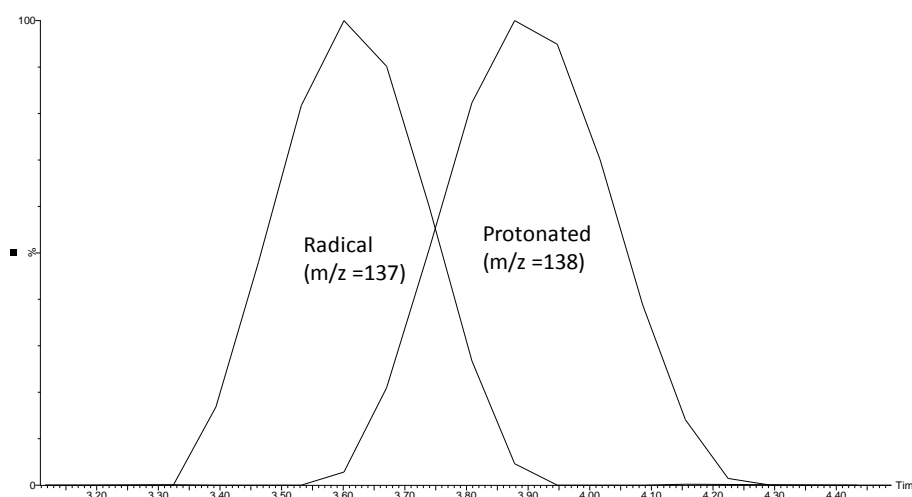


**Figure 3.31** - ATDs for the charged radical and protonated molecule ion of methyl nicotinate produced by ASAP ionisation.

The ATD of the protonated methyl nicotinate ion generated by ASAP, was similar to the ATD observed when protonated methyl nicotinate ions were generated by TA-EESI, ESI and DESI (not shown). No comparison could be made for the radical cation, as it is only generated by ASAP. The mobility separated product ion spectra for the protonated ion and radical cation are shown in Figure 3.32 A and B. A comparison of the product ion spectrum generated for the radical cation by ASAP and a spectrum generated by EI and listed in the National Institute of Standards and Technology (NIST) database are well matched (Figure 3.32 B,C). There is therefore the potential to rapidly characterise small molecules by the ASAP technique and then identify and/or confirm the structure of the unknown with a comparison of the MS/MS spectrum of the radical cation with well established EI databases.

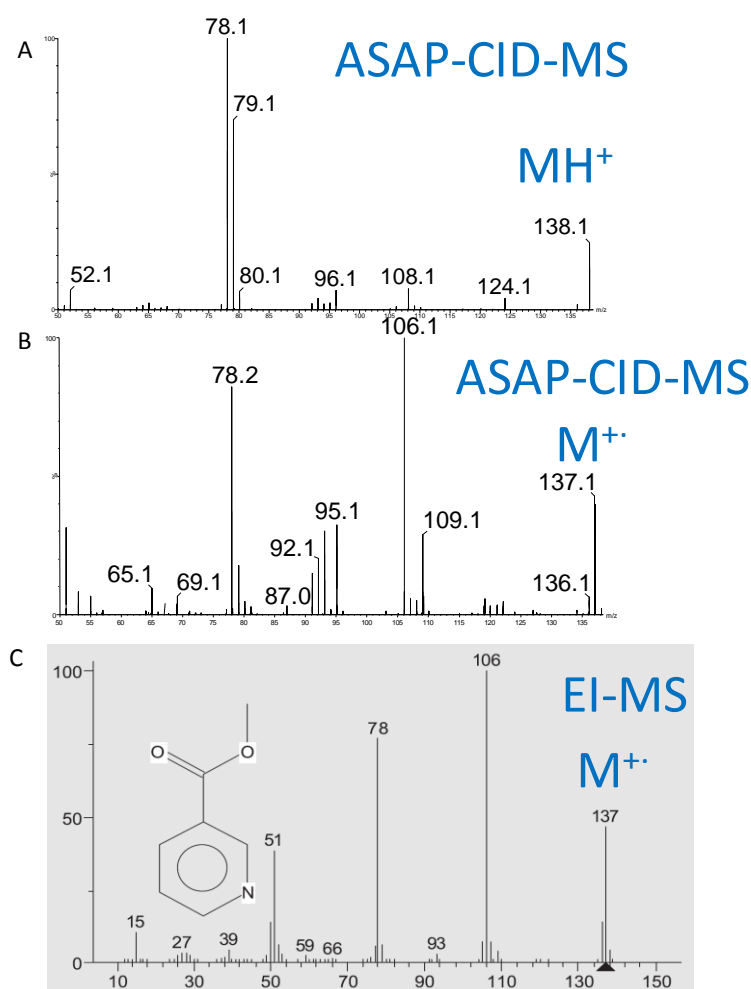


**Figure 3.32** - (A) Mobility separation spectrum of protonated methyl nicotinate, (B) corresponding radical cation product ion spectrum (C) NIST spectrum generated by EI.

MS/MS analysis of the protonated ion formed from TA-EESI, ASAP, DESI and ESI resulted in a product ion that was -14 daltons less than the precursor ion. It is very unlikely that this is a direct loss. A number of experiments were devised to characterise this product ion. The MS/MS spectrum of methyl nicotinate (a meta isomer (Figure 3.32A)) was compared with the MS/MS spectra of the ortho and para isomers. Both isomers resulted in the observation of a product ion 14 daltons below that of the protonated molecule ion (Figure 3.33).

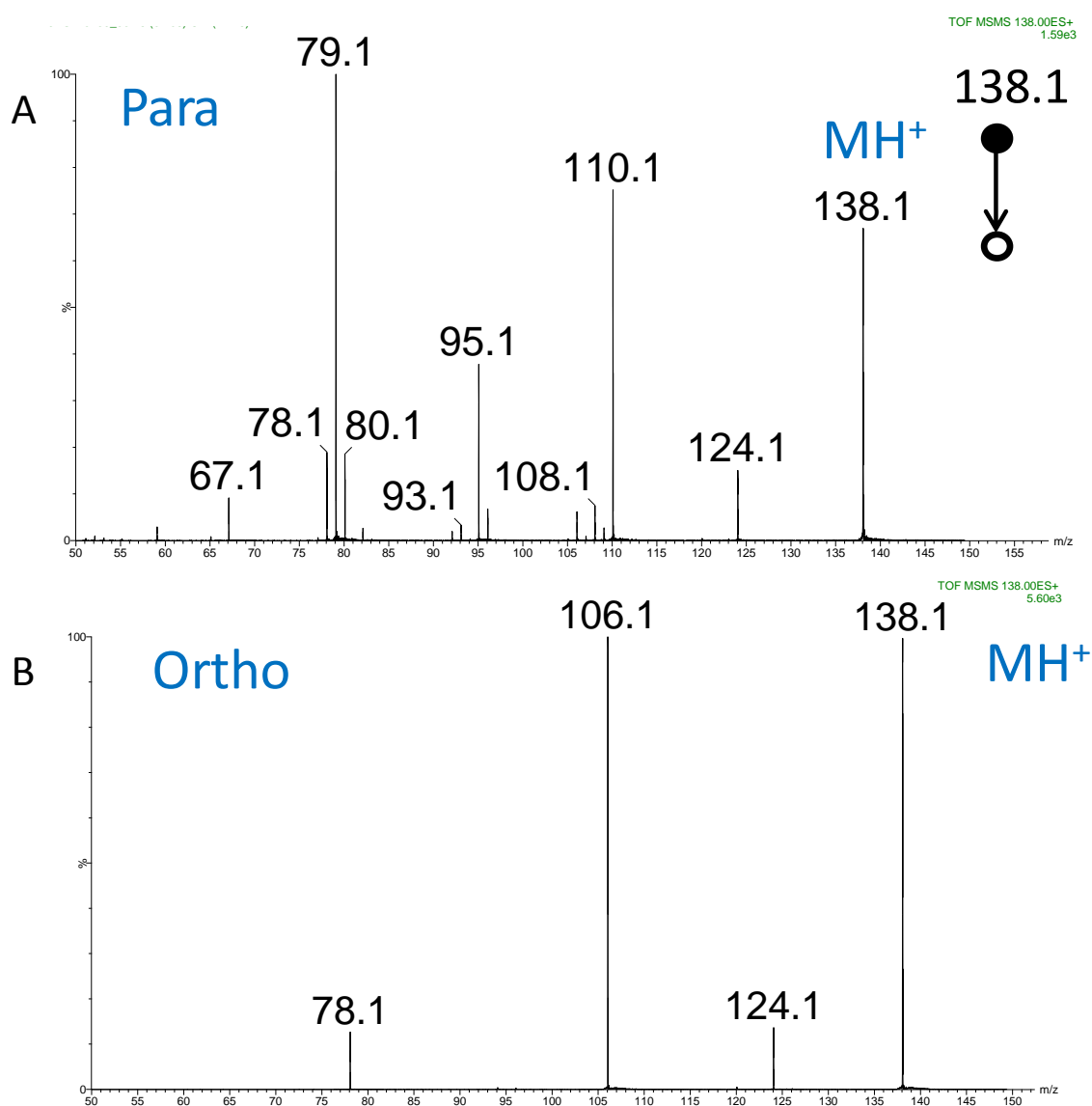


**Figure 3.33** - MS/MS of para (A) and ortho (B) isomers of methyl nicotinate

The difference of 14 daltons corresponds to a difference of CH<sub>2</sub>, in which case the structure of the product ion could be that of nicotinic acid (Figure 3.34).

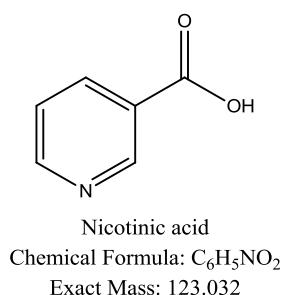


**Figure 3.34** - Structure, formula and exact mass of nicotinic acid.

A pseudo MS<sup>3</sup> experiment was carried out where the cone voltage was increased resulting in cone induced fragmentation. The *m/z* 124 ion (from methyl nicotinate) was then precursor selected and fragmented to produce the spectrum in Figure 3.35A. A comparison with the MS/MS spectrum of nicotinic acid (Figure 3.35B) shows that product ions generated are very similar.

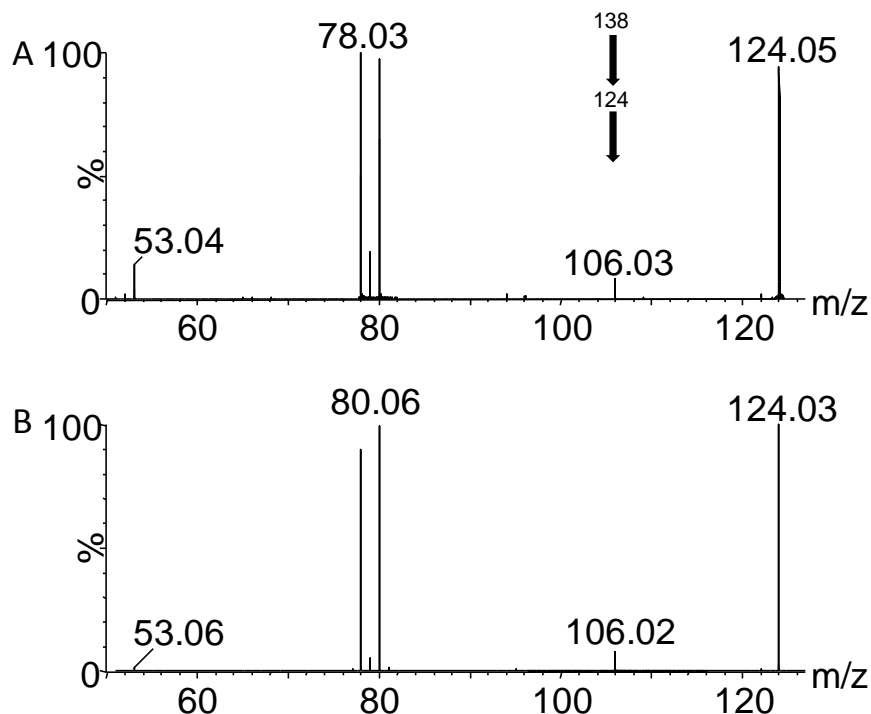


**Figure 3.35** - Pseudo MS<sup>3</sup> of *m/z* 124 ion from methyl nicotinate (A) and MS/MS of nicotinic acid (B).



Further evidence that the product ion at  $m/z$  124 corresponds to nicotinate acid is shown in Figure 3.36. Fragmentation was performed in the trap cell. This allows the ATD of the -14 Da product ion of methyl nicotinate (Figure 3.36A) to be compared with the ATD of the nicotinic acid precursor (Figure 3.36B) under similar conditions. The ATD are identical and reproducible. The ATD is 3.46 ms, and with an estimated cross section of  $68.3 \text{ \AA}^2$ .

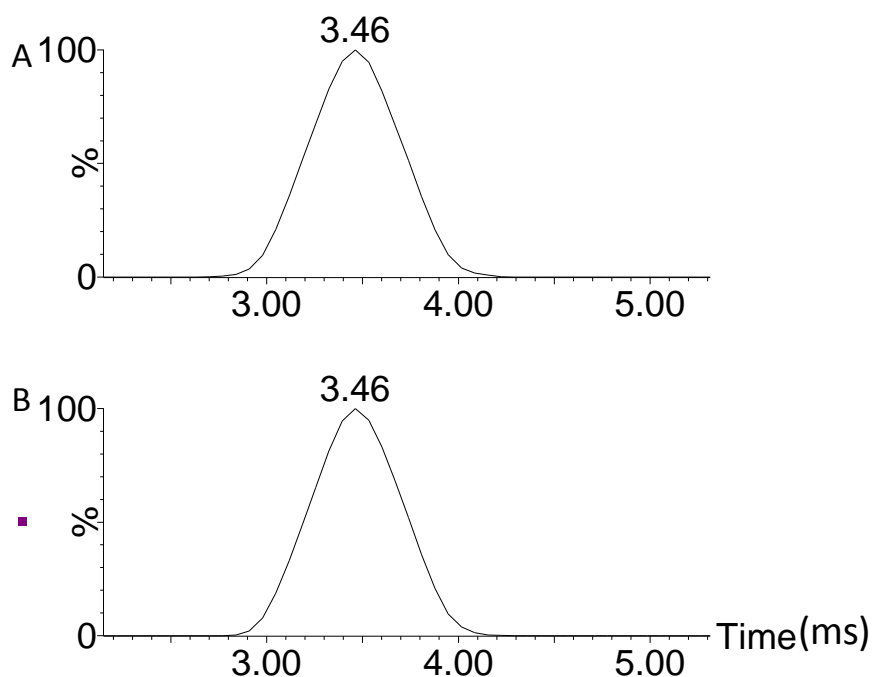


**Figure 3.36** - ATD of methyl nicotinate product ion with  $m/z$  124 (A) compared with ATD of nicotinic acid (B)

A potential explanation for the generation of protonated nicotinic acid from the fragmentation of protonated methyl nicotinate may be given by the observation of a hydration reaction whereby water reacts with methyl nicotinate. Fragmentation of this product could then result in protonated nicotinic acid and methanol. The loss of 14 daltons was also observed in spectra generated by means of QQQ and FT-ICR instrumentation.

### 3.9 Conclusions

Thermal assistance can increase the information content of the container based EESI technique for the analysis of semi and non volatile analytes. The ASAP technique can allow for the generation of both protonated molecule ions and radical cations. This adds additional information, and can help identify unknowns by comparison of MS/MS data of radical cations with the extensive databases of EI spectra. Both techniques rely on temperature, and limitations of both techniques include heat induced fragmentation, which is possible if the temperature is high enough for sample decomposition.

Thermal fractionation of components in formulations, can aid in the simplification of spectra obtained. Protonated molecule ions and radical cations may be mobility separated, indicating shape and/or mass differences. It would be interesting to follow up these observations with theoretical calculations of specific radical cations and protonated molecule ions.

The TA-EESI technique is more suitable for those samples that contain components that can be volatilised (such as found in liquid, spray and vapour samples). Solid samples may also be analysed via this method but may decompose within the sample container. ASAP is better suited for solid analysis, but liquids can also be analysed by dipping the glass capillary into a liquid sample container.

Compounds that contain components of significant volatility may not be detected by the ASAP technique (for example camphor in the oxymetazoline formulation), but may be observed using the TA-EESI technique. The data obtained from both techniques is similar to data obtained by conventional ESI analysis. When utilised, IM-MS provides additional information and an additional separation step.

The protonated molecular ion of benzocaine ( $m/z$  166) has two observed peaks in the mobility spectrum. These two peaks have different product ion MS/MS spectra which, when added, are in good agreement with the MS/MS spectrum generated from the non-mobility separated and ESI generated protonated molecule ion.

### 3.10 References

- Aguado, E., Longarte, A., Alejandro, E., Fernández, J. A. and Castaño, F.** (2006). "ZEKE-PFI Spectroscopy of Benzocaine." *The Journal of Physical Chemistry A* **110**(18): 6010-6015.
- Chen, H., Venter, Andre., Cooks, R. Graham.** (2006). "Extractive electrospray ionization for direct analysis of undiluted urine, milk and other complex mixtures without sample preparation." *Chemical Communications*(19): 2042-2044.
- Chernetsova, E. S. and Morlock, G. E.** (2011). "Determination of drugs and drug-like compounds in different samples with direct analysis in real time mass spectrometry." *Mass Spectrometry Reviews* **30**(5): 875-883.
- Creaser, C. S., Griffiths, J. R. and Stockton, B. M.** (2000). "Gas-phase ion mobility studies of amines and polyether/amine complexes using tandem quadrupole ion trap/ion mobility spectrometry." *European Journal of Mass Spectrometry* **6**(2): 213-218.
- Görög, S., Rényi, M. and Herényi, B.** (1989). "The changing rôle of ultraviolet spectroscopy in drug analysis." *Journal of Pharmaceutical and Biomedical Analysis* **7**(12): 1527-1533.
- Gu, H. W., Hu, B., Li, J. Q., Yang, S. P., Han, J. and Chen, H. W.** (2010). "Rapid analysis of aerosol drugs using nano extractive electrospray ionization tandem mass spectrometry." *Analyst* **135**(6): 1259-1267.
- Hansen, S., Pedersen-Bjergaard, S. and Rasmussen, K.** (2011). "Titrimetric Methods. Introduction to Pharmaceutical Chemical Analysis, "John Wiley & Sons, Ltd: 65-82.
- Harry, E. L., Reynolds, J. C., Bristow, A. W. T., Wilson, I. D. and Creaser, C. S.** (2009). "Direct analysis of pharmaceutical formulations from non-bonded reversed-

phase thin-layer chromatography plates by desorption electrospray ionisation ion mobility mass spectrometry." *Rapid Communications in Mass Spectrometry* **23**(17): 2597-2604.

**Huang, G., Chen, H., Zhang, X., Cooks, R. G. and Ouyang, Z.** (2007). "Rapid screening of anabolic steroids in urine by reactive Desorption Electrospray ionization." *Analytical Chemistry* **79**(21): 8327-8332.

**JackSon, A. T., Williams, J.P., Scrivens, J.H.** (2006). "Desorption electrospray ionisation mass spectrometry and tandem mass spectrometry of low molecular weight synthetic polymers." *Rapid Communications in Mass Spectrometry* **20**(18): 2717-2727.

**Janin-Bussat, M.-C., Strub, J.-M., Wagner-Rousset, E., Colas, O., Klinguer-Hamour, C., Corvaia, N., Dorsselaer, A. and Beck, A.** (2010). "Structural Characterization of Antibodies by Mass Spectrometry." *Antibody Engineering* 613-634.

**Karpas, Z. and Tironi, C.** (1991). "The mobility and ion structure of protonated aminoazoles." *Structural Chemistry* **2**(7): 655-659.

**Kauppila, T. J., Talaty, N., Kuuranne, T., Kotiaho, T., Kostinen, R. and Cooks, R. G.** (2007). "Rapid analysis of metabolites and drugs of abuse from urine samples by desorption electrospray ionization-mass spectrometry." *Analyst* **132**(9): 868-875.

**Kauppila, T. J., Wiseman, J. M., Ketola, R. A., Kotiaho, T., Cooks, R. G. and Kostinen, R.** (2006). "Desorption electrospray ionization mass spectrometry for the analysis of pharmaceuticals and metabolites." *Rapid Communications in Mass Spectrometry* **20**(3): 387-392.

**Klyuev, N. A.** (2002). "Application of Mass Spectrometry and Chromatography–Mass Spectrometry in Drug Analysis." *Journal of Analytical Chemistry* **57**(6): 462-479.

**Lalli, P. M., Iglesias, B. A., Toma, H. E., de Sa, G. F., Daroda, R. J., Silva Filho, J. C., Szulejko, J. E., Araki, K. and Eberlin, M. N.** (2012). "Protomers: formation, separation and characterization via travelling wave ion mobility mass spectrometry." *Journal of Mass Spectrometry* **47**(6): 712-719.

**Li, M., Hu, B., Li, J. Q., Chen, R., Zhang, X. and Chen, H. W.** (2009). "Extractive Electrospray Ionization Mass Spectrometry toward in Situ Analysis without Sample Pretreatment." *Analytical Chemistry* **81**(18): 7724-7731.

**Li, Y.-J., Wang, Z.-Z., Bi, Y.-A., Ding, G., Sheng, L.-S., Qin, J.-P., Xiao, W., Li, J.-C., Wang, Y.-X. and Wang, X.** (2012). "The evaluation and implementation of direct analysis in real time quadrupole time-of-flight tandem mass spectrometry for characterization and quantification of geniposide in Re Du Ning Injections." *Rapid Communications in Mass Spectrometry* **26**(11): 1377-1384.

**Manicke, N. E., Abu-Rabie, P., Spooner, N., Ouyang, Z. and Cooks, R. G.** (2011). "Quantitative Analysis of Therapeutic Drugs in Dried Blood Spot Samples by Paper Spray Mass Spectrometry: An Avenue to Therapeutic Drug Monitoring." *Journal of the American Society for Mass Spectrometry* **22**(9): 1501-1507.

**McCullough, B. J., Bristow, A.T., O'Connor, G. and Hopley, C.** (2011). "On-line reaction monitoring by extractive electrospray ionisation." *Rapid Communications in Mass Spectrometry* **25**(10): 1445-1451.

**Meier, L., Berchtold, C., Schmid, S. and Zenobi, R.** (2012). "Extractive Electrospray Ionization Mass Spectrometry Enhanced Sensitivity Using an Ion Funnel." *Analytical Chemistry* **84**(4): 2076-2080.

**Meier, L., Berchtold, C., Schmid, S. and Zenobi, R.** (2012). "Sensitive detection of drug vapors using an ion funnel interface for secondary electrospray ionization mass spectrometry." *Journal of Mass Spectrometry* **47**(5): 555-559.

**O'Donnell, R. M., Sun, X. and Harrington, P. d. B.** (2008). "Pharmaceutical applications of ion mobility spectrometry." *TrAC Trends in Analytical Chemistry* **27**(1): 44-53.

**Powers, R.** (2009). "Advances in nuclear magnetic resonance for drug discovery." *Expert Opinion on Drug Discovery* **4**(10): 1077-1098.

**Ratcliffe, L. V., Rutten, F. J. M., Barrett, D. A., Whitmore, T., Seymour, D., Greenwood, C., Aranda-Gonzalvo, Y., Robinson, S. and McCoustra, M.** (2007). "Surface analysis under ambient conditions using plasma-assisted desorption/ionization mass spectrometry." *Analytical Chemistry* **79**(16): 6094-6101.

**Ray, A. D., Hammond, J. and Major, H.** (2010). "Molecular ions and protonated molecules observed in the atmospheric solids analysis probe analysis of steroids." *European Journal of Mass Spectrometry* **16**(2): 169-174.

**Samms, W. C., Jiang, Y. J., Dixon, M. D., Houck, S. S. and Mozayani, A.** (2011). "Analysis of Alprazolam by DART-TOF Mass Spectrometry in Counterfeit and Routine Drug Identification Cases." *Journal of Forensic Sciences* **56**(4): 993-998.

**Twohig, M., Skilton, S., Fujimoto, G., Ellor, N. and Plumb, R. S.** (2010). "Rapid detection and identification of counterfeit of adulterated products of synthetic phosphodiesterase type-5 inhibitors with an atmospheric solids analysis probe." *Drug Testing and Analysis* **2**(1-2): 45-50.

**Van Berkel, G. J. and Kertesz, V.** (2006). "Automated sampling and imaging of analytes separated on thin-layer chromatography plates using desorption electrospray ionization mass spectrometry." *Analytical Chemistry* **78**(14): 4938-4944.

**Weston, D. J., Bateman, R., Wilson, I. D., Wood, T. R. and Creaser, C. S.** (2005). "Direct analysis of pharmaceutical drug formulations using ion mobility spectrometry/quadrupole-time-of-flight mass spectrometry combined with desorption electrospray ionization." *Analytical Chemistry* **77**(23): 7572-7580.

**Williams, J. P., Lock, R., Patel, V. J. and Scrivens, J. H.** (2006). "Polarity switching accurate mass measurement of pharmaceutical samples using desorption electrospray ionization and a dual ion source interfaced to an orthogonal acceleration time-of-flight mass spectrometer." *Analytical Chemistry* **78**(21): 7440-7445.

**Williams, J. P., Nibbering, N. M. M., Green, B. N., Patel, V. J. and Scrivens, J. H.** (2006). "Collision-induced fragmentation pathways including odd-electron ion formation from desorption electrospray ionisation generated protonated and deprotonated drugs derived from tandem accurate mass spectrometry." *Journal of Mass Spectrometry* **41**(10): 1277-1286.

**Williams, J. P. and Scrivens, J. H.** (2008). "Coupling desorption electrospray ionisation and neutral desorption/extractive electrospray ionisation with a travelling-wave based ion mobility mass spectrometer for the analysis of drugs." *Rapid Communications in Mass Spectrometry* **22**(2): 187-196.

**Williams, J. P., Scrivens, J.H.** (2005). "Rapid accurate mass desorption electrospray ionisation tandem mass spectrometry of pharmaceutical samples." *Rapid Communications in Mass Spectrometry* **19**(24): 3643-3650.

**Zhang, Z., Xu, W., Manicke, N. E., Cooks, R. G. and Ouyang, Z.** (2012). "Silica Coated Paper Substrate for Paper-Spray Analysis of Therapeutic Drugs in Dried Blood Spots." *Analytical Chemistry* **84**(2): 931-938.

**Zhao, Y., Lam, M., Wu, D. and Mak, R.** (2008). "Quantification of small molecules in plasma with direct analysis in real time tandem mass spectrometry, without sample preparation and liquid chromatographic separation." *Rapid Communications in Mass Spectrometry* **22**(20): 3217-3224.

# **Chapter 4**

## **Polymer Characterisation**



#### **4.1 Introduction to synthetic polymers**

Polymers are typically large molecules that are composed of smaller building blocks called monomers. The structure of such molecules may be linear, branched or composed of more complicated architectures. Polymers may be naturally occurring, including polypeptides and proteins which may be composed of repeating amino acids, and polysaccharides which are composed of repeating carbohydrate monomers. A synthetic polymer is a type of polymer that is not found naturally. The polymeric repeat units will have been systematically reacted and may be capped by end groups. The majority of synthetic polymers produced commercially can be split into three major groupings based on mechanical properties: - (1) plastics, (2) elastomers (otherwise known as rubbers) and (3) fibres. (Gnanou 2008; Nicholson 2012)

The application range of polymeric materials is wide and varied due to the ability of synthetic polymers to exhibit a range of properties. A few examples of applications and industries that are heavily reliant on synthetic polymers include packaging, the construction industry, electronics, transport, furniture, toys, textiles, medical implants and agriculture (Koenig 2004). While some synthetic polymers such as polypropylene (PP) and polyethylene (PE) are mass produced and also well characterised (Scrivens 2000), there are thousands of speciality products that tend to be more chemically complex and thus more challenging to characterise.

The end product that a manufacturer sells is a polymer formulation, and in addition to the synthetic polymer, other components including un-reacted catalyst, low molecular weight oligomers, intact monomers and polymer additives that have been blended into the formulation to modify or enhance certain properties of the synthetic polymer. There are many types of additive including fillers, pigments, plasticisers, antioxidants, lubricants, fire retardants, heat stabilisers, flow enhancers and fragrances. An impact modifier enables certain plastics including polyvinylchloride (PVC), to absorb shocks and resist impact without cracking, while an anti-oxidant can prevent the polymer from interacting with oxygen radicals. Autoxidation can result in surface cracks and discolouration.

A more specific example of how an additive can modify the property of a polymer is shown with polyethylene glycol (PEG). PEG is a mass produced polymer with numerous applications including insulation of electrical wires, as a bulk reagent in cosmetic products, and as a calibration standard in mass spectrometry. When used as an electrical wire insulator, additives such as plasticisers, flow enhancers and heat stabilisers may be added, so that the wire will be flexible and protect users from receiving electrical shocks. When used as a cosmetic product bulk, additives including UV absorbers and fragrances will be present. When used as a mass calibrant, no additives are required.

Synthetic polymers can be classified by the method in which they were generated. The two main categories of polymerisation are step-growth polymerisation and chain growth polymerisation (Stille 1981; Nicholson 2012). In the step-growth method, the polymer backbone is generated by a reaction between two molecules. The molecular mass of the polymer increases slowly, thus if the polymer is required to have a higher mass, then a longer reaction time will be needed. An example of step wise polymerisation is with the synthesis of polyethylene terephthalate (PET). PET is commonly found in plastic bottles. The synthetic pathway is shown in Figure 4.1.

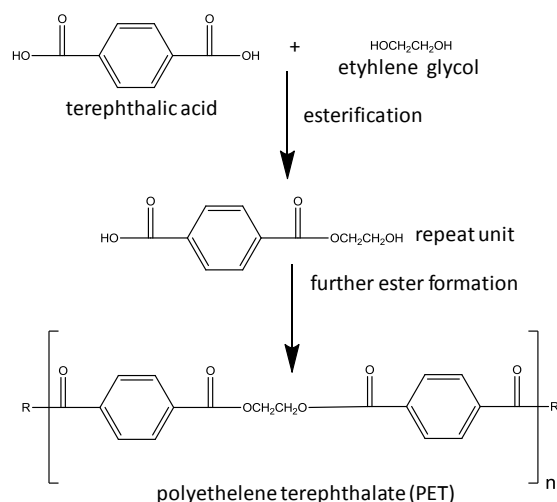
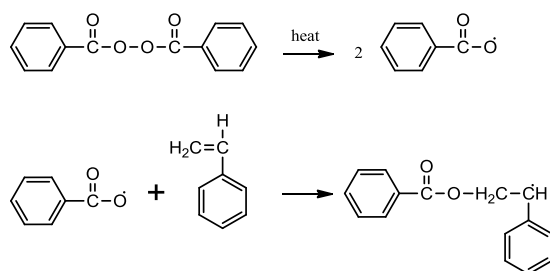
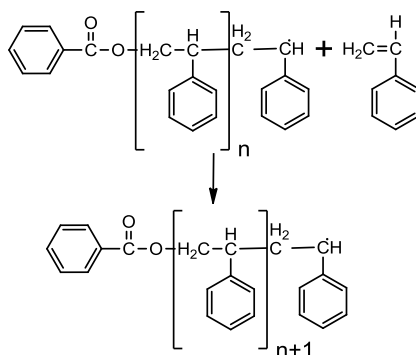


**Figure 4.1** - Generation by step-wise polymerisation of PET.

#### Initiation



#### Propagation



#### Termination (Combination)

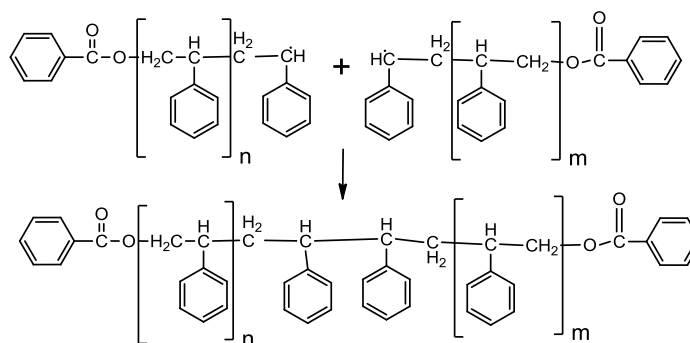


**Figure 4.2** - Chain growth of polystyrene via free radical polymerisation with benzoyl peroxide as initiator, and combination termination.

Chain growth polymerisation consists of three phases: - initiation, propagation and termination. In the initiation stage, a free radical is generated by excitation of unstable chain initiators such as azobisisobutyronitrile (AIBN) by UV light or simply by heating. In the propagation phase the reactive intermediate reacts with successive monomers resulting in chain growth. At each stage the free radical is regenerated, usually by reaction with a double bond. In the termination phase the polymerisation process terminates. Termination may be by coupling, where two free radicals join together. In coupling termination, the molecular mass of that specific

polymer will be significantly increased. In disproportionation termination, the two radicals interact, with abstraction of a hydrogen atom in one molecule, and double bond formation in the other. Chain growth polymerisation normally results in polymers with higher mass compared to step wise generation. An example of the chain growth polymerisation for polystyrene is shown in Figure 4.2.

## **4.2 Existing characterisation techniques for polymer formulations**

Characterisation of synthetic polymers is a necessity, because an understanding of the relationship between the molecular and bulk properties of such systems is essential to assess its performance in specific applications. The technique used to characterise the system is dependent on what type of information is required.

The bulk properties of synthetic polymers can be determined by a number of techniques including rheology which is predominantly used to investigate viscoelasticity (Ross-Murphy 1994), mechanical testing which is used to test for properties such as tensile strength (Swallowe 1999) and numerous thermal analysis methods such as differential scanning calorimetry (DSC) (Groenewoud 2001) that generate data on properties such as thermal stability and glass transition temperature. The performance of polymeric materials can also be affected by surface properties, and techniques such as X-ray photoelectron spectroscopy (XPS) (Thomas and O'Malley 1979) and secondary ion mass spectrometry (SIMS) (Briggs 1989) can be used to detect surface defects and imperfections. A number of microscopic techniques including atomic force microscopy (AFM), light microscopy (LM) and both transmission and scanning electron microscopy (TEM, SEM) can be used to probe the morphology of synthetic polymers (Sawyer 2008). At the molecular level, information such as molar-mass, repeat unit, sequence analysis, end-group analysis and conformational data are often desired.

Two of the most important characteristics of a synthetic polymer are average molecular weight and molar-mass distribution. In contrast to proteins where the chain length is constant, synthetic polymers always possess a certain polydispersity, which can be influenced by the polymerisation process used. A variation in the

average molecular weight can affect the physical and/or chemical properties of the polymer (Montaudo 2002). A simple example of this can be seen in a straight chain hydrocarbon series, the lower weight molecules such as methane and ethane are gases and are used as fuels, straight chain hydrocarbons containing thousands of carbons such as PE are solids and used for a variety of applications. There is often a molar-mass range for which a given polymer property will be optimal for a particular application

There are two widely used measurements of the average molecular weight. These are number average molecular weight  $M_n$  and weight average molecular weight  $M_w$ . Equations 4.1 and 4.2 show how these values are calculated.

The number-average molar mass  $M_n$  is defined by:

$$M_n = \frac{\sum m_i N_i}{\sum N_i}$$

Equation 4.1

where  $m_i$  is the mass of an observed oligomer and  $N_i$  is the number of oligomers observed, thus the total weight of the polymer sample is  $\sum m_i N_i$ , and the total number of molecules is  $\sum N_i$ .

The weight-average molar mass  $M_w$  is given by:

$$M_w = \frac{\sum m_i^2 N_i}{\sum m_i N_i}$$

Equation 4.2

The polydispersity index (PDI) (also known as the heterogeneity index) of a polymer is a measure of the distribution of its mass, and is calculated from the  $M_n$  and  $M_w$  values (Equation 4.3).

$$D = \frac{M_w}{M_n}$$

Equation 4.3

The value of  $M_w$  is always larger than  $M_n$ , except in a monodisperse system (where all molecules present have the same mass, as is the case with polypeptides). The value of  $D$  is thus equal to or greater than one. Polymers with a narrow molecular weight distribution have  $D$  values close to one, while broad molecular weight distributions are characterised by  $D$  values around two. Some distributions have two maxima and may be described as bimodal (Montaudo 2002).

Techniques such as osmometry, end group titrimetry, gel permeation chromatography (GPC) and a number of spectroscopic techniques including nuclear magnetic resonance (NMR) and Fourier transform infrared spectroscopy (FTIR) are conventional methods used to determine the  $M_n$  and  $M_w$  value of a polymer.

GPC, a type of size exclusion chromatography (SEC) is the most widely used technique with low cost equipment and is arguably the method preferred by polymer scientists for determination of both the  $M_n$  and  $M_w$  values. In the technique a polymer sample is injected into a GPC column, where components will be separated according to their size and shape within solution. The columns are packed with porous beads and will retain smaller molecules for a longer period of time, thus elution is in order of decreasing size. A comparison is then made with the elution times of known GPC calibrants to calculate the molecular weight of a polymer sample. The elution order is dependent on molecular shape and this can in some circumstances be a disadvantage. For example, the shape of low molecular weight polymers can be affected substantially when the end group is altered, generating inaccurate molecular weight data.

#### 4.2.1 Characterisation of polymers by established mass spectrometry techniques

Techniques such as light scattering, viscometry, NMR and FTIR can provide the polymer scientist with a lot of information, but are limited in that the information provided is an ensemble average for the polymer formulation. Mass spectrometry is a high sensitivity molecule specific technique, and should be viewed as both a complementary and alternative technique for polymer characterisation. MS does not require polymer standards to assign molecular weights to polymer species.

Initial attempts at mass spectrometry characterisation of polymers were limited by the inability to ionise due to the in-volatile nature and/or high molecular weight distributions of such systems. Prior to the development of ESI and MALDI, analysis of polymers by mass spectrometry was limited to in-direct methods such as pyrolysis where the synthetic polymer would be extensively degraded to generate structural information (Scrivens 2000; Montaudo 2002; Peacock and McEwen 2006), while the only ionisation method capable of generating data directly was by field desorption (FD) (Lattimer, Harmon et al. 1979). FD experiments can require a number of hours of careful experimentation to obtain a spectrum, and thus FD can be considered to be a challenging ionisation method.

The interest in mass spectrometry characterisation of polymers has surged with the development of MALDI and ESI. MALDI analysis of synthetic polymers can give information on the mass of individual polymers within a complex mixture, and from this information on repeat unit, end-group, presence of cyclic components and molar mass distributions can be obtained. The MALDI experiment can take place on the timescale of minutes, and is less experimentally challenging than FD, and can be utilised by polymer scientists whose area of expertise is not mass spectrometry. As discussed in chapter one, MALDI requires the co-crystallisation of the analyte with a matrix, and in contrast with naturally occurring polymers such as proteins and peptides, it can be challenging to achieve the correct balance of sample, salt, matrix and solvent with synthetic polymers (Scrivens 2000). Comparisons between MALDI and GPC for data obtained such as  $M_n$  and  $M_w$  are in good agreement for those polymers with a polydispersity of less than approximately 1.2 (Martin, Spickermann et al. 1996). The higher the polydispersity then the more challenging it is to obtain

an accurate result using MALDI. There have been a number of suggestions as to why there are significant mass discrimination effects when MALDI is used to analyse polymers with a high polydispersity. These include the method of sample preparation, laser power, detector design and analyser performance (Scrivens and Jackson 2000).

Cationisation of polymers can be more effective than protonation in MALDI analysis. Alkali or transition metals may be used, but are dependent on the polymer, due to different cation attachment mechanisms involved. Smaller polymers such as polyethers are more readily ionised with smaller cations such as lithium or sodium, larger polymers such as polystyrene are more readily ionised by larger cations such as silver, (Deery, Jennings et al. 1997; Chen and Li 2001). The molecular weight distribution may not be reflected accurately on the mass spectrum if an inappropriate cation is chosen (i.e. small cation with large oligomer, or large cation with small oligomer) (Deery, Jennings et al. 1997).

In contrast to MALDI, when polymers are ionised by ESI, multiply charged species may be generated, and this can be useful when the mass analyser has an upper  $m/z$  limited that is lower than the upper mass of a polymer distribution. ESI spectra can be more complicated and thus more difficult to interpret when compared with MALDI, but significantly, ESI can be used to couple gel permeation chromatography (GPC) with a mass spectrometry.

Lattimer demonstrated that MS/MS can be used to generate structural information (Lattimer 1992; Lattimer 1994) of polymers by providing end-group information. Both Lattimer and Jackson have proposed mechanisms to account for the fragmentation of the lithiated molecular ions formed, improving characterisation confidence (Lattimer 1992; Lattimer 1992; Lattimer 1994; Jackson, Scrivens et al. 2000). Lithiated precursor polyether ions have been shown to generate more structurally relevant fragmentation information when compared with that obtained from protonated or other alkali metal cationised species.



#### **4.2.2 Use of Direct Analysis techniques for polymer analysis**

The use of ambient ionisation techniques for polymer and polymer additive analysis has been limited. DESI has been coupled with MS/MS analysis for the analysis of lower molecular weight oligomers found in polyether formulations (Nefliu, Venter et al. 2006; Jackson 2007; Williams 2007; Whitson 2008). The Scrivens group demonstrated that the use of different cations could ionise polymers in a DESI experiment (Williams 2007). DESI has also been used for the analysis of polymer additives (Reiter, Buchberger et al. 2011). The ability of DESI to examine surfaces was exploited for surface polymer analysis to investigate the degradation products resulting from the radiolysis of polyurethane (Bonnaire 2010). DESI has also been interfaced with an on-probe pyrolyser for the analysis of non volatile pyrolysis products of synthetic polymers (Zhang, Shin et al. 2007).

ASAP has been utilised for the analysis of polymer additives (Trimpin, Wijerathne et al. 2009). Liquid extraction surface analysis (LESA) has also been used for the direct analysis of polymer additives and degradation products (Paine, Barker et al. 2012).

#### **4.2.3 Use of ion mobility-mass spectrometry for polymer analysis**

The structure of a synthetic polymer can be related to its performance, and it is believed that structural changes may affect its properties (Pethrick 1986). The development of IM-MS has enabled the gas-phase conformations of simple synthetic polymers to be investigated (Trimpin and Clemmer 2008). Polyether mixtures with the same nominal mass have been studied, and isomeric precursor ions may be separated by ion mobility prior to MS/MS characterisation (Hilton, Jackson et al. 2008). In a recent example IM-MS was used to assess the cyclic polymer purity in a formulation. The polymer investigated can either be linear or cyclic, and is isobaric, but only exhibits certain properties when cyclic, thus synthetic chemists required the formulation to be composed of only the cyclic oligomer (Hoskins, Trimpin et al. 2011).

### 4.3 Aims of work reported in chapter

Both ambient ionisation and IM-MS have been evaluated for the characterisation of a number of polymer formulations. Results have been split into three self contained sections.

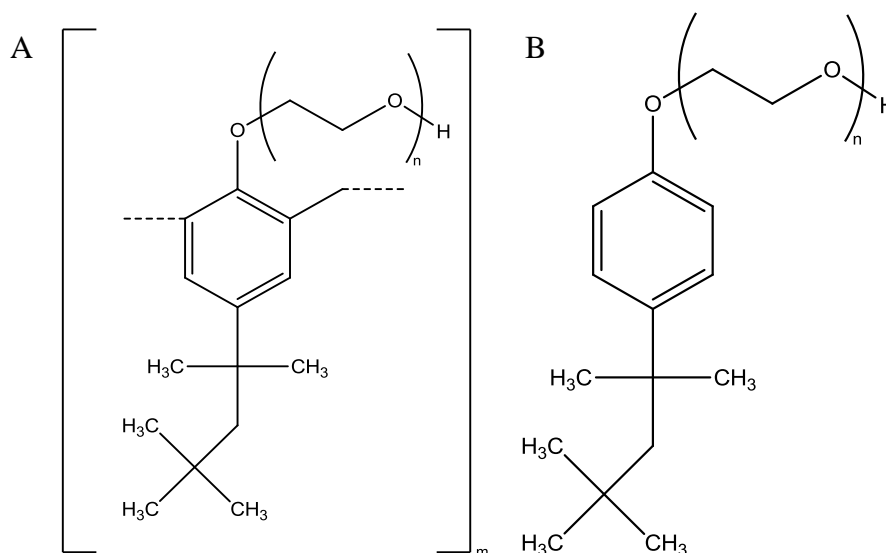
- 1) A comparison of the use of two ambient ionisation techniques (TA-EESI and ASAP) for a polyether formulation is shown in section 4.4. Comparisons have been made with spectra generated by ESI and MALDI. These techniques have the potential to speed up the analysis time of such formulations. The capability of both techniques to lithiate polyethers was assessed, and is important as lithiated polyethers produce more structural information in an MS experiment.
- 2) The characterisation of four polysorbate formulations is described in section 4.5. The use of ASAP to provide complementary information to conventional MALDI analysis is evaluated. The percentage fatty acid content of a formulation is important as will indicate the emulsifying properties of a polymer formulation. Conventionally this is assessed by gas chromatography – mass spectrometry (GC-MS), here the capability of ASAP to determine this attribute of a polysorbate formulation is assessed, and has the potential to increase analysis time, and increase information content. The formulations studied are complex, and so the capabilities of ion mobility coupled to MALDI to characterise these formulations are evaluated.
- 3) A novel fragmentation method (TAP) and TWIM-MS have been used to investigate a polymer system with a mechanically locked architecture (section 4.6). These techniques have the potential to analyse individual components and to provide gas-phase conformation information. Conventionally, these novel synthetic polymers would be characterised by ensemble techniques such as NMR, which may not reveal the true complexity of such systems.

#### 4.4 Results – Ambient ionisation for tyloxapol analysis

The suitability of two temperature driven ambient ionisation techniques for the analysis of polymer formulations has been evaluated for the characterisation of a polyether formulation sold as Tyloxapol. For materials and methods, see Chapter 2.

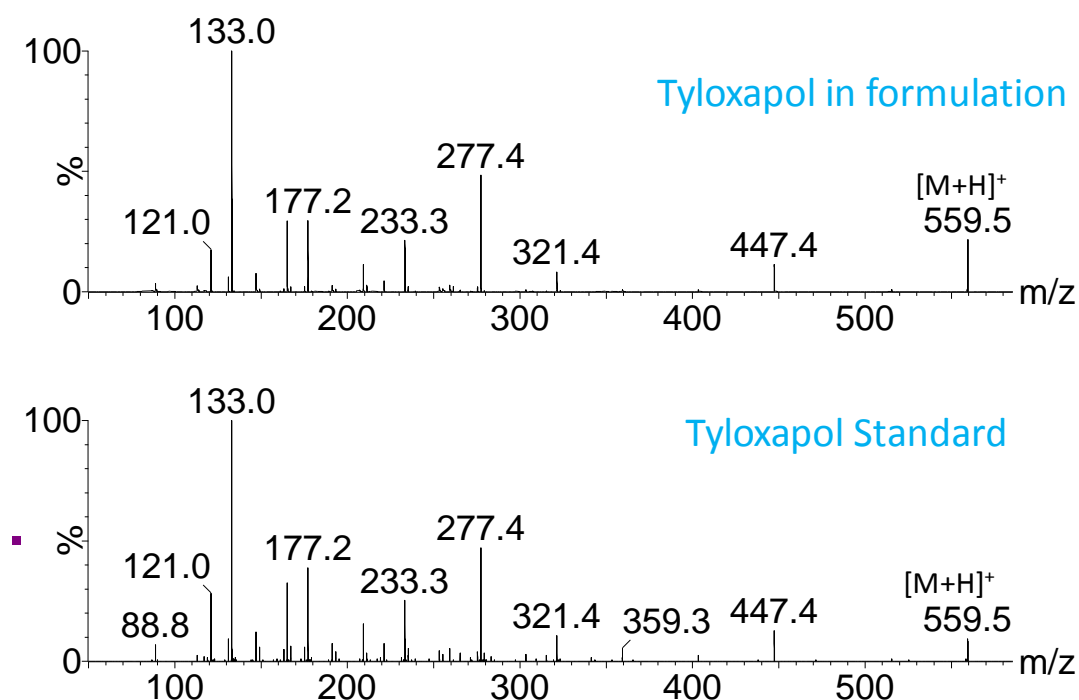
##### 4.4.1 Comparison of ionisation techniques for a Tyloxapol formulation

Analysis of a spray formulation containing oxymetazoline as the active ingredient in Chapter 3 by TA-EESI resulted in the observation at higher temperature of an ethoxylated polymer series. The specification sheet from the manufacturer indicated that the only polyether present in the formulation was Tyloxapol (Figure 4.3a). Tyloxapol is a non-ionic surfactant and is present within the formulation and has two major functions. The first is to act as an emulsifying agent, while a secondary property results in the expectoration of phlegm. The monomer of Tyloxapol consists of an alkyl aryl ether which can differ in the degree of ethoxylation from monomer to monomer. When there is just one monomer present ( $m=1$ , but  $n$  variable), the resulting structure would be identical to the structure of p-tert octylphenol ethoxylate, whose structure is shown in Figure 4.3B.



**Figure 4.3** - Chemical Structures of (A) Tyloxapol, and the structurally similar (B) p-tert octylphenol ethoxylate.

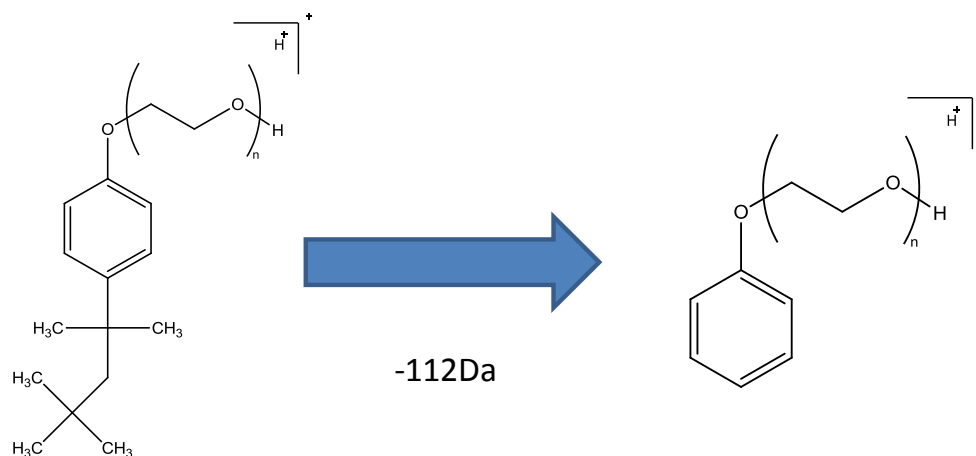
MS/MS analysis was performed on an ion observed at  $m/z$  559 from the formulation. This could correspond to p-tert octylphenol ethoxylate with 8 ethylene oxides moieties. A comparison has been made with the MS/MS product ion spectrum of the ion at  $m/z$  559 selected from a tyloxapol standard (Figure 4.4).



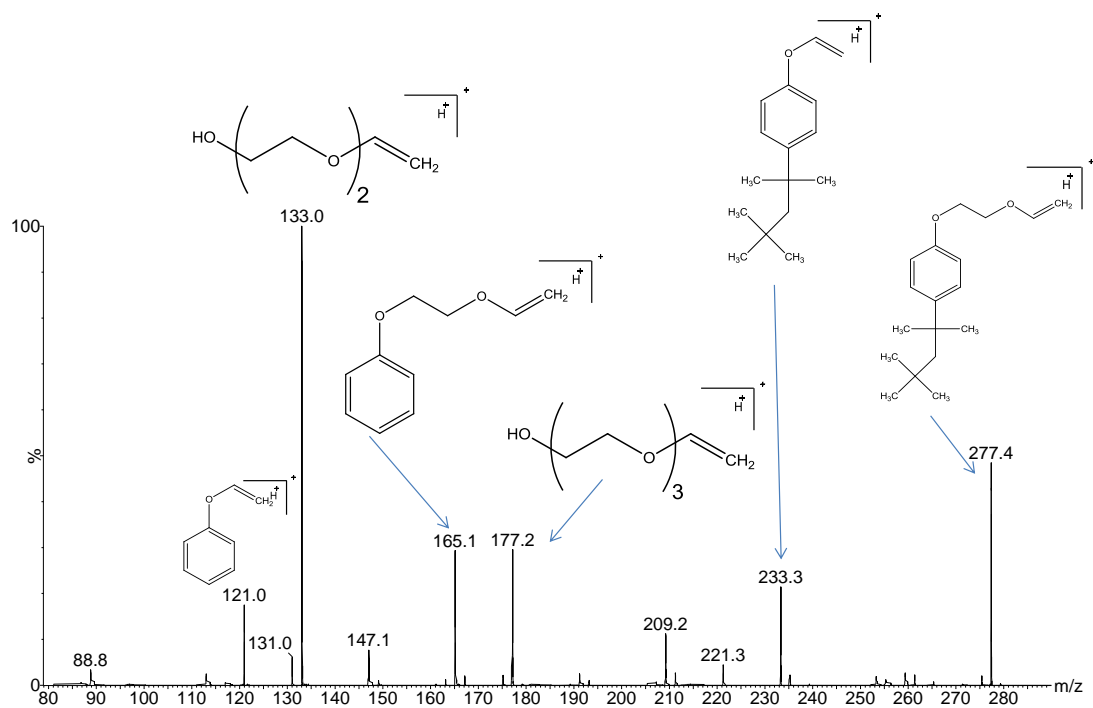
**Figure 4.4** - Comparison of TA-EESI-MS/MS spectra when  $m/z$  559.5 ion precursor selected.

The MS/MS product ion spectra obtained are in good agreement, indicating that the polymeric distribution observed in the formulation is indeed derived from Tyloxapol and not from another polyether that has not been described on the specification sheet. The series to which the ion at  $m/z$  559 belongs is thus structurally identical to p-tert octylphenol ethoxylate. The MS/MS product ion spectra shown in Figure 4.4 are similar when TA-EESI, ASAP, MALDI and ESI ionisation techniques are used. The MS/MS spectra for all polymers in the  $m/z$  559 series (i.e.  $m/z$  471, 515, 559, 603, 647, etc) fragmented in a similar way. A prominent characteristic loss of 112 daltons was observed, and the proposed fragmentation pathway is shown in Figure 4.5. The

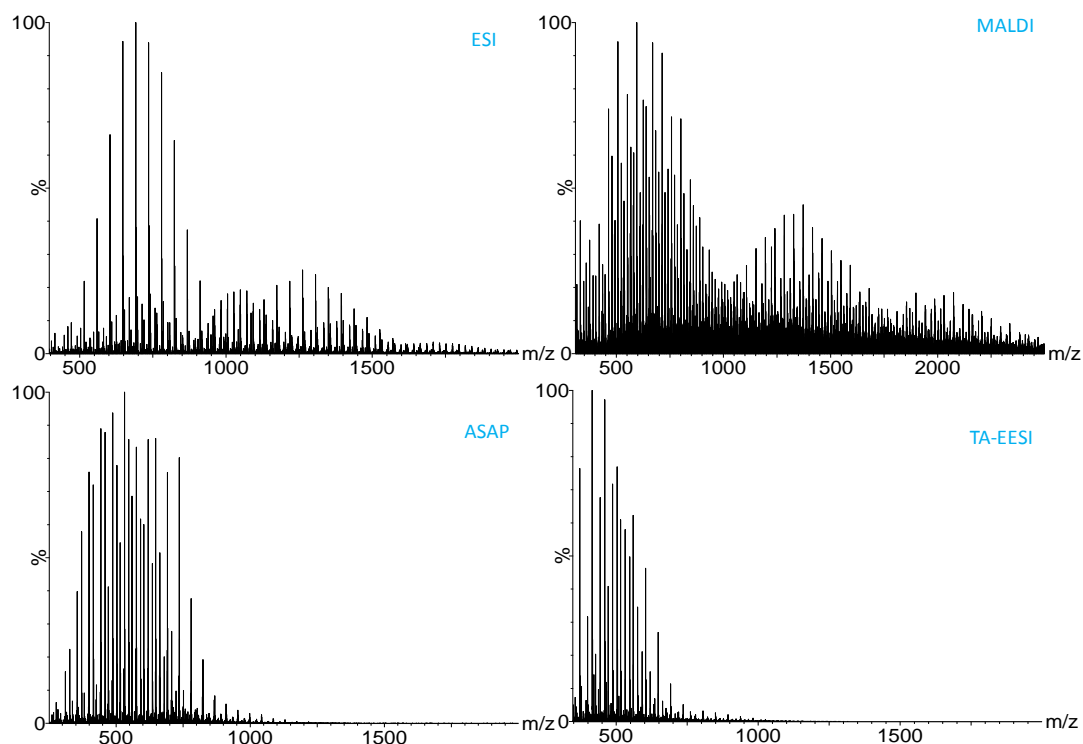
product ions generated below  $m/z$  300 were very similar for all molecules in the series, and the proposed structures for those peaks are shown in Figure 4.6.



**Figure 4.5** - Proposed formation of product ion that has a neutral loss of 112 Daltons



**Figure 4.6** - Proposed structures for ions below  $m/z$  300. This region is very similar for all the p-tert octyl phenol ethoxylate series observed from a Tyloxapol formulation.



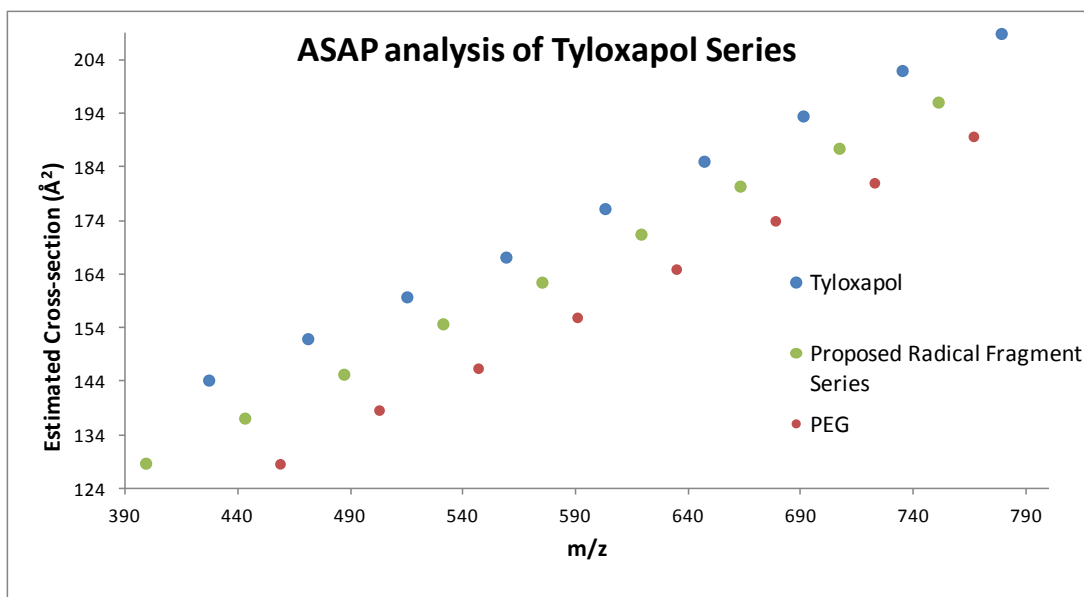
**Figure 4.7** - Spectra obtained when a 99% pure tyloxapol standard analysed using four different ionisation techniques.

Figure 4.7 shows the mass spectra observed when a Tyloxapol formulation was ionised using four different techniques. When the components in the formulation were ionised by ESI, major series observed included singly charged  $m=1$  and  $m=2$  and doubly charged  $m=3$ . The individual tyloxapol monomers are connected to one another via a  $\text{CH}_2$  group situated between the two aryl rings. The majority of the  $m=1$  tyloxapol are structurally *p*-tert octylphenol ethoxylate, but there are minor levels of ions that would correspond to one or two additional carbons present (i.e. +14 or +28).

The spectrum obtained when the components were ionised by MALDI contains more easily interpreted information than the spectrum obtained by ESI. All components are singly charged, and the presence of  $m=1$  through to  $m=3$  tyloxapol families can be observed. Spectra obtained by TA-EESI and ASAP are limited to around  $m/z$  1000 (when maximum temperature applied). There is no observation of any

tyloxapol species corresponding to  $m=2$  or  $m=3$ . Both of the ambient ionisation techniques presented here require heat to vapourise the sample. There are two probable explanations for why only  $m=1$  species were observed in these two techniques. The first is that the heat required to evaporate the polymers intact is greater than the temperature required to fragment the  $m=2$  and  $m=3$  species. The second is that the  $m=2$  and  $m=3$  species require a higher temperature than the upper heat limit of the two techniques employed to facilitate evaporation.

Three major ion series can be observed when ion mobility is used to resolve peaks that have been generated by means of the ASAP method (Figure 4.8). The estimated cross sections of the three series increases linearly with increase in mass. Mobility extracted spectra are shown in Figure 4.9. One of the extracted spectra corresponded to a tyloxapol species structurally similar to p-tert octylphenol ethoxylate and another was characterised as di-hydroxyl end capped polyethylene glycol (PEG). During ASAP analysis radical cationisation of the sample may occur, and it is proposed that the third series observed is generated by fragmentation of unstable radical cations. This is supported by MS/MS analysis of an ion at  $m/z$  646, which is the radical cation of p-tert octylphenol ethoxylate with 10 ethylene oxide repeats. An intense ion at  $m/z$  575 is observed representing a 71 dalton loss, presumed to be loss of  $C_5H_{11}$ . This loss was not present when the protonated ion at  $m/z$  647 was fragmented. A comparison of these ions is shown in Figure 4.10. CID of other radical cations within the  $m=1$  series also resulted in a loss of 71 daltons (data not shown).



**Figure 4.8** - Estimated cross sections of 3 extracted ion series generated by means of ASAP.

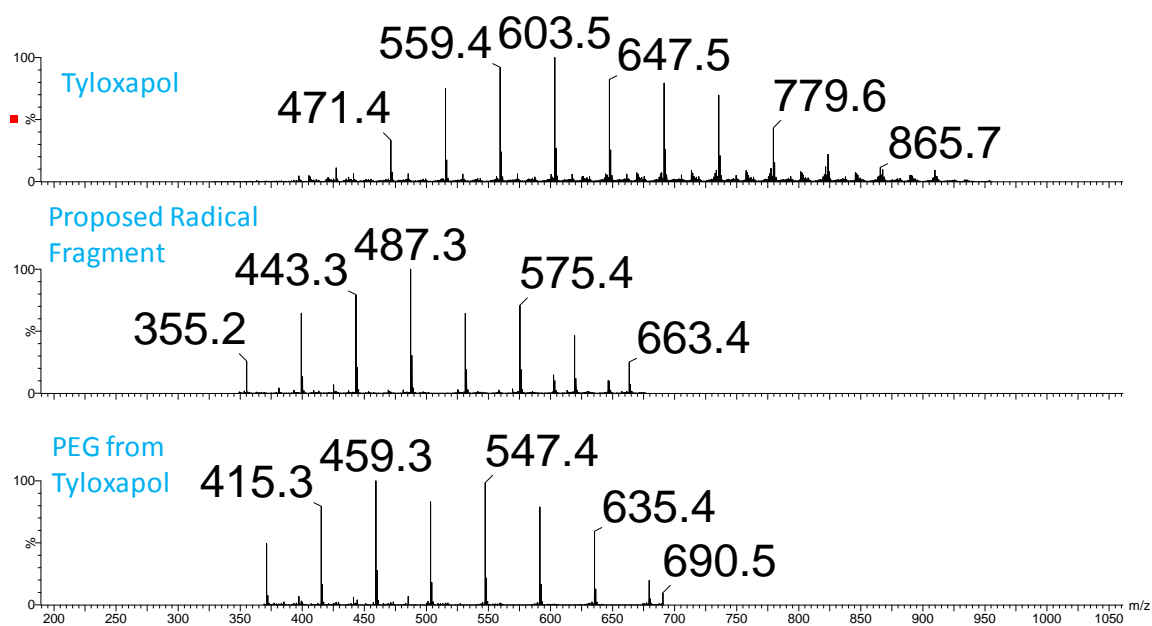


**Figure 4.9** - Mobility-extracted ASAP MS spectra observed in a Tyloxapol formulation.



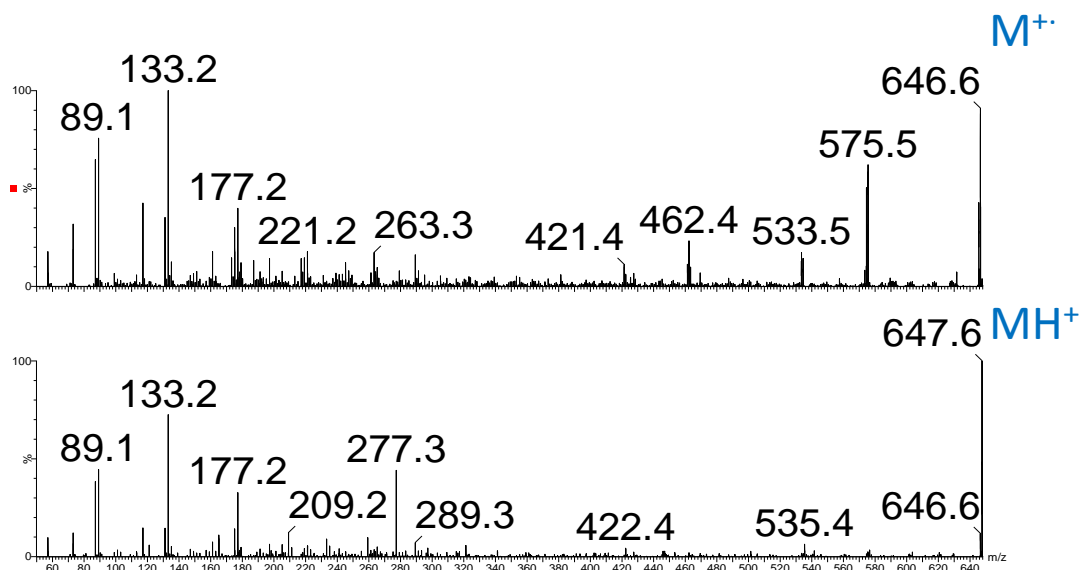


**Figure 4.10** - Comparison of MS/MS spectra for the radical cation (top) and the protonated molecule ion (bottom) of p-tert octylphenol ethoxylate with 10 ethylene oxide repeat units.

Evidence from the ASAP experiments indicate that oligomers from the p-tert octylphenol ethoxylate series had the largest estimated CCS. Loss of the alkyl chain (-71 daltons) results in a smaller estimated CCS for oligomers in the series, and the di-hydroxyl end capped PEG which does not contain the alkyl chain or the aryl ring, had the smallest CCS.

Analysis of the spectrum generated when TA-EESI was performed on a tyloxapol formulation indicated that, as with ASAP, three polymer distributions were detected. The ATD for the p-tert octylphenol ethoxylate molecules generated by TA-EESI did not differ to those generated using ASAP. The same is true for the di-hydroxyl end capped PEG species. The third series was composed of molecules with the same nominal  $m/z$  as the radical cation fragment series observed in the ASAP spectrum. It is not likely that a radical ion will be formed by TA-EESI, because the basic approach is based on ESI. Accurate mass results obtained for the unknown series were significantly different from the series acquired with the ASAP. The estimated

CCS for the three major series observed when TA-EESI used to ionise components is shown in Figure 4.11.

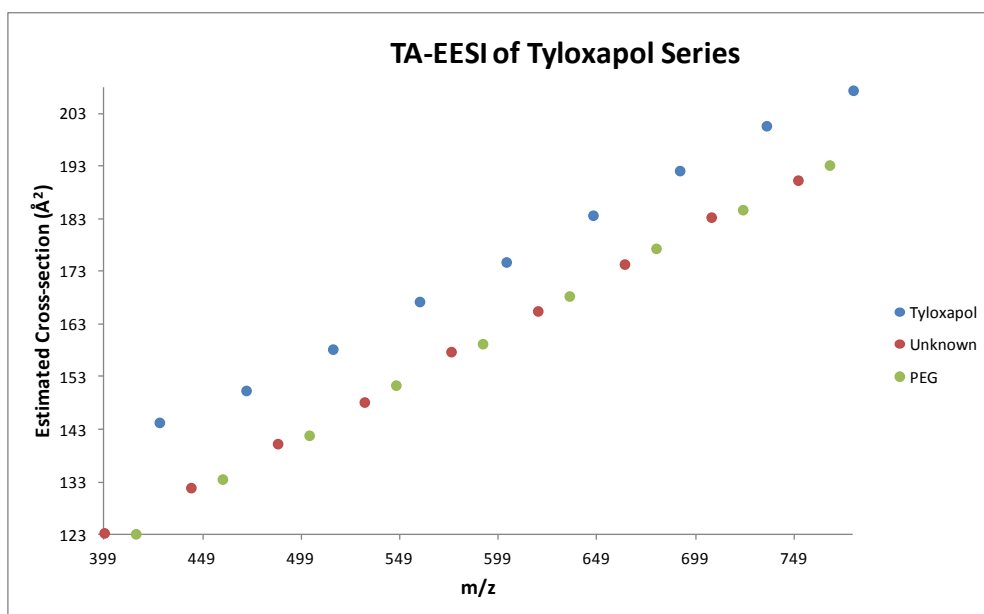


**Figure 4.11** - Estimated Cross sections of 3 extracted ion series observed when TA-EESI used to generate ions.

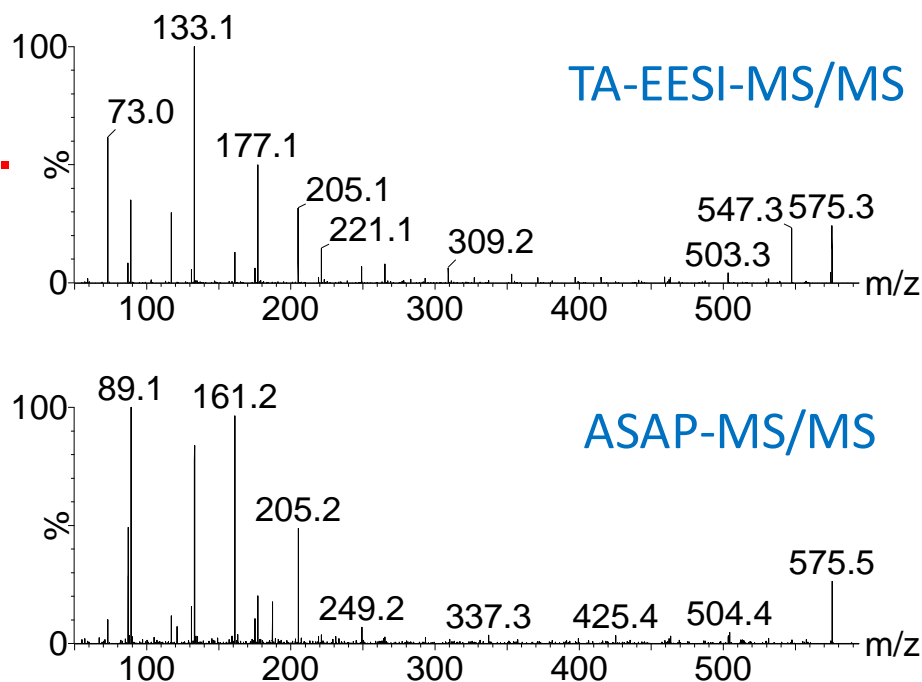


**Figure 4.12** - Comparison of MS/MS spectra for  $m/z$  575 ion generated by TA-EESI (top) and ASAP analysis (bottom).

The estimated CCS for the third series generated by TA-EESI has a trend line that is within the trend line for the di-hydroxyl end-capped PEG. This indicates that the gas phase conformation of this series is similar to that of di-hydroxyl end-capped PEG, and that there is no aryl ring present. This series is likely a side product from the synthesis of the component. The MS/MS product ion spectrum of the  $m/z$  575 ion generated by TA-EESI, and the proposed radical cation fragment ion at  $m/z$  575 generated by the ASAP are shown in Figure 4.12. At the lower end of both spectra, the  $m/z$  of the product ions produced are similar, although there are some differences in their relative intensity. The precursor ion generated by TA-EESI, fragments to produce an ion at  $m/z$  547, corresponding to a nominal loss of 28 daltons. This loss of 28 daltons is not observed in the product ion spectrum of the  $m/z$  575 ion generated by the ASAP. There are two likely possibilities for a loss of 28 daltons, the first is the neutral loss of carbon monoxide (CO), while the second is a neutral loss of ethene (C<sub>2</sub>H<sub>4</sub>). The exact mass of CO is 27.994915 daltons, while C<sub>2</sub>H<sub>4</sub> is 28.0313000 daltons. An average of three accurate mass experiments revealed that the loss was 27.9950 daltons, which would indicate that the loss is due to CO. The

measurement error for CO is calculated as 3.03 ppm. If the loss was due to C<sub>2</sub>H<sub>4</sub> this would indicate a mass error of 1296.4 ppm. This is not possible as external calibration of Synapt G2 instrument result in an error of less than 5ppm.

#### 4.4.2 Metal Ion adduct formation in ambient ionisation techniques

All Tyloxapol formulation ions formed by the ambient ionisation techniques in previous spectra have either been radical cations, protonated, or decomposition products of radical cations. As explained in the introduction, structurally informative product ions may form when the precursor polymer has been ionised by metal ion transfer. The type of metal is chosen is dictated by the nature of the polymer. Lithium adduct formation is preferred for polyether species.

A comparison of the lithiation of p-tert octylphenol ethoxylate by TA-EESI and ASAP compared to that formed from MALDI is shown in Figure 4.13. The spectra show an expanded region for the p-tert octylphenol species with 9 ethylene oxide units. The top spectrum shows that there is almost complete lithiation of the molecule, with the peak at  $m/z$  609 indicative of a lithiated ion. The ESI result (not shown) is similar to the MALDI result. All other ions in both ESI and MALDI are predominately lithiated.

The central spectrum shows the spectrum obtained when TA-EESI is used for ionisation. The majority of ions formed are protonated ( $m/z$  603) but a significant minority are lithiated ( $m/z$  609). This observation could be due to gas phase fusion of neutral molecules into an ESI droplet. The majority of the molecules are protonated because it is likely that the process of lithiation is more difficult to facilitate in the time period between the fusion event and total desolvation of droplet and release of ions. It is possible that lithiated reagent ions are created in solution and are ejected from the ESI droplets as gas phase reagent ions. These ions could then react with the neutral polymers resulting in a transfer of the lithium ion. The proportion of molecules that are lithiated by TA-EESI decreases as the  $m/z$  increases.

No lithiated ions, or radical cations were observed when molecules were ionised by means of ASAP (and solution infused). Lithium chloride solution was infused into

the ASAP source housing at the same flow rate as during TA-EESI experiments. The use of the solvent in the ASAP method has been shown in Chapter 3 to influence the type of ion formed. When no solvent is infused, and the source temperature is high to enable desorption, radical cations are predominately formed. When a solvent is used the proportion of protonated ions increases. While the desorbed polymer interacts with water clusters to form the protonated ion, it may not be possible for metal ion transfer to occur on the timescale of the ASAP experiment.

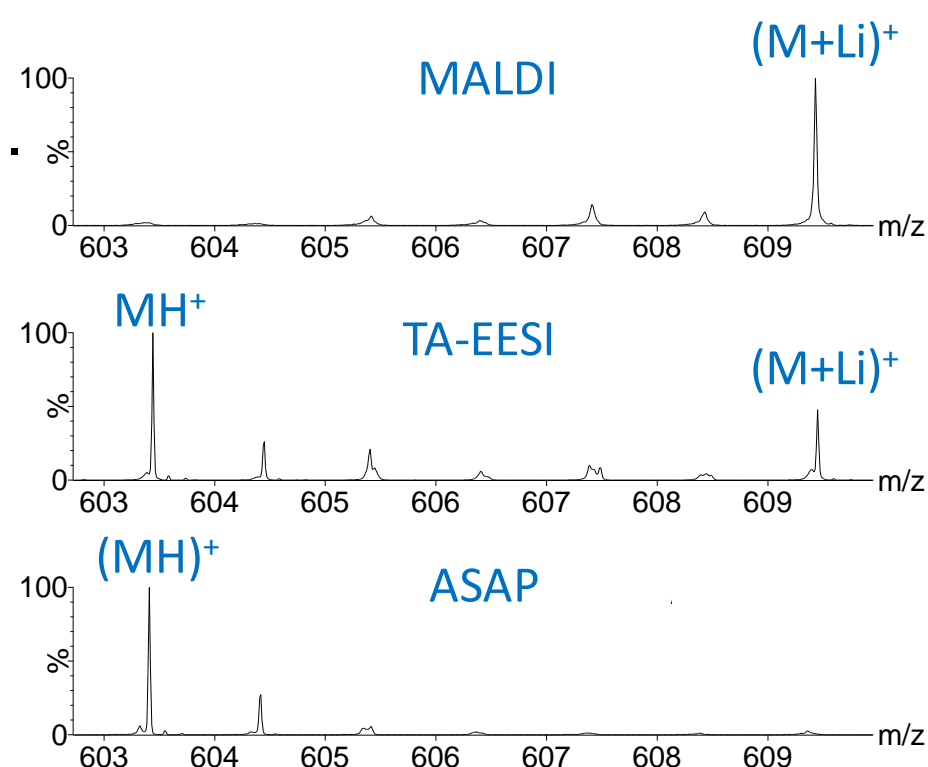


**Figure 4.13** - Spectra observed during investigation into lithiation by different ionisation techniques.

#### **4.4.3 Analysis of Tyloxapol by ambient ionisation conclusions**

ASAP and TA-EESI were not able to reproducibly ionise molecules with a mass larger than approximately 1000 Da. This is likely due to two reasons:

1. Heat induced decomposition may precede sample evaporation.
2. Higher temperatures than can be generated by these approaches are required for sample evaporation.

All common ions that were produced had the same ATDs, within experimental error, in TA-EESI and ASAP experiments, and these were also the same whether MALDI or ESI was used. Both ambient ionisation techniques produced singly charged ions.

Three major series were observed with the same nominal masses. Two of the series, PEG and p-tert-octylphenol ethoxylate, were generated in both ASAP and TA-EESI. The third series differed in terms of mobility and MS/MS spectra. The ASAP series was characterised as a radical cation fragment series, while the series generated by TA-EESI has a gas phase conformation similar to di-hydroxyl end-capped PEG. MS/MS analysis reveals that this series results in a loss of CO, while other ions are characteristic of the ethylene oxide repeat units. This series was not observed in ESI or MALDI.

Lithiation can partially occur in TA-EESI, which can improve the structural information in the MS/MS experiments. No metal ion transfer was observed with ASAP, but the formation of radical cations could potentially provide additional structural information as well as allowing comparison with EI spectral libraries.

## 4.5 Polysorbate formulations

*The majority of this section has been published in Analytical Chemistry (Snelling, Scarff et al. 2012).*

Emulsifiers are an industrially important class of excipients. These chemicals facilitate the mixture of otherwise immiscible substances, including other excipients, and active ingredients in pharmaceutical formulations. The use of emulsifiers results in a stable emulsion being formed. Surfactants are molecules that contain both a hydrophobic tail and a hydrophilic head, and are described as being amphiphilic, a key property for emulsifying agents. Surfactants are typically categorised into four groups, anionic, cationic, zwitterionic and non-ionic surfactants. Polysorbates are classified as non-ionic surfactants and are used as emulsifiers, but may also act as dispersants, stabilizers and defoamers.

The synthesis of polysorbate formulations starts with the dehydration of sorbitol. This results in anhydrides, (mainly 1:4 sorbitan) and sorbitol dianhydrides (1:4, 3:6 isosorbide), being formed at temperatures of around 250 °C. At this temperature, little acyclic sorbitol remains. Long-chain fatty acids are then reacted with the sorbitol anhydrides, in the presence of an acid catalyst. This results in the synthesis of sorbitan and isosorbide mono and di-esters. These sorbitol-derived esters are commercially available under the trade name SPAN. Chemically these are surfactants, and will act as emulsifiers. These materials have a low hydrophilic - lipophilic balance (HLB), and will form water in oil (W/O) emulsions, which is not always desirable. Ethoxylation increases the hydrophilicity of non-ionic surfactants, and more desirable oil in water emulsions (O/W) will be formed. Sorbitan and isosorbide esters are therefore reacted with ethylene oxide resulting in ethoxylated chemical families, commercially available as Tween. The specifications provided by the manufacturers of these products indicate that, on average, 20 moles of ethylene oxide are reacted with one mole of the reaction intermediates. This often provides the formulation its name, for example Tween 40, a widely used material, is also known as sorbitan polyethoxylate (20) mono-palmitate. It should be noted that this is only one of the components present in the complex mixture that makes up a typical Tween 40 formulation.

Figure 4.14 shows the synthesis route for the production of a desired sorbitan polyethoxylate monoester (other synthesis pathways may be employed, for example ethoxylation may precede esterification). The four major, commercially available Tween formulations (20, 40, 60, 80) differ in the major fatty acid component used in the synthesis. In all Tween formulations, fatty acids with varying alkyl chain lengths may be used, which can complicate their analysis. During ethoxylation the esters that are synthesised may be liable to hydrolysis. The resulting products may react, during the synthesis, with ethylene oxide chains. Species without the hydrophobic fatty tail are not considered surfactants since they are not amphiphilic in nature, and possess no emulsifying properties. Incomplete esterification can also result in non-amphiphilic molecules being produced.

A complex mixture of additional chemical species may also be formed in these formulations including PEG, PEG esters, sorbitan polyethoxylate mono and di-esters, isosorbide polyethoxylate mono and di-esters, isosorbide and sorbitan polyethoxylates. This molecular heterogeneity poses an interesting analytical challenge. Many chemical species are also isobaric, increasing the difficulty of characterisation.

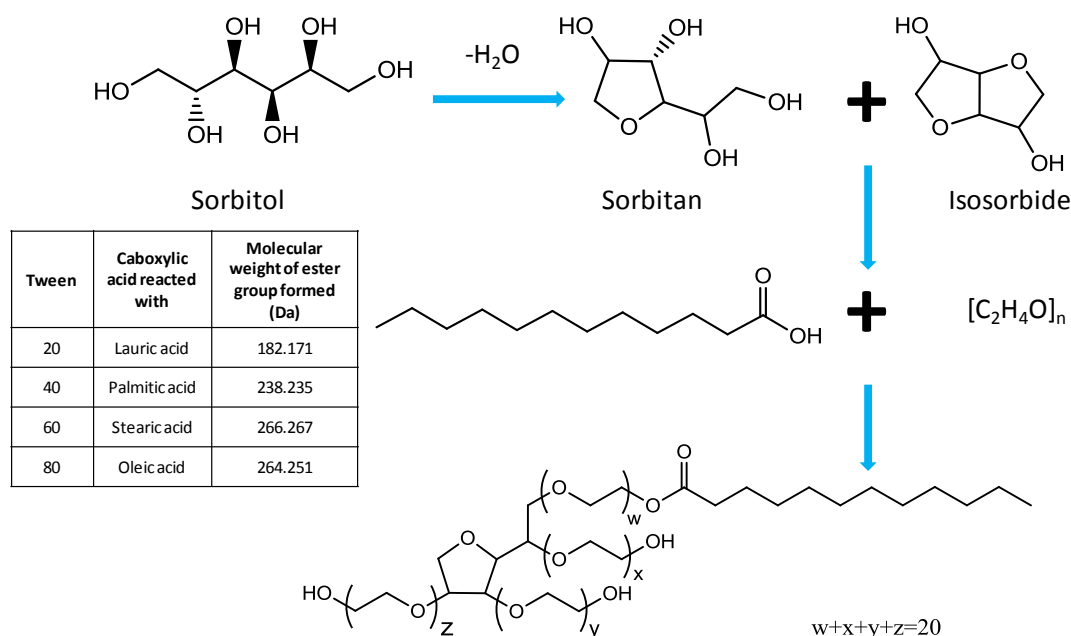


**Figure 4.14** - Schematic of Tween synthesis, inset shows the carboxylic acid.



An example of this isobaric complexity may be demonstrated by considering the Tween 80 formulation, where the major ester formed is an oleate ester. This has a nominal molecular weight of 264 Da. This is the same nominal mass as six ethylene oxide units and results in families with different structures but isobaric molecular distributions. Sorbitan polyethoxylate (20) monooleate is the desired product of the described synthesis. This has a nominal  $m/z$  of 1309, which is isobaric with the di-ester containing 14 ethylene oxide units, and the sorbitan polyethoxylate (26) molecule.

A number of analytical techniques have been reported in the literature for the characterisation of these complex formulations. The vast majority utilise mass spectrometry as the detection tool. Exceptions to this include the use of evaporative light scattering detection (ELSD) (Hewitt, Zhang et al. 2008), NMR (Dang, Gray et al. 2006), colorimetry (Kato, Nagai et al. 1989), infrared spectrophotometry (Kato, Nagai et al. 1989), fluorescence (Mehrnaz, Kao et al. 2002) and thin layer chromatography (Kato, Nagai et al. 1989). There are a number of characterisation approaches that employ separation techniques such as gas chromatography (Kato, Nagai et al. 1989) and liquid chromatography (Hewitt, Zhang et al. 2008), but which do not employ mass spectrometry as the detection technique. Negative ion chemical ionisation mass spectrometry (Brumley, Warner et al. 1985) utilising  $\text{OH}^-$ , has also been shown to be an effective approach in the characterisation of polysorbate formulations by mass spectrometry.

Liquid chromatography – mass spectrometry (LC-MS) with ESI has been evaluated for the compositional analysis of polysorbate 60 (Borisov, Ji et al. 2011). Both mixed-mode and reversed-phase liquid chromatography were compared as approaches to study both composition and base hydrolysis of polysorbate 20 and polysorbate 80 (Hewitt, Alvarez et al. 2011). A recent report by Borisov *et al* (Borisov, Ji et al. 2011) described the application of LC-MS to this problem. Tandem mass spectrometry (MS/MS), coupled with liquid chromatography separation, has been used to determine the concentration of polysorbate 80 in human plasma (Sparreboom, Zhao et al. 2002). The authors made the assumption that the Tween 80 formulation may be represented by a single sorbitan ethoxylate

monooleate, and, as such, MS/MS, multiple reaction monitoring (MRM) experiments were performed on the  $m/z$  1309 ion alone.

In a recent paper, Abrar *et al* (Abrar and Trathnigg 2011), developed a method that fractionated polysorbate formulations by liquid chromatography on a hydrophilic interaction chromatography (HILIC) column. These separated fractions were subsequently analysed by means of MALDI-TOF-MS. The use of MALDI-MS has been shown to be well suited to the analysis of ethoxylated materials. In a seminal paper, Ayorinde *et al* (Ayorinde, Gelain et al. 2000) utilising MALDI-MS, determined the chemical compositions of polysorbate formulations. The mass spectra revealed for the first time the true complexity of these formulations through the observation of the intermediates and by-products formed during sorbitan polyethoxylate monoester synthesis. The molecular complexity of Tween 60, 61, 80 and 85 was further confirmed by Frison-Norrie *et al* (Frison-Norrie and Sporns 2001), and Raith *et al* (Raith, Schmelzer et al. 2006) also utilising MALDI-TOF-MS.

MALDI-TOF-MS has been previously used extensively for the analysis of ethoxylated species, but can be limited by an inability to distinguish between isobaric compounds. There are no significant studies reported which make use of tandem mass spectrometry (MS/MS) for the characterisation of polysorbates.

The polysorbate ester formulations described here are typical of many commercial products. They show a wide range of major products and by-products, carbon number distributions of the feedstocks employed, ethylene oxide distributions (which may vary for each significant ethoxylated component) and a large dynamic range of compounds. The properties of the formulation are clearly dependent on the structures and the relative concentration of individual components, but the determination of these properties presents a major challenge. Chromatography-based approaches have successfully been used to separate individual components but the challenges in separating the, often chemically similar, species, the need to characterise novel components when present and the time required for optimal separation can restrict their use.

#### 4.5.1 ASAP analysis of Tween formulations for ester determination

The principal method, which has been employed to determine the fatty acid composition of polysorbate formulations has been gas chromatography - mass spectrometry (GC-MS) (Frison-Norrie and Sporns 2001; Dang, Gray et al. 2006) and this is the protocol recommended by the European and US Pharmacopoeias for quantitative studies. A major problem is that the fatty acids need to be released from the ester, increasing the timescale of analysis, and potentially introducing error. Borisov *et al* (Borisov, Ji et al. 2011), recently demonstrated an LC-MS based method for the identification of fatty acid content in polysorbate 20 and 80, influenced by results observed by Dang. They performed in-source CID resulting in dioxolanylium ions which are characteristic for certain fatty acids, and thus ester moieties. A number of laurate containing species observed were subsequently fragmented resulting in the formation of characteristic resonance-stabilized cyclic dioxolanylium ions. Manufacturers classify commercial Tween formulations according to the major fatty acid component used in the synthesis. Each commercial Tween formulation may contain more than one type of ester, differing in chain length reflecting the commercial origin of the feedstock used. This molecular complexity makes the characterisation analytically challenging. The type and degree of esterification used will also affect the emulsifying properties of the Tween formulation.

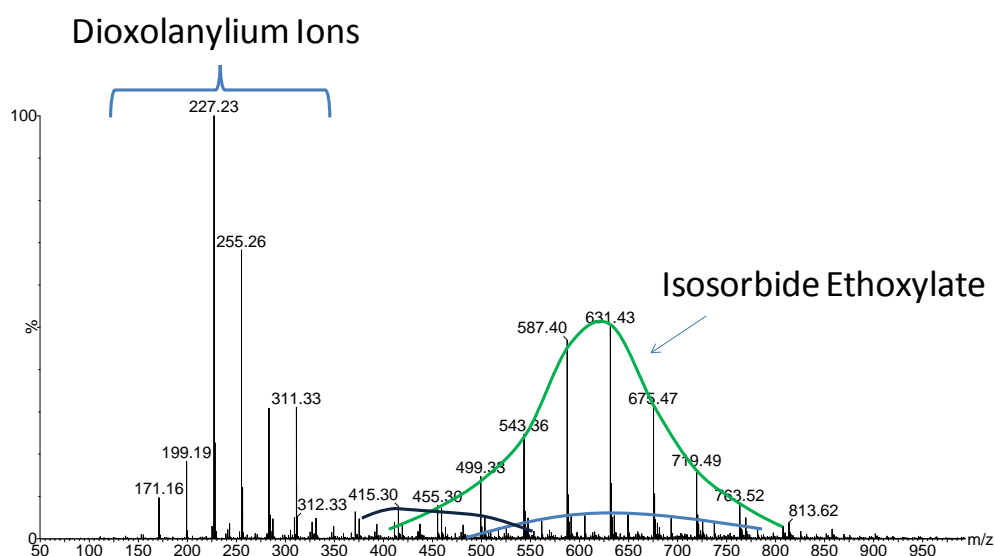


**Figure 4.15** - Typical mass spectrum observed when Tween 20 formulation is analysed by ASAP (600C).

When Tween formulations were ionised using ASAP, characteristic dioxolanylium ions were observed. Isosorbide polyethoxylate was observed as the major ethoxylated species with trace amounts of sorbitan polyethoxylate present. Trace amounts of species that we both ethoxylated and esterified were present. Figure 4.15 shows a spectrum of Tween 20 ionised using ASAP-MS. This is typical for all formulations with two regions corresponding to dioxolanylium ions and isosorbide ethoxylate observed.

The relative intensities of each of these ions remains relatively constant, independent of the nitrogen flow temperature. The use of ASAP is however not appropriate for the overall analysis of the formulation. The temperature required for desorption of formulation molecules results in trace amounts of sorbitan families, which could be due to gas-phase dehydration of the sorbitan-related chemicals in the formulation, into isosorbide-related molecules. The approach is however well suited for obtaining fatty acid compositional data.

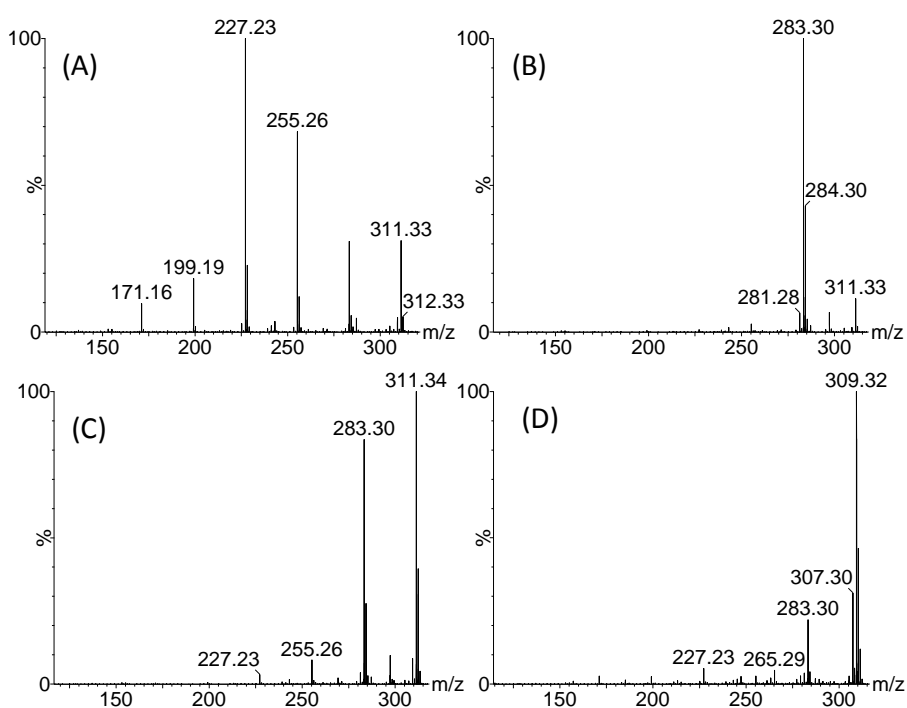


**Figure 4.16** - Characteristic dioxolanylium ions observed for (A) Tween 20, (B) Tween 40, (C) Tween 60, (D) Tween 80.

Figure 4.16 shows the dioxolanyium ions observed in an ASAP study of the TWEEN formulations with the temperature of the nitrogen gas set at 600°C, and a flow rate of 1000 L/hr. By summing the intensities of each of the specific dioxolanylium ions and dividing by the total summed ion intensity an estimation of the relative abundance of fatty acids in the Tween formulations may be calculated. This simple approach does not give an estimation of all of the species present, only the percentage content of fatty acid, since the signal observed may originate from all ester groups present within the formulation, including isosorbide and sorbitan mono and di-esters. Table 4.1 shows the approximate ester content for each Tween formulation studied. This is calculated from an average of three replicates (all replicate values differed by no more than 3%).

A comparison of observed composition was made with that supplied via the manufacturers (Sigma Aldrich) specification sheet. Product specification was independently determined by the manufacturer using methods such as thin layer chromatography (TLC) and titration. For example, the ester content determined by ASAP for Tween 20 indicated that lauric acid was the most abundant fatty acid reactant. This is in good agreement with the product specification sheet for Tween 20, which stated that the ester content was >40% lauric acid, with the balance primarily made up of myristate, palmitate and stearate esters.

A comparison of the experimental results obtained with the indicated composition of fatty acids in the commercial formulations is shown in Table 4.2. This showed good agreement for Tween 40 and 60 formulations. The Tween 80 material has an experimentally determined oleate concentration slightly lower than that indicated in the manufacturer's specification.

This represents the first use of the ASAP technique for complex polysorbate formulations, and has enabled the fatty acid/ester content of different Tween formulations to be rapidly assessed

**Table 4.1** - Approximate ester content measured, by percentage, for each Tween formulation studied

<b>Tween</b>	<b>Laurate</b>	<b>Myristate</b>	<b>Palmitate</b>	<b>Stearate</b>	<b>Oleate</b>	<b>Other Esters</b>
20	39%±2%	26%±1%	12%±1%	12%±2%	Not Detected	11%±2%
40	<1%	2%	87%±2%	10%±1%	Not Detected	<1%
60	2%±1%	4%±1%	43%±1%	51%±2%	Not Detected	<1%
80	<1%	2%	22%±2%	11%±2%	66%±1%	<1%

**Table 4.2** - Commercial specification (Sigma Aldrich). Ticks indicate manufacturer includes these in the balance of the formulation, crosses indicate not listed by manufacturer as part of formulation

<b>Tween</b>	<b>Laurate</b>	<b>Myristate</b>	<b>Palmitate</b>	<b>Stearate</b>	<b>Oleate</b>
20	40%	✓	✓	✓	×
40	×	×	90%	✓	×
60	×	×	30-50%	47-55%	×
80	×	×	✓	✓	70%

#### **4.5.2 ESI-IMMS analysis of Tween formulations**

ESI-IM-MS experiments were performed on the Tween formulations. The ESI spectra obtained contained less information than the MALDI experiments in section 4.5.3, and thus no further ESI experiments on these formulations was performed. Some species are singly charged, are doubly or triply charged. The difference in ATD between species decreased with addition of charge (compared to singly charged), and thus mobility separation of multiply charged isobaric species was ineffective. The top spectrum in Figure 4.17 shows data from an ESI-IM-MS experiment on Tween 80. The full spectrum reveals singly, doubly and triply charged species. Analysis of the spectra reveals that the major species that are singly charged are predominantly composed of an isosorbide core. Doubly charged species can contain an isosorbide or sorbitan core, while triply charged species were predominately sorbitan families. The mobilogram in Figure 4.17 reveals that there are two major regions – (A) – singly charged region and (B) multiply charged region. The corresponding extracted spectra for each region are shown in the bottom of Figure 4.17.

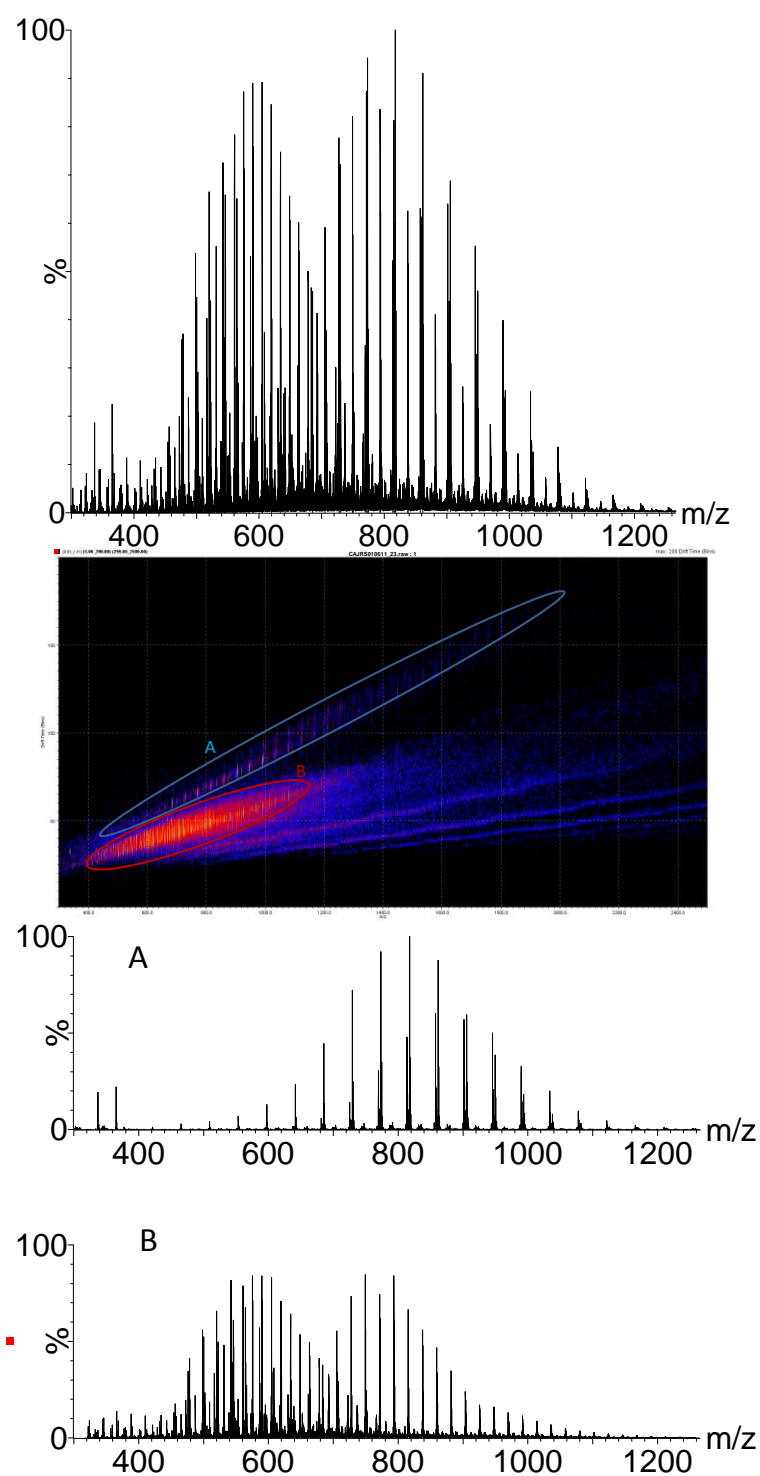


**Figure 4.17** - ESI-Mobility spectra of Tween 80 formulation (top), mobilogram of formulation (middle) with two trendlines A and B, and respective extracted spectra (bottom).



#### 4.5.3 MALDI-IMMS analysis of Tween formulations

**Table 4.3**

Chemical families observed by MALDI-IMS-MS, categorised as major, minor and trace series.

<b>Tween</b>	<b>Polyethylene Glycol</b>	<b>Polyethylene Glycol Esters</b>	<b>Isosorbide Polyethoxylate</b>	<b>Isosorbide Polyethoxylate Monoesters</b>	<b>Isosorbide Polyethoxylate Diesters</b>	<b>Sorbitan Polyethoxylate</b>	<b>Sorbitan Polyethoxylate Monoesters</b>	<b>Sorbitan Polyethoxylate Diesters</b>
20	Minor	Trace	Major	Major	Trace	Major	Major	Trace
40	Minor	Trace	Major	Major	Minor	Major	Major	Minor
60	Minor	Minor	Major	Major	Minor	Major	Major	Minor
80	Minor	Trace	Major	Major	Minor	Major	Major	Minor

Table 4.3 shows the chemical families observed experimentally for each of the formulations. The various families have been categorised into minor, major and trace components. Here major refers to values between 50 and 100%, minor to values between 10 and 50%, and trace to values less than 10%, where the percentage value refers to the most abundant peak for a polymer in a series compared to the most abundant peak overall. All species observed were lithiated, simplifying the data considerably. Tri- and tetra-esterified sorbitan species have not been listed, since only a very small proportion of peaks which could have been attributed to these were observed, and then only with poor signal to noise. Sorbitol based species were not observed in any of the Tween formulations tested, supporting the hypothesis that complete hydration of sorbitol is carried out in the manufacturing process.

In the Tween 20 formulation, the expected major product sorbitan polyethoxylate monolaurate (and other sorbitan polyethoxylate monoesters) were seen as major components. Isosorbide polyethoxylates, isosorbide polyethoxylate monolaurate (and other polyethoxylate isosorbide monoesters), together with sorbitan polyethoxylates, were also observed. An average spectrum is presented in Figure 4.18. The presence of non-esterified species in the data indicates that complete esterification during the manufacturing process did not occur, and/or ester interchange reactions may have taken place (Borisov, Ji et al. 2011). These non-esterified species lack amphiphilic properties and do not provide any additional emulsifying capacity to the overall formulation. While isosorbide polyethoxylate monolaurate is amphiphilic in nature, there are only two reactive hydroxyl groups on the isosorbide core compared with four on the sorbitan core. This results in a molecule series, which contains approximately half the number of ethylene oxide residues compared to a sorbitan polyethoxylate monoester. The presence of isosorbide species will also lower the hydrophilic-lipophilic balance (HLB) (Griffin 1949) of the formulation, and this may result in undesirable water in oil (W/O) emulsions. The presence of PEG as a minor component in Tween 20 is expected since, during the reaction, ethylene oxide can react with water molecules which are formed during sorbitan and isosorbide formation, and can also be formed as a by-product of the condensation reaction between esters and sorbitans/isosorbides.

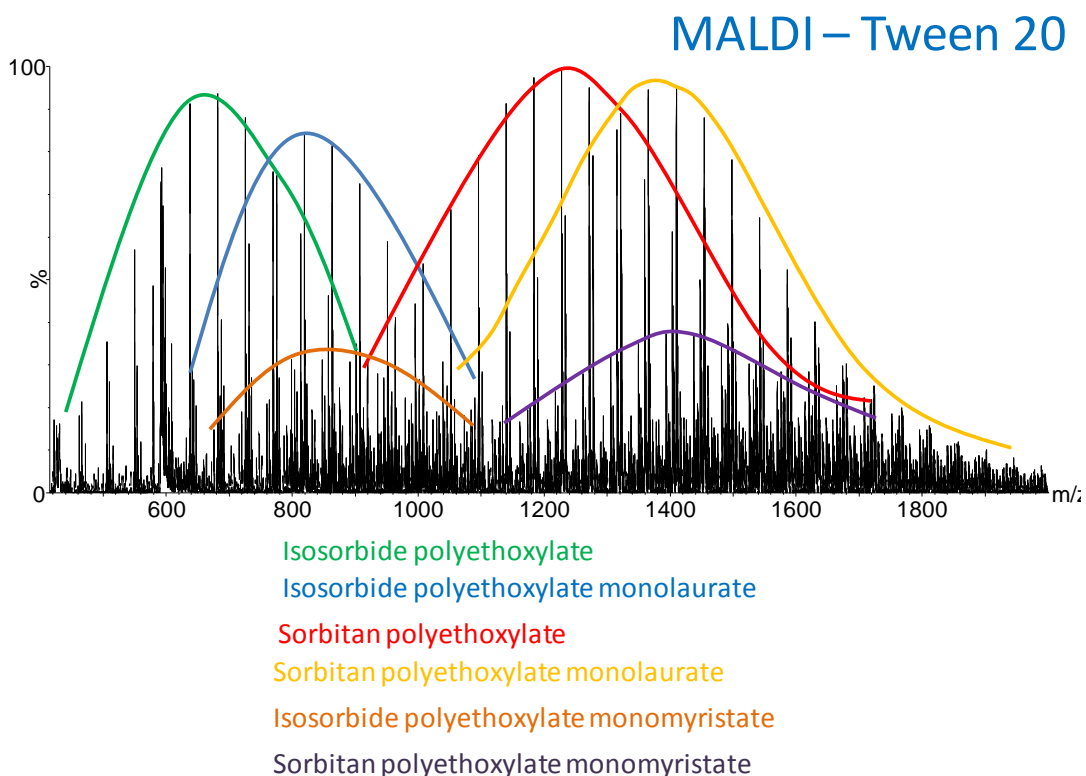


**Figure 4.18** - Summed MALDI-TWIM-MS spectrum of Tween 20, with major chemical families highlighted.

The Tween 40 formulation is similar to that of the Tween 20 formulation, the main difference being the presence of sorbitan polyethoxylate di-esters as a minor series. With Tween 40 the majority of the esterified species observed were palmitates. This is in good agreement with the diagnostic dioxolanylium ions observed. Mobility separation enabled the observation of isosorbide polyethoxylate dipalmitate as a minor series. This family is isobaric with sorbitan polyethoxylate monopalmitate, which is a major species in the formulation. Comparisons between the intensity of the ATDs obtained from isosorbide polyethoxylate dipalmitate and sorbitan polyethoxylate monopalmitate showed that the signal intensity of the former was approximately half that observed from the sorbitan polyethoxylate monopalmitate series. From the  $m/z$  versus arrival time plot, which was obtained from the MALDI-IM-MS experiments, it is possible to classify families of chemical species. Regions of the 2D-mobility space can be selected and the corresponding mobility-separated mass spectra observed. Figure 4.19A shows the estimated cross section versus  $m/z$  value for the isobaric isosorbide polyethoxylate dipalmitate and sorbitan

polyethoxylate monopalmitate series observed. Figure 4.19B shows the mobility-isolated spectra of the two series. The distribution of the isosorbide polyethoxylate dipalmitate species is observed to be lower in mass than that shown by the sorbitan polyethoxylate monopalmitate species. This is expected due to the lower degree of ethoxylation involved.

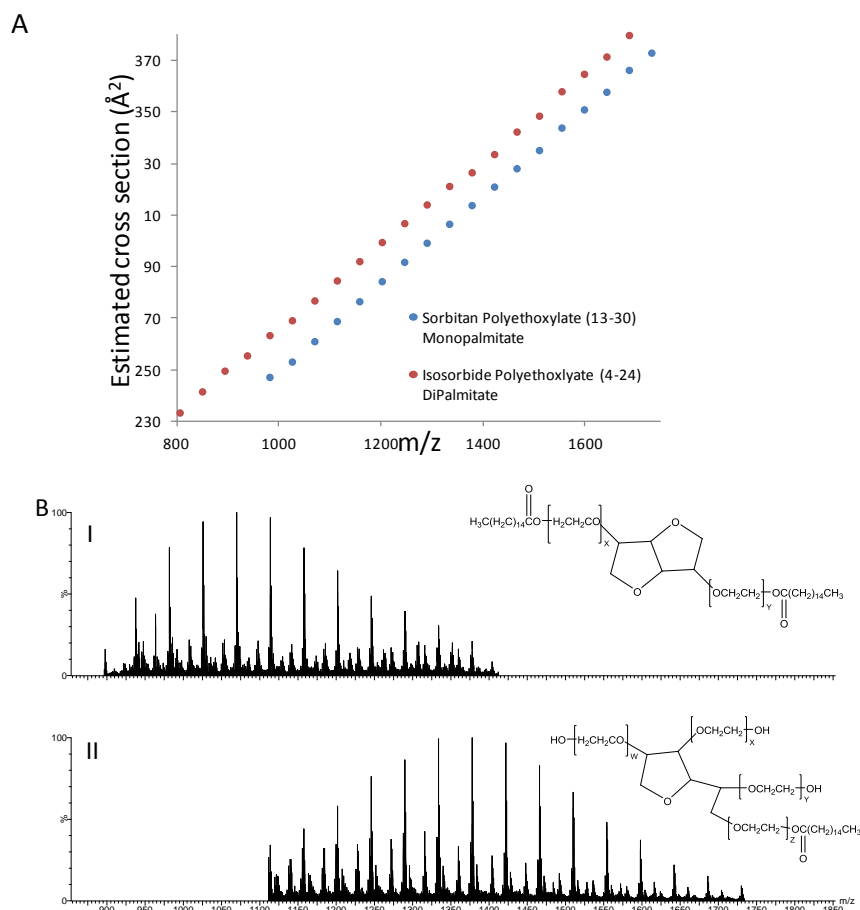


**Figure 4.19** - (A) Estimated cross section versus  $m/z$  comparison for sorbitan polyethoxylate monopalmitate and isosorbide polyethoxylate dipalmitate and (B) (I) Extracted mass spectrum for isosorbide polyethoxylate dipalmitate (II) Extracted Mass spectrum for sorbitan polyethoxylate monopalmitate.

In the Tween 60 formulation data, the sorbitan polyethoxylate monoesters were observed as minor components (along with other esterified species). The major series observed were the isosorbide polyethoxylate and sorbitan polyethoxylate families. Palmitate and stearate esters are present in approximate similar concentrations. PEG esters (PEG monostearate and PEG monopalmitate) (Ayorinde, Gelain et al. 2000; Borisov, Ji et al. 2011) were observed as minor series in the Tween 60 formulation and are trace by-products in the other formulations.

The chemical families observed as major, minor and trace species in the Tween 80 formulation are similar to those seen in the Tween 40 formulation. The nominal mass of the oleate group in the Tween 80 formulation is equivalent to the nominal mass of six ethylene oxide units and very significant isobaric overlap is present in the spectra.

Figure 4.20A shows a comparison of the estimated cross sections obtained experimentally for each  $m/z$  value of the three major isobaric isosorbide-based families. The use of ion mobility enables the clear differentiation of these species, providing an additional dimension of shape-selective information to the MALDI-MS spectra. This enables differentiation between compounds of the same isobaric molecular mass. To further characterise the isosorbide series, ions with a nominal  $m/z$  value of 1165 were selected using the quadrupole analyser, mobility-separated and then fragmented in the transfer cell. It was expected that the lithiated isosorbide polyethoxylate 23-mer ion, the lithiated isosorbide polyethoxylate monooleate 17-mer and the isosorbide polyethoxylate dioleate 11-mer, would all be observed at the nominal  $m/z$  of 1165. Figure 4.20B shows the separation of these three isobaric oligomers ( $m/z$  1165) by ion mobility, while Figure 4.20C shows the mobility-separated product ion spectra for each of the mobility-separated peaks in Figure 4.20B. The product ion spectrum shown in Figure 4.20C(I), extracted from the peak at an arrival time of 6.67 milliseconds, confirms that this ion is isosorbide polyethoxylate 23-mer. The estimated rotationally-averaged cross-section of this ion is  $260 \text{ \AA}^2$ . The mobility separated product ion spectrum in Figure 4.20C(II) is that of isosorbide polyethoxylate monooleate 17-mer. This was extracted from the peak with an arrival time of 7.22 milliseconds, and has an estimated cross-section of  $274 \text{ \AA}^2$ . The product ion spectrum clearly showed that the end group was an oleate

moiety. A loss of oleic acid is observed, as expected for isosorbide polyethoxylate monooleate 17-mer. Figure 4.20C(III) shows the product ion spectrum extracted from the peak at 7.81 milliseconds, and shows the loss of two oleic acid groups, indicative of the di-ester isosorbide polyethoxylate dioleate 11-mer. The rotationally-averaged cross-section for this species is estimated at  $287 \text{ \AA}^2$ . All of the data in Figure 4.20 were obtained in a single experiment.

Figure 4.21A shows the separation of three isobaric sorbitan chemical families by ion mobility, with similar results observed to those seen in the isosorbide series. The distribution of ions in the sorbitan series is higher in  $m/z$  due to the presence of additional reactive sites for ethylene oxide attachment. In this case oligomers with a nominal mass of  $m/z$  1227, were selected for further study. Three peaks were observed in the arrival time distribution (Figure 4.21B). The peak at 6.99 milliseconds with a cross-section of  $268 \text{ \AA}^2$  was characterised by use of the extracted product ion spectrum as sorbitan polyethoxylate 24-mer. The ion with an arrival time of 7.55 milliseconds was characterised by use of the mobility-separated product ion spectrum as sorbitan polyethoxylate monooleate 18-mer. This ion has an estimated cross-section of  $283 \text{ \AA}^2$ . The peak with an arrival time distribution centred at 8.17 milliseconds (which had a lower relative intensity than the other two peaks) was characterised by use of the mobility-separated product ion spectrum as sorbitan polyethoxylate dioleate 12-mer (Figure 4.21C). It is observed that, for these isobaric ions, the presence of an ester group increases the estimated cross-section and the presence of two ester groups further increases this value.

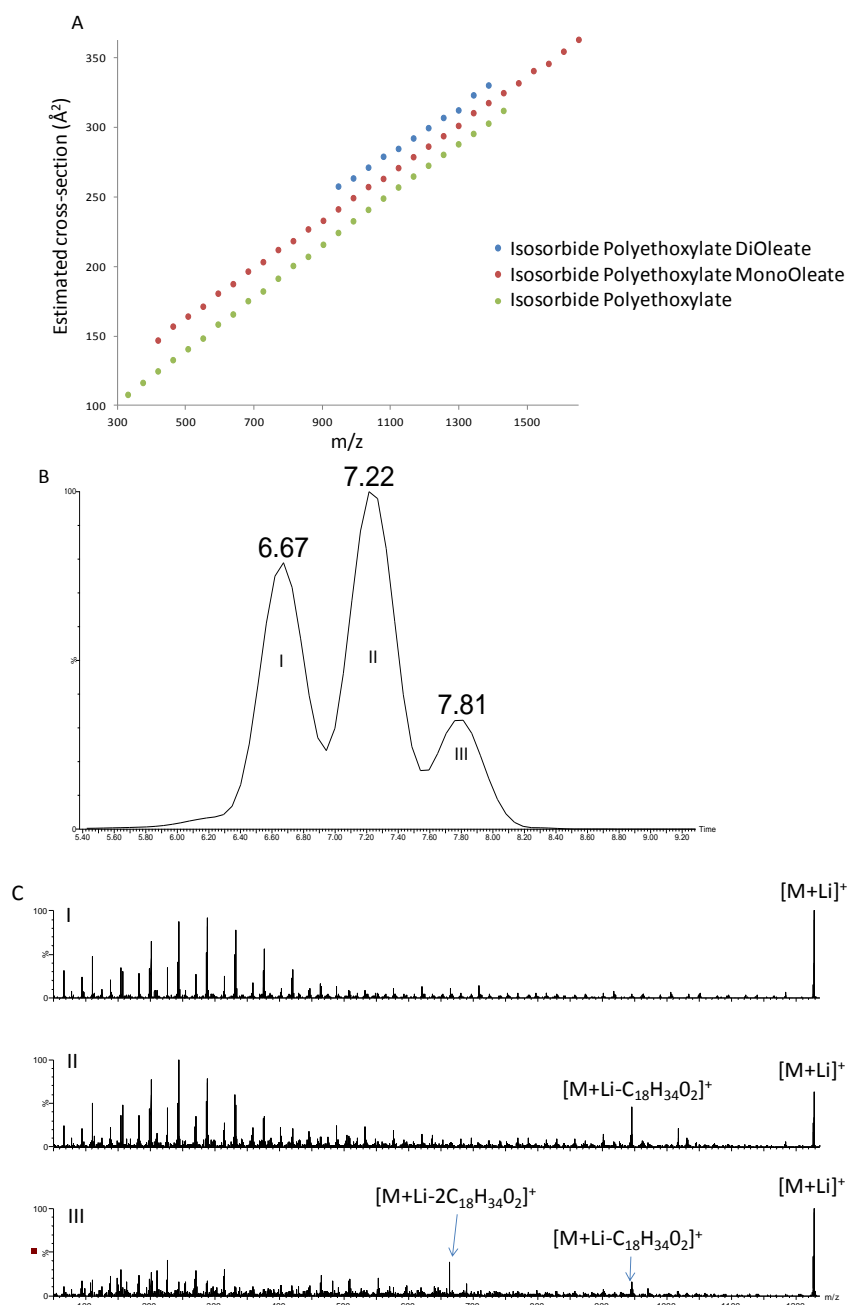


**Figure 4.20** - (A) - Estimated cross-section versus  $m/z$  for three isobaric isosorbide families (B) - ATD for nominal  $m/z$  of 1165 and (C) - (I) Mobility separated product ion spectrum for isosorbide polyethoxylate 23-mer. (II) Isosorbide polyethoxylate oleate 17-mer and (III) isosorbide polyethoxylate dioleate 11-mer.

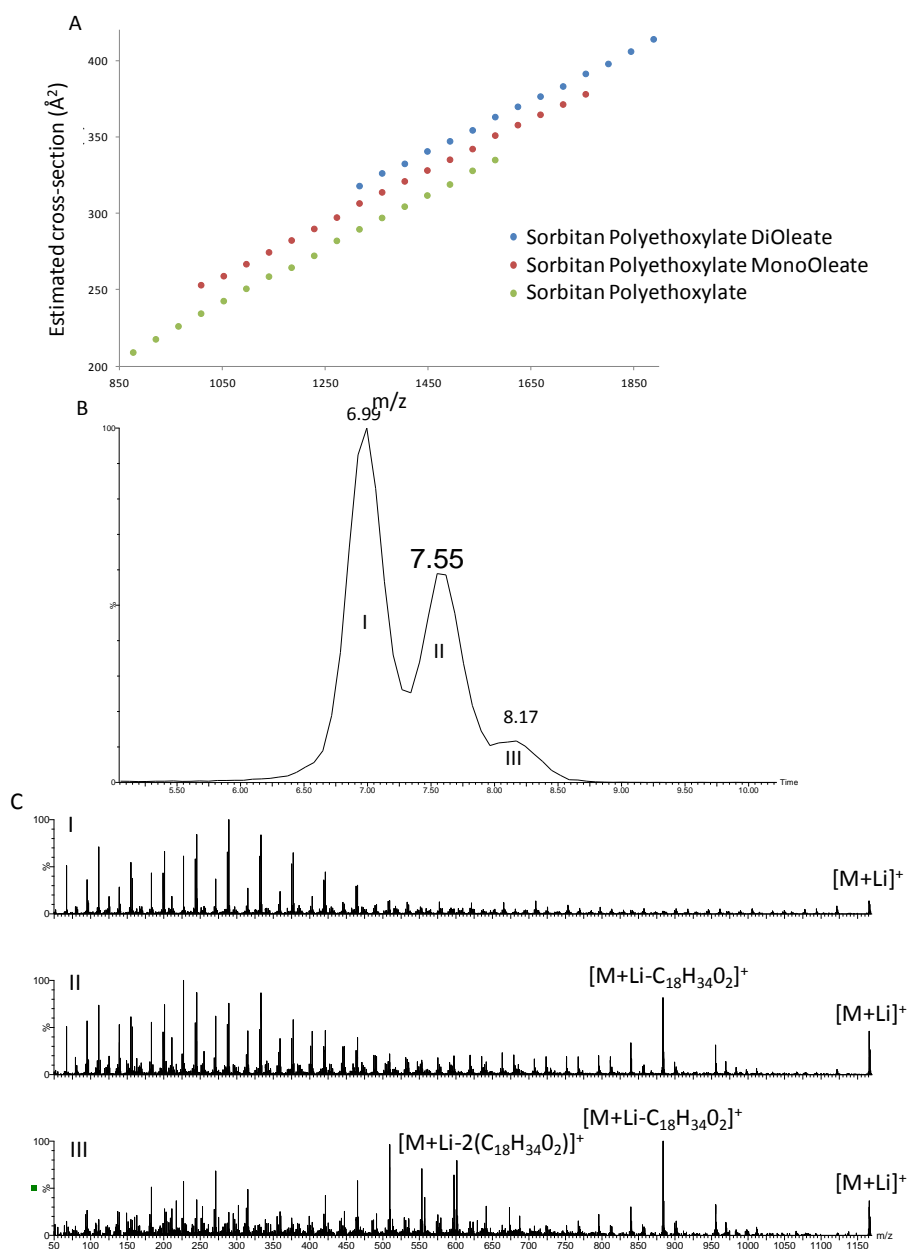


**Figure 4.21** - (A) - Estimated collision cross section versus m/z for three isobaric sorbitan families. (B) - ATD signal for m/z of 1227. (C) - Mobility separated product ion spectrum for (I) Sorbitan Polyethoxylate 24-mer (II) Sorbitan ethoxylate monooleate 18-mer (III) Sorbitan polyethoxylate dioleate 12-mer.



Information regarding the polydispersity index (PDI) measured on selected species found in each of the four formulations is presented in Table 4.4. The use of mobility data has enabled separation of isobaric species for calculation of PDI, providing an alternative approach to LC-MS measurements. The manufacturer did not give polydispersity data for individual species, but rather the entire formulation. The manufacturer gave formulation dispersities of 1.09, 1.08, 1.04 and 1.06 for Tween 20, 40, 60 and 80 respectively. The experimentally derived polydispersities for components within the formulations ranges from 1.01 to 1.12.

**Table 4.4 A-D** - Polydispersity index (PDI), number average molecular weight (Mn) and weight average molecular weight (Mw) for selected species in (A) Tween 20, (B) Tween 40, (C) Tween 60 and (D) Tween 80. Data derived from three replicates carried out on different days SD < 0.2%.

(A)	Isosorbide polyethoxylate	Isosorbide Polyethoxylate monolaurate	Sorbitan polyethoxylate	Sorbitan Polyethoxylate monolaurate	Sorbitan polyethoxylate monomyristate
<b>Mw</b>	697.7	916.6	1200.1	1345.0	1426.2
<b>Mn</b>	650.9	875.7	1176.8	1321.7	1405.3
<b>PDI</b>	1.07	1.05	1.02	1.02	1.01

(B)	Isosorbide polyethoxylate	Isosorbide polyethoxylate monopalmitate	Isosorbide Polyethoxylate dipalmitate	Sorbitan Ethoxylate	Sorbitan Polyethoxylate monopalmitate	Sorbitan Polyethoxylate dipalmitate
<b>Mw</b>	703.7	924.5	1128.3	1170.8	1385.6	1521.8
<b>Mn</b>	653.6	880.3	1111.5	1149.3	1366.7	1511.0
<b>PDI</b>	1.08	1.05	1.02	1.02	1.01	1.01

(C)	Isosorbide polyethoxylate	Isosorbide polyethoxylate monopalmitate	Isosorbide Polyethoxylate monostearate	Sorbitan Ethoxylate	Sorbitan Polyethoxylate monopalmitate	Sorbitan Polyethoxylate Monostearate
<b>Mw</b>	670.6	1046.9	940.7	1083.8	1360.4	1360.3
<b>Mn</b>	597.9	968.2	882.3	1052.4	1336.9	1338.4
<b>PDI</b>	1.12	1.08	1.07	1.03	1.02	1.02

(D)	Isosorbide polyethoxylate	Isosorbide polyethoxylate monooleate	Isosorbide Polyethoxylate dioleate	Sorbitan Ethoxylate	Sorbitan Polyethoxylate monooleate	Sorbitan Polyethoxylate dioleate
<b>Mw</b>	731.6	988.6	1119.8	1232.4	1409.6	1670.6
<b>Mn</b>	659.1	911.8	1109.6	1206.5	1381.5	1648.0
<b>PDI</b>	1.11	1.08	1.01	1.02	1.02	1.01

#### 4.5.4 Polysorbate case study conclusions

ASAP has enabled an estimation of the percentage fatty acid content of the Tween formulations to be obtained on a sub-second timescale without sample preparation. The combination of ion mobility separation with mass spectrometry enables extremely complex oligomeric formulations to be characterised in detail. No external chromatographic step is involved, the analysis is rapid and requires only preparation of MALDI plates. The experiment enables molecule-specific detail to be obtained on major, minor and trace products and by-products of the synthesis, including carbon number distributions of the feedstocks used and the ethoxylation distribution of the various ethoxylated moieties present. Series containing isobaric molecule ions have been separated and mobility-separated product ion spectra extracted, which enabled characterisation of the various products.

This approach to complex formulation characterisation has been evaluated using a series of commercial polysorbate formulations (Tweens) and has been shown to provide a high level of information content, difficult, if not impossible, to obtain by any other existing technique. The quantitation of the complex systems is relative but the reproducibility of the experiments, as shown by replicate analyses, which provide relative errors of less than 1%, enables formulations from different sources, or synthesised using varying approaches, to be easily differentiated. Quantitation using internal standards would be possible and would enable the relative ionisation efficiencies of the different chemical species to be established, but this would require synthesis or preparation of appropriate reference materials.

This method has very significant potential to be utilised in the characterisation of many other complex oligomeric and polymeric systems providing scientists using these materials with a rapid, reproducible, high information content technique to monitor the composition of these formulations. Another potential strength of the proposed approach is the capability to deal with additional components in these extremely complex mixtures providing the potential to identify (from mass spectrometry, tandem mass spectrometry (MS/MS) and mobility separated MS/MS experiments) and relatively quantify unknown components. This could be used to compare nominally equivalent feedstocks from different suppliers, degradation

products and/or changes in composition of feedstocks from the same supplier. These observations could then be related, via structure/property relationships to product quality.

## 4.6 Polyrotaxane characterisation

*The majority of this section has been published in JACS (Scarff, Snelling et al. 2012)*

### 4.6.1 Rotaxanes

Rotaxanes are molecules consisting of one or more mechanically interlocked macrocycles which encircle a dumbbell-shaped thread composed of an axle and two stopper groups (Figure 4.22). The macrocycle and thread cannot be dissociated from one another without the cleavage of one or more covalent bonds (Amabilino and Stoddart 1995; Stoddart 2009). The mechanical bond as seen in rotaxane molecules is more flexible than covalent bonds (Frisch, Martin et al. 1953), and can also be found in the molecular architectures of catenanes and molecular knots.

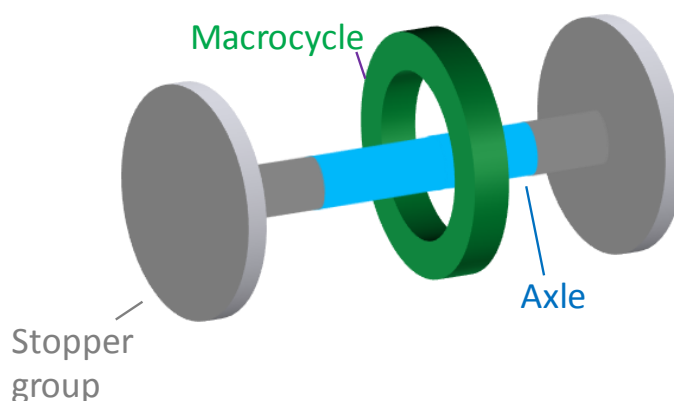


**Figure 4.22** - Schematic of a simple rotaxane molecule.

### 4.6.2 Polyrotaxanes

A polyrotaxane molecule is a type of rotaxane where the axle is composed of a polymer (Huang and Gibson 2005). Mechanically interlocked polymers such as polyrotaxanes and polycatenanes have been shown to possess unique, structural properties in comparison to their constituent parts (Harada, Hashidzume et al. 2009; Niu and Gibson 2009). For instance, cyclodextrin based polyrotaxanes are soluble in water, and other polar solvents, although the underlying polymer can be hydrophobic (Huh, Ooya et al. 2001).

There is potential to use polyrotaxanes as injectable drug delivery systems for the controlled and targeted release of macromolecular drugs, by end cap biodegradation (Yui, Katoono et al. 2009). The use of polyrotaxanes for gene therapy delivery is another potential application (Yang, Li et al. 2009). A recent example enables an organocatalyst to be mechanically switched on or off by simply changing the potential hydrogen (pH). In acidic conditions the macrocycle conceals the catalytic region (an ammonium moiety) of the axle rendering the molecule non-catalytic. When pH is increased, the macrocycle binds to triazolium sites, resulting in the exposure of the ammonium moiety thus permitting catalysis (Blanco, Carlone et al. 2012).

The physical properties of these systems can be affected by their topologies, and thus it is important to determine the overall topology, in addition to characterisation at the molecular level. NMR can be used to determine the overall threading efficiency of a polyrotaxane system, but as an ensemble analysis technique is unable to determine the structures of specific compounds within a mixture that contribute to this value.

#### **4.6.3 Characterisation Methods**

MS based approaches have been used to study supramolecular structure and assign structural properties (Baytekin, Baytekin et al. 2006; Engeser, Rang et al. 2006; Jiang, Schäfer et al. 2010; Pasquale, Di Stefano et al. 2010). These methods can be used to identify the presence of multiple components in heterogeneous mixtures and can be coupled with IM separation to allow determination of the rotationally-averaged collision cross-sections of each of these components. Recently IM-MS was successfully used to determine the structures of metallosupramolecular coordination assemblies (Brocker, Anderson et al. 2010) and to characterise and resolve hexameric metallomacrocycles from their linear isomers (Chan, Li et al. 2009; Li, Chan et al. 2011). IM-MS has also been used in the characterization of polymer systems, as a separation tool to allow for the improved identification of isobaric components and separation of oligomers from within complex systems (Trimpin, Plasencia et al. 2007; Hilton, Jackson et al. 2008; Trimpin and Clemmer 2008).

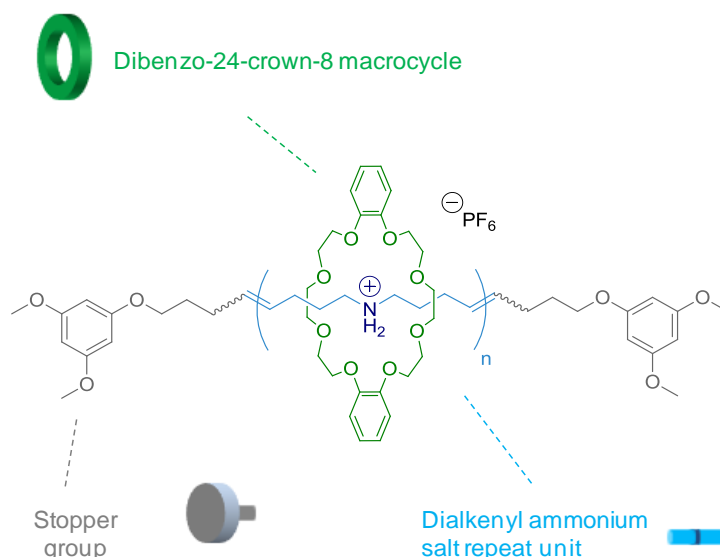


**Figure 4.23** - Structure of polyrotaxane system studied.

The polyrotaxane system studied here and shown in Figure 4.23, consists of dibenzo[24] crown-8 ether (DB24C8) macrocycles threaded onto the polymeric backbone of dialkenyl ammonium salt repeat units that have been end-capped by a derivative of trimethoxybenzene. This generously donated system was synthesised by the Grubbs group by means of a one-pot acyclic diene metathesis polymerisation process, details of which can be found elsewhere (Momčilović, Clark et al. 2011). Proton NMR spectroscopy carried out by that group confirmed efficient threading, which was postulated to be due to the rapid association of DB24C8 to the dialkenyl ammonium salts prior to metathesis events. The use of TWIM-MS for a more in depth characterisation of this system is described here.



#### 4.6.4 Results

Figure 4.24 shows the components observed during MALDI-MS analysis of the Grubbs polyrotaxane system. Ions corresponding to the presence of polyrotaxane species with repeat unit: macrocycle ratios of 1:1 through to 5:4 were observed with a single charge.

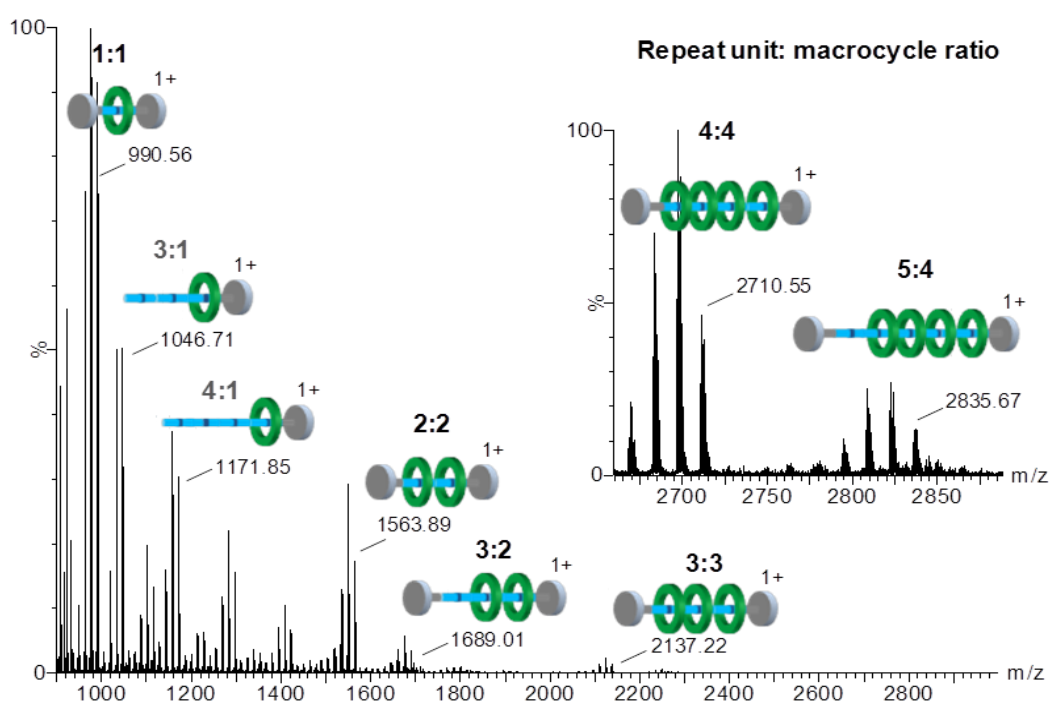


**Figure 4.24** - MALDI-MS spectrum of Grubbs polyrotaxane system.

Species where one or both of the stopper groups are not covalently bonded to the polymer backbone are referred to as polypseudorotaxanes, and species lacking one of the stopper groups were observed in the spectrum at  $m/z$  values of 921.57, 1046.71, 1171.85 and 1296.99 corresponding to repeat unit:macrocycle ratios of 2:1, 3:1, 4:1 and 5:1 respectively. No polypseudorotaxane species associated with more than one crown ether was observed. It is feasible that additional crown ethers were associated with the polypseudorotaxane species, but have been lost through a dethreading mechanism. Momčilović *et al* determined via proton NMR that not all species were

threaded (Momčilović, Clark et al. 2011), and thus the polypseudorotaxane species observed are likely side-products from the synthetic method used.

Carbon number distributions were observed within the spectrum, and this can be due to the nature of the feedstock used for the synthesis. The presence of polyrotaxane species containing these distributions and differing in the number of CH<sub>2</sub> groups can also be the result of the metathesis method used to synthesis due to alkene isomerisation prior to cross metathesis (Hong, Sanders et al. 2005). Figure 4.25 shows the MS/MS spectra of polyrotaxane species containing a repeat unit: macrocycle ratio of 1:1 but differing in the number of carbons in the polymer axle.

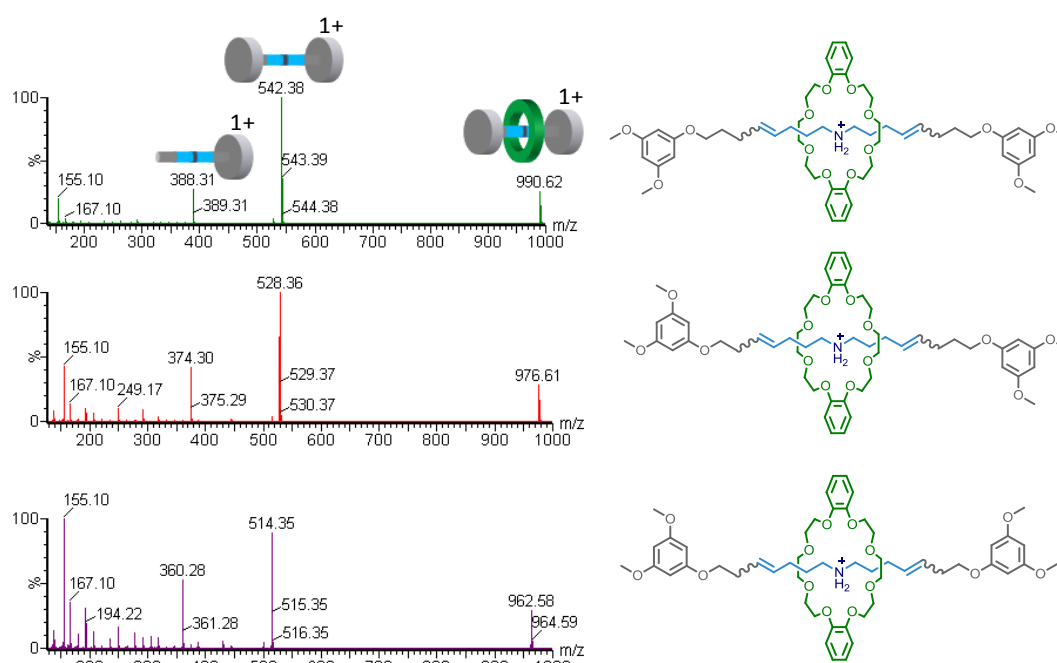


**Figure 4.25** - MS/MS spectra of 1:1 species differing in carbon number.

As can be seen in the spectra in, a decrease of 14 daltons is observed for the parent ion from the desired  $m/z$  990.62 to 976.61 and then a further 14 dalton decrease to 962.58. This corresponds to one and two fewer CH<sub>2</sub> groups respectively. It is important to note that standard proton NMR experiments can not differentiate these differences, highlighting the importance of the inclusion of MS methods into a characterisation methodology for such systems. The carbon number distributions

observed could potentially affect the properties of such systems, thus could affect their applicability.

Similar fragmentation pathways were observed for the protonated quasi-molecular ions of polyrotaxane species with repeat unit: macrocycle ratios of 1:1, 2:2 and 3:3 when MS/MS analysis is performed (Figure 4.26).

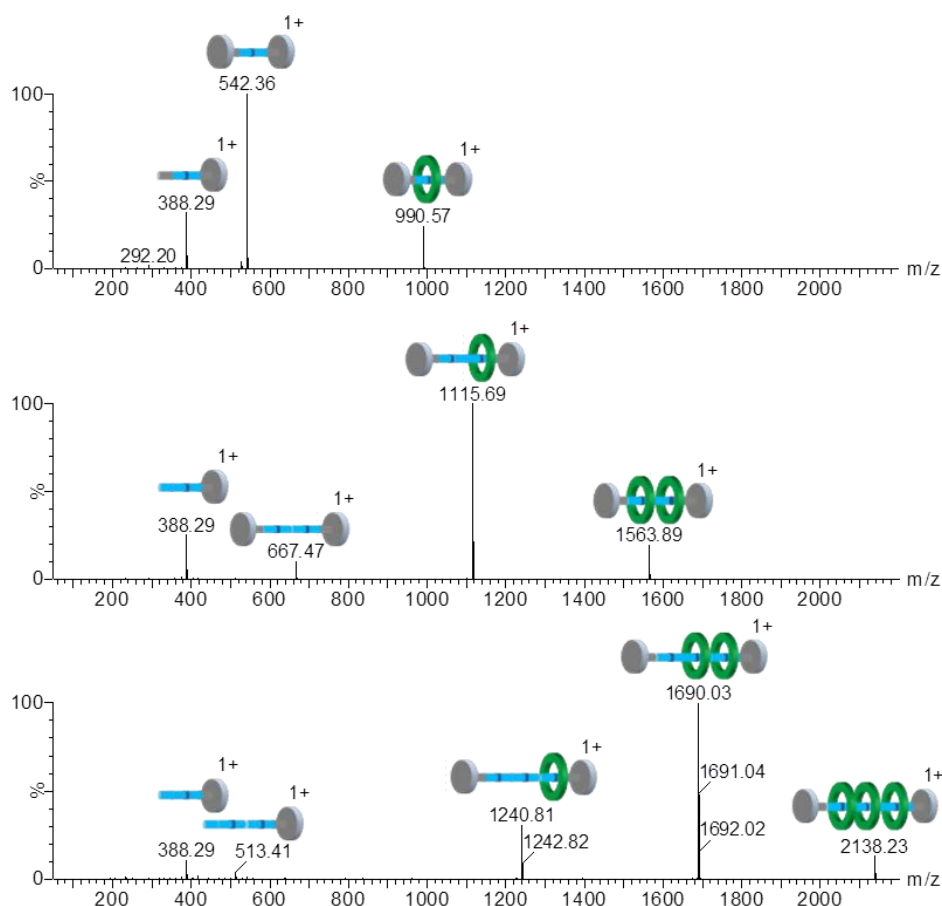


**Figure 4.26** - MS/MS analysis of species with 1:1 (top), 2:2 (middle) and 3:3 (bottom).

The product ion spectra observed indicated that there is dissociation of the crown ethers prior to fragmentation of the polymer backbone. This is likely due to fragmentation of crown ether ether bonds during the MS/MS experiment. The only other, unlikely explanation is that the macrocycle is able to dethread the axle while the stopper groups are still present.

The ion at  $m/z$  388.29 is a value could result from fragmentation of the crown ether, or of the polymer backbone. TAP analysis experiments, where product ions produced from a selected precursor ion are mobility separated prior to further CID, determined that this ion was due to axle fragmentation rather than macrocycle fragmentation (Figure 4.27).

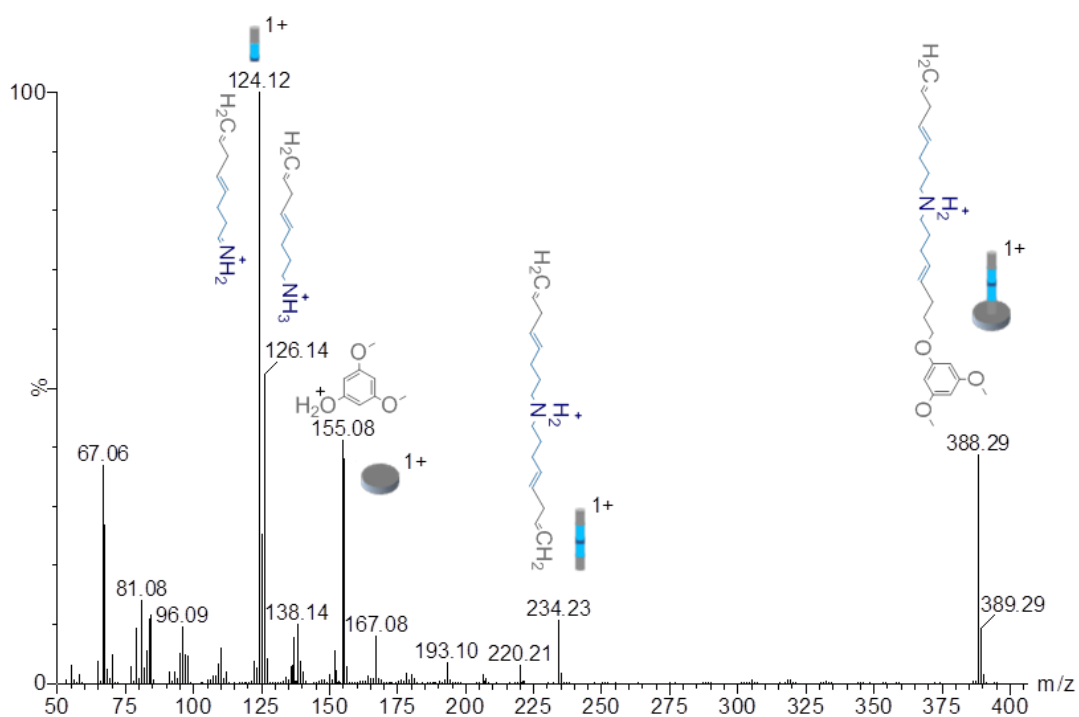


**Figure 4.27** - MS/MS spectra for  $m/z$  388, which has been mobility extracted from the TAP fragmentation of  $m/z$  990.

There was no evidence of crown ethers or their fragments from MS/MS spectra. The most probable explanation is that the charge is retained on the polymer backbone by one of the ammonium moieties, and that any crown ether or fragment formed in a MS/MS experiment is neutral.

A comparison of the spectra obtained by MALDI was made with ESI. Figure 4.28 shows the ESI-MS analysis of the Grubbs polyrotaxane system. The base peak is observed at  $m/z$  976.57 which corresponds to the 1:1 species but with one less  $\text{CH}_2$

than desired. This species is singly charged. The 2:2 species is observed with two charges at  $m/z$  782.98. The 3:3 species is triply charged and the 4:4 species has four charges. Interestingly a sodiated crown ether was observed during ESI-MS analysis. This is not unexpected as the method of synthesis did not result in 100% threading, and thus its presence can be explained as it being a side product.

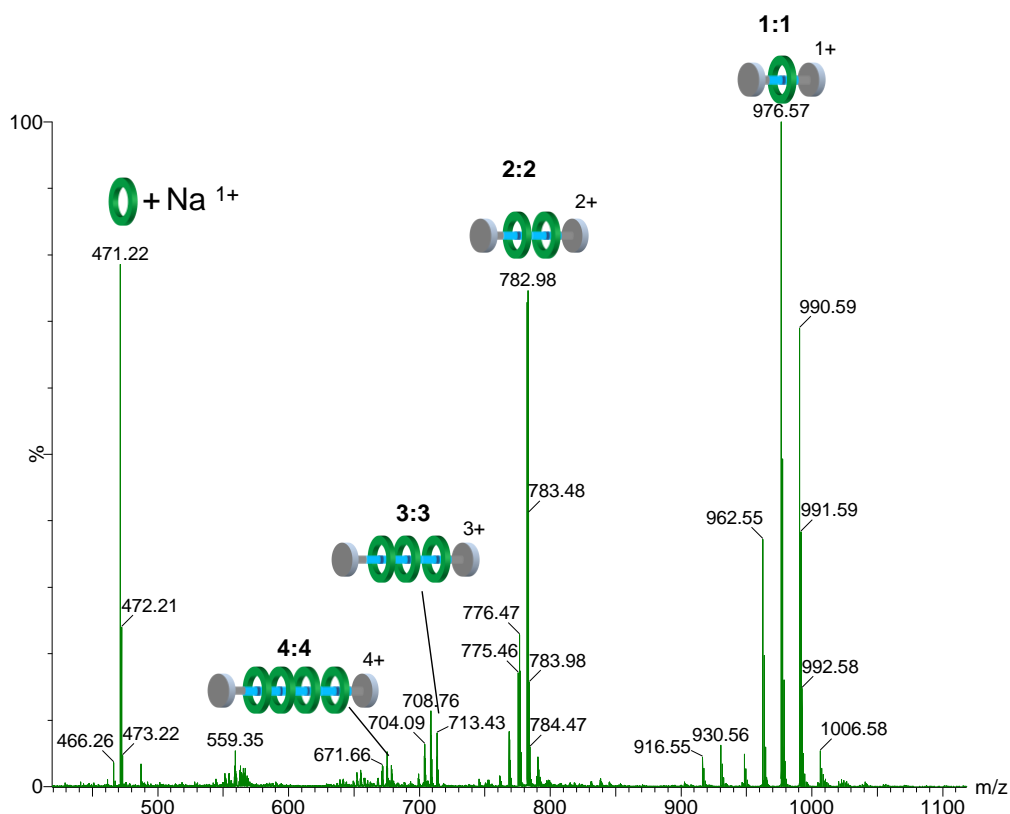


**Figure 4.28** - ESI-MS spectrum of polyrotaxane system.

Investigations into whether the fragmentation of the polyrotaxane system was dependent on the ionisation mechanism utilised were carried out by comparing the MS/MS spectrum and the ATD of the  $m/z$  990.6 ion (1:1 system) from ESI and MALDI experiments (Figure 4.29).

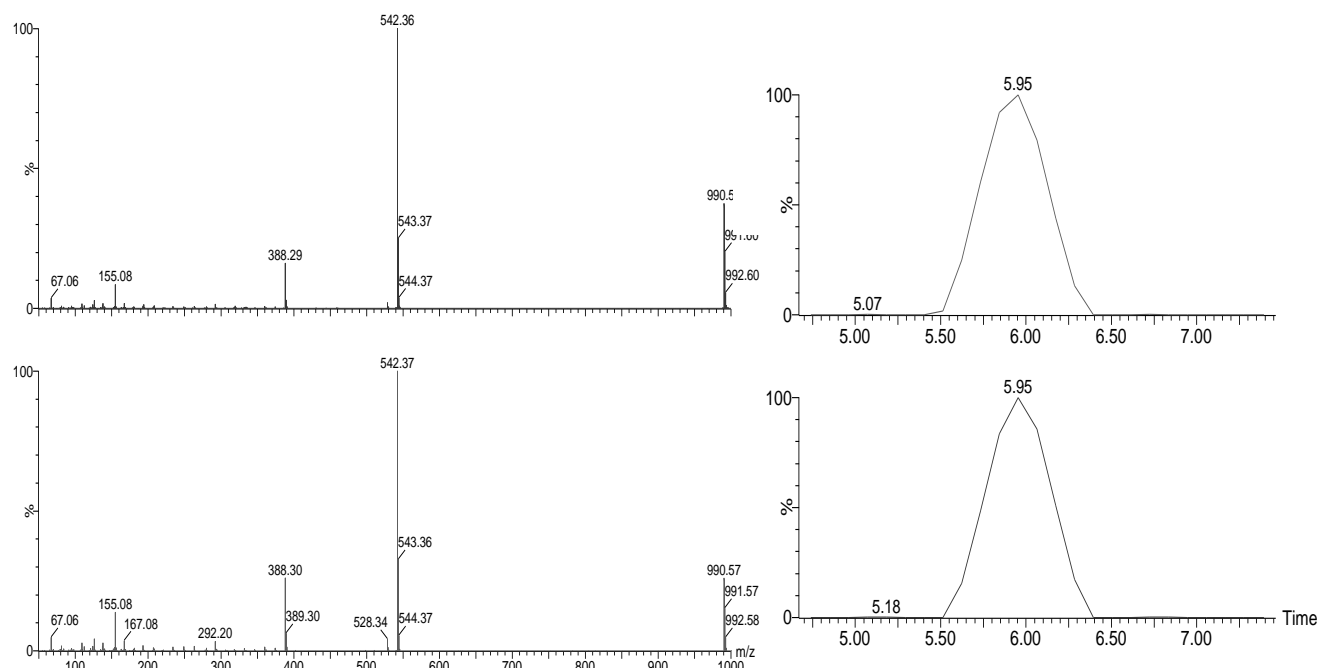


**Figure 4.29** - MALDI-MS/MS and ATD (top) and ESI-MS/MS and ATD (bottom) spectra of  $m/z$  990.6 ion.

The fragmentation spectra are comparable, and the ATDs match one another, and thus indicates that the structure of the ion is not dependant on the ionisation method, though the ionisation mechanism is likely different. In ESI, the polyrotaxanes are ionised by the loss of the hexafluorophosphate ( $F_6P$ ) anions, which are already partially displaced from the locality of the ammonium moiety positive charge by the crown ether, as has previously been commented on by Jiang *et.al* (Jiang, Schäfer et al. 2010). It is also possible that neutralisation of the species precedes protonation. In MALDI analysis samples are usually only singly charged, but these species could potentially be multiply charged due to the presence of precharged species. Only singly charged ions were observed during the MALDI analysis. It is postulated that desorption of these species results in neutral rotaxane and  $HF_6P$  species. The

polyrotaxane species are then presumed to ionise via conventional MALDI mechanisms.

Some of the polyrotaxane species observed in Figure 4.24 had an uneven repeat unit: macrocycle ratio (for instance 4:3, 4:2 or 4:1). When these species were fragmented by CID, there were additional fragment ions compared to the product ion spectra of species with even repeat unit : macrocycle ratios. The product ion spectrum of a 4:3 species ( $m/z$  2262.3) is shown in Figure 4.30, together with the TAP fragmentation spectrum for one of the additional product ions ( $m/z$  2109.3).

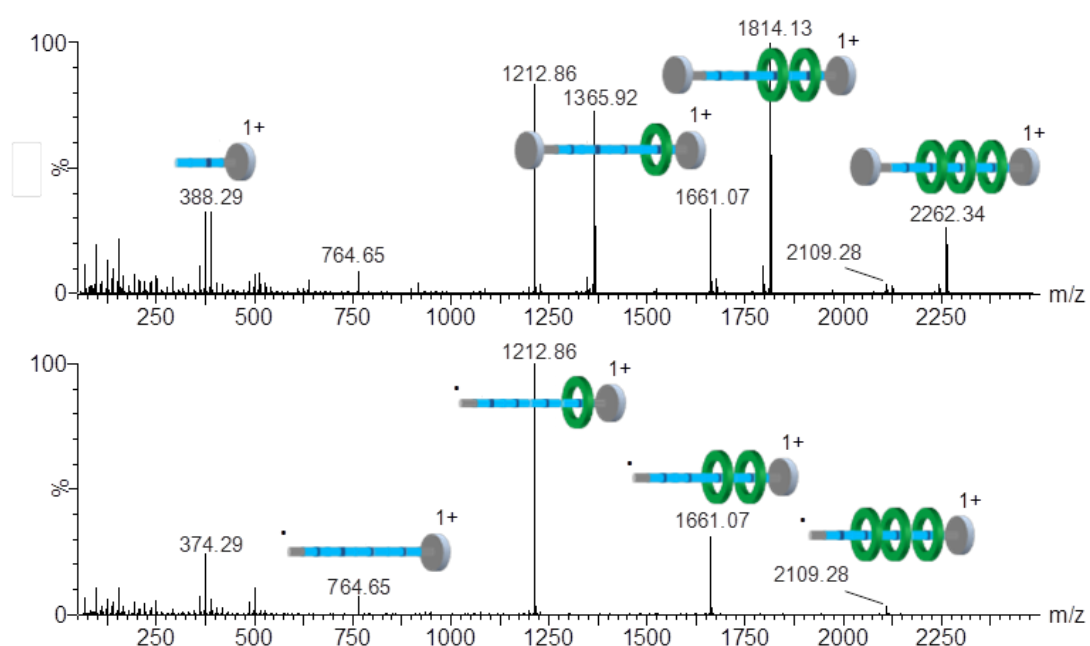


**Figure 4.30** - Product ion spectrum for  $m/z$  2262.3 (top). The MS/MS spectrum for  $m/z$  2109.3 (bottom) was mobility extracted from a TAP fragmentation of the  $m/z$  2262.3 ion.

Additional fragment ions for the product ion spectrum of  $m/z$  2262.34 (4:3) were observed at  $m/z$  2109.28, 1661.07, 1212.86 and 764.65, and appear to result from the fragmentation of the polymer backbone, prior to crown ether dethreading. The product ion at  $m/z$  2109.28 corresponds to a loss of a resonance stabilised end group fragment from the polymer backbone. Fragmentation of the  $m/z$  2109.28 ion via TAP

analysis reveals prominent fragments that are the result of macrocycle de-threading, and these ions correspond to the additional peaks observed during MS/MS analysis of the 4:3 species.

The Grubbs system analysed here was synthesised to showcase a novel synthetic method rather than for a specific application. In many applications of polyrotaxanes, the macrocycle is required to shuttle along the axle for a certain property to be displayed. The additional ions are not observed when there is a full complement of macrocycles, indicating that fragmentation of the end group is more likely to occur when the repeat unit : macrocycle ratio is not equal. A proposed explanation for this observation is that the macrocycles in this system largely remain associated with the ammonium moieties of the polymer backbone, and that the crown ethers are not freely moving along the axle. It is reasonable to assume that the ammonium moiety devoid of a macrocycle in the 4:3 system is at one of the ends of the axle next to a bulky end group. This may be expected from the synthesis route employed, since before end-capping, the macrocycle at the end of an uncapped axle would be capable of de-threading and would need to do so before subsequent macrocycles were able to do so.

This could indicate that when a macrocycle is associated with the ammonium moiety adjacent to the end-group, then the end-group is somehow stabilised by the presence of the macrocycle, and is more labile when macrocycle absent. The loss of the end group corresponds to a radical ion fragmentation of the axle, and the proposed pathway is shown in Figure 4.31.



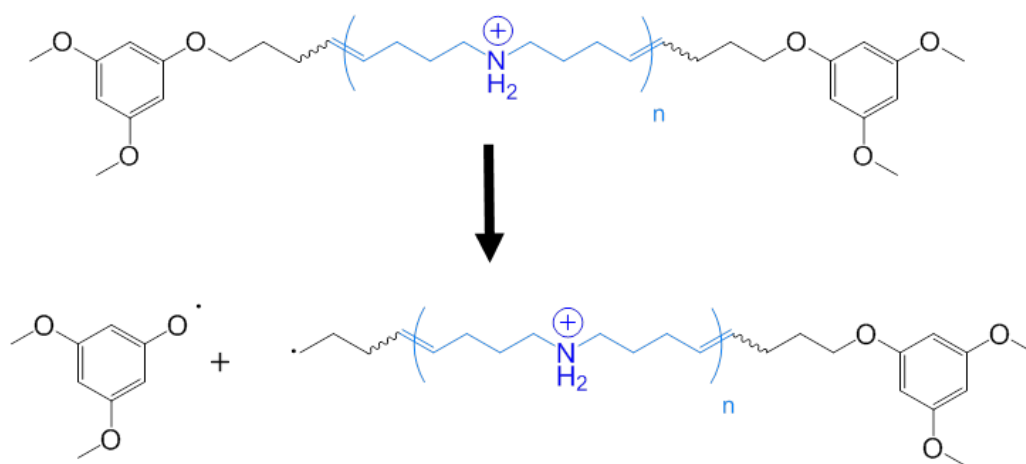


**Figure 4.31** - Proposed radical fragmentation

This proposed radical ion loss is not common and was unexpected, but is the most likely explanation. Radical cation rearrangement is likely to occur and has previously be reported (Williams, Nibbering et al. 2006).

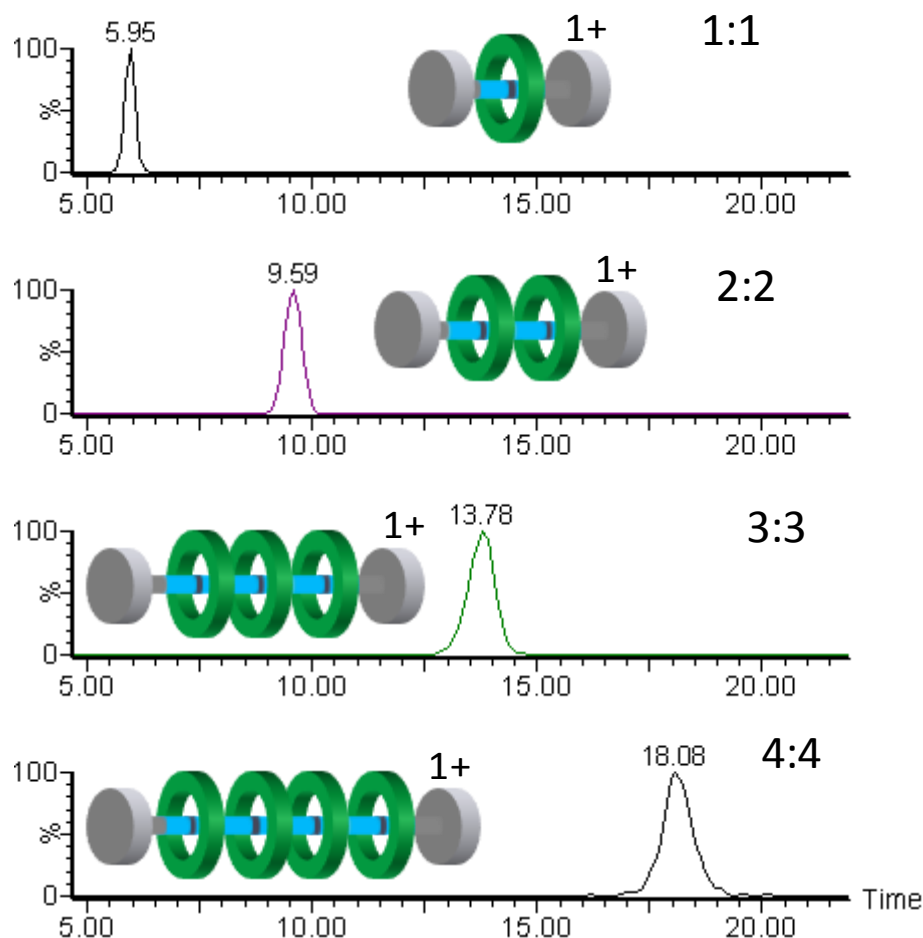


**Figure 4.32** - ATD for polyrotaxane species.

The ATDs of four of the polyrotaxane species with repeat unit:macrocycle ratios of 1:1, 2:2, 3:3 and 4:4 reveal that the species exist with a single conformation or multiple conformations that could not be separated by mobility due to differences in cross-section of less than 5% (Figure 4.32). The increase in estimated cross section is linear with increase in mass ( $R^2 = 0.9995$ ). Calibration with an external standard (see Chapter 2) allowed for estimated CCS to be determined from the ATD. The 1:1 species has an estimated CCS of  $232 \text{ \AA}^2$ , the 2:2 species  $313.9 \text{ \AA}^2$ , 3:3 species an estimated CCS of  $395.8 \text{ \AA}^2$  and the 4:4 species a CCS of  $470.8 \text{ \AA}^2$ .

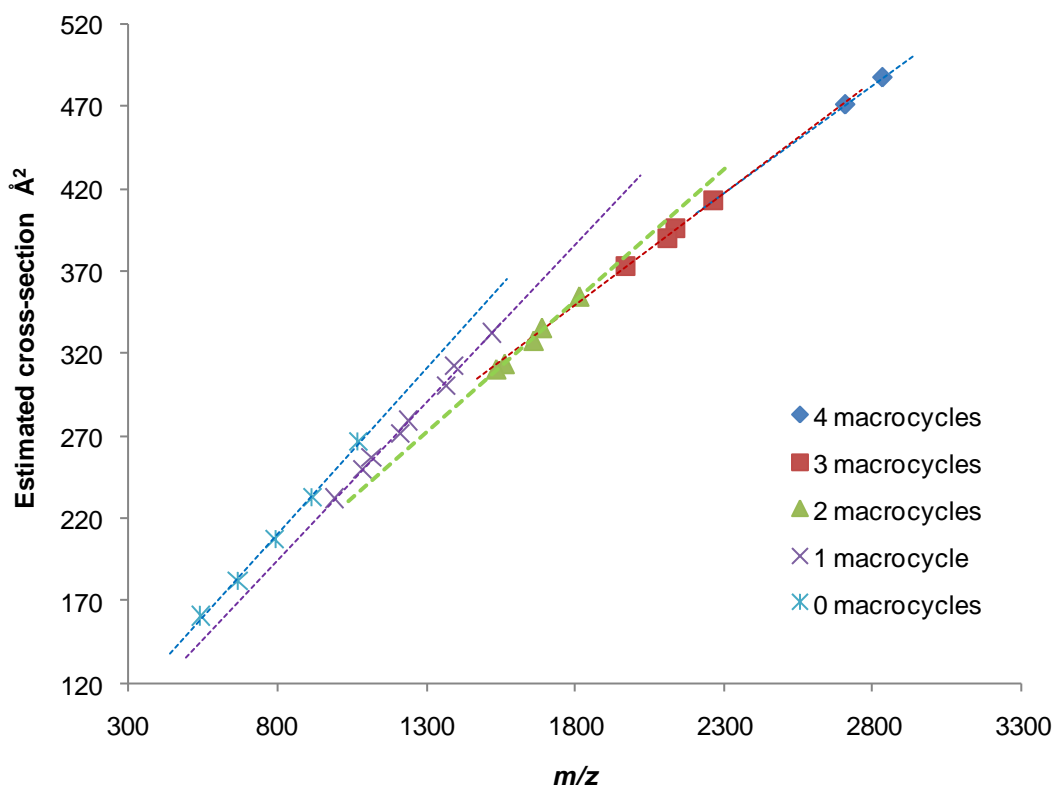


**Figure 4.33** - Estimated CCS for polyrotaxane species and their fragments.

A comparison of estimated cross sections of many species in the Grubbs formulation is shown in Figure 4.33. The number of crown ethers associated with a polyrotaxane or related species would appear to slightly influence the rate of increase in CCS with increase in mass. For instance the increase in CCS for those species with no crown ether associated is greater than for when there is one crown ether associated, which in turn is greater than those species with three crown ethers associated and so on. All species regardless of number of macrocycles present increase in a linear fashion with increase in mass. This observation indicates that the polymer axle remains rigid and linear with increase in mass, and that presence or absence of associated macrocycles does not affect the axle conformation.

#### 4.6.5 Polyrotaxane case study conclusions

IM-MS can be used to investigate the topology of a novel polyrotaxane system. The topologies of such systems can have an effect on the overall properties of the system and thus their practical applicability. Common ions formed from ESI and MALDI have experimentally identical mobilities and product ion spectra. In MALDI, it is likely that the species observed have been neutralised prior to protonation, while in ESI the charge is thought to be due to loss of an anion.

While NMR has been the characterisation method of choice for such systems, IM-MS can reveal molecular specific information about structure and shape. Further characterisation was allowed with pseudo-MS<sup>3</sup> experiments using TAP analysis. Synthetic chemists could potentially benefit from a characterisation protocol incorporating IM-MS in addition to NMR. IM-MS analysis, which is based on single molecule observation, rather than an ensemble average, has been shown to add useful structural information regarding these complex mechanically interlocked molecules, which could enable researchers to adjust the method of synthesis to increase the yield of molecules with the desired properties.

#### 4.7 References

**Abrar, S. and Trathnigg, B.** (2011). "Separation of polysorbates by liquid chromatography on a HILIC column and identification of peaks by MALDI-TOF MS." *Analytical and Bioanalytical Chemistry* **400**(7): 2119-2130.

**Amabilino, D. B. and Stoddart, J. F.** (1995). "Interlocked and Intertwined Structures and Superstructures." *Chemical Reviews* **95**(8): 2725-2828.

**Ayorinde, F. O., Gelain, S. V., Johnson, J. H. and Wan, L. W.** (2000). "Analysis of some commercial polysorbate formulations using matrix-assisted laser desorption/ionization time-of-flight mass spectrometry." *Rapid Communications in Mass Spectrometry* **14**(22): 2116-2124.

**Baytekin, B., Baytekin, H. T. and Schalley, C. A.** (2006). "Mass spectrometric studies of non-covalent compounds: why supramolecular chemistry in the gas phase?" *Organic & Biomolecular Chemistry* **4**(15): 2825-2841.

**Blanco, V., Carlone, A., Hänni, K. D., Leigh, D. A. and Lewandowski, B.** (2012). "A Rotaxane-Based Switchable Organocatalyst." *Angewandte Chemie International Edition* **51**(21): 5166-5169.

**Bonnaire, N., Dannoux, A., Pernelle, C., Amerkraz, B., Moulin, C.** (2010). "One the use of electrospray ionisation and desorption electrospray ionisation mass spectrometry for bulk and surface polymer analysis." *Applied Spectroscopy* **64**(7): 810-818.

**Borisov, O. V., Ji, J. A., Wang, Y. J., Vega, F. and Ling, V. T.** (2011). "Toward Understanding Molecular Heterogeneity of Polysorbates by Application of Liquid Chromatography "Mass Spectrometry with Computer-Aided Data Analysis." *Analytical Chemistry* **83**(10): 3934-3942.

**Briggs, D.** (1989). "Recent advances in secondary ion mass spectrometry (SIMS) for polymer surface analysis." *British Polymer Journal* **21**(1): 3-15.

**Brocker, E. R., Anderson, S. E., Northrop, B. H., Stang, P. J. and Bowers, M. T.** (2010). "Structures of Metallosupramolecular Coordination Assemblies Can Be Obtained by Ion Mobility Spectrometry–Mass Spectrometry." *Journal of the American Chemical Society* **132**(38): 13486-13494.

**Brumley, W. C., Warner, C. R., Daniels, D. H., Andrzejewski, D., White, K. D., Min, Z., Chen, J. Y. T. and Sphon, J. A.** (1985). "Characterization of polysorbates by OH<sup>-</sup> negative ion chemical ionization mass spectrometry." *Journal of Agricultural and Food Chemistry* **33**(3): 368-372.

**Chan, Y.-T., Li, X., Soler, M., Wang, J.-L., Wesdemiotis, C. and Newkome, G. R.** (2009). "Self-Assembly and Traveling Wave Ion Mobility Mass Spectrometry Analysis of Hexacadmium Macrocycles." *Journal of the American Chemical Society* **131**(45): 16395-16397.

**Chen, R. and Li, L.** (2001). "Lithium and transition metal ions enable low energy collision-induced dissociation of polyglycols in electrospray ionization mass spectrometry." *Journal of the American Society for Mass Spectrometry* **12**(7): 832-839.

**Dang, H. V., Gray, A. I., Watson, D., Bates, C. D., Scholes, P. and Eccleston, G. M.** (2006). "Composition analysis of two batches of polysorbate 60 using MS and NMR techniques." *Journal of Pharmaceutical and Biomedical Analysis* **40**(5): 1155-1165.

**Deery, M. J., Jennings, K. R., Jasieczek, C. B., Haddleton, D. M., Jackson, A. T., Yates, H. T. and Scrivens, J. H.** (1997). "A Study of Cation Attachment to Polystyrene by Means of Matrix-assisted Laser Desorption/Ionization and Electrospray Ionization-Mass Spectrometry." *Rapid Communications in Mass Spectrometry* **11**(1): 57-62.

**Engeser, M., Rang, A., Ferrer, M., Gutiérrez, A., Baytekin, H. T. and Schalley, C. A.** (2006). "Reactivity of self-assembled supramolecular complexes in the gas

phase: A supramolecular neighbor group effect." *International Journal of Mass Spectrometry* **255-256**: 185-194.

**Frisch, H., Martin, I. and Mark, H.** (1953). "Zur Struktur der Polysiloxene. I." *Monatshefte für Chemie* **84**(2): 250-256.

**Frison-Norrie, S. and Sporns, P.** (2001). "Investigating the Molecular Heterogeneity of Polysorbate Emulsifiers by MALDI-TOF MS." *Journal of Agricultural and Food Chemistry* **49**(7): 3335-3340.

Gnanou, Y., Fontanille, M. (2008). Organic and Physical Chemistry of Polymers, Wiley.

**Griffin, W. C.** (1949). "Classification of Surface Active Agents by HLB." *J. Soc. Cosmet. Chem.* **1**: 311-326.

**Groenewoud, W. M.** (2001). Chapter 1 - Differential scanning calorimetry. Characterisation of Polymers by Thermal Analysis. Amsterdam, Elsevier Science B.V.: 10-60.

**Harada, A., Hashidzume, A., Yamaguchi, H. and Takashima, Y.** (2009). "Polymeric Rotaxanes." *Chemical Reviews* **109**(11): 5974-6023.

**Hewitt, D., Alvarez, M., Robinson, K., Ji, J., Wang, Y. J., Kao, Y.-H. and Zhang, T.** (2011). "Mixed-mode and reversed-phase liquid chromatography-tandem mass spectrometry methodologies to study composition and base hydrolysis of polysorbate 20 and 80." *Journal of Chromatography A* **1218**(15): 2138-2145.

**Hewitt, D., Zhang, T. and Kao, Y.-H.** (2008). "Quantitation of polysorbate 20 in protein solutions using mixed-mode chromatography and evaporative light scattering detection." *Journal of Chromatography A* **1215**(1-2): 156-160.

**Hilton, G. R., Jackson, A. T., Thalassinou, K. and Scrivens, J. H.** (2008). "Structural Analysis of Synthetic Polymer Mixtures Using Ion Mobility and Tandem Mass Spectrometry." *Analytical Chemistry* **80**(24): 9720-9725.

**Hong, S. H., Sanders, D. P., Lee, C. W. and Grubbs, R. H.** (2005). "Prevention of Undesirable Isomerization during Olefin Metathesis." *Journal of the American Chemical Society* **127**(49): 17160-17161.

**Hoskins, J. N., Trimpin, S. and Grayson, S. M.** (2011). "Architectural Differentiation of Linear and Cyclic Polymeric Isomers by Ion Mobility Spectrometry-Mass Spectrometry." *Macromolecules* **44**(17): 6915-6918.

**Huang, F. and Gibson, H. W.** (2005). "Polypseudorotaxanes and polyrotaxanes." *Progress in Polymer Science* **30**(10): 982-1018.

**Huh, K. M., Ooya, T., Sasaki, S. and Yui, N.** (2001). "Polymer Inclusion Complex Consisting of Poly( $\epsilon$ -lysine) and  $\alpha$ -Cyclodextrin." *Macromolecules* **34**(8): 2402-2404.

**Jackson, A. T., Scrivens, J. H., Simonsick, W. J., Green, M. R. and Bateman, R. H.** (2000). "Generation of structural information from polymers and copolymers using tandem mass spectrometry." *Abstracts of Papers of the American Chemical Society* **219**: U363-U363.

**Jackson, A. T., Williams, J.P., Scrivens, J.H.** (2007). "Desorption electrospray ionisation mass spectrometry and tandem mass spectrometry of low molecular weight synthetic polymers." *Rapid Communications in Mass Spectrometry* **20**: 2717.

**Jiang, W., Schäfer, A., Mohr, P. C. and Schalley, C. A.** (2010). "Monitoring Self-Sorting by Electrospray Ionization Mass Spectrometry: Formation Intermediates and Error-Correction during the Self-Assembly of Multiply Threaded Pseudorotaxanes." *Journal of the American Chemical Society* **132**(7): 2309-2320.



**Kato, H., Nagai, Y., Yamamoto, K. and Sakabe, Y.** (1989). "Determination of polysorbates in foods by colorimetry with confirmation by infrared spectrophotometry, thin-layer chromatography, and gas chromatography." *J Assoc Off Anal Chem* **72**(1): 27-29.

**Koenig, J. L.** (2004). The application of molecular spectroscopy to characterization of polymers. *Physical Properties of Polymers, Cambridge University Press.*

**Lattimer, R. P.** (1992). "Tandem Mass-Spectrometry of Lithium-Attachment Ions from Polyglycols." *Journal of the American Society for Mass Spectrometry* **3**(3): 225-234.

**Lattimer, R. P.** (1992). "Tandem Mass-Spectrometry of Poly(Ethylene Glycol) Proton-Attachment and Deuteron-Attachment Ions." *International Journal of Mass Spectrometry and Ion Processes* **116**(1): 23-36.

**Lattimer, R. P.** (1994). "Tandem Mass-Spectrometry of Poly(Ethylene Glycol) Lithium-Attachment Ions." *Journal of the American Society for Mass Spectrometry* **5**(12): 1072-1080.

**Lattimer, R. P., Harmon, D. J. and Welch, K. R.** (1979). "Characterization of low molecular weight polymers by liquid chromatography and field desorption mass spectroscopy." *Analytical Chemistry* **51**(8): 1293-1296.

**Li, X., Chan, Y.-T., Newkome, G. R. and Wesdemiotis, C.** (2011). "Gradient Tandem Mass Spectrometry Interfaced with Ion Mobility Separation for the Characterization of Supramolecular Architectures." *Analytical Chemistry* **83**(4): 1284-1290.

**Martin, K., Spickermann, J., Räder, H. J. and Müllen, K.** (1996). "Why Does Matrix-assisted Laser Desorption/Ionization Time-of-flight Mass Spectrometry Give Incorrect Results for Broad Polymer Distributions?" *Rapid Communications in Mass Spectrometry* **10**(12): 1471-1474.

**Mehrnaz, K., Kao, Y.-H., Mrsny, R. J. and Sweeney, T. D.** (2002). "Analysis Methods of Polysorbate 20: A new method to assess the stability of polysorbate 20 and established methods that may overlook degraded polysorbate 20." *Pharmaceutical Research* **19**(5): 634-639.

**Momčilović, N., Clark, P. G., Boydston, A. J. and Grubbs, R. H.** (2011). "One-Pot Synthesis of Polyrotaxanes via Acyclic Diene Metathesis Polymerization of Supramolecular Monomers." *Journal of the American Chemical Society* **133**: 19087–19089.

Montaudo, G., Lattimer, R.P (2002). Mass Spectrometry of Polymers. Boca Raton, Florida, CRC Press LLC.

**Nefliu, M., Venter, A. and Cooks, R. G.** (2006). "Desorption electrospray ionization and electrosonic spray ionization for solid- and solution-phase analysis of industrial polymers." *Chemical Communications*(8): 888-890.

**Nicholson, J. W.** (2012). The Chemistry of Polymers. *Cambridge, UK, RSC Publishing*.

**Niu, Z. and Gibson, H. W.** (2009). "Polycatenanes." *Chemical Reviews* **109**(11): 6024-6046.

**Paine, M. R. L., Barker, P. J., MacLaughlin, S. A., Mitchell, T. W. and Blanksby, S. J.** (2012). "Direct detection of additives and degradation products from polymers by liquid extraction surface analysis employing chip-based nanospray mass spectrometry." *Rapid Communications in Mass Spectrometry* **26**(4): 412-418.

**Pasquale, S., Di Stefano, S. and Masci, B.** (2010). "Electron transfer from wheel to axle in a rotaxane. A mass spectrometric investigation." *New Journal of Chemistry* **34**(3): 426-431.

**Peacock, P. M. and McEwen, C. N.** (2006). "Mass Spectrometry of Synthetic Polymers." *Analytical Chemistry* **78**(12): 3957-3964.

**Pethrick, R. A.** (1986). "Physical properties of polymers. Edited by J. E. Mark, A. Eisenberg, W. W. Graessley, Mandelkern and J. L. Koenig, American Chemical Society, Washington, D.C., 1984. pp. ix+246, price \$44.95 (USA Canada), \$53.95 (rest of world). ISBN 0-8412-0851-4." *British Polymer Journal* **18**(1): 65-65.

**Raith, K., Schmelzer, C. E. H. and Neubert, R. H. H.** (2006). "Towards a molecular characterization of pharmaceutical excipients: Mass spectrometric studies of ethoxylated surfactants." *International Journal of Pharmaceutics* **319**(1-2): 1-12.

**Reiter, S., Buchberger, W. and Klampfl, C.** (2011). "Rapid identification and semi-quantitative determination of polymer additives by desorption electrospray ionization/time-of-flight mass spectrometry." *Analytical and Bioanalytical Chemistry* **400**(8): 2317-2322.

**Ross-Murphy, S. B.** (1994). "Rheological characterization of polymer gels and networks." *Polymer Gels and Networks* **2**(3-4): 229-237.

**Sawyer, L., Grubb, D.T** (2008). *Polymer Microscopy\_Springer*.

**Scrivens, J. H. and Jackson, A. T.** (2000). "Characterisation of synthetic polymer systems." *International Journal of Mass Spectrometry* **200**(1-3): 261-276.

**Scrivens, J. H., Jackson, A.T.** (2000). "Characterisation of synthetic polymer systems." *International Journal of Mass Spectrometry* **200**: 261-276.

**Sparreboom, A., Zhao, M., Brahmer, J. R., Verweij, J. and Baker, S. D.** (2002). "Determination of the docetoxal vehicle, polysorbate 80, in patient samples by liquid chromatography - tandem mass spectrometry." *Journal of Chromatography B* **773**: 183-190.

**Stille, J. K.** (1981). "Step-growth polymerization." *Journal of Chemical Education* **58**(11): 862.

**Stoddart, J. F.** (2009). "The chemistry of the mechanical bond." *Chemical Society Reviews* **38**(6): 1802-1820.

**Swallowe, G. M.** (1999). *Mechanical Properties and Testing of Polymers*. Netherlands, *Kluwer Academic Publishers*.

**Thomas, H. R. and O'Malley, J. J.** (1979). "Surface Studies on Multicomponent Polymer Systems by X-ray Photoelectron Spectroscopy. Polystyrene/Poly(ethylene oxide) Diblock Copolymers." *Macromolecules* **12**(2): 323-329.

**Trimpin, S. and Clemmer, D. E.** (2008). "Ion Mobility Spectrometry/Mass Spectrometry Snapshots for Assessing the Molecular Compositions of Complex Polymeric Systems." *Analytical Chemistry* **80**(23): 9073-9083.

**Trimpin, S., Plasencia, M., Isailovic, D. and Clemmer, D. E.** (2007). "Resolving Oligomers from Fully Grown Polymers with IMS-MS." *Analytical Chemistry* **79**(21): 7965-7974.

**Trimpin, S., Wijerathne, K. and McEwen, C. N.** (2009). "Rapid methods of polymer and polymer additives identification: Multi-sample solvent-free MALDI, pyrolysis at atmospheric pressure, and atmospheric solids analysis probe mass spectrometry." *Analytica Chimica Acta* **654**(1): 20-25.

**Whitson, S. E.** (2008). *The Development, Implementation and Application of Ambient Ionization Mass Spectrometry to Complex Polymeric Systems*. Chemistry. Akron, University of Akron. Doctor of Philosophy: 171.

**Williams, J. P., Hilton, G.R., Thalassinis, K., Jackson, A.T., Scrivens, J.H** (2007). "The rapid characterisation of poly(ethylene glycol) oligomers using desorption electrospray ionisation tandem mass spectrometry combined with novel product ion peak assignment software." *Rapid Communications in Mass Spectrometry* **21**: 1693.

**Williams, J. P., Nibbering, N. M. M., Green, B. N., Patel, V. J. and Scrivens, J. H.** (2006). "Collision-induced fragmentation pathways including odd-electron ion formation from desorption electrospray ionisation generated protonated and deprotonated drugs derived from tandem accurate mass spectrometry." *Journal of Mass Spectrometry* **41**(10): 1277-1286.

**Yang, C., Li, H., Wang, X. and Li, J.** (2009). "Cationic supramolecules consisting of oligoethylenimine-grafted  $\alpha$ -cyclodextrins threaded on poly(ethylene oxide) for gene delivery." *Journal of Biomedical Materials Research Part A* **89A**(1): 13-23.

**Yui, N., Katoono, R. and Yamashita, A.** (2009). "Functional cyclodextrin polyrotaxanes for drug delivery." *Advances in Polymer Science* **222**: 55-77.

**Zhang, S. F., Shin, Y. S., Mayer, R. and Basile, F.** (2007). "On-probe pyrolysis desorption electrospray ionization (DESI) mass spectrometry for the analysis of non-volatile pyrolysis products." *Journal of Analytical and Applied Pyrolysis* **80**(2): 353-359.

## **Chapter 5**

# **Conclusions and Future Perspectives**

## 5.1 Conclusions and Future Perspectives

The introduction of ambient ionisation techniques and the commercialisation of IM-MS represent two of the most significant developments in mass spectrometry over the last 10 years. The research presented in this thesis evaluates the capabilities of these approaches for the characterisation of pharmaceutical and polymer formulations.

### Thermally assisted extractive electrospray (TA-EESI)

TA-EESI has been developed and utilised in the characterisation of a number of spray pharmaceutical formulations. This technique can allow for the rapid analysis of formulations containing components with a wide range of volatilities. This technique has been coupled with IM-MS and enables the acquisition of multiple product ion spectra without precursor selection, on a sub-second timescale, with no sample pre-treatment. This technique is not as suitable for solid or viscous samples, as these may degrade within the sample container, and a volatile headspace is not always formed. At elevated temperatures, heat induced fragmentation may occur. Care needs to be taken to determine an appropriate temperature for a specific sample, i.e. – a temperature that is higher than the temperature required for headspace formation but lower than that which results in fragmentation. The upper  $m/z$  limit with the TA-EESI technique is related to the temperature employed.

The TA-EESI technique would benefit from the inclusion of quantitative analysis. This would be challenging given the temperature nature of the experiment. A potential method to perform quantitative analysis could be to use a chemically similar external standard at different concentrations at a temperature that is optimal for the formation of sample headspace for both sample and external standard. This technique is very useful for the rapid analysis of formulations with components of differing volatility.

### Atmospheric pressure solids analysis probe ASAP

The ASAP approach was employed for the characterisation of both pharmaceutical and polymer formulations. Sampling by this method is very simple, and only requires contact of the sample with the glass capillary. The formation of radical cations or protonated ions of active pharmaceutical ingredients was investigated, and optimal conditions for the formation of both or one or the other were developed.

Metal cation adduction was not observed during analysis of polyethers by the ASAP technique, and this can present a problem when analysing unknowns, as the products of metal adduct precursor ions can be more structurally informative.

The technique was also used to rapidly profile the ester content of a number of polysorbate formulations, and the results obtained were in good agreement with the manufacturer's specifications. The type and levels of these esters govern many of the properties of these formulations. The ASAP technique was shown to offer good precision. While very interesting from an academic point of view, for the technique to be adapted by large scale industrial laboratories, the ASAP technique would need to be compared with a well established method such as GC-MS for a number of formulations. Currently the ASAP ester determination method could be used to provide a snap-shot during the manufacturing process prior to analysis by methods listed in pharmacopoeias.

The use of the ASAP technique would not be able to provide an analysis that could characterise all the components in a polymer formulation, as most will either be involatile, or will fragment as a result of the temperature. In the future, the ASAP technique, will potentially be used in a number of applications, as a screening tool to rapidly determine the nature of a sample, and to assess if additional characterisation by established techniques such as ESI-MS is needed.



### Ion mobility – mass spectrometry (IM-MS)

IM-MS was coupled to both ambient and well established ionisation techniques such as ESI and MALDI for the analysis of both pharmaceutical and polymer formulations. The analysis of a pain relief active ingredient resulted in the observation of two peaks on the ATD. A number of explanations as to the reason for this observation were made, however none of them could explain the result with confidence. A possible explanation for the observation is that protonation on the benzocaine molecule at different sites results in the formation of two species with well resolved mobilities, and this is possibly due to a rearrangement. Differences in mobility due to differences in protonation site have been observed and commented on in the early 90's (Karpas and Tironi 1991) and very recently by the group of Marcos Eberlin, who utilising a Synapt G1 investigated if they could separate species termed protomers (Lalli, Iglesias et al. 2012).

IM-MS was also used to provide additional information in the investigation of molecule that upon CID produced a product ion spectrum containing a peak 14 Da lower than the mass of the precursor ion.

IM-MS was used as a high resolution separation technique to simplify spectra and to separate out isomeric species within polymeric formulations. The sensitivity between the non-mobility and mobility modes of the Synapt G2 was very similar however the instrument conditions had to be modified to maintain sensitivity during MALDI analysis of polymers. The use of ESI with IM-MS for the analysis of polysorbates resulted in more complex spectra than MALDI due to the presence of multiply charged species.

IM-MS has been used to structurally characterise the components in a polyrotaxane formulation synthesised by a novel synthetic approach. Molecule specific information about the shape of various components in the formulation was obtained from calculated cross-sections.

IM-MS would benefit from developments in software to increase the information that can be extracted from complex spectra and mobilograms. Recently Waters Corporation has developed a software approach called HDMS Compare which can compare mobilograms of complex systems. Figure 5.1 shows an example of the difference and similarities of species highlighted by the software when comparing mobility separated spectra of Tween 40 and Tween 80.

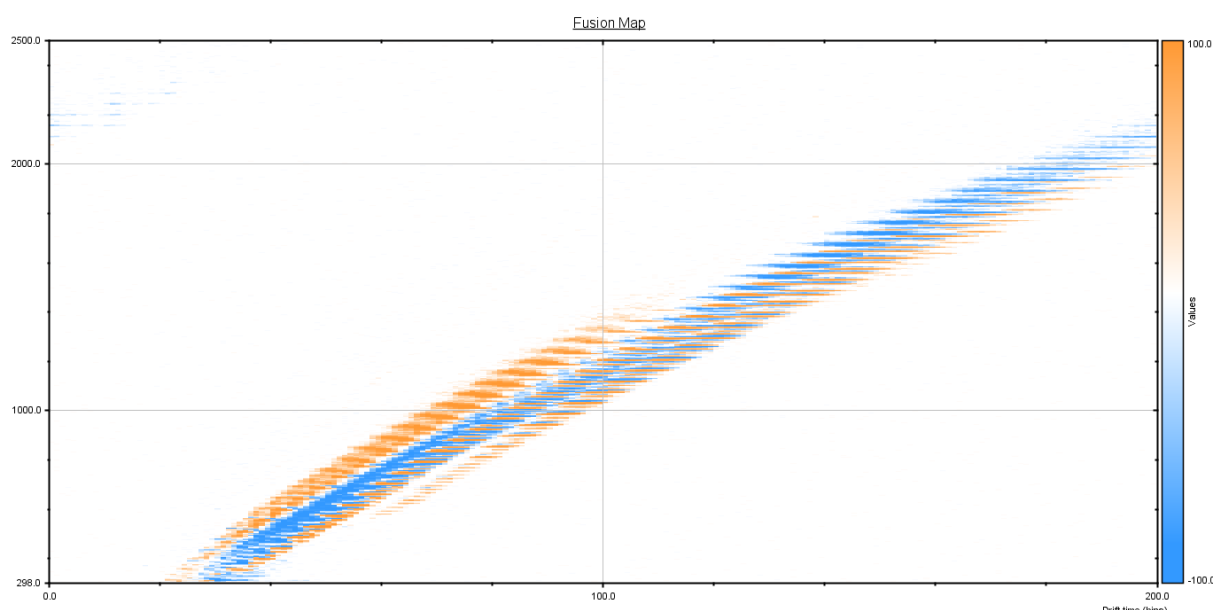


**Figure 5.1** - Comparison showing differences (orange) and similarities (blue) between Tween 40 and Tween 80.

The software could be used to aid in quality control measurements on batches of the same formulation within a manufacturing facility.

IM-MS approaches will have a more significant impact than ambient ionisation in mass spectrometry research. A number of applications would benefit including proteomics, the characterisation of synthetic macromolecules and structural biology.

The interest in ambient ionisation has decreased after the initial excitement, but a number of exciting avenues of research including breath analysis (Martinez-Lozano and de la Mora 2007; Ding, Yang et al. 2009) and the real time analysis of tissue during surgical procedures (Balog, Szaniszló et al. 2010; Guenther, Schoefer et al. 2011; Hinz, Gelhausen et al. 2011; Schaefer, Balog et al. 2011) are likely to result in

the continued use of techniques that require little or no sample preparation and that allow for the acquisition of results on a rapid time scale.

## 5.2 References

**Balog, J., Szaniszlo, T., Schaefer, K.-C., Denes, J., Lopata, A., Godorhazy, L., Szalay, D., Balogh, L., Sasi-Szabo, L., Toth, M. and Takats, Z.** (2010). "Identification of Biological Tissues by Rapid Evaporative Ionization Mass Spectrometry." *Analytical Chemistry* **82**(17): 7343-7350.

**Ding, J. H., Yang, S. P., Liang, D. P., Chen, H. W., Wu, Z. Z., Zhang, L. L. and Ren, Y. L.** (2009). "Development of extractive electrospray ionization ion trap mass spectrometry for in vivo breath analysis." *Analyst* **134**(10): 2040-2050.

**Guenther, S., Schoefer, K.-C., Balog, J., Denes, J., Majoros, T., Albrecht, K., Toth, M., Spengler, B. and Takats, Z.** (2011). "Electrospray Post-Ionization Mass Spectrometry of Electrosurgical Aerosols." *Journal of the American Society for Mass Spectrometry* **22**(11): 2082-2089.

**Hinz, K. P., Gelhausen, E., Schaefer, K. C., Takats, Z. and Spengler, B.** (2011). "Characterization of surgical aerosols by the compact single-particle mass spectrometer LAMPAS 3." *Analytical and Bioanalytical Chemistry* **401**(10): 3165-3172.

**Karpas, Z. and Tironi, C.** (1991). "The mobility and ion structure of protonated aminoazoles." *Structural Chemistry* **2**(7): 655-659.

**Lalli, P. M., Iglesias, B. A., Toma, H. E., de Sa, G. F., Daroda, R. J., Silva Filho, J. C., Szulejko, J. E., Araki, K. and Eberlin, M. N.** (2012). "Protomers: formation, separation and characterization via travelling wave ion mobility mass spectrometry." *Journal of Mass Spectrometry* **47**(6): 712-719.

**Martinez-Lozano, P. and de la Mora, J. F.** (2007). "Electrospray ionization of volatiles in breath." *International Journal of Mass Spectrometry* **265**(1): 68-72.

**Schaefer, K.-C., Balog, J., Szaniszlo, T., Szalay, D., Mezey, G., Denes, J., Bogнар, L., Oertel, M. and Takats, Z.** (2011). "Real Time Analysis of Brain Tissue

by Direct Combination of Ultrasonic Surgical Aspiration and Sonic Spray Mass Spectrometry." *Analytical Chemistry* **83**(20): 7729-7735.